UNIVERSITÀ DI TRENTO

Doctoral Programme in

Agrifood and Environmental Sciences

Amulya Jain Dinesh Kothari

Deciphering the biocontrol mechanisms of *Lysobacter capsici* AZ78 against plant pathogenic oomycetes using omics-based approaches

Supervisor

Prof. Gerardo Puopolo

38th cycle, 2025

ACKNOWLEDGEMENTS

This PhD scholarship and research project were supported by the University of Trento in collaboration with the Edmund Mach Foundation, to whom I extend my sincere gratitude.

First and foremost, I would like to express my deepest gratitude to my parents and my brother and Bhavika back in India for their unconditional love and support throughout this journey. For three years, they supported me from a distance, believing in my abilities from day one. This accomplishment belongs as much to them as it does to me. Thank you for believing in me, for trusting me to follow my dreams, and for always being my home no matter the distance. I love you.

I am also profoundly grateful to Manish, my boyfriend, who has stood by my side through every stage of this journey. Thank you for sharing both the challenges and the successes. Knowing that you were always there gave me the strength to keep moving forward, and for that I will always be grateful.

I would like to express my sincere appreciation to my supervisor, Prof. Gerardo Puopolo, for his invaluable guidance and encouragement throughout this journey. His scientific insight, constructive feedback, and dedication to research have profoundly influenced my development as a scientist. I am forever grateful for the opportunities he provided and for all that I have learned under his supervision.

I would also like to thank Prof. Aziz Aziz, my supervisor during my research period abroad at the University of Reims Champagne-Ardenne, for his guidance and support. My sincere thanks also go to my colleagues there for their collaboration, kindness, and hospitality.

My gratitude extends to all my colleagues and friends, both in Italy and abroad, whose support, knowledge sharing, and friendship contributed greatly to my personal and professional growth. In particular, I would like to thank Mehdi, whose kindness and friendship have meant more than words

can adequately express. Despite knowing each other for only a short time, your friendship has been invaluable.

I am especially grateful to Carmela and Oscar, who have helped me throughout these three years.

I would also like to thank my flatmates, Greta and Letizia, for their friendship, understanding, and constant support. Living far from home can often be challenging, but your warmth and companionship made Italy feel like home.

My sincere appreciation goes to Valentina from Consiglio Nazionale delle Ricerche - Area di Ricerca di Firenze, as well as Alessia and Prof. Francesco Vinale from the University of Napoli Federico II, for their collaboration, assistance during experiments, and the enriching professional and personal interactions we shared throughout this work.

I am grateful to PLAGRON for providing materials that were essential for conducting several of the experiments presented in this thesis.

I would also like to acknowledge all those whose contributions may not be explicitly mentioned here but whose support, encouragement, and inspiration accompanied me throughout this journey. Every interaction, whether large or small, played a role in shaping this experience and helping me reach this milestone.

Finally, I would like to thank myself for having the courage to embark on this journey. What began as a passion for science and a curiosity to explore a new country became a path filled with challenges, growth, uncertainty, and discovery. Completing this PhD required perseverance, adaptability, and determination, and I am proud to have carried it through to the end. Moving thousands of kilometres away from home was one of the most difficult decisions I have ever made, but it allowed me to grow

in ways I could never have imagined. I am proud of the person I have become through this experience.

I did it!!

TABLE OF CONTENTS

Contents

LIST OF TABLES

LIST OF FIGURES

LIST OF SYMBOLS AND ABBREVIATIONS

BCA	Biocontrol agent
PTMs	Polycyclic tetramate macrolactams
ROS	Reactive oxygen species
SDS	Self-digestive solution
mBCAs	Microbial biocontrol agents
VOCs	Volatile organic compounds
SA	Salicylic acid
JA	Jasmonic acid
ET	Ethylene
RMA	Rhizosphere mimicking agar
T4SS	Type 4 secretion system
T4P	Type 4 pili
HSAF	Heat stable antifungal factor
FHB	Fusarium head blight
SAR	Systemic acquired resistance
ISR	Induced systemic resistance
C/N	Carbon-to-nitrogen ratio
DMP	Dihydromaltophilin
MP	Maltophilin
AZ78	*Lysobacter capsici* AZ78
DH5α	*Escherichia coli* DH5α
NA	Nutrient agar
LBA	Luria-Bertani agar

PDA	Potato dextrose agar
PDB	Potato dextrose broth
CFU	Colony forming unit
Dpi	Days post inoculation
RH	Relative humidity
BION 50 WG	Benzothiadiazole-7-carbothioicacid S-methyl ester 50%
EPPO	European and Mediterranean Plant Protection Organization
DAB	3,3'-diaminobenzidine
DMSO	5,6-carboxyfluorescein diacetate
TLC	Thin layer chromatography
CC	Column chromatography
SPE	Solid phase extraction
HPLC	High-Performance Liquid Chromatography
ESIMS	Electrospray ionisation mass spectrometry
ACN	Acetonitrile
MeOH	Methanol
EtoH	Ethanol
KCl	Potassium chloride
H_2O	Water
$MgSO_4$	Magnesium sulphate
KH_2PO_4	Monopotassium phosphate
$((NH_4)_2SO_4)$	Ammonium sulphate
ANOVA	One-way analysis of variance
NMR	Nuclear magnetic resonance
t_n	Retention time

PAMP/MAMP	Pathogen- or microbe-associated molecular pattern
AOS	Allene oxide synthase
ACC	Ainocyclopropane-1-carboxylate synthase
PR	Pathogenesis related
ABA	Abscisic acid
PAL	Phenylalanine ammonia lyase
STS	Stilbene synthase
OMVs	Outer membrane vesicles
L-SDS	Unheated self-digestive solution
D-SDS	Heat-treated self-digestive solution
PYKM	Peptone, yeast, KH_2PO_4, $MgSO_4.7H_20$ growth medium
OD	Optical density
RNA	Ribonucleic acid
cDNA	Complementary deoxyribonucleic acid
qRT-PCR	Quantitative real time polymerase chain reaction
UPLC	Ultra-performance liquid chromatography
HR	Hypersensitive reaction
Da	Dalton
GC-MS	Gas chromatography mass-spectrometry
GS-GOAT	Glutamine synthase glutamate synthase
pH	Potential of hydrogen
OA	Organic amendment
RSD	Relative standard deviation
R2A	Reasoner's 2A agar
PCA	Principal component analysis

PCoA	Principal coordinate analysis
N	Nitrogen
NAS	Nitrogen assimilation
DNIT	Denitrification
NIT	Nitrification
ANR	Assimilatory nitrogen reduction
DNR	Dissimilatory nitrogen reduction
° C	Degree Celsius
H	Hours
G+C	Guanine-Cytosine
v/v	Volume to volume ratio
w/v	Weight to volume ratio

ABSTRACT

Plants are susceptible to numerous biotic and abiotic factors that negatively affect their performance in the field and ultimately reduce crop yield. Among the biotic factors, oomycetes are responsible for several devastating plant diseases that lead to substantial agricultural losses worldwide. Oomycetes are a group of eukaryotic microorganisms known for causing economically important plant diseases across diverse cropping systems. These diseases contribute significantly to global agricultural losses, resulting in reduced productivity and potential food shortages. Among the well-known oomycete genera, *Plasmopara*, *Peronospora*, and *Pythium* are prominent plant pathogens responsible for foliar and soil-borne diseases in a wide range of host plants. *Plasmopara viticola* and *Peronospora belbahrii* are the causal agents of downy mildew diseases in different hosts. In this study, we focused on grapevine and basil downy mildews caused by *P. viticola* and *P. belbahrii*, respectively. In addition to these foliar pathogens, *Pythium ultimum*, a soil-borne oomycete pathogen, poses a serious threat to various crops by causing pre-emergence and post-emergence damping-off diseases.

Current control strategies for oomycete plant pathogens largely rely on the application of fungicides to plants or soil. However, complete eradication of these pathogens from infected fields is nearly impossible. Although breeding programs aimed at developing resistant plant varieties are ongoing, this process is laborious and often challenged by the rapid evolution of pathogen resistance to both host resistance traits and chemical fungicides. Furthermore, extensive use of chemical control measures has raised concerns due to their negative impacts on human health and the environment. Consequently, farmers, scientists, and consumers are increasingly shifting toward sustainable pest management strategies. Modern disease management therefore emphasizes integrated approaches combining physical, chemical, and biological methods rather than relying on a single control strategy. Within this framework, biological control agents (BCAs) have gained considerable attention because

of their ability to suppress a broad range of pathogens through direct mechanisms such as antagonism, nutrient and space competition, and mycoparasitism, as well as indirect mechanisms including activation of plant defense responses that enhance plant resistance against pathogens.

The bacterial genus *Lysobacter* has emerged as a promising BCA and has been extensively studied for its antimicrobial activity against plant pathogenic fungi, oomycetes, nematodes, and both Gram-positive and Gram-negative bacteria. Several species, including *Lysobacter enzymogenes*, *L. antibioticus*, *L. gummosus*, and *L. capsici*, have demonstrated strong antimicrobial properties. These bacteria exert their effects through the secretion of lytic enzymes and a diverse array of secondary metabolites. Among them, *L. capsici* AZ78, isolated from the tobacco rhizosphere, has been widely investigated for its antimicrobial potential. Previous studies have demonstrated strong antagonistic activity of this strain against the foliar oomycete *P. viticola*, with efficacy comparable to commercially used copper-based fungicides in vineyards. Regarding soil-borne pathogens, volatile organic compounds (VOCs) emitted by *L. capsici* AZ78 have shown inhibitory effects on *P. ultimum* in *in vitro* split Petri dish assays. Despite multiple studies confirming the effectiveness of *L. capsici* AZ78 against both foliar and soil-borne oomycete plant pathogens, important knowledge gaps remain. In particular, the effects of *L. capsici* AZ78 and its antimicrobial secondary metabolites on host plants and the precise mechanisms of action against oomycete plant pathogens have not been fully elucidated. Moreover, studies involving soil-borne pathogens have largely been limited to laboratory conditions, with limited evaluation under realistic soil environments.

To address these knowledge gaps, this study investigated the effects of *L. capsici* AZ78 cells and their metabolites against two major foliar oomycete pathogens, *P. viticola* and *P. belbahrii*. We examined the direct effects of bacterial cells and their secondary metabolites, particularly thermostable polycyclic tetramate macrolactams (PTMs), on pathogen development while also

evaluating how plant protection responses were mediated in the host. Callose deposition and reactive oxygen species (ROS) accumulation were analysed in host plants treated with both bacterial cells and thermostable PTMs. To further understand grapevine responses to *L. capsici* AZ78 applications, gene expression analyses were performed on plants treated with a self-digestive solution (SDS) derived from the autolysis of *L. capsici* AZ78 cells grown in liquid culture for extended periods, allowing the accumulation of bioactive secondary metabolites in the growth medium. These analyses provided insights into the expression patterns of grapevine genes associated with defense-related functions against *P. viticola*. Simultaneously, phytoalexin accumulation was evaluated to determine whether *L. capsici* AZ78 and its metabolites could induce the production of antimicrobial compounds toxic to *P. viticola*.

The second part of the study focused on the soil-borne oomycete plant pathogen *P. ultimum*. Experiments evaluated the effects of *L. capsici* AZ78 cells and their VOCs on damping-off disease development in tomato plants. To gain deeper insight into the interactions among host plants, pathogens, and the BCA, metagenomic analyses were conducted to assess how *L. capsici* AZ78 and the VOCs influenced soil microbial communities and contributed to the establishment of disease-suppressive soil conditions that limit *P. ultimum* growth. The effects of these interactions were further enhanced through the addition of organic amendments, which served as nutrient-rich substrates supporting bacterial growth and promoting the emission of antimicrobial volatiles. The combined application of organic amendments and *L. capsici* AZ78 improved both plant growth promotion and disease protection under soil conditions.

Collectively, this study provides a comprehensive understanding of the mechanisms underlying the anti-oomycete activity of *L. capsici* AZ78. The results demonstrate that this bacterium employs multiple direct and indirect mechanisms to protect plants against pathogens. These include

direct antagonism, production of secondary metabolites such as thermostable PTMs, emission of antimicrobial VOCs, activation of plant immune responses, induction of phytoalexin accumulation toxic to pathogens, and modification of the soil microbiome to establish disease-suppressive environments. By integrating multiple experimental approaches, this work advances our understanding of this BCA and supports its application under practical agricultural conditions.

Furthermore, this study represents the first evaluation of the plant protection efficacy of *L. capsici* AZ78 against *P. belbahrii*. Currently, only a limited number of BCAs are available for controlling this pathogen, and they are typically applied in combination with chemical fungicides. Our results demonstrate that *L. capsici* AZ78 alone can provide more than 90% disease protection under semi-realistic greenhouse conditions. Additionally, this work expands upon previous *in vitro* studies on *P. ultimum* by validating the efficacy of *L. capsici* AZ78 under realistic soil conditions, thereby strengthening its potential for practical agricultural application.

CHAPTER 1.

INTRODUCTION

1.1 Oomycete plant pathogens: biology, epidemiological impact, and disease management

Oomycetes are eukaryotic microorganisms with a cosmopolitan distribution, capable of thriving both as saprobes or pathogens across diverse ecological niches (Burki *et al.*, 2020). Historically, these organisms were classified as fungi due to similarities in filamentous morphology, heterotrophic lifestyle, and life cycle characteristics. Both fungi and oomycetes occupy similar habitats, including soil, plant surfaces, and aquatic environments, and they frequently exhibit filamentous growth with extensive hyphal networks. These superficial similarities contributed to long-standing taxonomic confusion (Wang *et al*., 2025). However, several fundamental biological differences distinguish oomycetes from true fungi. Oomycetes possess coenocytic hyphae, generally lack pigmentation, and produce biflagellate motile zoospores. Most notably, their cell walls are primarily composed of cellulose and β-glucans, whereas fungal cell walls predominantly contain chitin (Latijnhouwers *et al*., 2003).

Many oomycetes are highly destructive plant pathogens and are often referred to as “plant killers” due to their capacity to cause severe agricultural losses worldwide. Beyond plants, some species also infect algae, fish, and mammals (Wang *et al*., 2025). Historical records illustrate the profound socio-economic impact of oomycete diseases. A prominent example is potato late blight, caused by *Phytophthora infestans*, which triggered the nineteenth-century Great Irish Famine, resulting in approximately one million deaths (Bourke, 1964). Grapevine downy mildew, caused by *Plasmopara viticola*, similarly devastated European vineyards in the late nineteenth century (Koledenkova *et al.*,

2022). Under favourable environmental conditions, this disease can infect 40-90% of plants in affected fields (Toffolatti *et al.*, 2018a) and cause yield losses of up to 75% in grapevine production (Stummer *et al.*, 2005; Jermini *et al*., 2010; Gessler *et al*., 2011). Historical outbreaks resulted in substantial economic damage, including vineyard losses of up to 33% in Germany between 1907 and 1916 and repeated production failures in Italy during multiple epidemic years. In France, vineyard production declined by approximately 70% in 1915, with wine losses reaching 20 million litres in 1930 (Koledenkova *et al.*, 2022). Another economically significant foliar oomycete pathogen is *Peronospora belbahrii*, the causal agent of basil downy mildew, which severely affects sweet basil (*Ocimum basilicum*). This disease has rapidly spread across Europe, the Americas, the Middle East, Asia, and Africa (Gilardi *et al*., 2020). Growers frequently report near-complete crop failure in susceptible cultivars, resulting in losses amounting to tens of millions of dollars annually (Wyenandt *et al.*, 2015). In addition to foliar pathogens, soil-borne oomycetes belonging to the genus *Pythium* represent major threats to agricultural production. These pathogens commonly inhabit agricultural soils and infect germinating seeds, seedlings, and young roots, causing pre- and post-emergence damping-off (Schroeder *et al.*, 2013). *Pythium* species possess broad host ranges and variable aggressiveness, contributing to estimated annual losses of approximately US$25 million in the United States alone (Bickel and Koehler, 2021). Disease incidence can exceed 60% seedling mortality in nurseries and fields, with annual yield losses ranging from 25-75% (Manoranjitham *et al*., 2001). In tomato nurseries, damping-off incidence has been reported between 41.3% and 85% under favourable epidemiological conditions (Kumar and Meenu, 2018).

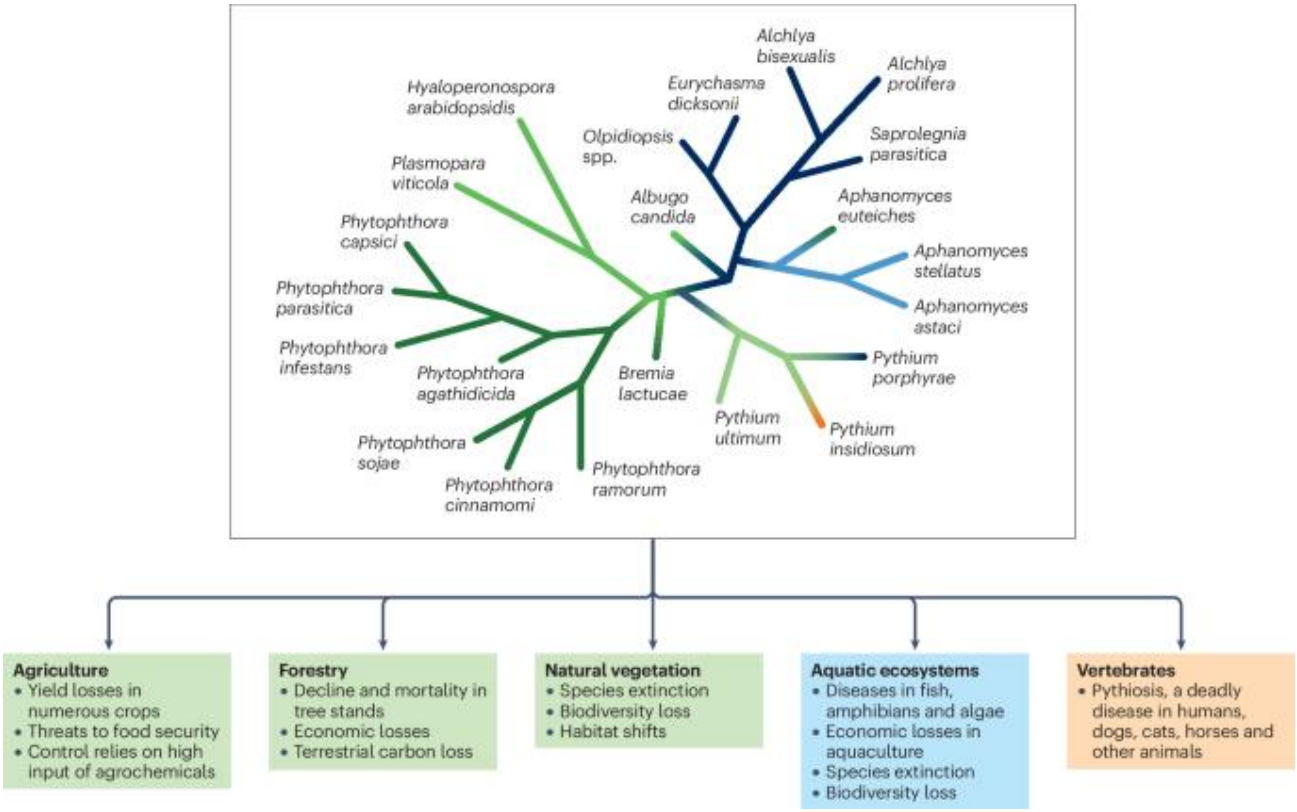

Figure 1. The phylogenetic tree highlights representative oomycete pathogens of plants (green), aquatic organisms (blue) and vertebrates (orange). Reference: *Wang Yan, Govers Frabcine and Wang Yuanchao*., 2025. Oomycete plant pathogens: biology, pathogenesis and emerging control strategies. *Nature Reviews Microbiology*.

Oomycete infection processes are closely linked to environmental moisture and specialized reproductive structures. Members of the order Peronosporales, including *Phytophthora, Pythium*, and numerous downy mildew genera, produce asexual sporangia dispersed by wind or water (Tyler, 2002). These sporangia germinate either directly via hyphal growth or indirectly through the release of motile zoospores. In *P. viticola*, biflagellate zoospores released under moist conditions swim toward stomata, encyst, and form germ tubes that penetrate leaf tissues. As an obligate biotroph, the pathogen derives nutrients from living host cells. Following approximately five days of incubation at optimal temperatures (~25 °C), sporangiophores emerge through stomata and release new sporangia, facilitating secondary infection cycles (Gessler *et* al., 2011). Similarly, *P. belbahrii* sporulates at temperatures between 10-25 °C and relative humidity above 85%, producing spores that germinate

within two hours and initiate infection within four hours under favourable conditions (Wyenandt *et al.*, 2015). In contrast, *Pythium* species are primarily soil-borne pathogens whose survival and infection are favoured by high soil moisture (>70%), low light, and nutrient-poor conditions (Van der Plaats-Niterink, 1981). Infection typically begins with oospore germination, followed by invasion of root hairs and root tips. The production of pectinolytic enzymes facilitates tissue degradation and pathogen spread within host tissues. Motile zoospores released from sporangia further infect nearby seedlings, ultimately leading to root rot, stem lesions, damping-off, and seedling collapse (Goodwin, 1997).

Symptoms caused by oomycete pathogens vary depending on host and pathogen biology. Grapevine downy mildew manifests as yellow or reddish-brown oil-like lesions on the upper leaf surface accompanied by white sporulation on the lower surface. Lesions may become angular along veins and later develop into mosaic patterns, while older leaves exhibit reduced susceptibility (Musetti *et al.*, 2005). Basil downy mildew symptoms often resemble nitrogen deficiency, with chlorotic leaves and dark purplish-brown sporulation on the abaxial surface under favourable conditions (Wyenandt *et al.*, 2015). *Pythium* infections cause both pre- and post-emergence damping-off in tomato and other crops, characterized by seed decay, water-soaked stem lesions, tissue maceration, wilting, and eventual seedling collapse. Severe infections may result in extensive root decay, fruit rot, and stunted plant growth (Weindling and Fawcett, 1936; Cram, 2003; Olson *et al.*, 2016).

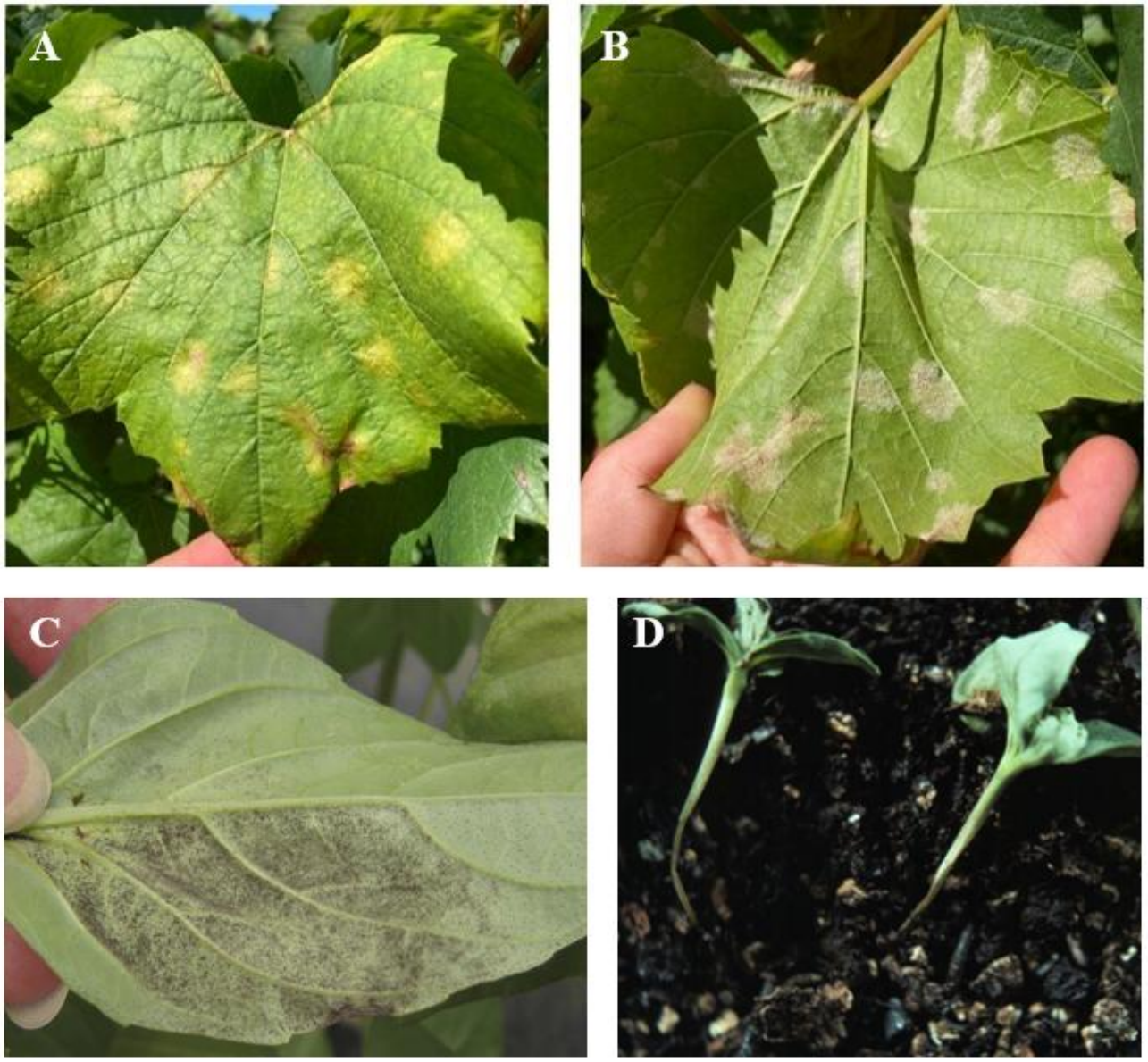

Figure 2. (A and B) A Foliar grapevine downy mildew signs and symptoms. Reference: *Kanaley Kathleen, Combs David B, Paul Angela, Jiang Yu, Bates Terry,* and *Gold Kaitlin M*., 2024. Assessing the Capacity of High-resolution commercial satellite imagery for grapevine downy mildew Detection and Surveillance in New York State. *Phytopathology*. (C) *Peronospora belbahrii* sporulating on the abaxial side of an infected sweet basil leaf (*Ocimum basilicum*). Reference: *Wyenandt Christian A, Simon James E, Pyne Robert M, Homa Kathryn, McGratch Margaret T, Zhang Shouan, Raid Ruchard N, Ma Li-Jun, Wick Robert, Guo LI,* and *Madeiras Angela*., 2015. Basil Downy Mildew (*Peronospora belbahrii*): Discoveries and Challenges Relative to Its Control. *Disease control and pest management*. (D) Lower stem collapse of *Zinnia* seedlings due to damping-off. *Hudelson Brian*. Damping-Off. *UW plant diseases facts*.

Management of oomycete diseases aims to maintain pathogen populations below economically damaging thresholds, as complete eradication is rarely feasible (Babadoost, 2017). Historically, disease control has relied heavily on chemical treatments. The first targeted control measure was the Bordeaux mixture, a combination of copper sulphate and lime developed in the late nineteenth century to manage grapevine downy mildew and later also applied against potato late blight (Lamichhane *et al.*, 2018). Copper-based formulations remain widely used against oomycetes, fungi, bacteria, algae, and invertebrates (Capinera and Dickens, 2016; Schuder *et al.*, 2004). However, prolonged copper use has raised concerns regarding phytotoxicity, soil accumulation, environmental contamination, and the emergence of resistant pathogen populations (Lamichhane *et al.*, 2018), prompting the development of more sustainable disease management approaches.

Current grapevine downy mildew management integrates cultural practices, chemical fungicides, and biological alternatives. Strategies such as canopy management, sanitation, resistant cultivars, and site selection reduce disease pressure and enhance spray effectiveness (Bem *et al.*, 2016; Yaxiong *et al.*, 2017). Fungicides remain essential, contributing to approximately 95% of yield protection under favourable disease conditions, although systemic fungicides carry a high risk of resistance development due to single-site modes of action (Gianessi and Reigner, 2006; Klopping and Delp, 1980; Koledenkova *et al*., 2022). Resistance in *P. viticola* to several fungicide classes has already been documented (Kuhn *et al.*, 1991; Baudoin *et al.*, 2008; Blum *et al*., 2010). Increasingly Microbial BioControl Agents (mBCAs) and natural compounds are incorporated into integrated disease management programs to reduce chemical inputs and delay resistance evolution (Compant *et al.*, 2013; Puopolo *at al*., 2014a, b; Clippinger *et al.*, 2024). Management of basil downy mildew similarly relies on integrated approaches combining fungicides, cultural practices, and host resistance. Registered fungicides such as cyazofamid and mandipropamid, along with phosphorous acid-based

products, are widely used preventively (Homa *et al*., 2014; Wyenandt *et al*., 2010). Organic fungicides and biopesticides generally provide limited control, making organic basil production particularly vulnerable under conducive environmental conditions (Wyenandt *et al.*, 2010). Effective management therefore requires preventive applications, fungicide rotation, humidity control, sanitation, and protected cultivation systems. Although resistant commercial cultivars are currently limited, resistance sources identified in non-sweet basil species and advances in transcriptomic studies are supporting future breeding efforts (Gilardi *et al.*, 2013).

Control of *Pythium* diseases remains challenging due to the pathogen's wide host range and long-term survival via oospores and sporangia. Cultural practices such as crop rotation, resistant cultivars, and disease-free seeds provide partial control. Soil solarization has proven effective in reducing pathogen populations through hydrothermal treatment, particularly when combined with organic amendments that enhance microbial antagonism. mBCAs act primarily through competition and antagonism but are most effective as preventive measures. Chemical fungicides, including mancozeb, carbendazim, and ridomil, remain widely used despite environmental concerns, limited post-infection efficacy, and resistance risks, reinforcing the importance of integrated disease management strategies (Baudoin *et al*., 2008; Gamliel *et al*., 2000; Hadar and Mandelbaum, 1986; Katan, 2000; Lazarovits *et al*., 1991; Lumsden and Locke, 1989; Praveen and Shrma, 2015).

The extensive reliance on chemical fungicides and associated environmental risks, together with the emergence of resistant pathogen populations, underscore the need for sustainable alternatives. In this context, biological control has gained attention, utilizing BCAs to suppress oomycete plant pathogens. Integration of biological control into disease management programs offers a promising pathway toward sustainable and environmentally friendly control of oomycete diseases.

1.2 Soilborne plant pathogens cause significant yield losses in various crops.

Agricultural sustainability is a crucial goal in the 2030 agenda for sustainable development, driven by the increasing global population, dietary transformations, and global climate changes (Di Marco *et al.*, 2020). The world's population is expected to grow to nearly 9.1 billion by 2050, up from 7.7 billion today, necessitating at least a 70% increase in agricultural production to meet food demand (FAO, 2017). Simultaneously, many emerging economies are transitioning from plant-based to animal-based diets, leading to resource-intensive practices. This adds additional strain on agriculture and the planet (Wood *et* al., 2019). Along with these challenges, the intensive and indiscriminate use of agrochemicals has severely affected the health of soils and the broader agricultural ecosystem. Prolonged use of chemical fertilizers and pesticides has reduced soil biodiversity, disrupted natural nutrient cycles, and weakened soil structure. These practices have led to declining soil fertility, contamination of the water bodies through runoff, and an increase in disease incidence (Meena *et al.*, 2020).

Soil is a heterogeneous habitat that harbours both biotic and abiotic components. It has many (micro)organisms, including bacteria, fungi, archaea, insects, protists, and plants (Nannipieri *et al.*, 2017). Alongside this, soil also harbours a variety (micro)organism causing plant diseases. The damages include the death of germinating seeds and seedlings, root rot, xylem blockage, soft rot, stem base deformation, and necrotic lesions. Additionally, in many circumstances, even though the plant pathogen does not directly affect the underground parts of the plant, it can still reside in the soil. In such cases, the soil can be considered to be the reservoir of the plant disease-causing (micro)organisms (García *et al*., 2020). For example, soilborne plant pathogens can survive many years without a host plant by forming resistant structures such as microsclerotia, sclerotia, chlamydospores, or oospores (Mihajlovic *et al.*, 2017). Fungi are the most destructive of all the studied organisms, causing plant diseases such as wilts, root rots, club rot, and blight.

Soil also plays an important role in determining the survival of plant pathogens and their movement to the potential host plant. Furthermore, it can create humid conditions, promote plant diseases and ensure the survival of prolonged plant pathogen structures. These features make soilborne plant pathogens particularly difficult to predict, detect, diagnose, and control (Mihajlovic *et al.*, 2017).

Fumigants have been essential tools for soil disinfestation for a long time. However, their use has been increasingly restricted due to large harmful side effects, including health hazards, environmental pollution, and potential ozone depletion. For 30 years, methyl bromide has been widely used to control soilborne plant pathogens and pests in fruit and vegetable production with 100% efficiency. However, in 1992, it was listed as an ozone-depleting substance under the Montreal Protocol, and its production and use were gradually reduced (Katan, 1999). The phase-out of methyl bromide highlighted the risks of relying on a single method for controlling soilborne plant pathogens and pest management.

The use of chemical inputs not only modifies the soil's biochemical and physiological properties but also reduces microbial populations (Duke, 2018), impacting plant health. The extent of these effects depends on the type of chemicals used and the composition of the soil's microbiome. For instance, chemicals like clidon, benzene hexachloride, hexaconazole, and bavistin are toxic to many beneficial soil organisms (Uddin, 2022). Fluazifop-P-butyl, commonly applied to control weeds, can reduce plant-promoting bacteria while increasing harmful plant pathogens in the soil (Darine *et al.*, 2015). Similarly, the use of glyphosate has been linked to an increase in *Fusarium* spp., a soilborne plant pathogenic fungi responsible for diseases like root rot and plant wilting (Fernandez *et al.*, 2009).

1.3 Exploring microbial biocontrol agents for sustainable management of soilborne plant diseases.

In response to these growing challenges, biological control developed as a sustainable and promising strategy to manage plant diseases and reduce the dependency on chemical inputs. Biological control utilizes naturally occurring microbes to safeguard plant health, offering an environmentally friendly alternative to traditional chemical pesticides. mBCAs are agriculturally important microbes that can manage various plant health threats, including emerging and re-emerging plant diseases, insect vectors of plant pathogens, phanerogamic plant parasites, and invasive weeds. These plant beneficial microbes work through various mechanisms, including direct antagonism of plant pathogens, production of antibiotics, lytic enzymes, and toxins, and eliciting plant-mediated resistance responses that strengthen plant immunity (Tripathi *et al.*, 2020).

Fungi of the genus *Trichoderma*, and bacteria like *Bacillus* spp. or *Pseudomonas* spp. are among the most promising mBCAs able to effectively control soilborne plant pathogens. For example, the density of the plant parasitic nematode *Meloidogyne hapla* significantly decreased in the coffee fields where the soil treated with *T. asperellum* was seen to improve soil health and further enriched microbial diversity (Saikai *et al.*, 2023). In the tomato *F. oxysporum* f. sp. *lycopersici* phyto-pathosystem, it was noticed that *Bacillus* spp., and *Trichoderma* spp. along with compost, negatively impacted the plant pathogen, causing a reduction in the wilt disease by 70% (Cucu *et al*., 2020b). Cucu *et al*. (2020a) found that treatments with mBCAs (*Bacillus* spp. and *Trichoderma* spp.) and two different composts significantly reduced the abundance of *P. capsici* in naturally and artificially infested soils. The pathogen suppression was achieved through direct interactions. The application of the mBCAs also boosted the population of beneficial microorganisms, which were also seen to contribute to disease suppression in zucchini. *B. subtilis*, *B. amyloliquefaciens* and *P. stutzeri* previously showed colonisation of cucumber roots and disease prevention towards *P. capsici* (Islam *et al*., 2016). Jain *et al*. (2012) proved that a consortium of *P. aeruginosa*, *T. harzianum*, and *B. subtilis*

effectively suppresses *Sclerotinia sclerotiorum* on pea plants (*Pisum sativum* L. cv. Arkel). The mBCA *B. amyloliquefaciens* GB03 has also been proven to play a significant role in plant disease control by modulating the rhizosphere microbiota of plants. When tomato plants were treated with this bacterial strain, it triggered the release of Volatile Organic Compounds (VOCs) from the plant leaves. β-caryophyllene, one of the VOCs induced the secretion of salicylic acid (SA) in the root exudates of neighbouring plants. The increased secretion of SA helps enhance the defence against plant pathogens. This demonstrated how *B. amyloliquefaciens* GB03 can indirectly promote plant health and disease resistance through plant signalling pathways (Kong *et al.*, 2021).

One of the most significant advantages of using mBCAs is their reduced environmental impact compared to synthetic agrochemicals. mBCAs are often selected for their specificity in targeting particular plant pathogens, ensuring that they do not affect non-target (micro)organisms, thus preserving soil biodiversity (Villaverde *et al.*, 2014). Furthermore, because mBCAs are typically effective in small quantities and decompose rapidly, they minimize the environmental footprint and avoid long-term contamination of soils and waterways (Shukla *et al.*, 2019). Unlike chemical pesticides, which often harm beneficial organisms, mBCAs are highly selective in suppressing harmful plant pathogens. This selectivity ensures that the broader ecological balance is not disrupted, making them a more sustainable option for disease management (Ul Haq et al., 2024).

Despite their clear advantages, mBCAs face barriers to widespread adoption in agriculture, as they can be susceptible to environmental factors, such as extreme temperatures, UV radiation, or moisture levels, which can reduce their effectiveness in the field (Quesada-Moraga *et al.*, 2024). Additionally, competition with native soil microorganisms and difficulty in developing stable formulations that retain viability and efficacy during storage further hinder their commercial success

(Bejarano and Puopolo, 2022). Addressing these formulation challenges is critical to enhancing the practicality and consistency of mBCAs in large-scale agriculture.

Nevertheless, sustainable agriculture's future must include strategies promoting soil and plant microbial health. Applying mBCAs can play a vital role in mitigating the damage caused by conventional agricultural practices. By restoring microbial diversity, they reduce the prevalence of harmful plant pathogens, enhance soil resilience, and promote healthier root systems. In particular, they can stimulate beneficial microbial communities in the soil, suppressing disease-causing organisms through competitive exclusion, secretion of antimicrobial compounds, and nutrient cycling. This allows crops to thrive with reduced reliance on synthetic inputs.

1.4 The genus *Lysobacter*: classification, morphological characteristics and ecological distribution

Environmental concerns have been pushing people and researchers around the world to find alternatives to chemical pesticides for controlling soilborne plant pathogens and plant parasitic nematodes. Possible alternatives could be found in members of the bacterial genus *Lysobacter*, including bacterial species commonly found in agricultural soils (Reichenbach, 1992).

Lysobacter spp. are characterised by the ability to prey upon other soil dwelling microbes. This predatory life style led to an early taxonomic confusion, where *Lysobacter* species were mistakenly classified alongside myxobacteria due to their shared characteristics (Reichenbach, 1992).

However, despite their behavioural resemblance, *Lysobacter* and myxobacteria differ significantly at the genetic level. One of the key distinctions lies in the DNA composition. *Lysobacter* spp. have a notably high guanine-cytosine (G+C) content in their DNA, exceeding 60%, while

myxobacteria generally exhibit a much lower G+C content (Christensen and Cook, 1978; Reichenbach, 1992)

This genetic difference was crucial for reassigning misidentified bacterial strains to a new bacterial genus. In 1978, *Lysobacter* was formally established as a distinct genus by Christensen and Cook (Christensen and Cook, 1978). *Lysobacter* belongs to the family *Lysobacteraceae*, which was later proposed by Naushad and colleagues (Naushad *et al.*, 2015). The formation of the new family *Lysobacteraceae* was based on comprehensive phylogenetic and molecular analyses a significant evolutionary divergence from the family *Xanthomonadaceae*. The study utilized concatenated protein sequences and 16S rRNA gene sequences to construct phylogenetic trees, revealing distinct branching patterns that indicate *Lysobacteraceae* and *Xanthomonadaceae* represent separate evolutionary lineages. Additionally, the identification of unique conserved signature indels specific to members of *Lysobacteraceae* further supports this distinction. These molecular signatures serve as markers that differentiate *Lysobacteraceae* from *Xanthomonadaceae*, highlighting their unique evolutionary adaptations and histories (Naushad *et al.*, 2015).

Since its establishment in the 1970s, there has been a gradual increase in the number of species belonging to the genus *Lysobacter*. In 1978, it comprised four species: *L. antibioticus, L. brunescens, L. enzymogenes,* and *L. gummosus*. By 2016, there were almost 40 species (http://www.bacterio.net) including newly discovered species such as *L. hankyongensis* and *L. sediminicola* (Siddiqi and Im, 2016). The number of species increased by almost 75% to 70 with valid data and accurate names registered on LPSN (https://lpsn.dsmz.de/genus/Lysobacter; Feb 2023). Currently, this bacterial genus includes 73 species.

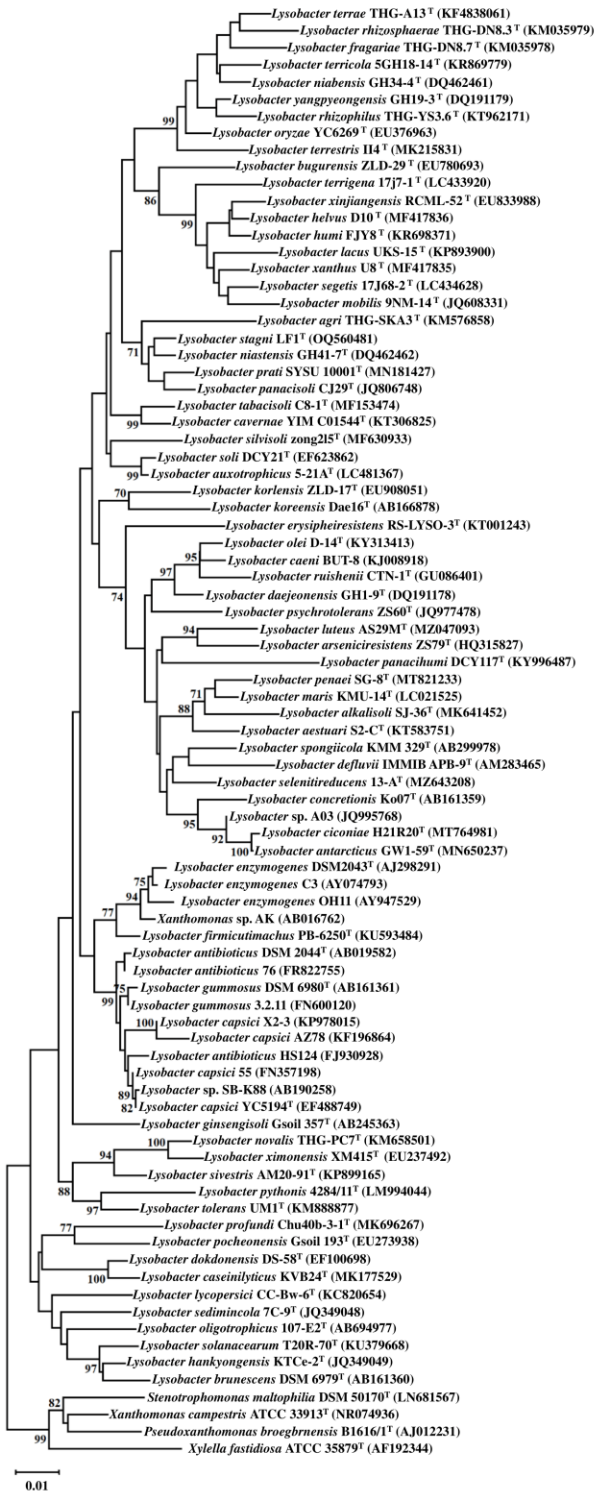

Figure 3. Phylogenetic tree resulting from analysis of the 16S rRNA gene sequences of *Lysobacter* species. GenBank was used to collect gene encoding 16S rRNA from *Lysobacter* species enlisted on the website https://lpsn.vsmz.de/genus/lysobacter at the time of writing. Once aligned by ClustalW,

the alignment profile was used to construct the optimal phylogenetic tree using the Neighbout-Joining method (Saitou and Nei, 1987) and the evolutionary distances were computed using the Kimura's two parameter model (Kimura, 1980). Bootstrap values (1000 replicates) higher than 70 are shown next to the branches (Felsenstein, 2009). All the phylogenetic analysis were carried out using MEGA11 (Tamura, Stecher and Kumar, 2021).

Lysobacter consists of non-motile, Gram-negative, rod-shaped bacteria widely distributed in nature. It derives its name, which translates to "the lysing rod," from its ability to lyse various organisms. In the past, *Lysobacter* was often mistaken for genera like *Stenotrophomonas* and *Xanthomonas*. A study by (Sullivan *et al.*, 2003) demonstrated this confusion, showing that bacterial strains N4-7 and C3, previously thought to belong to *St. maltophilia*, were members of *L. enzymogenes* (Folman *et al*., 2003). Similarly, *Xanthomonas* sp. AK was also seen to be more related to *Lysobacter* than to *Xanthomonas* in a phylogenetic analysis by Folman *et al*. (2003).

Lysobacter cells are rod-shaped and aerobic, typically measuring around 0.4-0.6 × 2-5 μm, and they possess a high G+C content in their DNA. Additionally, they utilize ubiquinone Q-8 as their primary respiratory quinone. Most species are non-motile due to the absence of flagella (Puopolo *et al*., 2018). However, some species, such as *L. spongiicola*, *L. arseniciresistens*, *L. lycopersici*, *L. rhizophilus,* and *L. mobilis*, are exceptions and have been reported to possess single polar flagella (Lin *et al*., 2015; Luo *et al*., 2012; Romanenko *et al*., 2008; Yan *et al*., 2016; Yang *et al*., 2015a). Additionally, strains like *L. helvus* and *L. xanthus* exhibit motility via monotrichous flagella *(Kim et al*., 2019). Recently discovered species, including *L. stagni, L. selenitireducens, L. auxotrophiocus,* have also demonstrated motility (Mao *et al.*, 2022; Saito *et al.*, 2023; Jung *et al.*, 2024). Cells of *L. luteus* were observed to be actively motile, with some displaying flagella, as confirmed by scanning electron microscopy (Lucena *et al.*, 2022).

While most species lack flagella, they exhibit other forms of motility, such as twitching or gliding. For example, *L. enzymogenes* exhibited twitching motility in the peripheral cells of the colony (Zhou

et al., 2015). Tomada *et al*. (2016) revealed that different *Lysobacter* spp., display various degrees of motility depending on the growth media and assay conditions, with *L. capsici* strains exhibiting significant swimming, swarming, and twitching motility, especially on pea agar medium, forming large dendritic colonies. Additionally, Brescia *et al*. (2020) found that the motility of *L. capsici* AZ78 cells was influenced by nutrient composition. *L. capsici* AZ78 cells grown on a growth medium mimicking the tomato rhizosphere nutrient conditions, rhizosphere mimicking agar (RMA) showed higher motility than those grown on Luria Bertani agar. This motility was assumed to be related to the formation of cell surface appendages and the lower abundance of nutrients in RMA (Brescia *et al*. 2020).

The colonies of *Lysobacter* spp. are typically mucoid and pale, with colours ranging from cream to pink, yellow-brownish, or brown (Christensen and Cook, 1978). A more recent study highlighted the diversity in colony morphology across different growth media, noting that *L. enzymogenes* OH11 had cream-yellow jagged colonies, *L. antibioticus* OH13 displayed shifts in colour from yellow to pink and brown, while *L. gummosus* OH17 and *L. bruneascens* OH23 exhibited creamy yellow and deep yellow colonies, respectively (Zhao *et al.*, 2021a).

Lysobacter spp. are distributed in various environments with diverse ecosystems, such as soil, rhizosphere, aquatic habitats (freshwater), and even extreme environments. With technological advancements, such as 16S rRNA gene sequencing, new *Lysobacter* species have been identified from various habitats. Several studies have documented *Lysobacter* spp. in agricultural soils and rhizospheres of diverse plants. For instance, strains have been isolated from ginseng fields in South Korea (Choi *et al*, 2014; Lee *et al*, 2006). *Lysobacter* spp. have also been identified in the rhizospheres of maize (García-Salamanca *et al.*, 2013), potato (Turnbull *et al*., 2012; Van Overbeek and Van Elsas, 2008), soybean (Kim *et al*., 2023; Liang *et al*., 2014), switchgrass (Rodrigues *et al.*, 2018), rice,

(Aslam *et al.*, 2009), green pepper (Qian *et al.*, 2009; Liu *et al.*, 2019), pepper (Park *et al.*, 2008), tobacco (Cheema and Qureshi, 2024; Puopolo *et al*., 2010; Xiao *et al*., 2019), common bean (Pérez-Jaramillo *et al.*, 2019), *Pteris vittata* (Wang et al., 2022b), tomato (Kim *et al.*, 2017), *Aglaia odorata* (Ngo *et al.*, 2015), marigold (Kim *et al.*, 2022), and strawberry (Singh *et al.*, 2015; Niu *et al.*, 2023). Recently, *Lysobacter* was also isolated form rhizospheric soil in Korea (Lee and Whang, 2021). *L. rhizophilus* was isolated from the rhizosphere of mugunghwa, the national flower of South Korea (Yan *et al.*, 2016). In addition to plant-associated environments, *Lysobacter* spp. have been found in human-associated habitats, such as *L. oculi* from human meibomian gland secretions (Bai *et al.*, 2020). Beyond common environments, *Lysobacter* spp., also thrive in extreme habitats, such as thermal vents and mudflows of Mt. Pinatubo (Sullivan *et al.*, 2003), *L. antarcticus* in a coastal sediment from the Chinese Great Wall Station, Antarctica (Z. Liu *et al.*, 2022), *L. luteus* isolated from activated sludge obtained from the sea water-based wastewater treatment plants (Lucena *et al.*, 2022). Analysis of 16s rRNA sequences from tar pits, also showed the presence of *Lysobacter* spp. (Kim and Crowley, 2007). Other environments from where *Lysobacter* spp. were isolated included Kentucky Bluegrass foliage (Giesler and Yuen, 1998), root tips of cucumber plants grown hydroponically (Folman *et al*., 2003), anaerobic sludge reactors (Bae *et al*., 2005), lake water in the Republic of Korea (Im *et al*., 2020; Jung *et al*., 2024), long sediment core collected in Republic of Korea (Jin *et al*., 2020), river sediment (Mao *et al.*, 2022), chitin-treated upland soils (Saito *et al.*, 2023), and in deep-sea sponge in Philippine (Romanenko *et al.*, 2008).

1.5 Mechanisms of action in plant pathogen suppression by *Lysobacter* spp.

1.5.1 Antimicrobial arsenal of Lysobacter*: antibiotics, enzymes, and volatile compounds*

In recent years, the genus *Lysobacter*, apart from other mBCAs, has garnered significant interest due to its potential to produce lytic enzymes and novel antimicrobial compounds. These compounds

could be valuable in combating plant pathogenic (micro)organisms (Panthee *et al.*, 2016; Puopolo *et al*., 2018). *Lysobacter* spp., are known to employ diverse strategies to target other microorganisms. A range of antimicrobial strategies, including the producing long-range, intermediate-range, and short-range weapons are used against plant pathogens. Short-range actions, such as the T6SS, enable *Lysobacter* spp. to inject toxic effectors directly into the cells of target plant pathogens, inducing cell death in a contact-dependent manner (Lin *et al*., 2021). Also, *L. enzymogenes* OH11 uses Type IV Secretion System (T4SS) for direct antagonism in the inter-bacterial killing system (Shen *et al.*, 2021). Intermediate-range mechanisms include lytic enzymes that inhibit plant pathogen growth. Long-range weapons involve diffusible antimicrobial compounds capable of disrupting fungal cell walls and membranes. These diverse modes of action make *Lysobacter* spp. versatile and effective mBCAs.

Among the antimicrobial compounds produced by *Lysobacter* spp., the Heat Stable Antifungal Factor (HSAF), also known as dihydromalthophilin, stands out as a promising broad-spectrum antifungal agent belonging to the family of polycyclic tetramate macrolactams (Graupner *et al*., 1997; Yu et al., 2007). *Lysobacter* spp. synthesize HSAF to protect themselves from oxidative damage and to preserve DNA from degradation in high concentrations of iron (Fe), H_2O_2, or under UV radiation (Yu *et al*., 2021). *L. enzymogenes* C3 mutants lacking HSAF production genes barely survived oxidative stress and exhibited significantly increased production of reactive oxygen species (ROS), highlighting the compound's vital role in microbial defence. HSAF isolated from *L. enzymogenes* C3 has been proven effective in controlling plant pathogens (Yu *et al*., 2007). HSAF is an antifungal compound that deteriorates the growth of the fungal cells by inducing cell wall thickening caused by disruption of sphingolipid biosynthesis (Li *et al*., 2009). HSAF treatment has been shown to inhibit the conidial germination and conidiation of *F. graminearum*, the causal agent of *Fusarium* head blight (FHB), achieving 100% inhibition when applied at concentrations as low as 1 to 6 µg/ml. Moreover,

ultrastructural changes such as cell wall thickening and plasmolysis were observed in *F. graminearum* cells, and HSAF field applications of HSAF was effective in controlling FHB (Zhao *et al.*, 2019). Additionally, HSAF's effectiveness extends to fungicide-resistant *F. graminearum* strains, making it a promising candidate for addressing the growing issue of fungicide resistance (de Chaves *et al.*, 2022). HSAF was also found to reduce virulence and toxin production and successfully inhibit both wild-type and fungicide-resistant strains of *F. graminearum*. A recent study identified FgORP1, an oxysterol-binding protein involved in mycelial growth, virulence, and ergosterol biosynthesis, as a direct target of HSAF in *F. graminearum* (Chen et al., 2024). *L. enzymogenes* OH11 was shown to deliver HSAF to the cell walls of plant pathogenic fungi by the production of outer membrane vesicles, which ensures its efficient delivery (Yue et al., 2021). Recently, *L. capsici* AZ78 also showcased the presence of HSAF in its metabolomic profile when grown on RMA. In particular, HSAF was accumulated in central core and the outer ring of *L. capsici* AZ78 macrocolonies (Brescia et al., 2020). Other examples of antibiotics belonging to the family of polycyclic tetramate macrolactams are lysobacteramides, alteramides (Li et al., 2018; Lou et al., 2011; Xu et al., 2015), dihydromaltophilin (Brescia et al., 2021), xanthobaccins (Islam et al., 2005; Nakayama et al., 1999). In addition to HSAF, *Lysobacter* spp. produce other antimicrobial compounds. The antibiotic profile of *L. capsici* AZ78 was recently characterized, revealing its ability to synthesize cyclic lipodepsipeptides, including WAP-8294A2, which is specifically toxic to Gram-positive bacteria (Brescia et al., 2021). WAP-8294A2 disrupts bacterial membranes by targeting menaquinone, a component crucial for membrane integrity in Gram-positive bacteria, ultimately causing cell lysis (Itoh *et al.*, 2018). This compound has shown remarkable activity against *Bacillus* spp., and *Staphylococcus* spp., including drug-resistant *S. aureus* isolates, and is currently under development as a pharmaceutical drug for systemic methicillin-resistant *S. aureus* infections (Chen *et al*., 2020). Another cyclic lipodepsipeptide, WBP-29479A1 was found in *L. antibioticus* (Sang *et al*., 2019). Similarly, cyclopeptides lysocin E

(Hamamoto *et al.*, 2015), I and J (Santiago *et al.*, 2018) are other antimicrobial compounds produced by *Lysobacter* sp. RH2180-5, was shown to target vitamin K_2 (menaquinone, MK), a membrane cofactor in the electron transport chain specific to various bacteria. Lysocin E has been shown to be highly effective against both drug-susceptible and drug-resistant *Mycobacterium tuberculosis* var. *tuberculosis*, as well as dormant mycobacteria, making it a promising lead compound for antituberculosis drugs (Geberetsadik et al., 2022). Additionally, *Lysobacter* spp. also produce phenazine-based antibiotics. For instance, *L. antibioticus* OH13 has a gene responsible for synthesizing myxin, a potent antibiotic derived from phenazine 1,6-dicarboxylic acid. It inhibits DNA synthesis and is highly toxic to both prokaryotic and eukaryotic cells (Zhao *et al.*, 2016).

Lysobacter spp. produce low-molecular weight antimicrobial compounds also, as the case of 4-hydroxyphenylacetic acid, isolated from *L. antibioticus* HS124, exhibits activity against the plant pathogen *P. capsici* and root-knot nematodes in tomatoes, offering another effective biological control method (Lee *et al*., 2013). Additionally, diketopiperazines such as cyclo(L-Pro-L-Tyr), cyclo(L-Pro-L-Val), and cyclo(L-Pro-L-Leu), have been identified as toxic secondary metabolites produced by *L. capsici* AZ78, with toxic activity against a variety of plant pathogens, including *P. infestans*, *P. viticola* and *Rhodococcus fascians* (Cimmino *et al*., 2021; Puopolo *et al*., 2014a, b). Cyclo (L-Pro-L-Tyr) showed effective inhibition of *F. oxysporum* and *R. solani,* which are both critical soilborne pathogens (Rahman *et al.*, 2019).

Moving beyond antibiotics, *Lysobacter* spp. also secrete a wide range of extracellular lytic enzymes, which play key roles in degrading complex macromolecules in the soil and attacking the cell walls of plant pathogenic fungi and oomycetes (de Bruijn *et al.*, 2015). Chitinases, for instance, target the chitin in fungal cell walls, insect exoskeletons, and nematode eggs, offering broad-spectrum defence against these organisms. In particular, the GH 19-type chitinase (Chi19MK) from *Lysobacter*

sp. MK9-1, when expressed in the transformed *Escherichia coli*, inhibited fungal growth, further supporting the antifungal potential of chitinases in *Lysobacter* spp. (Yano *et al.*, 2021). Proteases such as trypsin, secreted by *L. enzymogenes* B25, show nematicidal effects by destroying the hatched eggs of *Me. incognita* (Martínez-Servat *et al.*, 2023). Chitinases and proteases secreted by *L. antibioticus* HS124 showed efficient biocontrol of the lepidopteran pest *Hyphantria cunea*, both under *in-vitro* and filed conditions when applied to roots or leaves of poplar trees (Moon *et al.*, 2021). This highlights the potential role of *Lysobacter* members also as entomopathogenic microorganisms. Chitinases and proteases are not the only extracellular enzymes secreted by *Lysobacter* spp., involved in the biocontrol activity of plant parasitic nematodes. For instance, gelatinases produced by *L. capsici* YS1215 degraded the cuticle of root-knot nematodes, inducing mortality in nematodes during *in vivo* trials (Lee *et al*., 2015). Zhao *et al*. (2021a) demonstrated that the enzymes including, proteases, chitinases, cellulases, and glucanases are responsible for the antagonistic activity of *L. enzymogenes* OH11 and *L. gummosus* OH17 against a wide range of plant pathogens. This included *Colletotrichum fruticola*, *Botrytis cinerea, Botryosphaeria dothidea*, *R. solani*, *F. graminearum*, *S sclerotiorum*, and *P. capsici*.

Several *Lysobacter* spp. are also known to emit VOCs that exhibit antimicrobial activity against soilborne plant pathogens. Due to their physiochemical characteristics, these VOCs have been proposed as substitutes for chemical fumigants (De Boer *et al.*, 2019). For example, *L. enzymogenes* ISE13 releases 2,4-di-tert-butylphenol, which inhibits the growth of *C. acutatum* and *P. capsici* (Sang *et al*., 2011). When grown in a protein-rich growth medium, *L. antibioticus*, *L. capsici*, *L. enzymogenes*, and *L. gummosus* type strains release VOCs such as 2,5-dimethyl pyrazine, decanal, and pyrrole, which inhibit the *in vitro* growth of *P. Infestans* (Lazazzara *et al.*, 2017). In split Petri dish assays, VOCs produced by *L. capsici* AZ78 inhibit the growth of *Pythium* (*Py*) *ultimum*, *R. solani*,

and *Sc. minor*. GC-MS analysis revealed that *L. capsici* AZ78 produced 22 VOCs, the majority of which were identified as pyrazines such as 2,5-dimethylpyrazine, 2-ethyl-3-methoxypyrazine, and 2-isopropyl-3-methoxypyrazine (Vlassi *et al*., 2020a). *Lysobacter capsici* AZ78 emits also ammonia and subsequent bioassays showed that the inhibition of *R. solani* by *L. capsici* AZ78 volatiles is the result of the combination of ammonia, pyrazines and increase of pH in the growth medium (Vlassi *et al*., 2020b).

1.5.2 Colonization, biofilm formation, and motility in Lysobacter's biocontrol strategy

The ability of *Lysobacter* spp. to colonize plant tissues enables them to establish within the plant environment, where they can exert their antagonistic activities against plant pathogens. By colonizing the roots, shoots, or other plant surfaces, *Lysobacter* spp. form a protective barrier against invading (micro)organisms, preventing plant pathogens from establishing a foothold. The formation of biofilm plays an essential role in this. A biofilm is an assemblage of surface-associated microbial cells enclosed in polymeric matrix such as exopolysaccharides (Barceló *et al.*, 2016). The formation of biofilms not only increases the bacterium's resilience to environmental stresses such as desiccation, nutrient limitation, or pH changes but also helps in the accumulation of antimicrobial compounds and lytic enzymes at the site of colonisation (Velmourougane *et al*., 2017). For example, biofilm formation in *L. enzymogenes* OH11 helps it to form a dense microbial community for accumulating lytic enzymes and antimicrobial compounds (Xia *et al.*, 2018). Additionally, the suppression of the damping-off disease by *Lysobacter* sp. SB-K88 was found to be interlinked with its ability to densely colonize the roots of sugar beet and spinach plants by perpendicular attachment (Islam *et al*., 2005). *L. capsici* AZ78 produce biofilm in a growth media mimicking the nutrient content found in tomato rhizosphere. The cells that originated on RMA were equipped with surface external cell appendages known to help in colonisation processes (Brescia *et al.*, 2020).

Another essential factor in antagonistic behaviour is cell motility. Despite lacking flagella, *Lysobacter* spp. exhibit swarming motility, allowing it to move across the areas. In addition to swarming, *Lysobacter* spp. utilize twitching motility, driven by Type IV Pili (T4P; Tomada *et al.*, 2016). T4P mediates the extension and retraction of the pili, enabling the bacterium to "crawl" across surfaces (Chen *et al*., 2018). Twitching motility has been widely reported in *L. enzymogenes*, contributing to the colonisation of plant surfaces and the delivery of antimicrobial compounds (Chen *et al*., 2018; Zhou *et al*., 2015). Interestingly, *L. enzymogenes* B25 cell motility increases in the presence of plant pathogens like the plant pathogenic nematode *Me. incognita* (Martínez-Servat *et al.*, 2023). Similar behaviour was seen when *L. enzymogenes* OH11 was co-cultured with the plant pathogenic oomycete *P. aphanidermatum*, demonstrating the role of motility in its predatory behaviour (Zhao *et al*., 2017b). These results are consistent with the "wolf pack predation" attributed to the *Lysobacter* genus (Seccareccia *et al*., 2015) (Table 1).

Table 1: Types of interaction and different modes of action of biocontrol *Lysobacter* spp. strains.

Type of interaction	Microbial biocontrol agents	Modes of action	References
Long-range	*L. antibioticus* DSM 2044^{T}, *L. capsici* DSM 19286^{T}, *L. enzymogenes* DSM 2043^{T}, and *L. gummosus* DSM 6980^{T}	Emission of VOCs* such as decanal, pyrrole, and pyrazines	Lazazzara et al., 2017

Long-range	*L. enzymogenes* ISE13	Emission of VOCs such as 2,5-dimethylpyrazine	Sang et al., 2011
Long-range	*L. capsici* AZ78	Emission of VOCs such as pyrazines and ammonia	Vlassi et al., 2020a,b
Intermediate-range	*L. capsici* AZ78	Production of HSAF; cyclic lipodepsipeptides	Brescia et al., 2021
Intermediate-range	*L. enzymogenes* B25	Production of extracellular lytic enzymes (e.g., chitinases, proteases)	Martínez-Servat et al., 2023
Intermediate-range	*L. enzymogenes* C3	Production of HSAF; production of cyclic lipodepsipeptides	Li et al., 2009
Intermediate-range	*L. capsici* YS1215	Production of gelatinases	Lee et al., 2015
Intermediate-range	*L. enzymogenes* LE16	Production of cyclic lipodepsipeptides	Chen et al., 2020
Intermediate-range	*L. capsici* AZ78	Production of diketopiperazines such as cyclo(L-Pro-L-Tyr)	Puopolo et al., 2014a; Cimmino et al., 2021
Intermediate-range	*L. enzymogenes* OH11 and *L. gummosus* OH17	Production of extracellular lytic enzymes (e.g., proteases, cellulases, and glucanases)	Zhao et al., 2021a
Intermediate-range	*L. enzymogenes* OH11	Production of HSAF	Yue et al., 2021

Intermediate-range	*L. enzymogenes* M497-1	Production of Lysocin E	Santiago et al., 2018
Intermediate-range	*L. antibioticus* HS124	Production of extracellular lytic enzymes (e.g., chitinase, β-1,3-glucanase, lipase, protease) and 4-hydroxyphenylacetic acid	Ko et al., 2009
Intermediate-range	*L. antibioticus* OH13	Production of myxin	Zhao et al., 2016
Direct antagonism	*L. enzymogenes* OH11	Twitching motility via T4P; wolf pack predation	Chen et al., 2018; Zhao et al., 2017b; Zhou et al., 2015
Direct antagonism	*L. capsici* AZ78	Twitching motility via T4P; repression of biofilm formation; induction of cell death mechanisms	Tomada et al., 2017

***HSAF: Heat Stable Antifungal Factor; T4P: Type IV Pili; VOCs: Volatile Organic Compounds**

1.6 *Lysobacter* spp. as new plant defense stimulators

Plants defend themselves against plant pathogens through two primary mechanisms: Systemic Acquired Resistance (SAR) and Induced Systemic Resistance (ISR). SAR is activated in response to virulent plant pathogens and relies on the SA pathway, accumulating pathogenesis-related proteins, thus providing long-lasting immunity. In contrast, ISR is triggered by beneficial microorganisms, such as rhizobacteria, and depends on the jasmonic acid (JA) and ethylene (ET) signalling pathways, which

prime defence-related genes of the plant (Reimer-Michalski and Conrath, 2016). The cross-talk among SA, JA, and ET pathways allows the plant to modulate its defences optimally, depending on the nature of the threat (Durrant and Dong, 2004; koorneef and Pieterse, 2008; Pieterse *et al*., 2012). Studies have demonstrated that *Lysobacter* spp., contributes significantly to plant health by inducing resistance mechanisms and promoting plant growth (Expósito *et al.*, 2015).

Lysobacter enzymogenes C3 is known for its ability to induce localized and systemic resistance responses in various crops. For instance, foliar application of heat-killed C3 cells in tall fescue and wheat plants induced resistance against *Rhizoctonia solani* and *Bipolaris sorokiniana*, respectively, without directly inhibiting the plant pathogens. Instead, *L. enzymogenes* C3 stimulated peroxidase activity in the plants, signalling a primed defence response that enhanced pathogen resistance (Kilic-Ekici and Yuen, 2003). In greenhouse experiments, *L. enzymogenes* C3 also effectively controlled FHB, caused by *F. graminearum*, in hard red spring wheat (Jochum *et al*., 2006). Moreover, *L. enzymogenes* C3 has been shown to activate all three major defence hormone pathways SA, JA, and ET in soybean plants. Foliar treatments with C3 upregulated key marker genes, such as Allene Oxide Synthase and Aminocyclopropane-1-carboxylate Synthase, involved in the JA and ET pathways, respectively (Walnut, 2019).

In a recent study, *L. enzymogenes* OH11 demonstrated its ability to induce expression of defence-related genes involved in both SA and JA signalling pathways in *Nicotiana benthamiana* plants infected with the oomycetes *P. capsici* and *P. sojae*. The findings suggested that T4P on *L. enzymogenes* OH11 is essential in eliciting immune responses upon initial contact with the plant surface, similar to how flagellin functions in flagellated bacteria. This indicates that *Lysobacter* spp., not only primes the plant's defences but also helps coordinate a multifaceted immune response against pathogen attacks (Lin *et al*., 2023 b).

1.7 *Lysobacter* spp. as critical agents in soil suppressiveness: case studies and antagonism to soilborne plant pathogenic (micro)organisms

1.7.1 Effectiveness against soilborne plant pathogenic fungi and oomycetes

Several studies have showcased the antagonistic abilities of *Lysobacter* spp. strains against a range of soilborne plant pathogenic fungi and oomycetes. For example, *L. enzymogenes* C3 exhibits potent biocontrol activity against *P. ultimum*, as evidenced by clear antimicrobial zones on 10% tryptic soy agar (Kobayashi *et al*., 2005). Additionally, *L. enzymogenes* C3 produced β-1,3-glucanases, critical enzymes for breaking down plant pathogen cell walls. Mutant strains lacking these enzymes displayed reduced antagonistic activity against *B. sorokiniana* and *P. ultimum* (Kobayashi *et al.*, 2005). In tomato seedlings experiments, *L. enzymogenes* C3 effectively improved seedling emergence in soil infested with *P. ultimum*. Conversely, the *clp*-disrupted mutant strains did not show any significant difference in seedling emergence compared to the control, highlighting the importance of the *clp* gene in the biocontrol efficacy of *L. enzymogenes* C3 (Kobayashi *et al.*, 2005). In other *in vitro* tests, *L. enzymogenes* 3.1T8 produced surface-active compounds and low-molecular-weight metabolites that immobilized zoospores and inhibited cyst germination of *P. aphanidermatum*, which causes root and crown rot in cucumber (Folman *et al.*, 2004). *Lysobacter firmicutimachus* 5-7 showed relevant antagonistic activity against *P. arrhenomanes,* a root rot pathogen in rice seedlings. Culture filtrates from *L. firmicutimachus* 5-7 significantly reduced hyphal growth, sporangium formation, and zoospore germination of *P. arrhenomanes* (Tu *et al*.,2023). Furthermore, *L. enzymogenes* OH11 exhibited enhanced twitching motility and increased HSAF production in response to the presence of *P. aphanidermatum* (Zhao *et al.*, 2017b). *L. enzymogenes* OH11 also exhibited vigorous antifungal activity against several soilborne fungi, including *F. oxysporum*, *F. solani*, *P. capsici*, *P. aphanidermatum*, *R. solani*, *Rhizopus stolonifer*, and *S sclerotiorum*, (Qian *et al.*, 2009).

The *in vitro* antifungal activity of *L. capsici* AZ78 was tested using the classic dual-culture method and split Petri-dishes. In both assays, *L. capsici* AZ78 was able to significantly inhibit the mycelial growth of the highly important soilborne plant pathogens *P. ultimum*, *R. solani*, and *S. minor* (Puopolo *et al*., 2016; Vlassi *et al*., 2020 a,b).

In another *in vitro* study, *L. capsici* SB-K88 effectively suppresses *Aphanomyces cochlioides*, the causal agent of damping-off disease in sugar beet and spinach. The bacterium's supernatant and metabolite xanthobaccin A effectively immobilized zoospores with a minimum inhibitory concentration of 0.01 μg/ml. Seeds pre-treated with xanthobaccins A exhibited significant disease suppression, reducing preemergence damping-off in sugar beet seedlings. (Nakayama *et al.*, 1999; Islam *et al.*, 2005).

Greenhouse experiments have further validated *Lysobacter*'s biocontrol capabilities. For instance, *L. antibioticus* HS124 demonstrated significant efficacy against *P. capsici*, a major pathogen of pepper plants. This bacterial strain controlled significantly *P. capsici* and enhanced pepper plant growth in greenhouse (Ko *et al.*, 2009). Similarly, *L. capsici* PG4, isolated from the rhizosphere of tobacco plants, effectively reduced the disease incidence of tomato crown rot caused by *F. oxysporum* f. sp. *radicis-lycopersici* in both *in-vitro* and greenhouse settings (Puopolo *et al*., 2010).

Multiple studies have shown that the abundance of *Lysobacter* spp. in soil reduced disease caused by different fungal plant pathogens. Examples include a study in organic farms of the Netherlands by Postma *et al*. (2008), where soil suppressiveness against three soilborne pathogens (*R. solani* in sugar beet, *Streptomyces scabies* in radish, and *Verticillium longisporum* in oilseed rape) was evaluated alongside microbial, chemical, and physical soil properties. The results indicated that suppression of *R. solani* was notably linked to the presence of antagonistic *Lysobacter* spp., particularly *L. antibioticus* and *L. gummosus*. Grass-clover fields were especially effective in promoting *R. solani*

suppression by enhancing the abundance of *Lysobacter* spp. in clay soils. These findings highlight that *Lysobacter* spp. plays a significant role in soil disease suppressiveness, particularly in organic systems. Another study investigated four *Lysobacter* strains from clay soils in the Netherlands, which were closely related to *L. antibioticus, L. gummosus*, and *L. capsici*. DNA-DNA hybridization confirmed these strains as *L. capsici*, though phenotypic and DNA fingerprinting analyses indicated considerable diversity and niche specialization within this species. Notably, the new *L. capsici* strains showed strong suppression of *R. solani* AG2 and were found in soils naturally suppressive to *Rhizoctonia*, where *L. antibioticus* and *L. gummosus* were also present (Postma *et al*., 2010a).

Additionally, Postma *et al* (2010b) investigated two soils: one with a 40-year cauliflower history naturally suppressive to *R. solani*, and another soil with no recent cauliflower history conducive. Interestingly, over five successive cauliflower cropping cycles, disease suppressiveness developed in the initially conducive soil, especially when inoculated repeatedly with *R. solani*. This suppressiveness was biological, as it disappeared after soil sterilization. The suppressive soil was found to have a high proportion of bacteria that inhibited *R. solani in vitro*, including *Lysobacter* (56%) spp., *Streptomyces* (23%) spp., and *Pseudomonas* (21%) spp. *Lysobacter* spp. were particularly associated with suppressiveness, as shown by quantitative PCR, which indicated a larger *Lysobacter* population in the suppressive cauliflower soil compared to the conducive soil. The results suggest that successive planting of cauliflower and *R. solani* inoculation enhances disease suppressiveness, with *Lysobacter* spp. likely playing a key role in the biological control of *R. solani* through antagonistic activity (Postma *et al*., 2010b).

Zhang *et al.* (2020) showed that *Lysobacter* spp. introduced as probiotic consortia with other compatible microbes (*Bacillus* spp. and *Pseudomonas* spp.) improved the nutrient composition in the

rhizosphere of *Panax notoginseng* with a notable and remarkable suppression of the plant pathogen *F. oxysporum*.

Eighteen *Lysobacter* strains, including eleven isolated from Rhizoctonia-suppressive soils, were evaluated for their antifungal and plant growth-promoting activities. Based on 16S rRNA gene sequencing, these strains were classified into four species: *L. antibioticus*, *L. capsici*, *L. enzymogenes*, and *L. gummosus*. Among the selected strains most of them demonstrated significant *in vitro* antagonistic activity against *R. solani*, *P. ultimum*, and *F. oxysporum*. However, they showed less suppression towards *R. solani* in sugar beet and cauliflower when introduced into soil. This limited efficacy may be attributed to poor rhizosphere colonisation under field conditions. (Expósito *et al.*, 2015).

Field trials are still relatively limited for *Lysobacter* strains, but promising results have been observed. A study on soils treated with bio-organic fertilizers found that the abundance of *Lysobacter* spp. was six times higher than that of soils treated with chemical fertilizers. These soils exhibited enhanced suppressiveness against Fusarium wilt in vanilla plants (Xiong *et al.*, 2017).

Fu *et al*. (2017) studied the different composition of microbiome in biofertilizer and compost treated banana fields, showing the symptoms of Fusarium wilt. As a result, it was discovered that the abundance of *Lysobacter* spp. was negatively correlated to the abundance of the pathogen *F. oxysporum*.

Recently, Dai *et al*. (2023) investigated the effects of maize plants grown from seeds treated with *L. antibioticus* 13-6 on soil properties, plant growth, and rhizosphere microbiome composition. *In vivo* experiments demonstrated a positive effect on plant growth parameters and successful colonisation of the mBCA in the rhizosphere of treated plants. The treatment also altered the rhizosphere microbiome,

recruiting beneficial organisms and reducing negative microbial interactions. These findings highlight the potential of *Lysobacter* spp. as a sustainable strategy for controlling soil-borne plant pathogenic fungi and promoting plant health.

This indicates that *Lysobacter* spp. likely contributes to disease suppression in soil, potentially by interacting with other beneficial microbes, such as *Bacillus* spp. and *Trichoderma* spp., to enhance overall biocontrol efficacy (Table 2).

Table 2. Biocontrol activity of *Lysobacter* spp. against different plant pathogenic (micro)organisms in greenhouse and field conditions.

Microbial biocontrol agent	Plant pathogenic (micro)organism	Plant diseases	Modes of action	References
Lysobacter enzymogenes C3	*Heterodera schachtii*	Sugar beet cyst nematode	Production of HSAF*	Yuen et al., 2018
	Heterodera glycines	Soybean cyst nematode		
Lysobacter enzymogenes B25	*Meloidogyne* spp.	Root-knot nematode	Production of extracellular lytic enzymes and twitching motility	Martínez-Servat et al., 2023
Lysobacter spp.	*Pratylenchus neglectus*, *Meloidogyne chitwoodi*	Root-lesion and root-knot nematodes	Rhizosphere colonisation	Castillo et al., 2017

Lysobacter spp.	*Meloidogyne javanica*, *Pratylenchus brachyurus*	Root-knot nematode	Enhancement of soil microbial diversity and richness	do Rêgo Barros et al., 2022
Lysobacter antibioticus 13-6	*Meloidogyne spp.*	Root-knot nematode	Rhizosphere colonisation	Zhou et al., 2016
Lysobacter spp. strain YFY 02, 13-1, and HY	*Plasmodiophora brassicae*	Clubroot in cruciferous plants	Production of extracellular lytic enzymes	Zhou et al., 2014
Lysobacter capsici ZST1-2			Production of toxic secondary metabolites	Fu et al., 2018
Lysobacter spp.	*Streptomyces* spp.	Common potato scab	Rhizosphere colonisation	Rosenzweig et al., 2012
Lysobacter spp.	*Ralstonia solanacearum*	Bacterial wilt of tobacco	Rhizosphere colonisation	Li et al., 2023
Lysobacter enzymogenes C3	*Pythium ultimum*	Tomato damping-off	Production of β-1,3-glucanases	Kobayashi et al., 2005
Lysobacter capsici PG4	*Fusarium oxysporum* f. sp. *radicis-lycopersici*	Tomato crown rot	Production of lytic enzymes and rhizosphere colonisation	Puopolo et al., 2010

Lysobacter spp.	*Rhizoctonia solani*	Sugar beet damping-off	Rhizosphere colonisation	Postma et al., 2008
Lysobacter spp.	*Rhizoctonia solani*	Cauliflower root rot	Rhizosphere colonisation	Postma et al., 2010b
Lysobacter spp.	*Fusarium oxysporum*	*Panax notoginseng* Fusarium wilt	Influence on rhizosphere nutrient composition and rhizosphere colonisation	Zhang et al., 2020
Lysobacter spp.	*Fusarium oxysporum*	Vanilla Fusarium wilt	Rhizosphere colonisation	Xiong et al., 2017
Lysobacter antibioticus 13-6	*Fusarium oxysporum*	Fusarium wilt in maize	Rhizosphere colonisation and recruitment of plant beneficial microbes	Dai et al., 2023

***HSAF: Heat Stable Antifungal Factor.**

1.8 Understanding *Lysobacter*'s acclimatization process in different soil types

1.8.1 Influence of soil composition

Soil pH is pivotal in shaping microbial communities, including *Lysobacter* spp. In fact, *Lysobacter* species, particularly *L. antibioticus* and *L. gummous*, were predominantly found in clay soils with a higher pH, contributing to the suppression of *R. solani* AG2-2IIIB in sugar beet crops (Postma *et al*., 2008). These findings are supported by research showing that *Lysobacter* populations are more abundant in soils with higher pH, clay content, and a lower carbon-to-nitrogen (C/N) ratio. (Postma,

Schilder and van Hoof, 2011). In contrast, *Lysobacter* was rarely detected in sandy soils with lower pH levels, indicating that acidic conditions may hinder its proliferation. This is further reinforced by data from Craibstone Experimental Farm in Scotland, where *Lysobacter* sequences were identified exclusively in medium- and high-pH clusters but absent in low-pH soils (Bartram *et al.*, 2014). The analysis of 206 agricultural sites in northeastern China consistently indicated soil pH as the primary factor influencing microbial diversity, including the distribution of *Lysobacter* spp. (Wang *et al*., 2019).

Soil nutrient availability has a notable effect on *Lysobacter* spp. populations. In tobacco fields where pea, rapeseed, and wheat were used as cover crops, a positive correlation was observed between *Lysobacter* populations, organic matter, and nitrate nitrogen levels (Qi *et al.*, 2020).

Root exudates are another critical factor in shaping the soil microbiome and influencing *Lysobacter* spp. populations. These exudates, which include compounds like glucose, glycine, and citric acid, serve as substrates for microbial growth and play a key role in microbial assembly around the root zone (Hu *et al.*, 2018). For example, in soils cultivated with grass-clover crops, *Lysobacter* spp. isolates were more abundant, indicating that root exudates from specific plants can enhance the presence of *Lysobacter* spp. (Postma *et al.*, 2008). Moreover, the use of millet as a cover crop was found to strengthen *Lysobacter* populations, even in soils with high organic carbon and nitrogen content, suggesting a special relationship between certain crops and *Lysobacter* spp. (Xu et al., 2019).

Intercropping faba bean and maize significantly increased total crop yields and nitrogen fixation compared to monoculture. Using ^{13}C-DNA-SIP, it was observed that maize root exudates activated nine key bacterial genera in the faba bean rhizosphere, including *Lysobacter* spp., which directly fix nitrogen. This bacterium along with others promoted the expression of key genes in faba bean roots, facilitating nitrogen fixation and productivity (Hu et al., 2021).

Furthermore, it was seen that foliar application of nitrogen-doped carbon dots on maize significantly enhanced seedling biomass and photosynthesis. This treatment increased organic acid production, which were then secreted into the rhizosphere. Over time, these organic acids helped attract beneficial rhizobacteria, including *Lysobacter* spp., which showed a marked increase in relative abundance after one week of exposure. The enriched *Lysobacter* spp. and other beneficial microbes supported nitrogen and phosphorus cycling in the soil, thereby boosting nutrient uptake and contributing to maize growth (Yue *et al.*, 2023).

1.9 Integration with soil amendments

Soil amendments play a critical role in enhancing *Lysobacter* spp. populations and their disease-suppressive capabilities. Organic amendments, such as animal and green manure, compost, and peats, influence soil properties like structure, nutrient availability, and microbial ecology, promoting the growth of beneficial microbes (Bonanomi *et al.*, 2010). For instance, Postma and Schilder (2015) demonstrated that organic amendments such as chitin, yeast, fungal tissue, and protein-rich animal waste stimulated *Lysobacter* spp. populations, significantly improving the soil's suppressiveness against *R. solani* in sugar beet. Interestingly, other studies found that amendments, like spent mushroom substrate, led to an increase in populations of *Lysobacter* spp., *Pseudomonas* spp., and *Bacillus* spp., and were correlated with reduced incidence of Fusarium wilt in cucumber (Wang et al., 2020b).

In an experiment, it was seen that applying vermicompost, biochar, and their combination following soil sterilization effectively controlled Fusarium root rot in replanted American ginseng. The combined treatment significantly boosted the abundance of beneficial bacteria in the soil, particularly *Pseudomonas* spp., *Lysobacter* spp., *Variibacter* spp., and *Chryseolinea* spp. Vermicompost was found to enhance the presence of beneficial bacteria in the rhizosphere, while

biochar inhibited the degradation of phenolic acids. The increased abundance of these beneficial bacteria was negatively correlated with the disease index of the pathogen. (Tian *et al.*, 2021).

Wang *et al*. (2024) demonstrated that applying modified biochar significantly reduces root rot incidence and enhances rhizospheric soil quality. The biochar application improved soil aeration and positively impacted bacterial abundance, leading to notable improvements in the soil's physicochemical properties. Beneficial bacteria, including *Lysobacter* spp., became more abundant, contributing to suppression of harmful microbial groups such as *Bacteroidetes*, *Ascomycota*, and *Fusarium*. This study underscores the role of modified biochar in fostering a healthier soil microbiome that supports plant health and resilience.

Additionally, *Lysobacter* spp. plays a unique role in the decomposition of organic matter. In a study by Fu *et al*., (2022) when straw was used as an amendment in maize fields, *Lysobacter* spp. contributed to straw breakdown and increased its predatory behaviour on plant pathogens, enhancing plant health. This highlights *Lysobacter* spp. ability to function in organic matter degradation and plant pathogen suppression, making it a versatile agent in agricultural soils.

Moreover, dissolved organic matter extracted from fresh chicken manure and mature compost has been demonstrated to increase *Lysobacter* spp. when applied to the soil (Yang *et al*., 2024). Furthermore, in a recent study, co-compost of swine manure, human excrement, and rice straw fertilization increased soil quality and the relative abundance of *Lysobacter* spp. in soil previously treated with nitrogen fertilizers (Gao *et al.*, 2024). These studies implore the possible replacement of current fertilizers with beneficial mBCAs in the plant rhizospheric soil.

CHAPTER 2. AIM OF THE THESIS

Building on the knowledge described above, the overall aim of this PhD research was to gain deeper insight into the anti-oomycete activity of *Lysobacter capsici* AZ78 and to elucidate its role in biological control and integrated pest management strategies. Therefore, the study was structured around three main objectives:

Objective 1: To evaluate the biocontrol activity and mode of action of viable and heat-treated *Lysobacter capsici* AZ78 cells, as well as their derived polycyclic tetramate macrolactams, against the foliar oomycete pathogens *Plasmopara viticola* and *Peronospora belbahrii* (chapter 3).

Objective 2: To assess the biocontrol efficacy of unheated and heat-treated self-digestive solutions derived from *Lysobacter capsici* AZ78 against *Plasmopara viticola* in grapevine plants, and to investigate pathogen-induced responses in grapevine through gene expression analysis and phytoalexin accumulation (chapter 4).

Objective 3: To evaluate the biocontrol potential of *Lysobacter capsici* AZ78 against the soil-borne pathogen *Pythium ultimum* under soil conditions, and to characterize changes in the soil microbiome associated with bacterial application using omics-based approaches (chapter 5).

CHAPTER 3.

HEAT-INACTIVATED *LYSOBACTER CAPSICI* AZ78 CELLS AND THEIR POLYCYCLIC TETRAMATE LACTAMS EFFECTIVELY CONTROL DIRECTLY AND INDIRECTLY *PERONOSPORA BELBAHRII* AND *PLASMOPARA VITICOLA*.

Amulya Jain Dinesh Kothari[1,2*], Stefano Nadalini[1,2*], Linda Lucii[1,2], Nina Desiato[1,2], Jesus Garcia Zorilla[4], Marco Masi[3], Alessio Cimmino[3], Ilaria Pertot[1,2], Gerardo Puopolo[1,2]

[1]*Center Agriculture Food Environ. (C3A), University of Trento, Via E. Mach 1,38098 San Michele all'Adige, Italy*

[2]*Research and Innovation Centre, Fondazione Edmund Mach, Via E. Mach 1, 38098 San Michele all'Adige, Italy*

[3]*Department of Chemical Sciences, University of Naples Federico II, 80126 Naples, Italy*

[4]*Allelopathy Group, Department of Organic Chemistry, Facultad de Ciencias, Institute of Biomolecules (INBIO), University of Cadiz, C/Avenida República Saharaui, s/n, 11510 Puerto Real, Spain*

Published on **European Journal of Plant Pathology**, 2026, https://doi.org/10.1007/s10658-026-03207-4.

Abstract

The bacterial strain *Lysobacter capsici* AZ78 is an effective biocontrol agent against several plant-pathogenic oomycetes. This study demonstrates that heat-inactivated *L. capsici* AZ78 cells retain strong protective activity against *Plasmopara viticola* and *Peronospora belbahrii*, comparable to that of viable *L. capsici* AZ78 cells, as well as a copper-based fungicide and a plant resistance inducer. Microscopic analyses showed that both heat-inactivated and viable *L. capsici* AZ78 cells were toxic to *P. viticola* sporangia. Moreover, microscopic analyses revealed also their ability to induce callose deposition and reactive oxygen species production in basil and grapevine leaves, indicating the stimulation of plant resistance mechanisms. Chemical analyses led to the identification of dihydromaltophilin and maltophilin, two heat-stable polycyclic tetramate macrolactams, within the membranes of *L. capsici* AZ78 cells. Isolated dihydromaltophilin and maltophilin, individually or in combination, were highly effective against *P. viticola* and triggered callose accumulation in grapevine leaf discs. These findings demonstrate that *L. capsici* AZ78 and its heat-stable polycyclic tetramate macrolactams act through a dual mechanism, direct antimicrobial activity and induction of plant defence responses. The use of heat-inactivated *L. capsici* AZ78 cells and their secondary metabolites offers a promising, environmentally friendly alternative to copper-based products for the sustainable management of downy mildews.

Keywords: *Lysobacter,* Downy mildew, Biocontrol, Polycyclic Tetramate Macrolactams, Dihydromaltophilin.

3.1 Introduction

In the field, crop plants have to face diverse biotic and abiotic stresses continuously. Among these, plant diseases caused by (micro)organisms represent a major factor contributing to global yield losses and pose a serious threat to agricultural production (Savary *et al*., 2019). To sustain and improve crop plant productivity, it is therefore crucial to develop strategies that effectively manage plant pathogenic (micro)organisms. Given the environmental and regulatory concerns associated with the chemical input in agriculture, there is an increasing interest in environmentally friendly and

sustainable approaches for detecting and controlling plant pathogenic (micro)organisms (Helepciuc and Todor, 2022; Song and Liu, 2025).

One promising strategy involves the use of microbial biopesticides, plant protection products that employ microbial BioControl Agents (mBCAs) as active ingredients. These are effective in controlling plant pathogenic (micro)organisms, promote plant growth, and improve nutrient uptake (Ray et al., 2020). Interest in microbial biopesticides has grown rapidly, with 13 bacterial mBCAs already authorised for commercial use in the European Union (https://food.ec.europa.eu/plants/pesticides/eu-pesticides-database_en). The efficacy of mBCAs largely depends on their ability to produce a wide array of secondary metabolites, including lytic enzymes, siderophores, toxins, volatile organic compounds (VOCs), polyketides, and non-ribosomal peptides (Sarrocco, 2023). For example, *Bacillus subtilis* can suppress the growth of several plant-pathogenic (micro)organisms through the production of secondary metabolites (Kiesewalter *et al*., 2021). Similarly, certain secondary metabolites produced by *Pseudomonas* spp. exhibit antagonistic activity against bacteria, fungi, and oomycetes (Raio and Puopolo, 2021). Furthermore, secondary metabolites extracted from *Trichoderma* spp. are often more effective as plant protection products than the organisms themselves (Vinale *et al*., 2009). Plants have also evolved mechanisms to recognise mBCAs and their bioactive compounds, thereby enhancing their capacity to resist pathogen attacks by triggering plant resistance mechanisms (Hönig *et al*., 2023). In particular, cyclic lipopeptides such as orfamide and surfactins, produced respectively by plant-beneficial *Pseudomonas* spp. and *Bacillus* spp., can be perceived by plants and stimulate defence mechanisms against plant-pathogenic (micro)organisms (Nimbeshaho *et al*., 2024; Omoboye *et al*., 2019).

Within this context, the genus *Lysobacter* (family Lysobacteraceae) has emerged as an important reservoir of mBCAs and secondary metabolites. They are well recognised for their ability to produce a broad spectrum of antimicrobial compounds, enabling them to prey on other

microorganisms, particularly plant pathogenic (micro)organisms (Puopolo *et al*., 2018; Meers *et al*., 2018; Vlassi *et al*., 2020a). Among the most significant secondary metabolites are polycyclic tetramate macrolactams (PTMs), produced by many *Lysobacter* species (Li *et al*., 2021; Liu *et al*., 2022). One such PTM is dihydromaltophilin (DMP), also known as the heat-stable antifungal factor (HSAF) due to its stability at high temperatures, which exhibits a unique mode of action. Chemically, DMP is classified as a polycyclic macrolactam a structural motif common among natural bioactive products containing a tetramic acid, a class of compounds known for their antibiotic and anticancer properties (Schobert and Schlenk, 2008).

DMP was first isolated from *Streptomyces* sp. (Graupner *et al*., 1997) and later identified in *L. enzymogenes* C3, where it demonstrated antagonistic activity against plant-pathogenic fungi (Li *et al*., 2006). It exerts its antifungal activity by targeting specific sphingolipids that are essential for polarized filament growth in fungal cells. Studies have demonstrated the negative impact of this molecule on various fungi, including *Alternaria alternata*, *Aspergillus nidulans*, and *Candida albicans* (Ding *et al*., 2016; He *et al*., 2018; Li *et al*., 2006). Notably, DMP was found to disrupt fungal growth via a reactive oxygen species (ROS)-dependent pathway in *C. albicans*, and its unique and selective mode of action makes it highly suitable for the sustainable control of plant-pathogenic fungi. Specifically, DMP from *L. enzymogenes* C3 (previously identified as *Stenotrophomonas maltophilia* C3) inhibited the growth of plant-pathogenic fungi such as *Bipolaris sorokiniana* and *Uromyces appendiculatus* (Yuen *et al*., 2001; Zhang and Yuen, 1999), as well as oomycetes like *Pythium ultimum* (Kobayashi *et al*., 2005). In another study, DMP isolated from *L. enzymogenes* OH11 protected pear fruit against fungal decay caused by *Colletotrichum fruticola*. The protection was attributed to hyphal deformation and depolarisation, along with inhibition of conidial germination (Li *et al*., 2021). Similarly, Liu *et al*. (2022) reported that DMP from *L. enzymogenes* OH11 inhibited the growth of *Neurospora crassa* by activating fungal genes involved in cell wall formation. Additionally, crude DMP extracts from *L.*

enzymogenes OH11 showed efficacy in managing Fusarium head blight (Zhao *et al*., 2019) and suppressing *Pythium graminicola* in maize (Ren *et al*., 2020).

Recent studies have further provided insight into the delivery mechanisms of these bioactive PTMs. DMP and other secondary metabolites are transported via outer-membrane vesicles (OMVs), which facilitate long-distance delivery to target plant pathogenic fungi (Yue *et al*., 2021). This vesicle-mediated mechanism has also been reported in *L. enzymogenes* C3, highlighting its relevance as a general strategy in *Lysobacter*–plant pathogen interactions. Specifically, DMP comes into contact with the outer membranes of *L. enzymogenes* C3 cells, from which it is released into the environment, entrapped in OMVs, until it establishes physical contact with plant-pathogenic fungi, thereby inhibiting their growth (Meers *et al*., 2018).

Among *Lysobacter* biocontrol agents, *L. capsici* AZ78 (AZ78) exhibits strong antagonistic activity against several economically important plant pathogens, including *Phytophthora infestans* and *Plasmopara viticola*, the causal agents of potato late blight and grapevine downy mildew, respectively (Puopolo et al., 2014a, b). The biocontrol efficacy of AZ78 is associated with its production of multiple antagonistic factors, such as ammonia, antibiotics, lytic enzymes, and VOCs (Brescia *et al*., 2021; Puopolo *et al*., 2014a; Vlassi *et al*., 2020a, b). Metabolomic analyses confirmed the presence of PTMs, notably DMP and its precursor maltophilin (MP), both of which exhibit potent activity against plant pathogens (Brescia *et al*., 2021). However, although these secondary metabolites have been identified in AZ78, their role in the control of plant pathogenic oomycetes and their underlying mode of action remain poorly understood.

3.2 Aim of the work

To address this knowledge gap, we investigated whether the application of heat-inactivated AZ78 cells and the PTMs: DMP and MP could be effective in controlling *P. viticola* and *Peronospora*

belbahrii, the causal agent of grapevine and basil downy mildews, respectively. Based on the results, we examined the mechanisms involved in the control of both oomycetes through the application of heat-inactivated AZ78 cells and assessed the role of PTMs in these processes. Overall, this study provides new insights into the multifaceted mechanisms of AZ78-mediated plant protection and highlights the potential of heat-inactivated AZ78 cells and their PTMs as promising components of next-generation microbial biopesticides.

3.3 Material and methods

3.3.1 Maintenance of bacterial strains

AZ78 and *Escherichia coli* DH5α (DH5α) were stored as 40% (v/v) glycerol stocks at −80 °C. For routine culture, both bacterial strains were grown on Nutrient Agar (NA) in 90 mm Petri dishes and incubated for 48 h at 27 °C. To prepare bacterial cell suspensions, the Petri dishes were flooded with 5 mL of sterile distilled water, and the cells were gently scraped from the surface using sterile L-shaped spatulas. The resulting cell suspensions were homogenised in sterile distilled water. The absorbance at 600 nm was adjusted to 0.1, corresponding to approximately 1×10^8 colony-forming units (CFU)/mL, using a spectrophotometer (UV-2450, Shimadzu, Kyoto, Japan) (Puopolo *et al*., 2014b). This bacterial cell concentration was used in all experiments unless otherwise specified.

3.3.2 Preparation of heat-inactivated bacterial cells

AZ78 and DH5α cell suspensions were transferred into sterile 15 mL centrifuge tubes and exposed to a thermal shock at 90 °C for 20 min using a thermo-mixer (T-shaker EMS100 Euro Clone, IT), followed by incubation at -20 °C for five minutes (Brescia *et al*., 2021). After the thermal shock, cell viability was assessed by spot-inoculating 100 µL of each bacterial cell suspension onto NA. Once inoculated, Petri dishes were incubated at 27 °C. After 72 h of incubation, the occurrence of colonies was visually assessed. Five Petri dishes were prepared for each treatment.

3.3.3 Plants and respective plant pathogenic oomycetes

Sweet basil (*Ocimum basilicum* L.) plants were cultivated from seeds (cv. Italiano classico, Franchi Sementi, Italy) in a 1:1 (v/v) mix of peat and vermiculite in 0.5 L pots under controlled conditions (25 ± 1 °C, 70 ± 10% relative humidity (RH), and a 16/8 h day/night photoperiod) until

they reached the 8–10 leaf stage. *Peronospora belbahrii*, originally isolated from diseased basil plants in a local garden, was maintained by manually spraying the sporangial suspension onto both leaf surfaces until runoff occurred. Following inoculation, the plants were placed in a humid chamber (100% RH, 20 °C) to promote infection. After 20 h, basil plants were transferred to a growth chamber at 25 ± 1 °C, 70 ± 10% RH, and a 16/8-h day/night light regime to facilitate *P. belbahrii* colonisation. Six days post-inoculation (dpi), the plants were placed in the humid chamber at 20 ± 1 °C and 100% RH in darkness for 20 h to induce sporulation (Cohen and Rubin, 2015). To prepare *P. belbahrii* inoculum, diseased, chlorotic basil leaves bearing sporangia on the abaxial surface were harvested and rinsed with distilled water. The resulting sporangial suspension was filtered through cheesecloth to remove plant debris, and the sporangial concentration was adjusted to 1×10^5 sporangia/mL using a haemocytometer under a light microscope (Gilardi *et al*., 2013). This sporangial concentration was used in all experiments unless otherwise specified.

Vitis vinifera cv. Pinot Noir grapevine plants, grafted onto Kober 5BB rootstock, were grown in 2.5 L pots containing a 3:1 (v/v) mixture of peat and pumice in a greenhouse (20 ± 0.5 °C, 70 ± 10% RH) for 60 days, until the plants produced two shoots with at least nine leaves each. *Plasmopara viticola*, originally isolated from an untreated vineyard in San Michele all'Adige (Italy) in 2024, was maintained on healthy grapevine plants through weekly inoculations according to Puopolo *et al*. (2014b) under controlled conditions (20 ± 0.5 °C, 70 ± 10% RH). Briefly, grapevine plants showing oil-spot symptoms were kept overnight in the dark at 20 ± 0.5 °C and 100% RH. The inoculum was then prepared by rinsing sporulating lesions on the abaxial leaf surface with cold (4-5 °C) distilled water and adjusting the concentration to 2.5×10^5 sporangia/mL by counting under a light microscope using a haemocytometer. This sporangial concentration was used in all experiments unless otherwise specified.

3.3.4 Assessment of the efficacy of heat-treated and viable Lysobacter capsici *AZ78 cells in controlling* Plasmopara viticola *on grapevine leaf discs*

To prepare grapevine leaf discs, the third and fourth leaves from the top of healthy grapevine plants were collected and used to cut 12 mm discs using a cork borer. These discs were placed with the abaxial side facing upwards in 90 mm Petri dishes containing three layers of absorbent paper soaked in 8 mL of sterile distilled water to prevent the discs from drying out.

Once prepared, the grapevine leaf discs were sprayed with the following treatments: 1) sterile distilled water (untreated control); 2) copper-based fungicide Coprantol Hi Bio (copper hydroxide 20%, Syngenta; 2 g/L solution); 3) resistance inducer BION 50 WG (benzothiadiazole-7-carbothioic acid S-methyl ester 50%, Syngenta; 50 mg/L); 4) viable AZ78 cells; 5) heat-inactivated AZ78 cells; 6) viable DH5α cells; and 7) heat-inactivated DH5α cells. All treatments were applied manually using a nebuliser until complete runoff, followed by a five-minute drying period under a chemical fume hood. Petri dishes were then transferred to the greenhouse at 20 ± 0.5 °C.

After 24 h, the leaf discs were sprayed with *P. viticola* sporangial suspension (2 mL per Petri dish) and kept in darkness at 20 ± 0.5 °C and 80-99% RH overnight. Subsequently, the leaf discs were incubated for six days in a greenhouse at 25 ± 1 °C and 70-80% RH (Brescia *et al*., 2021). Disease severity (percentage of abaxial leaf area covered by sporulating lesions) was evaluated at seven dpi according to the EPPO standard scale (2004) and expressed as a percentage. Each treatment consisted of five Petri dishes containing five leaf discs, and the experiment was repeated.

3.3.5 Evaluation of the efficacy of heat-inactivated and viable Lysobacter capsici *AZ78 cells in controlling* Peronospora belbahrii *and* Plasmopara viticola in planta

Regarding efficacy against P. viticola, viable and heat-inactivated AZ78 cells were applied to both leaf surfaces of grapevine plants grown in the greenhouse using a hand sprayer. The treatments

applied were: 1) sterile distilled water (untreated control); 2) copper-based fungicide (Coprantol Hi Bio, 2 g/L); 3) viable AZ78 cells; and 4) heat-inactivated AZ78 cells. Once treated, grapevine plants were maintained at 25 □} 0.5 °C and 60–80% RH with a 16/8 h day/night light regime. After 24 h, *P. viticola* sporangial suspension was uniformly sprayed onto the abaxial surfaces of fully expanded grapevine leaves using a hand sprayer. Subsequently, the plants were incubated in the dark at 20 ± 0.5 °C and 80–99% RH for 24 h, followed by maintenance at 25 °C (60–80% RH) under a 16/8 h day/night regime. After six days, the plants underwent an overnight dark incubation at 20 ± 0.5 °C and 80–99% RH to induce sporulation (Puopolo *et al*., 2014b). Disease severity was evaluated at seven dpi using the EPPO standard scale (EPPO, 2004). Each treatment was applied to five plants (replicates), and the experiment was repeated three times. For efficacy against *P. belbahrii*, viable and heat-inactivated AZ78 suspensions were applied to basil plants. The treatments were: 1) sterile distilled water (untreated control); 2) copper-based fungicide Cuprotax S.D.I. (copper sulfite 15.20%, Sipcam; 0.594 mL/L) (Gilardi *et al*., 2020); 3) viable AZ78 cells; and 4) heat-inactivated AZ78 cells. Treatments 3 and 4 were used at an absorbance of 0.4 at 600 nm, corresponding to 1×10^9 CFU/mL. The treatments were applied using a hand sprayer (5 mL per plant), and the plants were maintained under controlled greenhouse conditions at 25 ± 1 °C (60–80% RH) with a 16/8 h day/night light regime. After 24 h, each plant was sprayed with *P. belbahrii* sporangial suspension (5 mL per plant) and transferred to a humid chamber set at 100% RH and 20 ± 0.5 °C for 20 h. Subsequently, the plants were moved to a greenhouse chamber at 25 ± 1 °C (60–80% RH) with a 16/8 h day/night regime. Six dpi, the plants were again placed overnight in a humid chamber at 100% RH (Cohen and Rubin, 2015). After seven days, disease severity was assessed on eight leaves per plant using a 0–100 scale, where 0 represented no symptoms and 100 indicated complete coverage of the leaf surface by sporulating lesions. Lower leaves were excluded from the evaluation (Elad *et al*., 2016). Each treatment was applied to five plants (replicates), and the experiment was repeated three times.

3.3.6 Determination of the ability of heat-inactivated and viable Lysobacter capsici AZ78 cells to stimulate the deposition of callose and accumulation of reactive oxygen species in basil and grapevine leaves

For the visualization of callose accumulation and ROS production, basil and grapevine leaf discs were used. Grapevine leaf discs were prepared as described above. The experimental treatments included: 1) distilled water (untreated control); 2) BION 50 WG (50 mg/L) as a positive control for callose accumulation; 3) laminarin at a concentration of 2 mL/L as a positive control for ROS production; 4) viable AZ78 cells; and 5) heat-inactivated AZ78 cells. All treatments were applied to grapevine leaf discs 24 h before inoculation with *P. viticola*.

In the case of basil, treatments 1-5 were applied to the plants one day before inoculation with the *P. belbahrii* sporangial suspension. Twenty-four hours after *P. belbahrii* inoculation, 12 mm leaf discs were carefully excised from each treated plant using a sterile cork borer. These leaf discs were cut immediately before staining to minimise potential wounding effects, thereby ensuring accuracy and reliability in subsequent analyses. In both cases, leaf discs were stained and observed at two dpi.

To assess callose accumulation in the guard cells of basil and grapevine leaf discs, a fluorescence microscopy method was used, staining plant tissues with 0.05% aniline blue in 0.06 M K_2HPO_4 (pH 8) (Palmieri *et al*., 2012). For staining grapevine leaf discs, samples were placed in 50 mL sterile centrifuge tubes containing 1 M KOH and immersed in a thermal bath at 95 °C for 15 min. After decantation, the discs were rinsed three times for 15 s each with sterile distilled water to remove KOH residues. Subsequently, the leaf discs were submerged in 0.05% aniline blue solution for 15 min before being mounted on glass slides. The slides were covered with coverslips, and the edges were sealed for long-term preservation. All slides were wrapped in aluminium foil until observation. Callose accumulation was visualised as blue fluorescence in guard cells. For basil leaf discs, aniline

blue staining followed the same steps, except that the boiling period in KOH was shortened to 11 min at 95 °C due to the delicate nature of the leaves.

To assess ROS production, 3,3′-diaminobenzidine (DAB) staining was used. Briefly, basil and grapevine leaf discs were incubated for five hours in 1 mg/mL DAB staining solution in HCl-acidified water at pH 3.8, as described by Thordal-Christensen et al. (1997). Afterwards, basil and grapevine leaf discs were incubated for 15 min at 90 °C in a destaining solution containing ethanol, acetic acid, and glycerol (3:1:1) to remove chlorophyll, carotenoids, and other plant pigments (Daudi and O'Brien, 2012). Due to their tenderness, the basil leaf discs were incubated in the destaining solution for only 11 min.

Subsequently, microscopic observations were conducted to assess callose accumulation and ROS production using a Leica LMD7000 microscope (Germany). ROS were visualised under bright field as dark reddish-brown spots resulting from DAB absorption and polymerisation. For callose accumulation, an A4 filter (BP 320-400 nm excitation, 400 nm dichroic mirror, BP 470 nm emission) was used for blue-fluorescence imaging. Five slides per treatment were prepared in both cases, and the experiments were repeated three times.

Callose accumulation surrounding stomata was quantified by counting the proportion of stomata exhibiting detectable aniline blue fluorescence. For each treatment, stained leaf discs were examined under a fluorescence microscope at the same magnification and exposure settings. From each biological replicate (n = 3), five randomly selected, non-overlapping fields of view were analysed. In each field, all clearly visible stomata were counted, and stomata were scored as callose-positive when a distinct blue, fluorescent ring or localised deposition was observed surrounding the guard cells. At least 100 stomata were evaluated per replicate. The percentage of stomata with callose accumulation was calculated as: Percentage of stomata with callose accumulation (%) = number of stomata with callose/ total number of stomata observed × 100.

For the ROS production, the digital images of the leaf discs obtained under bright field microscope were quantified using ImageJ software (version 1.53, NIH, USA) according to Sekulska-nalewajko et al. (2016) with some modifications. For each leaf disc, total leaf disc area was measured using the selection tool, followed by measuring the DAB deposits in each leaf disc. Five leaf discs were analysed per treatment. The percentage of leaf disc area stained with DAB was then calculated using the formula: Stained area (%) = (Stained leaf disc area/ total leaf disc area) × 100.

3.3.7 Determination of the toxicity of viable and heat-inactivated cells Lysobacter capsic*i AZ78 against* Plasmopara viticola *sporangia*

The toxicity of heat-inactivated and viable AZ78 cells towards *P. viticola* sporangia was evaluated according to Puopolo *et al*. (2014a), with slight modifications. Briefly, 50 µL of freshly prepared *P. viticola* sporangial suspension (2.5×10^5 sporangia/mL) was transferred into sterile 1.5 mL centrifuge tubes and kept on ice to prevent sporangial mortality. Subsequently, an equal volume of each treatment was added to the tube. The treatments consisted of 1) distilled water (untreated control); 2) copper-based fungicide (Coprantol Hi Bio, 2 g/L); 3) AZ78 viable cell suspension (1×10^9 CFU/mL); and 4) AZ78 heat-inactivated cell suspension (1×10^9 CFU/mL). After treatment, the tubes were transferred to an incubator at 17 °C for one hour.

After incubation, the mixtures were stained with 5,6-carboxyfluorescein diacetate (Sigma-Aldrich, 0.05%) in DMSO (Sigma-Aldrich, 0.01%) and propidium iodide (Sigma-Aldrich, 0.01%). The former dye conferred green fluorescence to viable sporangia, while the latter imparted red fluorescence to devitalised sporangia.

After staining, the mixtures were carefully spread onto glass slides and covered with coverslips. The prepared slides were examined under a Leica LMD7000 microscope (Germany) using the B/G/R filter to count dead sporangia (excitation filter: BP 550–590 nm; dichroic mirror: 590 nm; suppression

filter: BP 600-680 nm) and the H3 filter to count viable sporangia (BP 420-490 nm excitation; dichroic mirror: 510 nm; LP 515 nm emission) (Trouvelot *et al*., 2008). Low-intensity fluorescence was used to minimise dye degradation. The ratio of live to devitalised sporangia was then calculated for each treatment. Three slides per treatment were prepared, and 100 sporangia were randomly counted on each slide, with five replicates per treatment. The experiment was repeated three times.

3.3.8 Chemical analytical tools

Analytical and preparative thin-layer chromatography (TLC) was performed on silica gel plates (Kieselgel 60, F254, 0.25 and 0.5 mm, respectively) or reverse-phase plates (Kieselgel 60 RP-18 F254, 0.20 mm), and the compounds were visualised by exposure to UV light and/or iodine vapours and/or by sequential spraying first with 10% H_2SO_4 in MeOH and then with 5% phosphomolybdic acid in EtOH, followed by heating at 110 °C for 10 min. Column chromatography (CC) was performed using silica gel (Merck, Kieselgel 60, 0.063–0.200 mm). Solid-phase extraction (SPE) was carried out using SUPELCO Supelclean LC-18 SPE 2 g/12 mL cartridges (Merck, Darmstadt, Germany) on a SUPELCO Visiprep™ SPE Vacuum Manifold system (Merck, Darmstadt, Germany). Unless specified otherwise, all reagents were purchased from Sigma-Merck (Milan, Italy).

High-performance liquid chromatography (HPLC) was performed using a Hitachi 1260 Infinity system equipped with a 5160 pump and a 5410 spectrophotometric detector (Merck, Darmstadt, Germany). The HPLC separations were conducted with a Purospher STAR RP-18 column (5 µm, 125 × 4.0 mm; Merck, Darmstadt, Germany). Electrospray ionisation mass spectrometry (ESIMS) was performed using an LC/MS TOF AGILENT 6230B system (Agilent Technologies, Milan, Italy).
Clog P values were calculated using ChemOffice v20.1 (PerkinElmer, Waltham, MA, USA) with the corresponding tool in ChemDraw Professional (Vraka *et al*., 2017; Zorrilla *et al*., 2024).

3.3.9 Extraction and purification of bioactive metabolites from Lysobacter capsici AZ78 cells

A volume of 50 µL of AZ78 cell suspension was evenly distributed on the surface of 90 mm Petri dishes containing 15 mL of solid Luria-Bertani agar (LBA) 1:10 medium using sterile L-shaped spatulas and incubated at 27 °C. After 72 h, bacterial cells were scraped from the surface of the growth medium using sterile spatulas and placed into sterile flasks containing 30 mL of an extraction solution consisting of methanol (MeOH), acetonitrile (ACN), and water (1.5:1.5:1, *v/v/v*) plus 0.1% formic acid (*v/v*). The flasks were stirred for one hour at room temperature, and the extracts were then transferred into sterile 15 mL centrifuge tubes. Cell-free extracts were obtained by centrifugation at 35,000 × g for 30 min. The samples were frozen at -80 °C and lyophilised using a freeze dryer (FreeZone 6 Plus, Labconco, Kansas City, MO, USA) for 94 h. The dried samples were reconstituted in 3 mL of extraction solution. Five hundred microlitres of the concentrated extracts were centrifuged at 30,000 × g for 20 min at -4 °C. The supernatant was filtered through a Millex-GV PVDF syringe filter (0.22 µm, Merck, Darmstadt, Germany) and transferred to 2 mL HPLC vials, which were stored at −80 °C until analysis (Brescia *et al*., 2021).

The AZ78 cell-free extract (800 mL) corresponding to 240 Petri dishes (3.6 L of LBA 1:10) was concentrated under vacuum to 400 mL, and ammonium sulphate ($(NH_4)_2SO_4$) was added to a final concentration of 0.5 mg/mL. The solution was stirred for one hour, left overnight at 4 °C, and then centrifuged at 3,600 rpm for 50 min. The supernatant was discarded, and the pellet was washed twice with 3 mL of methanol and left for one hour at room temperature. The sample was centrifuged at 10,000 rpm for 30 min, and the supernatant was applied to a C18 SPE column. The SPE column was preconditioned with 6 mL of ACN and equilibrated with 12 mL of distilled water. The purification yielded five fractions (F1–F5), obtained by stepwise elution with H_2O (6 mL), ACN/H_2O (3:7, *v/v*; 12 mL), ACN/H_2O (1:1, *v/v*; 12 mL), ACN/H_2O (7:3, *v/v*; 12 mL), and ACN (12 mL), respectively.

Subsequently, the organic solvents were removed under reduced pressure, and the remaining aqueous phases were lyophilised. The residue of F3 (8.1 mg), which exhibited high anti-oomycete activity against *Pythium ultimum*, was analysed by ^{1}H NMR and further purified by TLC using the mixture CH_2Cl_2:MeOH:conc. NH_4OH (60:36:4, v/v/v) as the eluent. The main fractions obtained, F3.1C (1.7 mg, Rf 0.4) and F3.2E (1.0 mg, Rf 0.6), were purified by HPLC using multiple injections on a reverse-phase column.

The mobile phase used to elute the samples was a mixture of H_2O (0.1% formic acid) and ACN (0.1% formic acid) at a flow rate of 0.5 mL/min. The analysis was performed using a gradient starting from 60% ACN (0.1% formic acid), increased linearly to 80% over 20 min, and finally re-equilibrated to the initial conditions for 10 min. Detection was performed at 220 nm, and samples were injected using a 20 µL loop and monitored for 35 min.

3.3.10 Evaluation of the application of dihydromaltophilin and maltophilin for the control of Plasmopara viticola *on grapevine leaf discs*

To evaluate the potential of the isolated metabolites, namely dihydromaltophilin (DMP) and maltophilin (MP), they were individually tested on grapevine leaf discs against *P. viticola* at various concentrations. The treatments included: 1) distilled water (untreated control); 2) copper-based fungicide (Coprantol Hi Bio, 2 g/L); 3) DMP at 5 mg/L; 4) DMP at 2.5 mg/L; 5) DMP at 0.5 mg/L; 6) MP at 5 mg/L; 7) MP at 2.5 mg/L; and 8) MP at 0.5 mg/L. All treatments were mixed with equal volumes of *P. viticola* inoculum to reach the final concentrations and stored under cold conditions.

The treatments were applied by spotting five drops of 20 µL each onto each grapevine leaf disc. After application, the Petri dishes were wrapped in aluminium foil and incubated at 25 °C for 16 h. This was followed by a drying period of the Petri dishes under a chemical fume hood, after which they were transferred to the greenhouse at 25 °C (60-80% RH) with a 16/8 h day/night light regime.

Disease severity was measured on the seventh day post-inoculation. Each treatment consisted of five Petri dishes containing three leaf discs, resulting in 15 replicates (15 spots), and the experiment was repeated.

3.3.11 Assessment of the plant protection efficacy, toxicity against Plasmopara viticola *sporangia and induction of plant resistance mechanisms of a mixture of dihydromaltophilin and maltophilin*

To evaluate the plant protection efficacy of a mixture of DMP and MP against *P. viticola* on grapevine leaf discs, the following treatments were tested: 1) distilled water (untreated control); 2) DMSO 0.1% (v/v); 3) DMSO 0.05% (v/v); 4) copper-based fungicide (Coprantol Hi Bio, 2 g/L); 5) DMP and MP mixture at 50 mg/L; 6) DMP and MP mixture at 5 mg/L; 7) DMP and MP mixture at 2.5 mg/L; and 8) DMP and MP mixture at 0.5 mg/L. The DMSO concentrations corresponded to those present in the DMP and MP mixtures at 50 mg/L and 2.5 mg/L, respectively. The treatments were applied as described above.

The same DMP and MP mixtures, along with their respective controls, were also evaluated for their toxicity against *P. viticola* sporangia, following the procedure described above. Three slides per treatment were prepared, and 100 sporangia were randomly counted per slide (five replicates). The experiment was repeated three times.

DMP and MP mixtures at varying concentrations were also evaluated for their ability to stimulate callose accumulation and ROS production using the procedures previously described. The treatments were: 1) distilled water (untreated control); 2) DMSO 0.1%; and 3–6) leaf discs treated with DMP and MP mixture at 50 mg/L, 25 mg/L, 2.5 mg/L, and 0.5 mg/L, respectively. Each treatment consisted of five biological and three technical replicates, and all experiments were repeated three times.

3.3.12 Statistical analysis

Disease severity data obtained from all experiments were subjected to one-way analysis of variance (ANOVA) using R v4.3.0 in RStudio v2024.12.1-563. Data were analysed for normality using the Shapiro-Wilk test ($p > 0.05$) and for homogeneity of variances using Levene's test. Tukey's HSD post hoc test was performed using the 'emmeans' (v1.10.0) and 'agricolae' (v 1.3-7) package, with adjustments for multiple comparisons and a significance level of $\alpha = 0.05$. The percentage of stomata exhibiting callose accumulation and the leaf-stained area (%) for ROS production in the analysed leaf discs were also subjected to one-way ANOVA to evaluate differences among treatments. Different letters within the same column indicate statistically significant differences at ($p \leq 0.05$).

3.4 Results

3.4.1 Application of viable and heat-inactivated Lysobacter capsici AZ78 cells effectively controlled Plasmopara viticola on grapevine leaf discs

No colony formation occurred on NA dishes spot inoculated with AZ78 and DH5α cells after thermal shock, indicating that all treated bacterial cells died. The plant protection efficacy of heat-inactivated and viable AZ78 and DH5α cells was evaluated against *P. viticola*. Grapevine leaf discs treated with distilled water exhibited a disease severity of 90.00 ± 2.33%. In contrast, the copper-based fungicide provided the highest level of protection, resulting in a disease severity of 0.24 ± 0.16% (**Figure 4**). Similarly, the application of BION 50 WG significantly reduced disease severity (2.56 ± 0.62%). Application of heat-inactivated and viable DH5α cells resulted in only a slight but significant reduction in disease severity compared with the untreated control. Notably, the application of heat-inactivated and viable AZ78 cells significantly reduced *P. viticola* infections, performing better than BION 50 WG and equivalent to the copper-based fungicide (**Figure 4**).

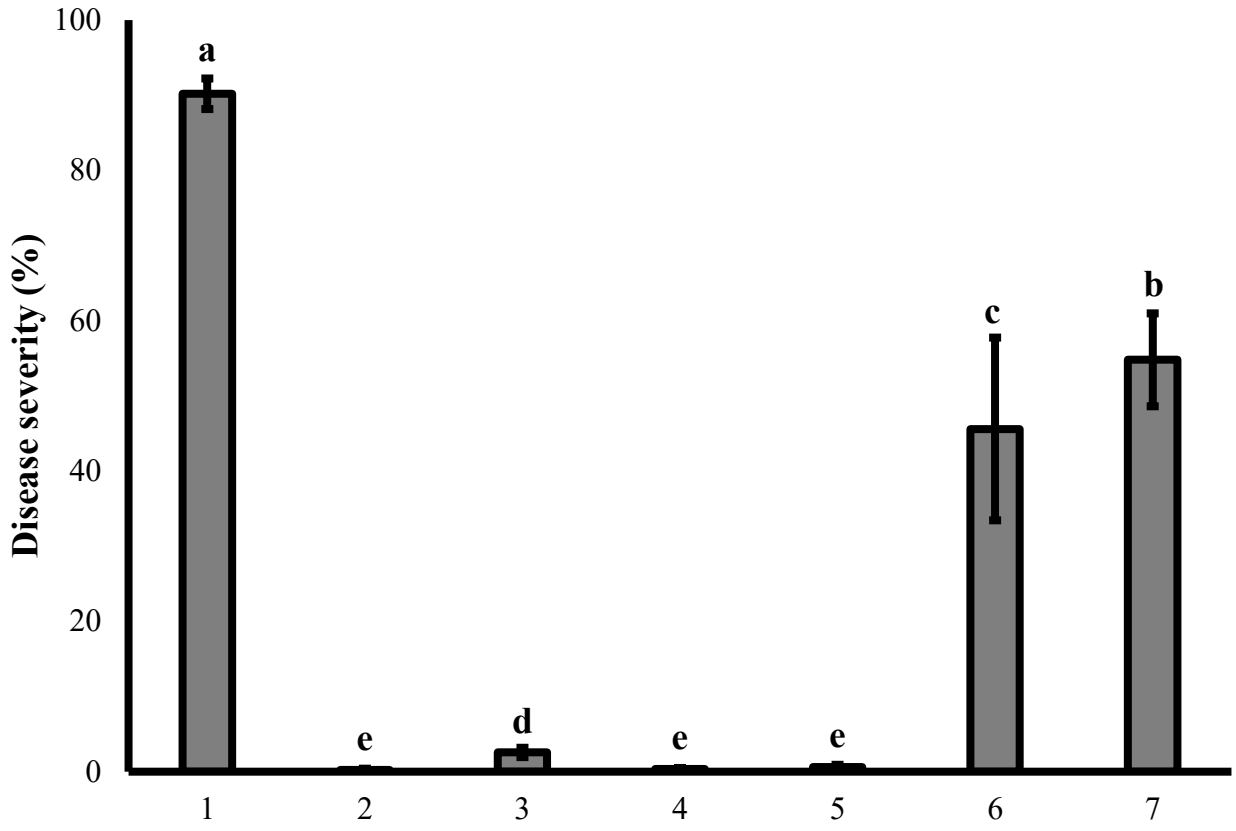

Figure 4. Control of *Plasmopara viticola* infections on grapevine leaf discs through the preventive application of viable and heat-treated *Lysobacter capsici* AZ78.cells The treatments included: **1)** distilled water (untreated control); **2)** copper-based fungicide [Coprantol Hi Bio (Copper hydroxide 20%, Syngenta; solution 2 g/L]; **3)** plant resistance inducer [BION 50 WG (acibenzolar-S-methyl 50%, Syngenta; 50 mg/L)]; **4)** viable *L. capsici* AZ78 cells (1×10^8 CFU/mL); **5)** heat-treated *L. capsici* AZ78 cells (1×10^8 CFU/mL); **6)** viable *Escherichia coli* DH5α cells (1×10^8 CFU/mL); and **7)** *heat-treated* E. coli DH5α cells (1×10^8 CFU/mL), applied 24 h prior to *P. viticola*. Disease severity is expressed as the mean percentage of symptomatic grapevine leaf disc area ± standard error (n = 5). Columns bearing the same letters are not significantly different according to Tukey's HSD test (a = 0.05).

3.4.2 Heat-inactivated and viable Lysobacter capsici AZ78 cells effectively suppressed downy mildew in grapevine and basil plants

In the next step, heat-inactivated and viable AZ78 cells were tested on whole grapevine and basil plants to evaluate their plant-protection efficacy under more complex conditions. For grapevine plants, the untreated control showed the highest disease severity (82.24 ± 2.18%), whereas the copper-based fungicide achieved the lowest (0.12 ± 0.12%; **Figure 5Figure *5***). The application of heat-

inactivated and viable AZ78 cells showed excellent efficacy, resulting in disease severities of 0.97 ± 0.23% and 0.34 ± 0.75%, respectively.

For basil plants, the untreated control exhibited a notably high disease severity (94.58 ± 0.75%). In contrast, the copper-based fungicide significantly reduced disease severity (1.46 ± 0.55%). Both viable and heat-inactivated AZ78 cells demonstrated strong plant-protection efficacy. Specifically, treatment with viable AZ78 cells (0.63 ± 0.36%) produced results comparable to those obtained with the copper-based fungicide. Heat-inactivated AZ78 cells reduced disease severity to 8.13 ± 2.01%, which was slightly higher than that achieved by the copper-based fungicide and viable AZ78 cells, but still significantly lower than the untreated control (**Figure 5**).

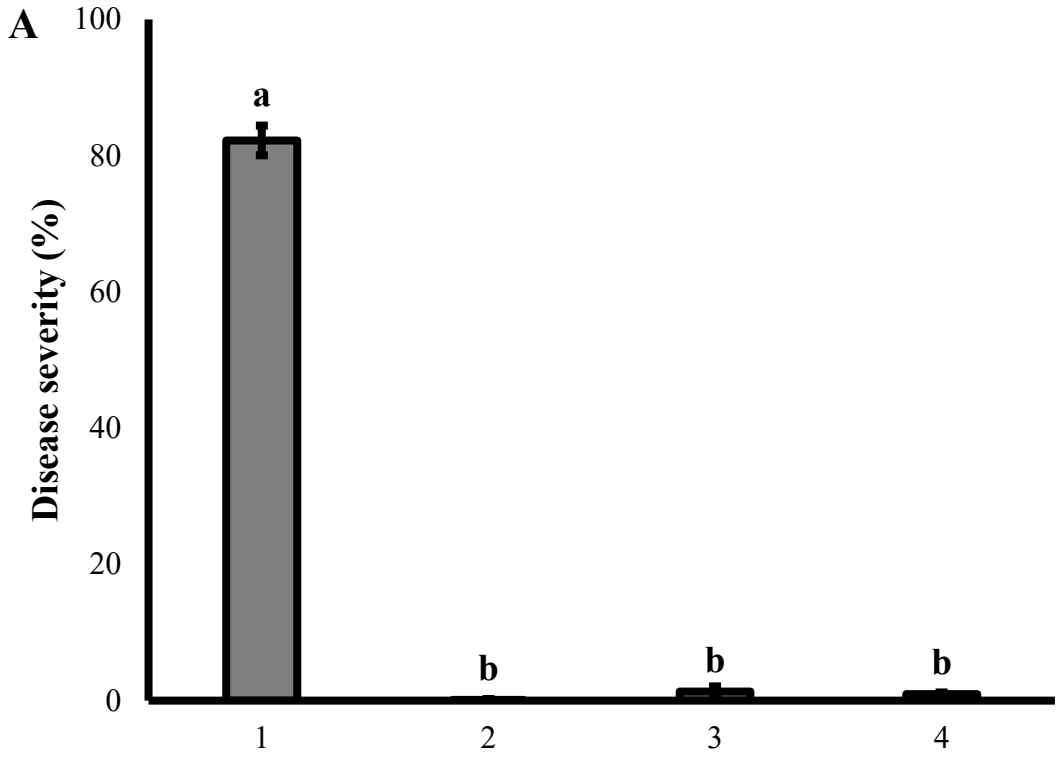

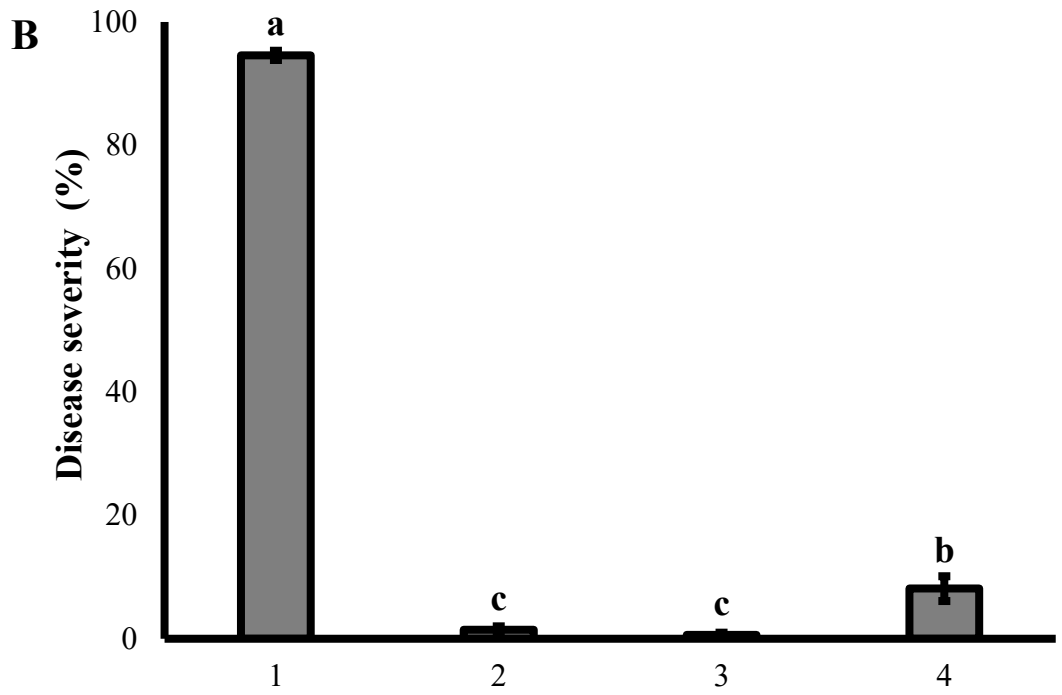

Figure 5. Preventive application of viable and heat-treated *Lysobacter capsici* AZ78 cells effectively protects basil and grapevine plants against plant pathogenic oomycetes. Viable and heat-treated *L. capsici* AZ78 cell suspension (1×10^8 CFU/mL) were applied to grapevine plants and treated with *Plasmopara viticola* after 24 h **(A)**. Similarly, viable and heat-treated *L. capsici* AZ78 cells suspension (1×10^9 CFU/mL) were applied to basil plants and inoculated with *Peronospora belbahrii* after 24h **(B)**. In both cases, treatments included: 1) distilled water (untreated control); 2) a copper-based product, in particular Coprantol Hi Bio (copper hydroxide 20%, 2 g/L) for grapevine plants and Cuprotax S.D.I. (copper sulfite 15.20%, 0.594 mL/L) for basil plants; 3) viable *L. capsici* AZ78 cells; and 4) heat-treated *L. capsici* AZ78 cells. Disease severity is expressed as the mean percentage of symptomatic grapevine leaf disc area ± standard error (n = 5). Columns bearing the same letters are not significantly different according to Tukey's HSD test (a = 0.05).

3.4.3 Application of heat-inactivated and viable Lysobacter capsici AZ78 cells stimulated callose accumulation and reactive oxygen species production in basil and grapevine leaf discs

Grapevine leaf discs treated with distilled water and inoculated with *P. viticola* showcased the presence of zoospores without callose formation at two days post-inoculation (dpi; **Figure 6**). BION 50 WG induced callose accumulation, consistent with its plant resistance-inducing activity. Notably, the application of heat-inactivated and viable AZ78 cells to grapevine leaf discs prevented the

presence of *P. viticola* zoospores or mycelium, and, similar to BION 50 WG, the grapevine leaf discs were characterised by pronounced callose accumulation around stomata (**Figure 6**).

In basil plants, untreated leaf discs exhibited minimal callose accumulation in response to infection, and the mycelial mat completely covered the leaf surface at two dpi (Fig. 6). The results for BION 50 WG-treated basil leaf discs were similar to those obtained with grapevine. Additionally, in basil plants treated with heat-inactivated and viable AZ78 cells, significant callose accumulation and a marked increase in stomatal cells containing callose plugs were observed (**Figure 6**).

For ROS production in grapevine, leaf discs treated with distilled water and inoculated with *P. viticola* displayed only minimal ROS production. However, the laminarin-treated grapevine leaf discs demonstrated a moderate increase in ROS production, as observed microscopically. Notably, leaf discs treated with heat-inactivated and viable AZ78 cells exhibited a significantly higher level of ROS production than the untreated control at two dpi (**Figure 7**).

Basil plants inoculated solely with *P. belbahrii* exhibited negligible ROS production at two dpi (Fig. 7), indicating a minimal oxidative response. The laminarin-treated plants showed a moderate reaction to DAB staining, characterised by low levels of ROS accumulation. In contrast, basil leaves treated with AZ78 cells demonstrated a substantial increase in ROS production, with both heat-inactivated and viable AZ78 cells inducing higher ROS levels than the other treatments (**Figure 7**).

Callose accumulation around stomata was significantly enhanced by viable and heat-treated *L. capsici* AZ78 cells compared with the untreated controls in both grapevine and basil treated ($p \leq 0.05$; Table 3) leaf discs. In grapevine, BION 50 WG (54.91 ± 3.03%), viable *L. capsici* AZ78 cells (53.66 ± 7.41%), and heat-treated AZ78 cells (48.41 ± 5.81%) markedly increased the proportion of stomata with callose compared with the untreated control (2.66 ± 0.93%). A similar trend was observed in basil leaf discs, where treated samples (40.67 ± 2.32% and 39.69 ± 4.00% for viable and heat-treated

L. capsici AZ78 cells, respectively) showed significantly higher callose accumulation than the untreated control (3.59 ± 1.28%).

ROS production, quantified as the percentage of DAB-stained leaf area, was significantly increased by all treatments compared with the untreated controls in both grapevine and basil (Table 4). In grapevine, viable *L. capsici* AZ78 cells (44.76 ± 0.95%) and heat-treated AZ78 cells (41.65 ± 4.70%) induced the highest ROS production, followed by the positive control laminarin (30.51 ± 2.98%), whereas the control exhibited minimal staining (3.93 ± 1.24%). A similar pattern was observed in basil, where viable (58.23 ± 1.57%) and heat-treated *L. capsici* AZ78 cells (53.77 ± 3.41%) triggered significantly greater ROS production than laminarin (34.31 ± 0.18%) and the untreated control (9.86 ± 2.08%).

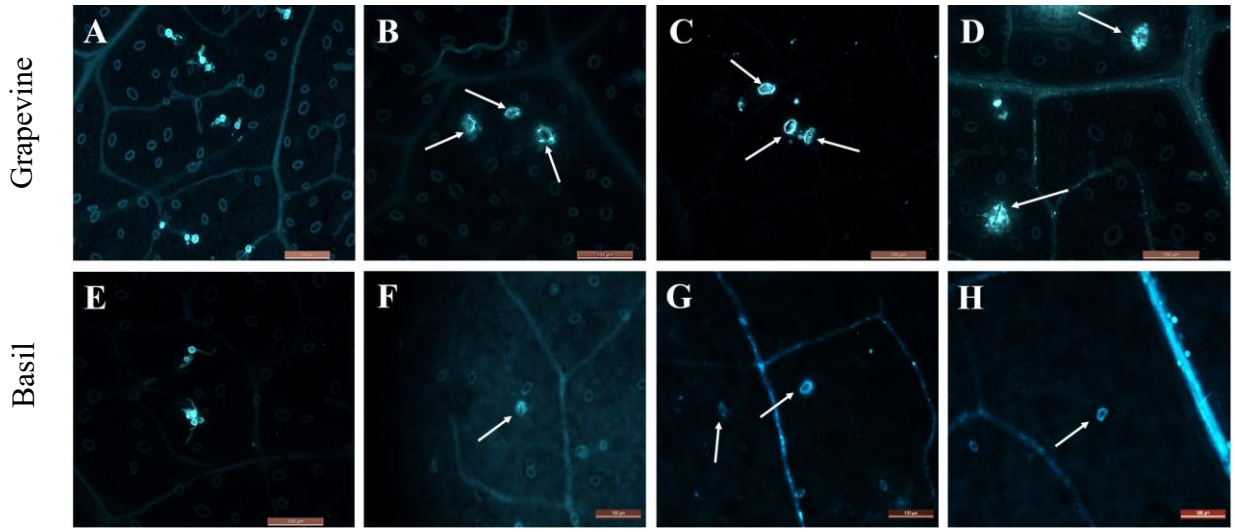

Figure 6. Application of viable and heat-treated *Lysobacter capsici* AZ78 cells promoted callose accumulation in grapevine and basil leaf discs. Viable and heat-treated *L. capsici* AZ78 cell suspension (1×10^8 CFU/mL) were applied to grapevine leaf discs. In contrast, basil plants were treated with viable and heat-treated *L. capsici* AZ78 cell suspension at 1×10^9 CFU/mL. Grapevine leaf discs (A-D) and basil plants (E-F) were inoculated with *Plasmopara viticola* (2.5×10^5 sporangia/mL) and *Peronospora belbahrii* (1×10^5 sporangia/mL) 24 h after the application of different treatments, respectively. After 48 h, callose deposition was assessed in basil and grapevine leaf discs using aniline blue staining. Representative micrographs illustrate callose accumulation in different treatments. The treatments included leaf discs treated with distilled water (untreated control) (A, E); leaf discs treated with BION 50 WG (acibenzolar-S-methyl, 50 mg/L) (B, F); leaf discs treated with viable *L. capsici* AZ78 cells (C, G) and heat-treated *L. capsici* AZ78 cells (D, H). Arrows indicate callose deposition around stomatal openings, visible as blue fluorescence. Scale bars: 100 µm.

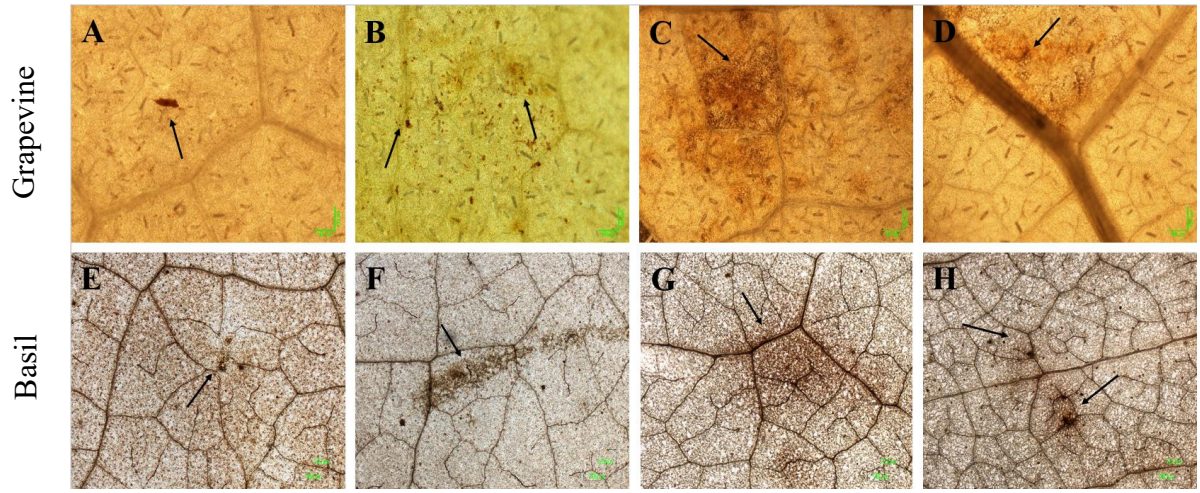

Figure 7. Promotion of reactive oxygen species (ROS) deposition in grapevine and basil leaf discs following the application of viable and heat-treated *Lysobacter capsici* AZ78 cells. Viable and heat-treated *L. capsici* AZ78 cell suspension (1×10^8 CFU/mL) were applied to grapevine leaf discs. In contrast, basil plants were treated with viable and heat-treated *L. capsici* AZ78 cell suspension a 1×10^9 CFU/mL. Grapevine leaf discs from grapevine **(A–D)** and basil **(E–H)** were inoculated with *Plasmopara viticola* (2.5×10^5 sporangia/mL) and *Peronospora belbahrii* (1×10^5 sporangia/mL), respectively, and assessed for ROS accumulation at 48 dpi using 3,3′-diaminobenzidine (DAB) staining solution. DAB-stained leaves revealed localized H_2O_2 accumulation. The treatments were as follows: leaf discs treated with distilled water (untreated controls) **(A, E)**; leaf discs treated with laminarin (2 mL/L) **(B, F)**; leaf discs treated with viable L. capsici AZ78 cells **(C, G)** and L. capsici AZ78 heat-treated cells **(D, H)**. Arrows indicate ROS accumulation, visible as brown precipitated spots. Scale bars: 100 µm.

Table 3. Callose accumulation quantification in grapevine and basil leaf discs treated with viable and heat-treated Lysobacter capsici AZ78 cells.

Treatments	Percentage of stomata with callose accumulation (%)	
	Grapevine	Basil
Untreated control	2.66 ± 0.93 [b]	3.59 ± 1.28 [c]
BION 50 WG	54.91 ± 3.03 [a]	48.19 ± 3.10 [a]
Viable *L. capsici* AZ78 cells	53.66 ± 7.41 [a]	40.67 ± 2.32 [b]
Heat-treated *L. capsici* AZ78 cells	48.41 ± 5.81 [a]	39.69 ± 4.00 [b]

Values are expressed as mean ± standard error (n = 3). Different letters within the same column indicate significant

Table 4. Reactive oxygen species production quantification in grapevine and basil leaf discs treated with viable and heat-treated *Lysobacter capsici* AZ78 cells.

Treatments	Quantification of ROS production areas in leaf discs (stained area%)	
	Grapevine	**Basil**
Untreated control	3.93 ± 1.24 [c]	9.86 ± 2.08 [c]
Laminarin	30.51 ± 2.98 [b]	34.31 ± 0.18 [b]
Viable *L. capsici* AZ78 cells	44.76 ± 0.95 [a]	58.23 ± 1.57 [a]
Heat-treated *L. capsici* AZ78 cells	41.65 ± 4.70 [a]	53.77 ± 3.41 [a]

Values represent mean ± standard error (n = 5). Different letters within the same column indicate significant differences according to Tukey's HSD test (P ≤ 0.05).

3.4.4 Effect of heat-treated and viable Lysobacter capsici AZ78 on the viability of Plasmopara viticola sporangia

Plasmopara viticola sporangia treated with distilled water demonstrated 51.02 ± 5.19% devitalised sporangia. In contrast, treatments with heat-inactivated and viable AZ78 cells significantly reduced sporangial viability, with 81.05 ± 1.50% and 80.08 ± 9.48% devitalised sporangia, respectively (**Figure 8**). Notably, the efficacy of viable AZ78 cells was higher than that of the copper-based fungicide, which caused 65.00 ± 2.00% sporangial devitalisation. Similarly, heat-inactivated AZ78 cells outperformed the untreated control, confirming their potential to reduce *P. viticola* sporangial viability and to suppress *P. viticola* infection (**Figure 8**).

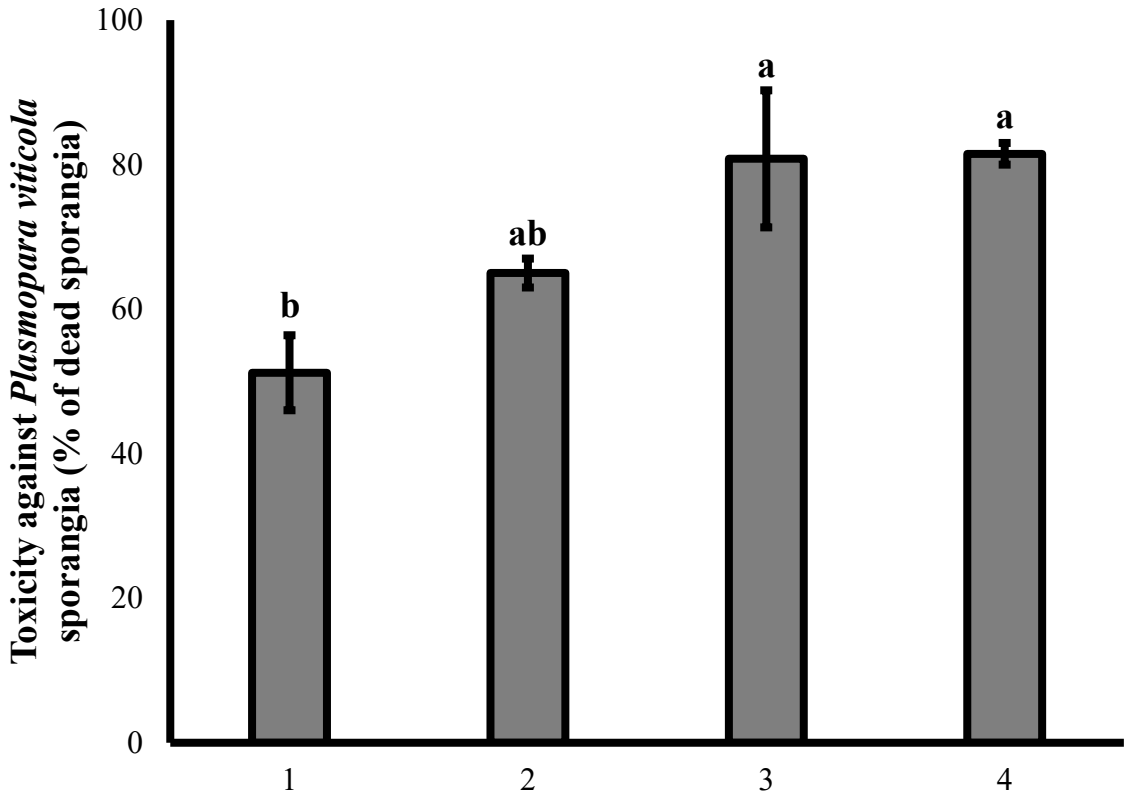

Figure 8. Toxicity of *Lysobacter capsici* AZ78 cells on the sporangia of *Plasmopara viticola*. The following treatments were evaluated: (1) untreated control; (2) Coprantol Hi Bio (Copper hydroxide 20%, Syngenta; 2 g/L solution); (3) viable *L. capsici* AZ78 cells (10^9 CFU/mL); and (4) heat-inactivated *L. capsici* AZ78 cells (10^9 CFU/mL). For each treatment, 100 sporangia were randomly counted per slide. Bars display the mean proportion of germinated and non-germinated sporangia, with dark grey indicating viable sporangia and light grey indicating devitalized sporangia. Error bars represent the standard error of the mean ± SE (n = 3). Different letters above the bars denote statistically significant differences between treatments ($p \leq 0.05$), as determined by Tukey's HSD test.

3.4.5 Identification of dihydromaltophilin and maltophilin in extracts from Lysobacter capsici *AZ78 cells*

As described above, the AZ78 cell-free extract was purified by precipitation with ammonium sulphate. The methanol-soluble compounds obtained were separated by C18 solid-phase extraction (SPE), yielding a fraction (F3) whose ^{1}H NMR spectrum (**Figure 9**) displayed signals corresponding to olefinic, methine, and methylene protons, similar to those reported for tetramic acid-containing metabolites (Graupner et al., 1997). This fraction was further purified through two successive steps of

TLC and HPLC, resulting in two pure compounds eluted at retention times (t_n) of 5.73 and 7.79 min (**Figure 10**and **Figure 11**, respectively). These were pooled, concentrated under reduced pressure, and lyophilised. Subsequently, the two compounds were identified as DMP, also known as HSAF (0.53 mg, t_n 5.73), and MP (MP; 0.83 mg, t_n 7.79 min) (Graupner et al., 1997). Their ESI-MS spectra showed the dimer protonated adduct [2M+H]+ and the protonated adduct [M+H]+ ions at *m/z* 1025 and 513 for DMP and at *m/z* 1021 and 511 for MP.

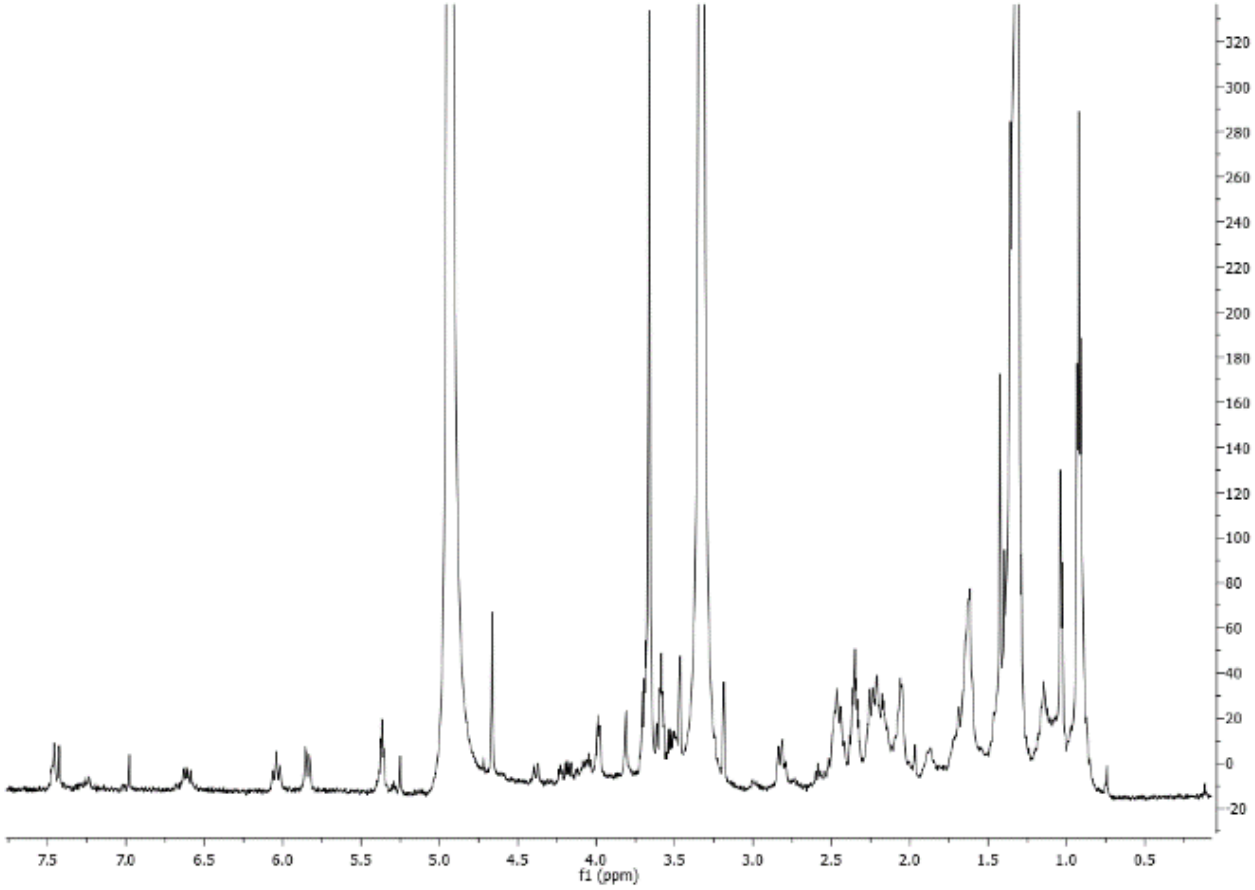

Figure 9. 1H NMR spectrum of F3 recorded in CD3OD at 400 Mhz

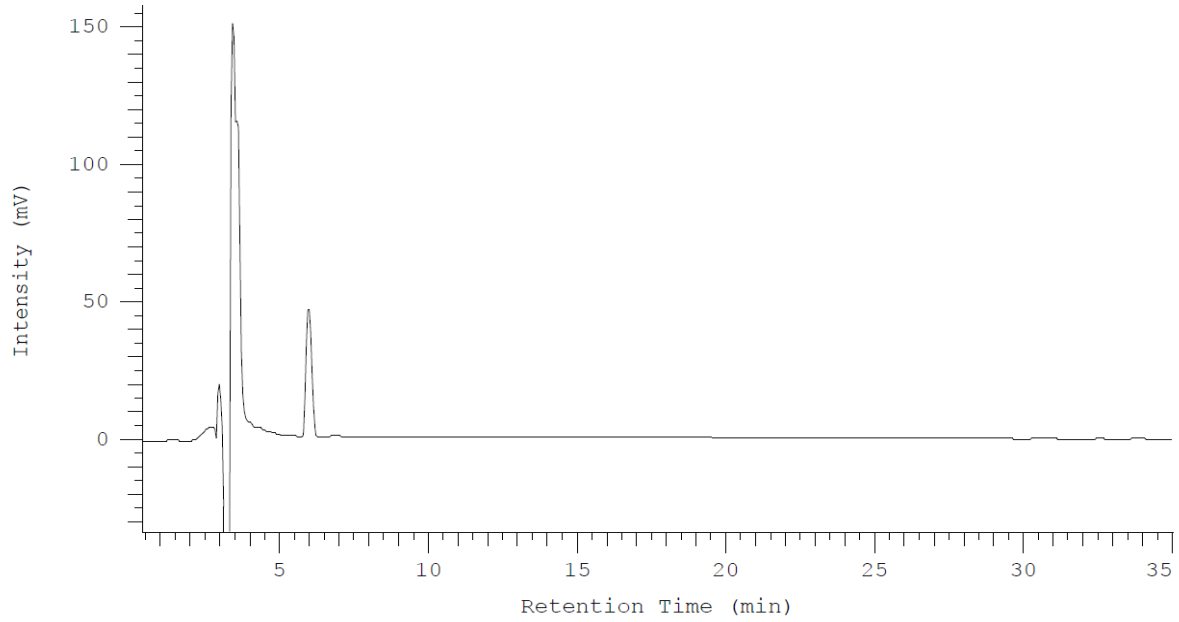

Figure 10. Chromatogram of dihydromaltophilin analysed at 1 mg/mL.

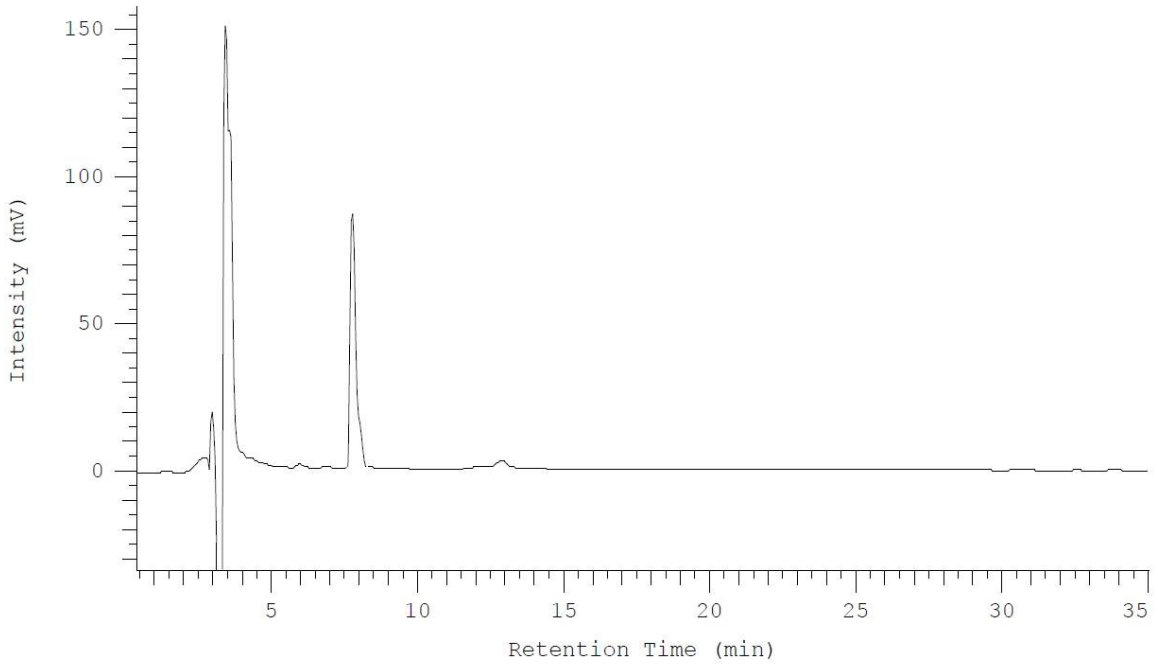

Figure 11. Chromatogram of maltophilin analysed at 1 mg/mL.

3.4.6 Impact of dihydromaltophilin and maltophilin application on Plasmopara viticola *infection in grapevine leaf discs*

The results demonstrated a strong protective effect of the two metabolites, DMP and MP, at varying concentrations on disease severity. In the control group, grapevine leaf discs exhibited a high disease severity (90.74 ± 6.23%; **Figure *12***. Effective control of Plasmopara viticola infections on grapevine leaf discs through the preventive application of dihydromaltophilin and maltophilin, individually at different concentrations. Grapevine leaf discs were subjected to various treatments, including: **1)** distilled water (untreated control); **2)** copper-based fungicide (Coprantol Hi Bio, copper hydroxide 20%, 2 g/L); **3)** DMP at 0.025 mg/L **4)** DMP at 0.005 mg/L; **5)** DMP at 0.0025 mg/L; **6)** MP at 0.025 mg/L **7)** MP at 0.005 mg/L; **8)** MP at 0.0025 mg/L. Disease severity is expressed as the mean percentage of symptomatic grapevine leaf disc area ± standard error (n = 5).). Treatments with DMP at 5 mg/L and 2.5 mg/L, as well as MP at 5 mg/L, completely suppressed disease development, resulting in the absence of symptoms, comparable to those observed with the copper-based fungicide. However, when applied at the lowest concentration (0.5 mg/L), both DMP and MP were less effective, with disease severity remaining high (77.41 ± 7.71% and 81.48 ± 3.76%, respectively; **Figure 12**). Additionally, MP applied at 2.5 mg/L exhibited a moderate reduction in disease severity (64.52 ± 3.96%).

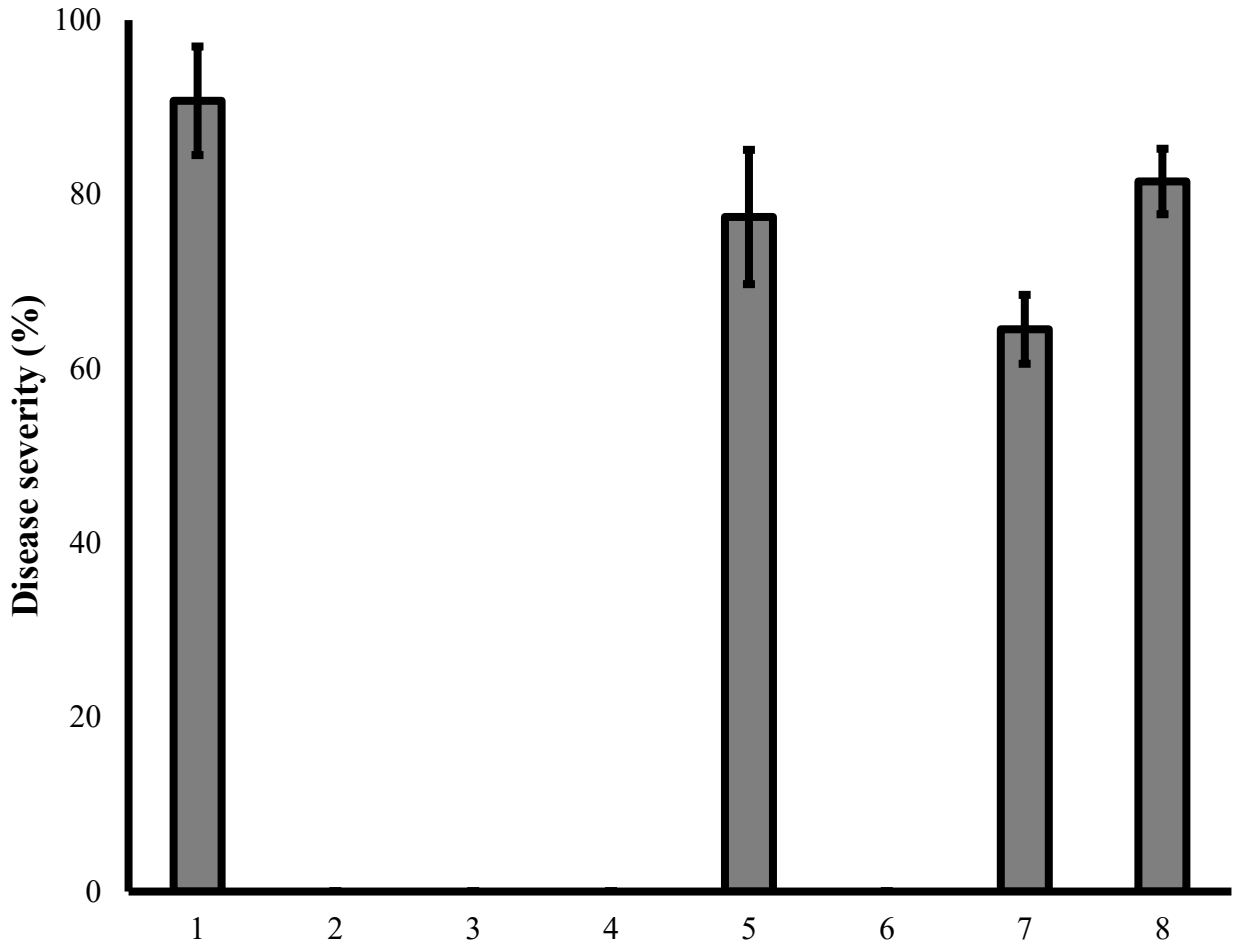

Figure 12. Effective control of *Plasmopara viticola* infections on grapevine leaf discs through the preventive application of dihydromaltophilin and maltophilin, individually at different concentrations. Grapevine leaf discs were subjected to various treatments, including: **1)** distilled water (untreated control); **2)** copper-based fungicide (Coprantol Hi Bio, copper hydroxide 20%, 2 g/L); **3)** DMP at 0.025 mg/L **4)** DMP at 0.005 mg/L; **5)** DMP at 0.0025 mg/L; **6)** MP at 0.025 mg/L **7)** MP at 0.005 mg/L; **8)** MP at 0.0025 mg/L. Disease severity is expressed as the mean percentage of symptomatic grapevine leaf disc area ± standard error (n = 5).

3.4.7 Impact of a mixture of dihydromaltophilin and maltophilin on Plasmopara viticola *infection in grapevine leaf discs*

Grapevine leaf discs treated with distilled water were covered entirely with sporulating *P. viticola* mycelium, showing 100% disease severity. Treatments with DMSO at lower concentrations (0.1% and 0.05%) and with the DMP and MP mixture at 0.5 mg/L exhibited high levels of disease severity, not significantly different from the untreated control (**Figure 13**). In contrast, the DMP and

MP mixture resulted in complete disease suppression (0% severity), matching the efficacy of the copper-based fungicide when applied at concentrations of 50 mg/L, 5 mg/L, and 2.5 mg/L (**Figure 13**).

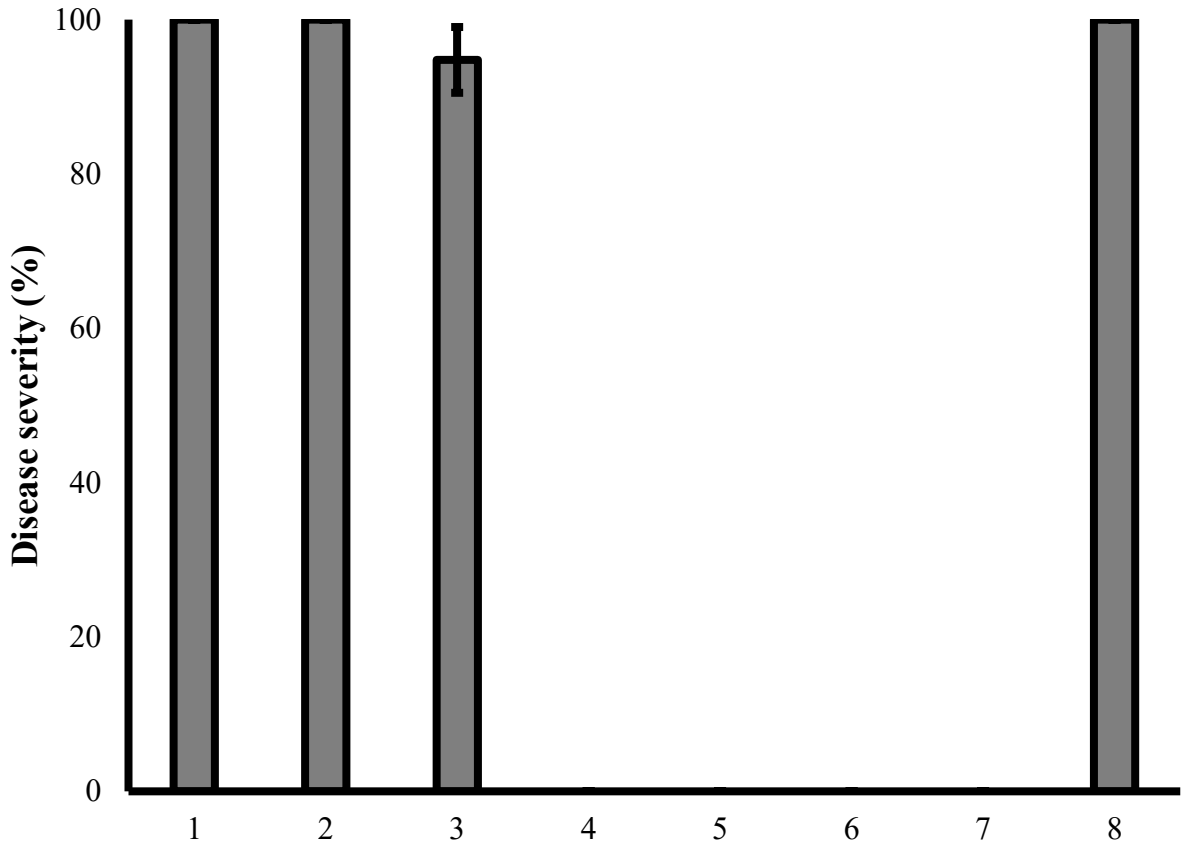

Figure 13. Control of *Plasmopara viticola* infections on grapevine leaf discs through the preventive application of a mixture of dihydromaltophilin and maltophilin. Grapevine leaf discs were subjected to various treatments, including: **1)** distilled water (untreated control); **2)** DMSO 0.1% (v/v); **3)** DMSO 0.05% (v/v); **4)** copper-based fungicide (Coprantol Hi Bio, copper hydroxide 20%, 2 g/L). The dihydromaltophilin and maltophilin mixture was applied at the following concentrations: **5)** 50 mg/L, **6)** 5 mg/L, **7)** 2.5 mg/L, and **8)** 0.5 mg/L. Disease severity is expressed as the mean percentage of symptomatic grapevine leaf disc area ± standard error (n = 5).

3.4.8 Effect of dihydromaltophilin and maltophilin mixture on Plasmopara viticola *sporangia*

Fluorescence microscopy revealed 26.00 ± 1.00% devitalised sporangia in the untreated control (Fig. 14). Varying concentrations of DMSO did not show any significant effect on sporangial viability,

with DMSO at 0.1% and 0.05% yielding 38.50 ± 1.50% and 45.00 ± 3.00% devitalised sporangia, respectively (**Figure 14**).

Conversely, the application of the DMP and MP mixture was highly toxic to *P. viticola* sporangia at concentrations as low as 2.5 mg/L. Notably, the DMP and MP mixture at 50 mg/L resulted in a higher percentage of devitalised sporangia than the copper-based fungicide (Coprantol Hi Bio). However, the DMP and MP mixture at 0.5 mg/L produced levels of sporangial devitalization comparable to those of the untreated control (**Figure 14**).

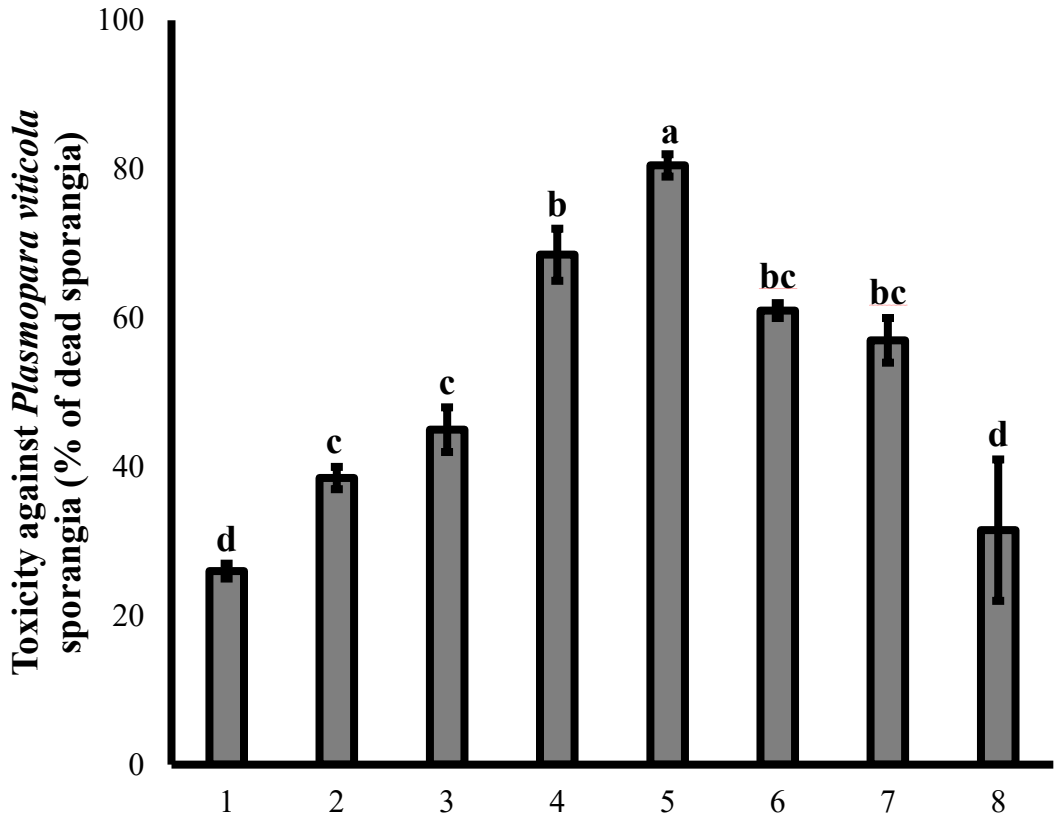

Figure 14. Toxicity of metabolite mixture on the sporangial germination ratio of *Plasmopara viticola*. The following treatments were evaluated: (1) untreated control; 2) DMSO 0.1%; 3) DMSO 0.05%; 4) Coprantol Hi Bio (2 g/L); and 5-8) DMP and MP mixtures at concentrations of 50 mg/L, 5 mg/L, 2.5 mg/L, and 0.5 mg/L. For each treatment, 100 sporangia were randomly counted per slide. Bars display the mean proportion of germinated and non-germinated sporangia, with dark grey indicating viable sporangia and light grey indicating devitalized sporangia. Error bars represent the standard error of the mean ± standard error (n = 3). Different letters above the bars denote statistically significant differences between treatments ($p \leq 0.05$), as determined by Tukey's HSD test.

3.4.9 Application of dihydromaltophilin and maltophilin mixture stimulates callose accumulation in grapevine leaf discs

Microscopic observations revealed that grapevine leaf discs treated with distilled water and 0.1% DMSO exhibited extensive *P. viticola* mycelial growth and no callose accumulation. Notably, callose deposition was clearly observed in grapevine leaf discs treated with the DMP and MP mixture at concentrations of 50 mg/L, 5 mg/L, and 2.5 mg/L, whereas the lowest concentration tested (0.5 mg/L) did not induce callose accumulation (**Figure 15**).

As reported above, treatment with distilled water did not increase the percentage of callose-positive stomata in grapevine leaf discs (0.94 ± 0.54%). However, this value was significantly higher than that observed in leaf discs treated with DMSO (0.1%), in which no callose-positive stomata were detected (Table 5). The DMP and MP mixture at various concentrations significantly induced callose deposition in grapevine leaf discs in a dose-dependent manner (**Table 5**Table 5). The highest response was observed at 50 mg/L (46.53 ± 2.35%), followed by 25 mg/L (18.19 ± 3.17%) and 2.5 mg/L (11.52 ± 0.81%). In contrast, the application of the DMP and MP mixture at 0.5 mg/L reached a percentage of callose-positive stomata (0.93 ± 0.53%) that was not significantly different from that observed on grapevine leaf discs treated with distilled water (untreated control).

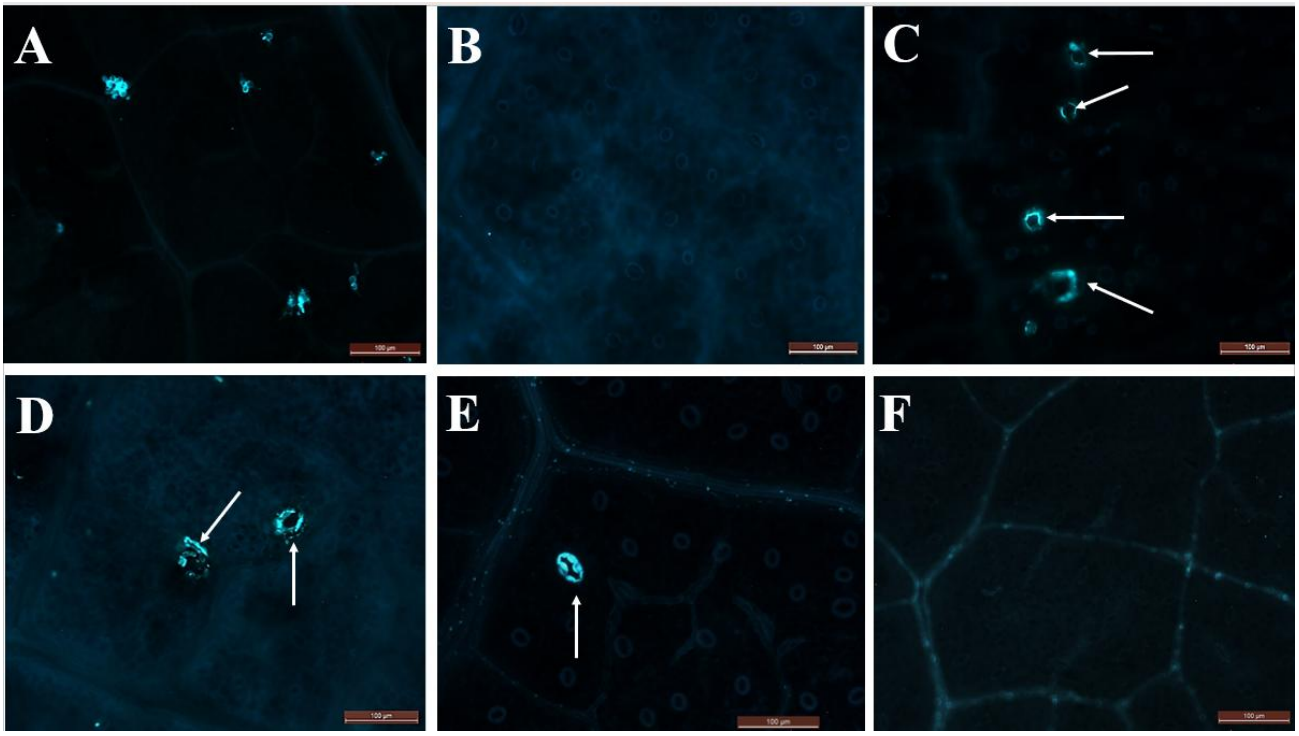

Figure 15. Callose deposition in grapevine leaf discs treated with a dihydromaltophilin and maltophilin mixture. The treatments included: leaf discs treated with distilled water (untreated control) **(A)**; leaf discs treated with DMSO 0.1% **(B)**; and leaf discs treated with the dihydromaltophilin-maltophilin mixture at 50 mg/L **(C)**, 25 mg/L **(D)**, 2.5 mg/mL **(E)**, and 0.5 mg/L **(F)**. Arrows indicate callose deposition around stomatal openings, visible as blue fluorescence. Scale bars: 100 µm.

Table 5. Callose accumulation quantification in grapevine leaf discs treated with dihydromaltophilin and maltophilin mixture at various concentrations

Treatments	Percentage of stomata with callose accumulation (%)
Untreated control	0.94 ± 0.54
DMSO (0.1%)	0.00 ± 0.00
*DMP+MP mixture (50 mg/L)	46.53 ± 2.35
DMP+MP mixture (25 mg/L)	18.19 ± 3.17
DMP+MP mixture (2.5 mg/L)	11.52 ± 0.81
DMP+MP mixture (0.5 mg/L)	0.93 ± 0.53

*** DMP: dihydromaltophilin; MP: maltophilin.**

Values are expressed as mean ± standard error (n = 3).

3.5 Discussion

Biocontrol *Lysobacter* spp. strains are emerging as promising candidates for the development of new, eco-friendly products suitable for the management of plant-pathogenic (micro)organisms (Puopolo *et al*., 2018). In particular, *Lysobacter* spp. strains have shown remarkable efficacy in controlling plant diseases caused by pathogenic oomycetes (Lin *et al*., 2021), with AZ78 being one of the few examples of a biocontrol agent capable of controlling *P. viticola* in vineyards (Markellou *et al*., 2022). In this study, we further characterised the mechanisms employed by AZ78 to control plant-pathogenic oomycetes, focusing on *P. viticola* and *P. belbahrii* on grapevine and basil plants, respectively. Recently, we showed that AZ78 can produce heat-stable PTMs, and since these secondary metabolites come into contact with the outer membranes of *Lysobacter* spp. cells (Yue *et al*., 2021), we hypothesised that applying heat-inactivated AZ78 cells could achieve the same efficacy as applying viable AZ78 cells.

To verify this hypothesis, we conducted efficacy trials on grapevine leaf discs, and the results clearly showed that heat-inactivated AZ78 cells provided significant plant protection efficacy, comparable to that of a copper-based fungicide and viable AZ78 cells. Similarly, heat-inactivated AZ78 cells drastically reduced infections caused by *P. viticola* on grapevine and *P. belbahrii* on basil under greenhouse conditions. Beyond the efficacy of heat-inactivated AZ78 cells, it is noteworthy that AZ78 is among the few bacterial biocontrol agents capable of efficiently controlling basil downy mildew, performing comparably to a copper-based fungicide. Until now, the development of resistant basil cultivars, the use of chemical active substances, physical control measures, and agronomic strategies have represented the main approaches for managing basil downy mildew (Ben-Naim *et al*., 2018; La Placa *et al*., 2025; López-López *et al*., 2014; Patel *et al*., 2021). Although several alternative

products have been tested for controlling basil downy mildew in the USA, most have failed to control *P. belbahrii* effectively (Patel *et al*., 2021; Wyenandt *et al*., 2015). Thus, AZ78 could represent a valuable new resource for the development of a commercial microbial biopesticide targeting basil downy mildew, providing an environmentally sustainable alternative to chemical fungicides.

Given the efficacy of both heat-inactivated and viable AZ78 cells, we proceeded to characterise their mode of action. Firstly, we assessed the toxicity of AZ78 cells on *P. viticola* sporangia and found that sporangia treated with AZ78 displayed a significantly higher proportion of dead cells. Notably, viable AZ78 cells resulted in a greater proportion of dead sporangia than the copper-based fungicide. Previously, we showed that AZ78 can kill *P. viticola* sporangia through the production of the 2,5-diketopiperazine cyclo(L-Pro-L-Tyr); thus, it is plausible that AZ78 also produces this metabolite when applied to grapevine leaf discs (Puopolo *et al*., 2014a). However, as heat-inactivated AZ78 cells also showed strong efficacy, the toxicity could additionally be associated with the presence of heat-stable secondary metabolites.

In greenhouse experiments, the application of heat-inactivated AZ78 cells efficiently controlled *P. viticola* on grapevine and *P. belbahrii* on basil, similarly to the copper-based fungicide and viable AZ78 cells. Since heat-inactivated AZ78 cells were non-viable, we postulated that their plant-protection efficacy could be related to the stimulation of host resistance mechanisms, similar to other bacterial biocontrol agents such as *Bacillus* spp. and *Pseudomonas* spp. (Meziane *et al*., 2005; Ali *et al*., 2025).

Among resistance mechanisms, we focused our attention on callose deposition and ROS production, as they are two processes commonly associated with induced resistance triggered by plant-beneficial (micro)organisms and chemical resistance inducers (Mersha *et al*., 2012; Palmieri *et al*., 2012; Trouvelot *et al*., 2008; Van der Ent *et al*., 2008). ROS are typically produced in response to

stress and play a pivotal role in activating plant-defence signalling pathways. The localised accumulation of ROS at plant pathogen entry sites leads to oxidative bursts that are toxic to invading (micro)organisms (Averyanov, 2009). For instance, ROS production is associated with the hypersensitive response in resistant grapevine plants following *P. viticola* infection (Kortekamp and Zyprian, 2003). Additionally, callose, a β-(1,3)-D-glucan, reinforces plant cell walls and restricts plant pathogen spread (Wang *et al*., 2021). Its deposition around stomata is crucial for preventing *P. viticola* infection in resistant grapevine plants (Gindro *et al*., 2003).

In our study, substantial callose deposition was observed near stomata in both basil and grapevine leaf discs treated with heat-inactivated or viable AZ78 cells, comparable to the response induced by the resistance activator BION. The ability of AZ78 cells, whether heat-inactivated or viable, to stimulate callose deposition near the stomata in basil and grapevine leaves is essential for limiting infection by *P. viticola* and *P. belbahrii*, as both plant pathogens use stomata as their primary penetration sites (Fröbel and Zyprian, 2019; Koroch *et al*., 2013). Similarly, a marked accumulation of ROS was detected in grapevine and basil leaf discs treated with both viable and heat-inactivated AZ78 cells, and this oxidative burst likely forms the basis of the host response to *P. viticola* and *P. belbahrii* infection. Alongside callose deposition, ROS production may play a significant role in protecting basil and grapevine plants by triggering a hypersensitive response against these plant pathogenic oomycetes (Delledonne *et al*., 2001). Based on these results, it is conceivable that AZ78 contributes to plant protection not only through the release of secondary metabolites toxic to sporangia but also by activating host-defence mechanisms.

Plant-beneficial and pathogenic bacteria possess cell components and secreted proteins that can be recognised by plants, and this recognition forms the basis of pathogen- or microbe-associated molecular pattern (PAMP/MAMP)-triggered immunity (Meziane *et al*., 2005; Willmann *et al*., 2011;

Yu *et al*., 2017). To exclude the possibility that heat shock could cause bacterial cells to release components and/or other compounds recognisable by plants, we also assessed the plant-protection efficacy of heat-inactivated *E. coli* DH5α, which has never been associated with resistance induction in plants. However, it is worth noting that another *E. coli* strain has been reported to promote resistance mechanisms in *Arabidopsis thaliana* (Seo and Matthews, 2012); thus, some *E. coli* strains may indeed possess elicitors that plants can recognise.

Neither heat-inactivated nor viable DH5α cells were effective in controlling *P. viticola*, confirming the inability of this strain to stimulate plant-resistance mechanisms. Based on these findings, it is plausible that AZ78 cells, unlike DH5α, contain metabolites and/or cell components capable of eliciting defence responses in grapevine, similarly to BION, which was used as a reference resistance inducer (Perazzolli *et al.*, 2011).

Among *Lysobacter* spp. biocontrol agents, similar results were obtained with the application of heat-inactivated *L. enzymogenes* C3 cells, which were able to control *Bipolaris sorokiniana* in tall fescue and *Fusarium graminearum* on wheat (Jochum *et al*., 2006; Kilic-Ekici and Yuen, 2003). Thus, AZ78 and *L. enzymogenes* C3 may share heat-resistant elicitors that can stimulate defence mechanisms in plants. Notably, both AZ78 and *L. enzymogenes* C3 release PTMs such as DMP and MP, which remain stable even after exposure to high temperatures (Brescia *et al*., 2021; Yu *et al*., 2007).

The involvement of DMP (also known as Heat-Stable Antifungal Factor) in the biocontrol efficacy of *L. enzymogenes* C3 has been thoroughly investigated. This PTM displays potent toxicity against a wide range of fungi (e.g. *Fusarium graminearum*), nematodes (e.g. *Heterodera schachtii*), and oomycetes (e.g. *Pythium ultimum*) (Jochum *et al*., 2006; Kobayashi *et al*., 2005; Yuen et al., 2018). Regarding its mode of action, DMP produced by *L. enzymogenes* C3 was shown to severely

impair the polarised growth of *Aspergillus nidulans* hyphae by influencing microfilament assembly at hyphal tips through interactions with the ceramide biosynthetic pathway (Li *et al*., 2006). Additionally, Ding *et al*. (2016) demonstrated that DMP application to *Candida albicans* induces apoptosis in yeast cells by stimulating ROS production. Interestingly, Tomada *et al*. (2017) reported that genes involved in PTM biosynthesis were upregulated in AZ78 during its interaction with *Phytophthora infestans*. The plant pathogen itself responded by upregulating genes associated with apoptotic processes (Tomada *et al*., 2017).

Alongside the characterisation of the DMP mode of action, Meers *et al*. (2018) demonstrated that *L. enzymogenes* C3 releases DMP and related analogues into the environment via outer membrane vesicles (OMVs). Thus, it is conceivable that PTMs come into direct contact with the cell membranes of *Lysobacter* spp. producing strains. Based on this assumption, we isolated and characterised secondary metabolites associated with AZ78 cell membranes. Purification of the extracts through chromatographic techniques (SPE C18, TLC, and HPLC) led to the identification of two key metabolites: DMP and MP.

Once isolated, we tested DMP, MP, and their mixture at varying concentrations against *P. viticola* only, due to the limited amount of metabolites obtained. When applied individually at 2.5 mg/L, only DMP achieved complete control of *P. viticola* on grapevine leaf discs. The same level of efficacy was achieved with the mixture of DMP and MP at 2.5 mg/L. Overall, these results are consistent with those obtained by applying heat-inactivated and viable AZ78 cells to grapevine leaf discs and plants. Moreover, these findings align with those of Graupner *et al*. (1997), who isolated and tested DMP and MP from a *Streptomyces* sp. strain in Indiana (USA) against *P. viticola* on grapevine plants, demonstrating high efficacy for both PTMs.

To further characterise how these PTMs could control *P. viticola*, we applied a mixture of DMP and MP, as both metabolites were extracted from AZ78 cells. Similar to heat-inactivated and viable AZ78 cells, the DMP and MP mixture significantly reduced the viability of *P. viticola* sporangia. A clear dose-dependent effect was observed, with higher concentrations of the DMP and MP mixture exhibiting greater efficacy in devitalising *P. viticola* sporangia. Notably, at 50 mg/L, the DMP and MP mixture was as effective as the copper-based fungicide, and at 500 mg/L, its efficacy surpassed that of the fungicide. Importantly, the DMP and MP mixture remained toxic at 2.5 mg/L, indicating that these PTMs may serve as promising candidates for the development of new active substances for the sustainable control of grapevine downy mildew within integrated pest management programmes.

Along with its toxic activity against *P. viticola* sporangia, the DMP and MP mixture also stimulated callose deposition near stomatal guard cells in grapevine leaf discs, even at a concentration of 2.5 mg/L. To the best of our knowledge, this is the first report demonstrating that these PTMs can influence plant tissues by modulating callose deposition in grapevine. Recently, Lin *et al*. (2023) reported that a *L. enzymogenes* OH11 mutant deficient in DMP production was still able to induce the expression of defence genes involved in the salicylic acid and jasmonic acid signalling pathways in the *Phytophthora capsici-Nicotiana benthamiana* pathosystem. Based on these findings, we cannot exclude the possibility that AZ78 cells also contain other elicitors capable of stimulating resistance mechanisms in grapevine plants.

In future studies, it will be essential to investigate the presence of additional potential elicitors in AZ78, alongside experiments aimed at elucidating the molecular pathways activated in grapevine following the application of the DMP and MP mixture. Furthermore, identifying the specific grapevine receptors that recognise and bind these PTMs will be a crucial step towards understanding the molecular basis of AZ78-induced resistance and developing novel, targeted biocontrol strategies.

3.6 Conclusions

This study demonstrates that heat-inactivated AZ78 cells retain significant biocontrol activity against *P. viticola* and *P. belbahrii* on grapevine and basil plants, respectively. Their efficacy is comparable to that of a commercial copper-based fungicide and a resistance inducer. The results showed that heat-inactivated AZ78 cells were highly toxic to *P. viticola* sporangia, similarly to viable AZ78 cells. Moreover, both heat-inactivated and viable AZ78 cells induced callose accumulation and ROS production in basil and grapevine leaves, thereby inhibiting plant pathogen entry during the early stages of infection.

We attribute this activity to the accumulation of thermostable polycyclic tetramate macrolactams (PTMs), specifically dihydromaltophilin (DMP) and maltophilin (MP), in AZ78 cell membranes. Indeed, we isolated these PTMs from AZ78 cells and demonstrated their toxicity against *P. viticola* sporangia, as well as their ability to stimulate callose deposition in grapevine leaf discs, mirroring the effects of heat-inactivated and viable AZ78 cells. These complementary modes of action, combining direct antimicrobial activity with plant resistance induction, highlight the potential of AZ78 and its metabolites as eco-friendly biocontrol agents for the sustainable management of downy mildews.

CHAPTER 4

ANTI-OOMYCETE ACTIVITY OF *LYSOBACTER CAPSICI* AZ78 AUTOLYSATES AND THEIR ROLE IN INDUCING GRAPEVINE DEFENSE RESPONSES

Abstract

Lysobacter capsici AZ78 and the derived thermostable polycyclic tetramate macrolactams (PTMs) are previously known to exhibit strong anti-oomycete activity against *Plasmopara viticola* and *Peronospora belbahrii*, the causal agents of grapevine and basil downy mildew, respectively. In the present study, we evaluated the plant protection potential of self-digestive solutions (SDS) obtained from prolonged liquid cultivation of *L. capsici* AZ78 in nutrient limited growth medium. Extended cultivation for a prolonged period induced bacterial autolysis, resulting in membrane disruption and release of membrane-associated metabolites, including PTMs, into the culture medium. Grapevine plants were treated with the obtained unheated and heat-treated SDS at full strength and at 1/10 dilution. Disease severity (%) assays revealed that diluted SDS collected at 96 h, corresponding to the autolysis phase, provided the highest level of protection against *P. viticola*. Protection assays were combined with gene expression analyses, showing that SDS treatments activated multiple grapevine defense responses and promoted accumulation of stilbene phytoalexins, including piceid, resveratrol, and trans-ε-viniferin, compounds previously reported to inhibit *P. viticola*. Most defense-related genes were strongly induced only after pathogen inoculation, indicating a priming effect triggered by SDS treatments.

Collectively, these results demonstrate that autolysate-derived metabolites from *L. capsici* AZ78 confer grapevine protection through a dual mode of action combining direct anti-oomycete

activity with activation of host immunity. This study highlights bacterial autolysates rich in antimicrobial secondary metabolites are stable and promising biocontrol tools with significant potential for sustainable management of grapevine downy mildew.

Keywords: *Lysobacter capsici* AZ78, grapevine downy mildew, self-digestive solution, phytoalexins, plant immune priming, defense gene expression.

4.1 Introduction

The obligate biotrophic oomycete *Plasmopara viticola* is the causal agent of grapevine downy mildew, one of the most destructive diseases affecting *Vitis vinifera* L. worldwide and causing substantial economic losses in viticulture (OIV, 2022). The pathogen infects living host tissues, including leaves, shoots, and berries, and under favourable environmental conditions disease severity may result in yield losses ranging from 40%-90% (Toffolatti *et al.*, 2018b). Originally endemic to North America, *P. viticola* was accidentally introduced into Europe, where highly susceptible Eurasian grapevine cultivars facilitated rapid disease spread (Fontaine *et al.*, 2013). Disease management still relies largely on repeated fungicide applications, while breeding programs aim to develop resistant cultivars (Delame *et al.*, 2019; Miclot *et al.*, 2020). . However, the rapid evolutionary potential of *P. viticola* has led to the emergence of fungicide-resistant populations(Chen *et al.*, 2007), and the limited availability of durable resistance sources continues to challenge breeding efforts (Peressotti *et al.*, 2010; Delmas, 2016). Consequently, integrating biological control agents (BCAs) into existing management strategies is increasingly considered essential for sustainable crop protection, offering environmentally safe alternatives that benefit plant health, farmers, and ecosystems (Nunez-Palenius *et al.*, 2022).

Among promising BCAs, species belonging to the genus *Lysobacter* have attracted considerable attention due to their ability to produce a broad antimicrobial arsenal composed of antibiotics, lytic enzymes, volatile organic compounds, and secondary metabolites (Puopolo *et al.*, 2014a; Fu *et al.*, 2018; Lin *et al.*, 2021; Nian *et al.*, 2021; Chen *et al.*, 2024). These bacteria employ multiple antagonistic strategies, including short-range secretion systems (T6SS and T4SS), intermediate-range enzymatic degradation via lytic enzymes, and long-range inhibition mediated by diffusible metabolites and volatiles (Shen *et al*., 2021; Lin *et al*., 2021). Beyond direct antimicrobial activity,

Lysobacter spp. can also function as plant defense stimulators. For example, *L. enzymogenes* induces resistance against *Rhizoctonia solani* and *Bipolaris sorokiniana* by enhancing peroxidase activity in tall fescue and wheat (Kilic-Ekici and Yuen, 2003), activates hormone-related pathways and defense marker genes such as allene oxide synthase (*AOS*) and aminocyclopropane-1-carboxylate synthase (*ACC*) in soybean (Walnut, 2019), and promotes defense gene activation in *Nicotiana benthamiana* against *Phytophthora* spp. (Lin *et al*., 2023). These findings highlight the dual mode of action of *Lysobacter* species involving both **direct antimicrobial activity against pathogens and indirect activation of plant immune responses**. Recent work on *L. enzymogenes* LE16 further demonstrated that self-digestive solutions (SDS) derived from bacterial cultures in liquid growth media retains strong antimicrobial activity due to extracellular enzymes, siderophores, and secondary metabolites released during autolysis. Notably, SDS maintained efficacy even after heat treatment or long-term storage, indicating that thermostable extracellular metabolites can retain biological activity independently of bacterial viability (Chen *et al*., 2020). These findings suggest that bacterial autolysates may represent a practical and durable form of biological control. Together, these findings demonstrate that *Lysobacter* BCAs function through integrated modes of action, combining direct pathogen suppression mediated by microbial cells or bioactive metabolites present in enriched SDS with indirect protection achieved through **activation of plant defence pathways and induction of defence-related genes and phytoalexin** accumulation. Within this genus, *Lysobacter capsici* AZ78 has emerged as an effective biocontrol strain against bacterial, fungal, and oomycete pathogens (Puopolo *et al.*, 2014a, b, 2016; Brescia *et al.*, 2021). Its efficacy is linked to the production of diverse antimicrobial metabolites, including cyclic lipodepsipeptides such as WAP-8294A2, diketopiperazines, volatile organic compounds, and polycyclic tetramate macrolactams (PTMs), notably heat-stable antifungal factor (HSAF)/dihydromaltophilin (DMP) and maltophilin (MP). These compounds exhibit strong antagonistic activity against pathogens such as *Phytophthora infestans*, *P.*

viticola, *R. solani*, *Rhodococcus fascians*, and *Sclerotinia minor* under both *in vitro* and greenhouse conditions (Puopolo *et al.*, 2014; Brescia *et al.*, 2020, 2021; Vlassi *et al.*, 2020a; Cimmino *et al.*, 2021). In our previous work, both viable and heat-treated *L. capsici* AZ78 cells retained strong anti-oomycete activity against *P. viticola* and *Peronospora belbahrii*. The plant protection offered by heat-treated *L. capsici* AZ78 cells was similar to viable cells and was attributed to thermostable PTMs produced by *L. capsici* AZ78 cells, as purified DMP and MP reproduced disease inhibition in grapevine even at low concentrations. Furthermore, these PTMs in addition to bacterial cells stimulated early plant defense responses, including **stomatal callose deposition and ROS** production, demonstrating for the first time the involvement of PTMs in grapevine plant protection and revealing their capacity act as **both direct antimicrobial agents and elicitors of host immunity**.

Despite these advances, the molecular mechanisms underlying host transcriptional responses induced by *L. capsici* AZ78 remain largely unexplored. Although early defense events such as ROS production and callose deposition have been described, plants activate additional multilayered defense strategies following pathogen perception. These include reinforcement of structural barriers, phytoalexin biosynthesis, activation of hormonal signalling pathways, and transcriptional regulation of defense-related genes, including pathogenesis-related (*PR*) proteins (Kaur *et* al., 2022; Al-khayri *et al.*, 2023; Singh and Hallan, 2024).

Beneficial microbes can stimulate plant immunity through systemic acquired resistance (SAR), typically associated with salicylic acid (SA) signalling and *PR* protein accumulation, or induced systemic resistance (ISR), primarily mediated by jasmonic acid (JA) and ethylene (ET) pathways (Nawrocka and Małolepsza, 2013; Salas-marina *et al*., 2011). Many BCAs function by priming plants, establishing a physiological state that enables faster and stronger defense activation upon pathogen attack while minimizing metabolic costs (Pozo *et al*., 2004; Verhagen *et al.*, 2010; Perazzolli *et al.*,

2011). Primed plants commonly exhibit enhanced ROS production, callose deposition, hypersensitive response activation, phytoalexin synthesis, and hormonal crosstalk involving JA, ET, SA, and abscisic acid (ABA) pathways (Koornneef and Pieterse, 2008; S Trouvelot *et al.*, 2008; Verhagen *et al.*, 2010; Gruau *et al.*, 2015; Aziz *et al.*, 2016). Although SA signalling is traditionally linked to resistance against biotrophic pathogens, increasing evidence highlights an important contribution of JA signalling during grapevine responses to *P. viticola* infection (Glazebrook, 2005; Figueiredo *et al*., 2015). Initial evidence for the participation of the JA pathway emerged from elicitor-based investigations demonstrating that treatments with β-aminobutyric acid and sulfated laminarin activated the expression of JA-related genes, including *LOX* and other JA-responsive genes (Hamiduzzaman *et al.*, 2007). Later studies showed that *P. viticola* infection makes several enzymes that are involved in JA biosynthesis and signalling work more, such as *AOC, AOS, LOX,* and *JAZ* genes (Polesani *et al.*, 2010; Marchive *et al.*, 2013; Gauthier *et al.*, 2014). Recent research indicates that the early up-regulation of JA biosynthesis genes (*LOX2, AOC, AOS,* and *OPR3*) and the activation of signalling components such as *JAR1* and *COI1* occur in the initial stages of infection, particularly in resistant cultivars (Figueiredo *et* al., 2015). Simultaneously, SA signalling is activated during the interaction, characterized by increased SA accumulation and the induction of SA-responsive genes such as *NPR1* and *PR1* following *P. viticola* inoculation (Dufour *et al.*, 2013). These results indicate that both JA- and SA-dependent pathways play a role in grapevine immunity against *P. viticola*, characterized by intricate interactions between the two hormonal signalling networks that govern the defense response (Mur *et al.*, 2006; Pieterse *et al.*, 2012). In transgenic *Vitis vinifera* cv. Shiraz plants possessing the *MrRPV1* resistance gene, a total of 1356 differentially expressed genes were identified post-pathogen infection. Genes implicated in JA and ET signalling, such as *LOX, AOS, ACO, ACS,* and *ERF*, exhibited significant upregulation between 18 and 36 hours post-infection, signifying the activation of JA/ET-mediated defense responses (Qu and Dry, 2021).

Among grapevine defense responses, stilbene phytoalexins play a central role and accumulate in response to both biotic and abiotic stresses (Langcake and Pryce, 1976; Jeandet *et al*., 2014). Stilbenes are synthesized via the phenylpropanoid pathway, where phenylalanine is converted into trans-cinnamic acid by *PAL*, leading to the formation of p-coumaroyl-CoA. *STS* then catalyses resveratrol production, the principal grapevine phytoalexin, which is further modified through methylation, hydroxylation, glycosylation, and oxidative coupling to generate diverse defense-related derivatives (Qian *et al.*, 2019; Jeandet *et al.*, 2021). (Qu and Dry, 2021) showed that genes implicated in secondary metabolite biosynthesis were markedly upregulated in transgenic *Vitis vinifera* cv. Shiraz plants possessing the MrRPV1 resistance gene, especially those related to stilbene production, including stilbene synthase (*STS*), phenylalanine ammonia-lyase (*PAL*), and resveratrol O-methyltransferase. After *P. viticola* infection, members of the *STS A* and *STS C* gene families showed a steady increase in activity.

Major grapevine stilbenes include resveratrol, its glycosylated form piceid, methylated derivatives such as pterostilbene, and oligomers such as ε-viniferin (Jeandet *et al.*, 2010). Accumulation of viniferin has been reported during *P. viticola* infection (Pezet *et al*., 2007) and several studies demonstrate that resveratrol moderately reduces *P. viticola* zoospore motility, whereas methylated stilbenes (e.g., pterostilbene) and dimeric stilbenes (e.g., ε-viniferin) exhibit stronger inhibitory effects, particularly on zoospore activity and sporulation (Langcake, 1981; Jeandet *et al.*, 2014; Gabatson *et al.*, 2017).

4.2 Aim of the work

Building on this knowledge and our previous findings, the present study investigated whether SDS derived from prolonged cultivation of *L. capsici* AZ78 in liquid medium, can promote the accumulation of enriched antimicrobial metabolites capable of conferring protection against *P.*

viticola in grapevine. PTMs which are often associated with bacterial membranes in *Lysobacter* spp., (Meers *et al.*, 2018) may be released through membrane disruption or via outer membrane vesicles (OMVs) formation during autolysis in the liquid medium. To evaluate their contribution to plant protection, unheated SDS (L-SDS) was subjected to heat treatment to generate heat-treated SDS (D-SDS), enabling the assessment of the **role of thermostable PTMs in plant protection activity.** Unlike L-SDS, D-SDS represents a cell-free biocontrol system that may overcome limitations related to microbial survival, formulation stability, and field variability while allowing direct assessment of PTM involvement in plant protection. Beyond assessing direct antagonistic activity, this study aimed to elucidate the mechanisms underlying SDS-mediated resistance in grapevine against *P. viticola* by evaluating disease protection efficacy focusing on defense gene regulation, priming responses, and the capability of SDS treatments to stimulate the accumulation of stilbene phytoalexins, as key markers of induced plant immunity and secondary metabolite-driven defence responses. This study represents the first investigation into the role of *L. capsici* AZ78 derived SDS in modulating host immune responses against *P. viticola*. By integrating disease protection assays, defense gene expression analysis, and phytoalexin accumulation, it provides new insights into **the role of bacterial autolysates in plant immune activation and biocontrol-mediated resistance.**

4.3 Material and methods

4.3.1 Maintenance of microorganism

The *L. capsici* AZ78 strain was routinely preserved in 40% (*v/v*) glycerol stocks at -80 °C. For experimental use, the bacterium was streaked onto Nutrient Agar (NA) plates (90 mm Petri dishes; Sarstedt, Nümbrecht, Germany) and incubated at 27 °C for 48 h. To prepare bacterial suspensions, each plate was flooded with 5 mL of sterile NaCl solution (0.85%; *w/v*), and cells were gently scraped using sterile L-shaped spreaders. The resulting suspension was homogenized and the optical density (OD_{600nm}) was adjusted to 0.1 using a spectrophotometer (UV-2450, Shimadzu, Kyoto, Japan), corresponding to approximately 1×10^8 colony-forming units (CFU)/mL, as previously described (Puopolo *et al*., 2014b).

4.3.2 Preparation of self-digestive solution of Lysobacter capsici *AZ78*

For the preparation of the self-digestive solution (SDS), PYKM medium (Peptone 10 g/L, Yeast Extract 5 g/L, KH_2PO_4 1.4 g/L, $MgSO_4 \cdot 7H_2O$ 1 g/L) was prepared as described by (Segarra *et al.*, 2015). Initially, viable *L. capsici* AZ78 cells were used to inoculate PYKM medium by adding 0.8 mL of AZ78 cell suspension (OD_{600} = 0.1) to 40 mL of PYKM sterile 50 mL centrifuge tubes, following Chen et al. (2020) with slight modifications. Cultures were incubated at 27 °C under continuous shaking (180 rpm) in the dark for up to 144 h. At each 24 h time point (i.e., 24, 48, 72, 96, 120, and 144 h), tubes were collected and subjected to thermal shock at 90 °C for 20 min using a thermo-mixer (T-shaker EMS100, Euro Clone, Italy), followed by incubation at -20 °C for 5 min (Brescia *et al.*, 2021) to obtain heat-treated SDS (D-SDS) from the unheated SDS (L-SDS). Both L-SDS and D-SDS were subsequently diluted 1/10 (*v/v*) with sterile distilled water to obtain diluted SDS (L-SDS 1/10 and D-SDS 1/10). Uninoculated PYKM medium and its corresponding 1/10 dilution

(PYKM 1/10) were included as control treatments. For each type of treatment, five independent replicates (centrifuge tubes) were prepared.

To verify the loss of viability, 100 µL D-SDS was spread onto NA plates, which were incubated at 27 °C for 72 h before visually evaluating colony formation. Five plates were prepared per treatment.

4.3.3 Growth curve measurement

Bacterial growth in L-SDS was monitored by measuring optical density at 600 nm (OD_{600}) at 24, 48, 72, 96, 120, and 144 h using a spectrophotometer (UV-2450, Shimadzu, Kyoto, Japan). At each time point, 1 mL of culture was withdrawn and used for OD_{600} measurement..

4.3.4 Maintenance of Plasmopara viticola *in grapevine*

Vitis vinifera cv. Pinot Noir plants grafted onto Kober 5BB rootstock were cultivated in 2.5 L pots containing a 3:1 (*v/v*) peat: pumice substrate in a greenhouse at 20 ± 0.5 °C and 70 ± 10% relative humidity (RH). Plants were grown for 60 days until each developed two shoots bearing at least nine fully expanded leaves. *Plasmopara viticola*, originally isolated in 2024 from an untreated vineyard in San Michele all'Adige, Italy, was maintained on healthy grapevine plants by weekly inoculations under controlled conditions (20 ± 0.5 °C, 70 ± 10% RH) as previously described (Puopolo *et al*., 2014b). Fresh inoculum of *P. viticola* was obtained from plants exhibiting oil-spot symptoms by incubating leaves overnight in darkness at 20 ± 0.5 °C and 100% RH to induce sporulation. Sporangia were collected by rinsing sporulating lesions on the abaxial leaf surface with cold (4-5 °C) sterile distilled water. The suspension was adjusted to 2.5×10^5 sporangia/mL using a haemocytometer under a light microscope and used in all subsequent experiments.

4.3.5 Evaluation of plant protection efficacy of self-digestive solution of Lysobacter capsici *AZ78 on* Plasmopara viticola

To assess the effectiveness of SDS derived from *L. capsici* AZ78, treatments including L-SDS, D-SDS, L-SDS 1/10, and D-SDS 1/10 SDS collected at the different time points, were sprayed onto both adaxial and abaxial leaf surfaces of greenhouse-grown grapevine plants using a handheld sprayer. Sterile distilled water-treated plants served as untreated controls, while plants treated with the copper-based fungicide Coprantol Hi Bio (2 g/L) served as positive controls. PYKM and PYKM 1/10 treatments were included as medium controls corresponding to the SDS treatments. The treatments for full strength SDS (L-SDS and D-SDS) were as follows: (1) sterile distilled water (untreated); (2) copper-based fungicide Coprantol Hi Bio (2 g/L); (3) PYKM; (4) 24L-SDS; (5) 24D-SDS; (6) 48L-SDS; (7) 48D-SDS; (8) 72L-SDS; (9) 72D-SDS; (10) 96L-SDS; (11) 96D-SDS; (12) 120L-SDS; (13) 120D-SDS; (14) 144L-SDS; (15) 144D-SDS. The treatments for diluted (1/10) SDS (L-SDS 1/10 and D-SDS 1/10) were as follows: (1) sterile distilled water (untreated); (2) copper-based fungicide Coprantol Hi Bio (2 g/L); (3) PYKM 1/10; (4) 24L-SDS 1/10; (5) 24D-SDS 1/10; (6) 48L-SDS 1/10; (7) 48D-SDS 1/10; (8) 72L-SDS 1/10; (9) 72D-SDS 1/10; (10) 96L-SDS 1/10; (11) 96D-SDS 1/10; (12) 120L-SDS 1/10; (13) 120D-SDS 1/10; (14) 144L-SDS 1/10; (15) 144D-SDS 1/10. Following application, plants were maintained under greenhouse conditions at 25 ± 0.5 °C, 60-80% RH, and a 16 h light / 8 h dark photoperiod.

Twenty-four hours after treatment, the prepared sporangial suspension of *P. viticola* was uniformly applied to the abaxial surfaces of fully expanded leaves using a hand sprayer. Inoculated plants were incubated in darkness at 20 ± 0.5 °C and 80-99% RH for 24 h to promote infection. Subsequently, plants were transferred to 25 °C under 60-80% RH with a 16/8 h light/dark cycle. Six days post-inoculation, plants were again incubated in darkness at 20 ± 0.5 °C and 80-99% relative

humidity overnight to induce sporulation, as previously described (Puopolo *et al*., 2014b). Disease severity was evaluated at 7 days post-inoculation (dpi) according to the EPPO standard evaluation scale (EPPO, 2004). Each treatment included five biological replicates (five plants per replicate), and the experiment was independently repeated.

4.3.6 RNA extraction and qRT-PCR

Leaf samples were collected prior to *P. viticola* infection (T0) and 24 h post-inoculation (T1). For the gene expression analysis, the following experimental groups were sampled: (1) sterile distilled water (untreated); (2) copper-based fungicide Coprantol Hi Bio (2 g/L); (3) PYKM; (4) PYKM 1/10; (5) 96L-SDS; (6) 96L-SDS 1/10; (7) 96D-SDS; and (8) 96D-SDS 1/10. Three biological replicate sets of leaves were collected for each treatment in both T0 and T1 conditions, with each replicate comprising four to five leaves pooled together. The experiment was independently repeated twice. Collected leaves were flash-frozen in liquid nitrogen and stored at -80 °C until RNA extraction.

Frozen leaf samples were homogenized using a mixer mill (Retsch Technology GmbH) at 45 Hz for 60 s. Total RNA was extracted from the powdered leaf tissue using the Spectrum™ Plant Total RNA Kit (Sigma-Aldrich) according to the manufacturer's instructions. RNA concentration was measured with a Qubit 4 Fluorometer (Thermo Fisher Scientific) using the Qubit™ RNA High-Sensitivity Broad Range Assay Kit (Invitrogen, USA) and further assessed with a NanoDrop 800 spectrophotometer (Thermo Fisher Scientific). RNA integrity was verified by electrophoresis on a 1% agarose gel. Extracted RNA was treated with DNase I (Invitrogen, Life Technologies) to remove residual genomic DNA prior to cDNA synthesis. First-strand cDNA was synthesized from 1 µg of total RNA using SuperScript III reverse transcriptase (Invitrogen, Life Technologies) and oligo (dT) primers, as previously described (Lenzi *et al.*, 2016). The resulting cDNA was diluted 1:10 with nuclease-free water and stored at -20 °C until quantitative RT-PCR analysis was performed.

Quantitative RT-PCR was performed on three biological replicates per treatment, with three technical triplicates per sample. No-template controls (NTC, using nuclease-free water) and no-RT controls (NRT, using DNase-treated RNA) were included to monitor for contamination and genomic DNA amplification. Reactions were conducted using qPCRBIO SyGreen Blue mix (Eurobio Scientific, Les Ulis, France) on a CFX Opus 384 real-time system (Bio-Rad, Hercules, USA). PCRs were assembled in 384-well white plates with a final volume of 5 µL per well, containing 1X SYBR Green mix (*Taq* polymerase and dNTPs), gene-specific forward and reverse primers at optimized concentrations, and 1:10 diluted cDNA. Primers were designed using Primer-BLAST (NCBI) and Primer3web v4.1.0 (**Table 6**).

Thermal cycling conditions were initial denaturation at 95 °C for 3 min, followed by 40 cycles of 95 °C for 5 s and 60 °C for 30 s. Specificity was confirmed by melting curve analysis, with each reaction yielding a single amplicon of the expected melting temperature. Transcript levels were normalized to *VvEF1α* (elongation factor 1α; XM_002284888.3) and *Vv60SRP* (60S ribosomal protein L18; XM_002270599.3) using Bio-Rad CFX Manager v.4.1, with expression stability validated using the GeNorm algorithm. Cycle threshold (Ct) values were determined with Maestro software using the second derivative maximum method, and relative expression was calculated by the ΔΔCt method relative to the untreated control group according to (Marant *et al.*, 2025). Fold change was obtained using the formula: $2^{(-\Delta\Delta Ct)}$.

4.3.7 Phytoalexin extraction and analysis

Phytoalexins were extracted from grapevine leaves following the protocol of (Gruau *et al.*, 2015). Leaves corresponding to the treatments described in Section 4.3.6 were collected, immediately frozen in liquid nitrogen, and ground into a fine powder. For each sample, 200 mg of fresh tissue powder were weighed, transferred into sterile 2 mL microcentrifuge tubes, and stored at -80 °C until

analysis. For extraction, 1 mL of 85% methanol (per 200 mg fresh weight) was added at room temperature. Samples were vortexed for 10 s and incubated for 2 h at 800 rpm on a rotary tube shaker in the dark. After centrifugation at 15,000 × g for 10 min at 4 °C, the supernatant was collected into 5 mL glass tubes, covered with aluminium foil. The pellet was re-extracted with 1 mL of 100% methanol, incubated for 1 h at room temperature in the dark, and centrifuged under the same conditions. The resulting supernatant was pooled with the first extract and evaporated to dryness using a SpeedVac concentrator in solvent evaporation mode at 40 °C, under dark conditions. The dried residues were resuspended in 1 mL of 100% methanol, vortexed, filtered through 0.22 µm polytetrafluoroethylene filters and transferred to 2 mL tinted ultra-performance liquid chromatography (UPLC) vials. Samples were analysed immediately or stored at -20 °C in the dark until use.

Phytoalexin analysis was performed using an Acquity Ultra Performance Liquid Chromatography (UPLC) system (Waters Corp.) coupled to a fluorescence detector. A 2 µL aliquot of each extract was injected onto an Acquity UPLC Cortex C18 column (1.6 µm, 2.1 × 100 mm) maintained at 40 °C. Separation was achieved using a binary gradient of water (A) and acetonitrile containing 0.1% phosphoric acid (B) at a flow rate of 0.5 mL/min. The gradient program was: 90% A initially; decreased to 10% A at 7 min; 0% A at 7.5 min (held until 8 min); returned to initial condition (90% A) at 8.5 min; and maintained until 10 min. Fluorescence detection was carried out an excitation wavelength of 330 nm and an emission wavelength of 375 nm. Data acquisition and processing were conducted using Empower 2 software (Waters), and quantification was performed by external calibration with authentic standards. Each treatment consisted of five biological replicates, and the experiment was independently repeated.

4.3.8 Statistical analysis

Disease severity data from all experiments were analysed using one-way analysis of variance (ANOVA) in R v4.3.0 (RStudio v2024.12.1-563 environment). Data normality was assessed using the Shapiro–Wilk test ($p > 0.05$), and homogeneity of variances was verified using Levene's test. When assumptions were met, mean comparisons were performed using Tukey's honestly significant difference (HSD) post hoc test implemented via the *emmeans* (v1.10.0) and *agricolae* (v1.3-7) packages, with adjustment for multiple comparisons at a significance level of $\alpha = 0.05$. Gene expression and phytoalexin accumulation experiments were conducted twice. Data obtained from these experiments were also analysed using one-way ANOVA followed by Tukey's HSD post hoc test in R ($\alpha = 0.05$) to determine statistically significant differences among treatments.

4.4 Results

4.4.1 Growth curve

The growth curve shows that *L. capsici* AZ78 cultivated in PYKM medium over a 144 h period **was monitored by measuring optical density at 600 nm (OD_{600})**. Bacterial growth was monitored at 24 h intervals from inoculation (0 h) to 144 h. The strain exhibited a very short lag phase, rapidly transitioning into the exponential phase by 24 h. Exponential growth continued progressively, with **OD_{600} values increasing steadily up to 96 h**. After 96 h, the culture entered a stationary/decline phasecharacterized by a progressive reduction in OD_{600} values, which persisted until the final time point at 144 h (**Figure 16**). For each time point, five biological replicates were analysed, and data from two independent experiments were pooled **prior to statistical analysis**.

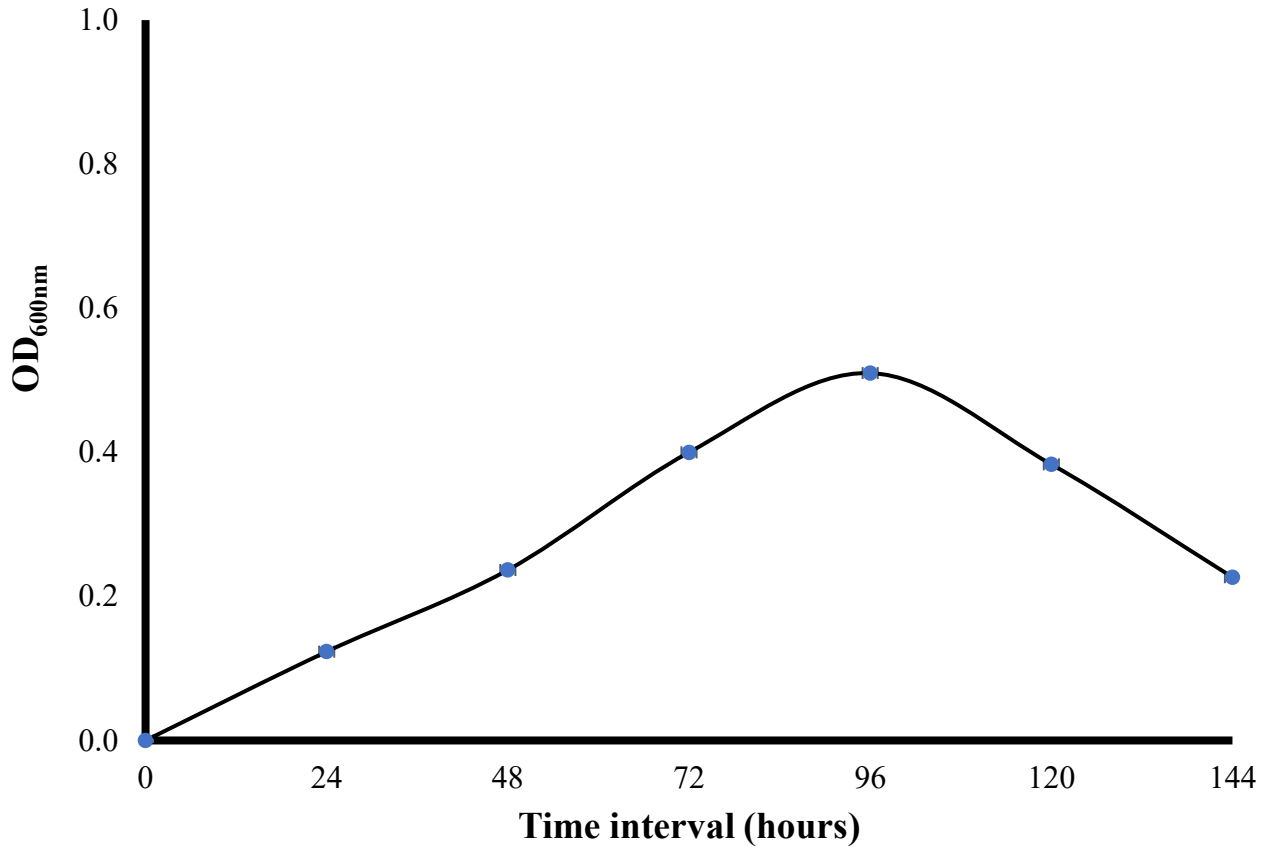

Figure 16. Growth curve of *Lysobacter capsici* AZ78 grown in PYKM medium under controlled conditions. Bacterial growth was monitored by measuring optical density at 600 nm (OD_{600nm}) at 0, 24, 48, 96, 120, and 144 h after inoculation. Data are presented as mean ± standard error.

4.4.2 Protective efficacy of Lysobacter capsici *AZ78 self-digestive solution against* Plasmopara viticola *on grapevine plants*

The protective activity of L-SDS and D-SDS obtained at different time points was evaluated on grapevine plants inoculated with *P. viticola*. Untreated plants exhibited the highest disease severity (63.43 ± 2.36%), followed by the copper-based fungicide, which significantly reduced disease severity to 14.81 ± 8.37%. The media control PYKM also resulted in comparable disease suppression (18.72 ± 3.93%), indicating a contributory effect of the medium itself.

Among the SDS treatments, L-SDS and D-SDS collected at 24 h, 48 h, and 72 h reduced disease severity to a range of 11-15%, which was significantly lower than the untreated control. However, these values were only slightly lower than those observed for the copper-based fungicide and PYKM, suggesting a moderate protective effect at earlier time points. A stronger protective effect was observed for SDS obtained from 96 h onward. The lowest disease severity was recorded at 96 h, with 96L-SDS showing 3.15 ± 1.47%, followed by 96D-SDS with 7.79 ± 1.53%. Treatments collected at 120 h and 144 h maintained disease severity within the range of 5–11%, remaining significantly lower than those observed for the 24-72 h treatments. Nevertheless, no statistically significant differences were detected among the copper-based fungicide, PYKM, and SDS treatments at full concentration (**Figure 17**).

When applied at 1/10 dilution, PYKM 1/10 showed reduced protective efficacy, with disease severity increasing to 40.21 ± 2.13%. In contrast, diluted SDS treatments maintained strong protective activity. The lowest disease severity was observed with 96L-SDS 1/10 (8.79 ± 2.09%), followed by 96D-SDS 1/10 (9.93 ± 2.04%). These values were lower than those recorded for the copper-based fungicide, indicating a **high level of efficacy even after dilution**.. Overall, these results indicate that SDS obtained at **96 h provides optimal protection** against *P. viticola* (**Figure 18**).

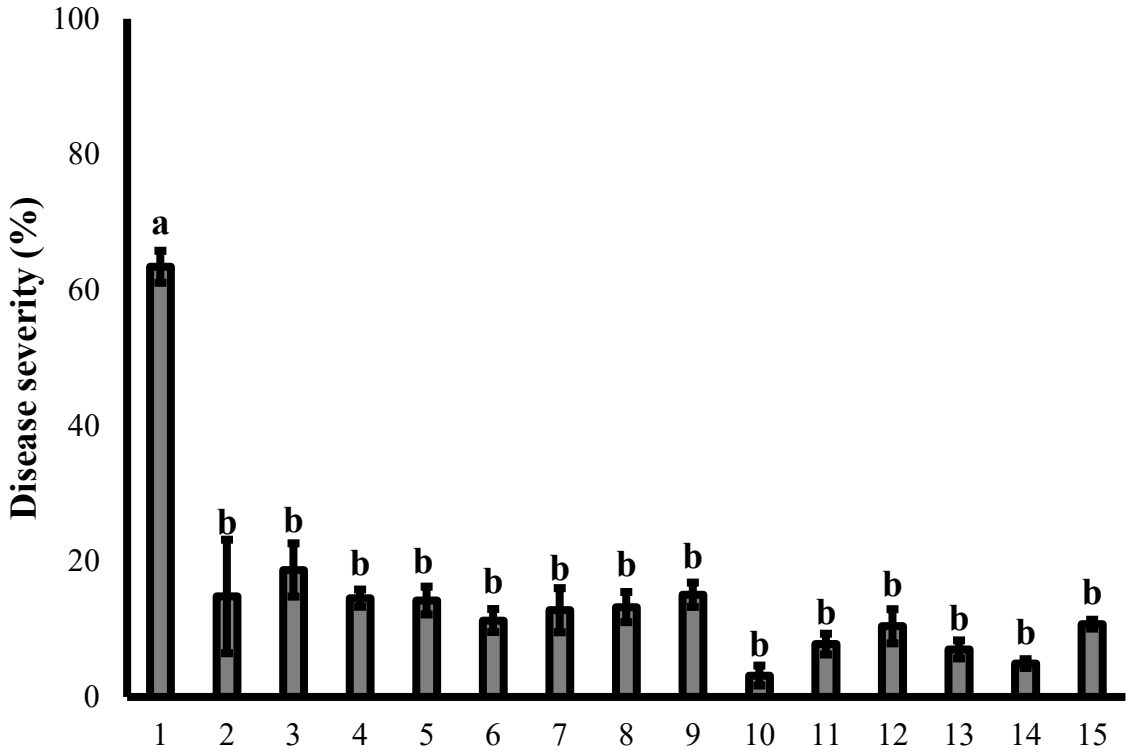

Figure 17. Preventive control of *Plasmopara viticola* infection on grapevine plants following application of full-strength unheated (L) and heat-treated (D) self-digestive solutions (SDS) derived from *Lysobacter capsici* AZ78. Treatments included: (1) sterile distilled water (untreated control); (2) copper-based fungicide Coprantol Hi Bio (2 g/L); (3) PYKM medium control; and SDS collected at different incubation times: (4) 24L-SDS; (5) 24D-SDS; (6) 48L-SDS; (7) 48D-SDS; (8) 72L-SDS; (9) 72D-SDS; (10) 96L-SDS; (11) 96D-SDS; (12) 120L-SDS; (13) 120D-SDS; (14) 144L-SDS; and (15) 144D-SDS. Treatments were applied 24 h prior to *P. viticola* inoculation. Disease severity is expressed as the mean percentage of symptomatic grapevine leaf disc area ± standard error (n = 5). Columns bearing the same letters are not significantly different according to Tukey's HSD test ($\alpha = 0.05$).

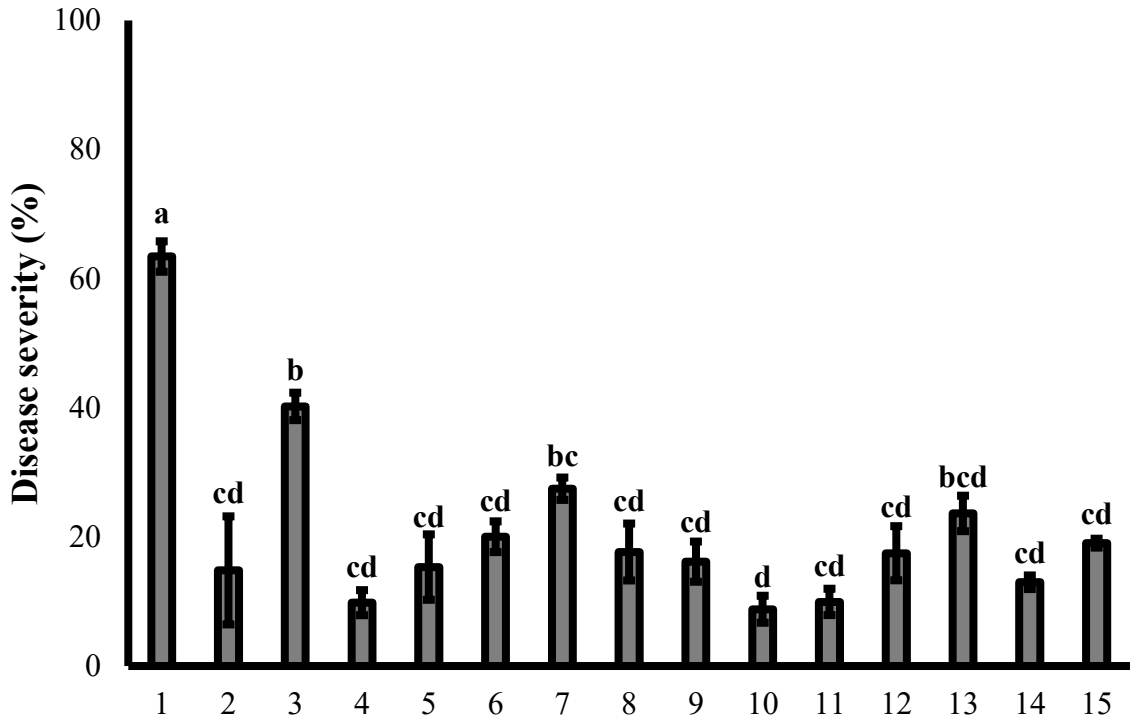

Figure 18. Preventive control of *Plasmopara viticola* infection on grapevine plants following application of diluted (1/10) unheated (L) and heat-treated (D) self-digestive solutions (SDS) derived from *Lysobacter capsici* AZ78. Treatments included: (1) sterile distilled water (untreated control); (2) copper-based fungicide Coprantol Hi Bio (2 g L^{-1}); (3) PYKM 1/10 medium control; and SDS collected at different incubation times: (4) 24L-SDS 1/10; (5) 24D-SDS 1/10; (6) 48L-SDS 1/10; (7) 48D-SDS 1/10; (8) 72L-SDS 1/10; (9) 72D-SDS 1/10; (10) 96L-SDS 1/10; (11) 96D-SDS 1/10; (12) 120L-SDS 1/10; (13) 120D-SDS 1/10; (14) 144L-SDS 1/10; (15) 144D-SDS 1/10.. Treatments were applied 24 h prior to *P. viticola* inoculation. Disease severity is expressed as the mean percentage of symptomatic grapevine leaf disc area ± standard error (n = 5). Columns sharing the same letters are not significantly different according to Tukey's HSD test ($\alpha = 0.05$).

4.4.3 Lysobacter capsici *AZ78 derived self-digestive solution primes grapevine plants and induces immune responses upon challenge with* Plasmopara viticola

Gene expression analysis was organized into five functional categories, including structural defense–related genes, signalling and hormone biosynthesis genes, pathogenesis-related (*PR*) effector genes, defense-related transcription factors, and phytoalexin biosynthesis genes. Relative transcript abundance was quantified using the $2^{-\Delta\Delta Ct}$ method and is therefore presented as fold change relative

to the untreated control at T0. Overall, inoculation with *P. viticola* (T1) induced a general transcriptional activation across all tested genes, whereas untreated plants showed **stable expression levels between T0 and T1**, indicating that pathogen challenge was the principal driver of gene induction in SDS treated plants.

Control treatments (untreated, copper-based fungicide, PYKM, and PYKM 1/10) consistently exhibited low basal expression levels at both time points, suggesting limited activation of defense pathways under these conditions (Fig. 19). Among structural defense genes, *CalS7* and *HSR* showed negligible upregulation at T0 across all treatments; however, following inoculation, SDS-based treatments triggered marked induction. For *CalS7*, full-strength treatments (96L-SDS and 96D-SDS) showed the highest fold change, followed by their diluted (1/10) counterparts, whereas *HSR* expression was most strongly induced by 96D-SDS, with comparatively lower induction in 96L-SDS (**Figure 19**). Regarding signalling and hormone biosynthesis genes, *ACO* expression was higher in diluted SDS treatments (96L-SDS 1/10 and 96D-SDS 1/10), whereas *AOC* showed stronger induction under full-strength SDS treatments compared to diluted forms. For *LOX9*, the highest fold change was observed in 96L-SDS 1/10, followed by 96D-SDS 1/10, while 96D-SDS displayed expression levels comparable to control treatments at T1. In the case of *PR* effector genes, *PR2* and *PR3* remained at basal levels in control treatments at both time points (T0 and T1), whereas full-strength SDS treatments significantly increased fold change, with 96D-SDS showing particularly strong induction of *PR3*. For defense-related transcription factors, *ERF1* exhibited higher fold change in diluted SDS treatments compared to full-strength treatments, while *JAZ1* showed the opposite trend, with stronger induction under full-strength SDS conditions. Finally, phytoalexin-related genes *PAL* and *STS* showed basal fold change at T0 and in all T1 control treatments; however, *PAL* was most strongly induced by

96L-SDS 1/10, whereas *STS* displayed **moderate but consistent induction across all SDS treatments at T1**, indicating a **less treatment-dependent response pattern** (**Figure 19**).

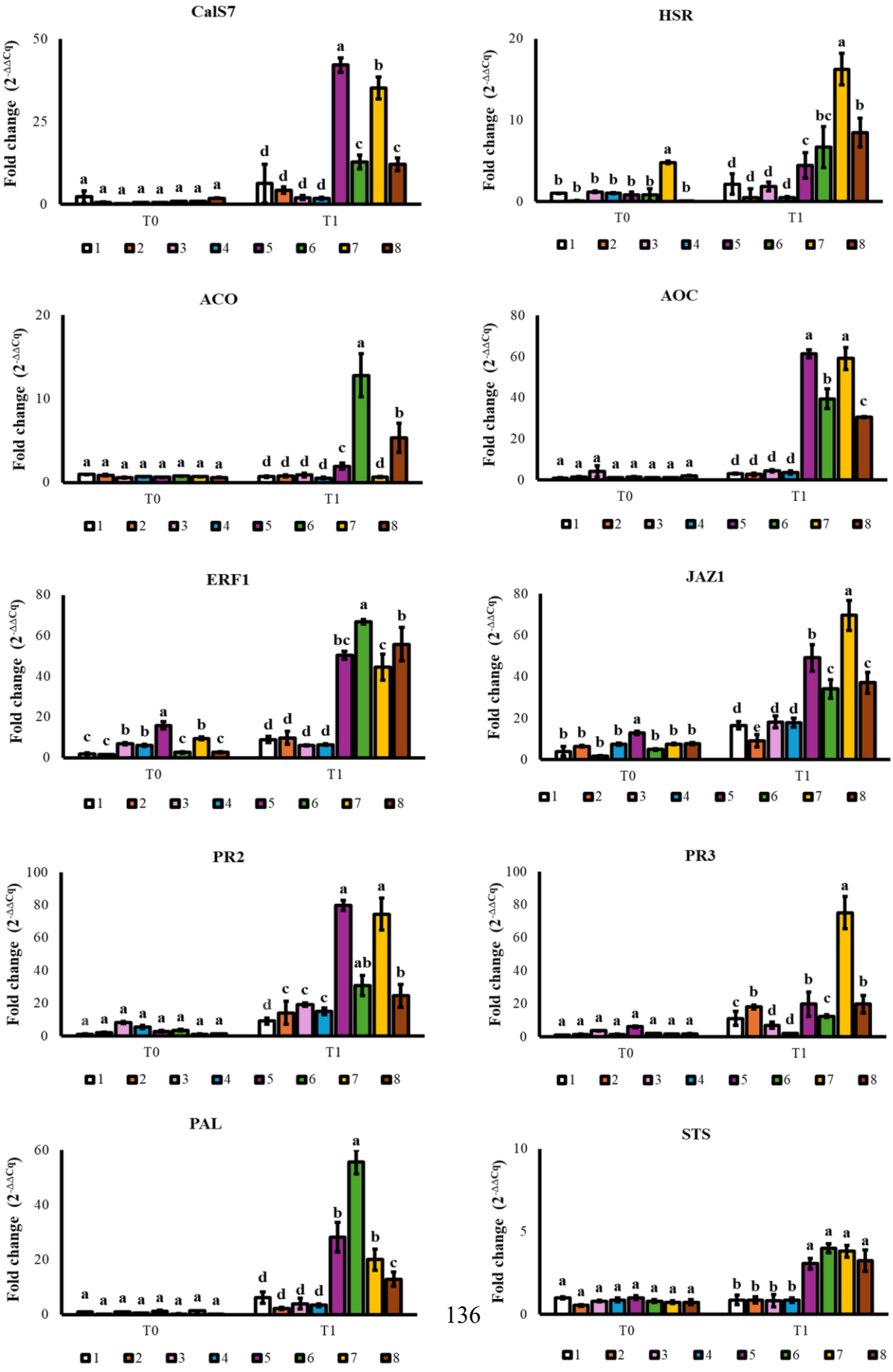
CalS7
HSR
ACO
AOC
ERF1
JAZ1
PR2
PR3
PAL
STS
Fold change (2-ΔΔCq)
T0
T1
1 2 3 4 5 6 7 8

Figure 19. Gene expression analysis in grapevine plants following treatment with (1) sterile distilled water (untreated control); (2) copper-based fungicide Coprantol Hi Bio (2 g/L); (3) PYKM medium; (4) PYKM diluted 1/10 (medium controls); and SDS collected after 96 h incubation: (5) 96L-SDS; (6) 96L-SDS 1/10; (7) 96D-SDS; and (8) 96D-SDS 1/10. Relative expression levels of *CalS7, HSR, ACO, AOC, LOX9, ERF1, JAZ1, PR2, PR3, PAL*, and *STS* were evaluated at T0 (before *Plasmopara viticola* inoculation) and T1 (24 h post inoculation). Gene expression levels were quantified by qRT-PCR and expressed as relative expression values [fold change ($2^{-\Delta\Delta Cq}$)]. Error bars represent mean ± standard error (n = 3). One-way analysis of variance (ANOVA) was conducted separately for each time point (T0 and T1), followed by Tukey's honestly significant difference (HSD) test ($\alpha = 0.05$). Columns sharing the same letter are not significantly different among treatments within the same time point.

Table 6. Primer sequences used for gene expression

Type	Genes	Gene description	Forward Primer/Reverse Primer Sequence	Accession number	Amplicon size (bp)
Reference genes	*Vv60SRP*	60S ribosomal protein L18	ATCTACCTCAAGCTCCTAGTC/ CAATCTTGTCCTCCTTCCCT	XM_002270599.3	166
	VvEF1α	Elongation factor 1-alpha	AACCAAAATATCCGGAGTAAAAGA/ GAACTGGGTGCTTGATAGGC	XM_002284888.3 / GU585871	150
Genes analysed	*VvGluc/PR2*	Class I beta-1,3-glucanase / Laminarinase	TCAATGGCTGCAATGGTGC/ CGGTCGATGTTGCGAGATTTA	NM_001280967.2 /DQ267748	155
	VvChit4c/ PR3	Class IV chitinase	TCCCCTGTCGAAACACCAAG/ TCGAATGCGATGGTGGAAA	NM_001281244.1	91
	VvHSR	Serine hydrolase-like	GGGACAGTGCTGGAGGAAAC/ ATCCAGTCGGTTAATGCCAAA	NM_001281193.1	181

VvACC/ACO	1-aminocyclopropane-1-carboxylate oxidase	AAGGTCAGCAACTACCCTCC/ CGCATGGGTGGAACATCAAT	XM_002273394.3	158
VvAOC	allene oxide cyclase	TGGGAGTAACAGCGGGGATA/ CCTGCACCGATATGTGACCA	NM_001280971.1	117
VvERF1	Ethylene response factor	CGGTGGTGGCGCTCAAGAGG/ TCACCCAGAAGAATCAACGGCTCT	AM443915.2	91
VvJAZ1	Jasmonate ZIM-Domain protein 1	GAGAAGGGCACGTTTGGAGA/ CATCGTCGTTGTTGTCGCTG	XM_002277121.3	102
VvCalS7	Callose synthase 7	AGAGGATACGGTGGGTGGAA/ GTTTGCACAGCTTCTCCACG	OZ353804.1	91
VvNCED-2	9-cis-epoxycarotenoid dioxygenase 2	CTCTTGGCCATGTCGGAAGA/ CGGAGCTGCTTGTCGAAGTC	NM_001281271	101
VvPAL	Phenylalanine ammonia-lyase	AGAAAATGCGTCCGGTTC/ TTGGCAAACACTGACGTCTC	XM_002268220.4 / X75967	101
VvSTS	Stilbene synthase	AGGAAGCAGCATTGAAGGCTC/	X76892 / NM_001281117 / FJ851185	101

		TGCACCAGGCATTTCTACACC		
VvLox9	Lipoxygenase	TTCCACCCACCTCGCCTGATG/ GCACCGCACCTGTTTCTTCG	AY159556 / NM_001281249.1 / XM_002280615.1	101

4.4.4 Lysobacter capsici *AZ78 derived self-digestive solution enhances phytoalexin accumulation in grapevine plants upon challenge with* Plasmopara viticola

To evaluate the role of *L. capsici* AZ78 in enhancing phytoalexin accumulation in grapevine plants challenged with *P. viticola*, phytoalexin levels were quantified at three time points: T0 (treated plants without pathogen inoculation), T24 (24 h post-inoculation), and T72 (72 h post-inoculation). Piceid content (μg/g fresh weight) showed no detectable accumulation at T0 across all treatments. Following pathogen inoculation, piceid levels increased at T24 in SDS-treated plants but declined at T72, whereas control treatments maintained relatively constant, lower concentrations across all time points (**Figure 20**). In contrast, resveratrol levels remained at basal concentrations in control plants throughout the experiment, while SDS-treated plants exhibited a progressive time-dependent increase, reaching maximum accumulation at T72. For trans-ε-viniferin, SDS-treated plants displayed the highest accumulation among all treatments, with a marked increase at T24 followed by a further gradual increase up to T72. Although control plants also showed a slight time-dependent increase in trans-ε-viniferin, their levels were consistently lower than those observed in SDS-treated plants. Overall, across all phytoalexins examined, control treatments exhibited basal or comparatively lower accumulation, whereas SDS treatments significantly enhanced phytoalexin production in response to pathogen challenge, highlighting a priming-like effect of SDS on stilbene biosynthesis (**Figure 20**).

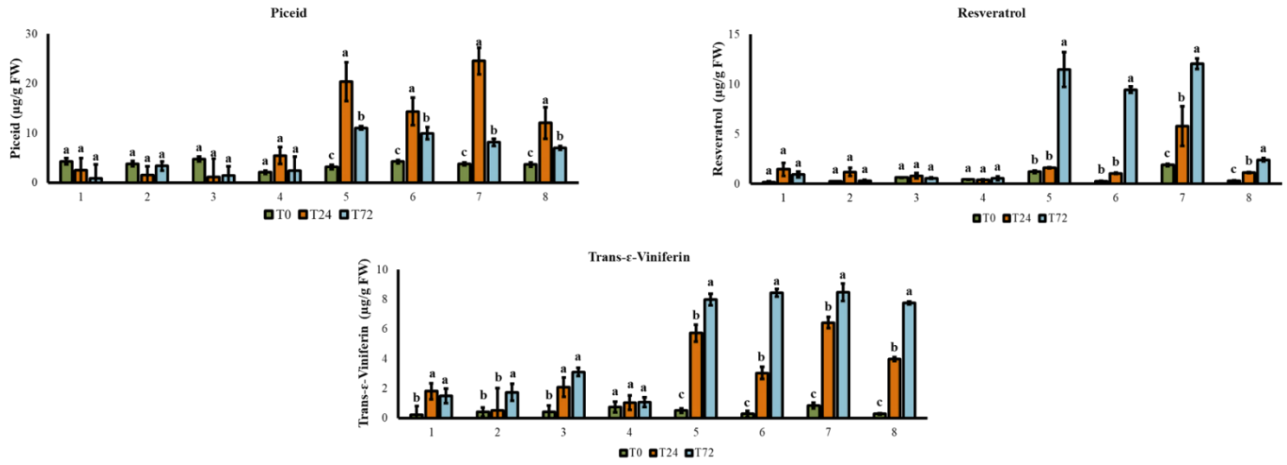

Figure 20. Phytoalexin production in grapevine leaves after treatment with self-digestive solutions (SDS) derived from *Lysobacter capsici* AZ78. Treatments included: (1) sterile distilled water (untreated control); (2) copper-based fungicide Coprantol Hi Bio (2 g/L); (3) PYKM medium; and (4) PYKM diluted 1:10 as medium controls; and SDS collected at 96 h incubation: (5) 96L-SDS; (6) 96L-SDS diluted 1:10; (7) 96D-SDS; and (8) 96D-SDS diluted 1:10. Phytoalexins piceid, resveratrol, and trans-ε-viniferin were quantified at T0 (before *Plasmopara viticola* inoculation), T24 (24 h after inoculation), and T72 (72 h after inoculation), and are expressed as µg/g fresh weight (FW). Error bars are shown as mean ± standard error, (n = 5). Columns sharing the same letter are not significantly different according to Tukey's honestly significant difference (HSD) test (α = 0.05).

4.5 Discussion

The present study aimed to elucidate the role of secondary metabolites enriched SDS in plant protection as well as to clarify the mechanisms underlying grapevine protection mediated by SDS derived from *L. capsici* AZ78. Members of the genus *Lysobacter* are well recognized for their rich antibiotic profiles and ability to produce diverse bioactive secondary metabolites with antagonistic activity against plant pathogens (Christensen and Cook 1978). Consistent with this, antibiotic profiling of *L. capsici* AZ78 previously revealed the production of multiple metabolite classes, including 2,5-diketopiperazines, cyclic lipodepsipeptides, and PTMs, compounds widely associated with antimicrobial and anti-oomycete activity (Puopolo *et al.*, 2016; Brescia *et al.*, 2021). Among these metabolites, PTMs represent a particularly relevant group due to their unique modes of action against fungal and oomycete pathogens, which differ from those of conventional antifungal compounds (Li

et al., 2006, 2009, 2021). PTMs such as heat-stable antifungal factor (HSAF) are commonly associated with bacterial membranes in *Lysobacter* spp. and can be released into the extracellular environment via outer membrane vesicles (OMVs), suggesting an important ecological role in microbe-plant interactions (Kudryakova *et al*.,2016; Meers *et al.*, 2018).

In our previous work, both viable and heat-inactivated *L. capsici* AZ78 cells provided significant protection against *P. viticola* in grapevine and *Peronospora belbahrii* in basil, achieving efficacy comparable to that of copper-based fungicides. Heat-treated *L. capsici* AZ78 cells retained the capacity to induce plant defense responses, including callose deposition and ROS accumulation, indicating that thermostable PTMs may be involved in plant protection activity. Subsequent extraction and chemical characterization of metabolites from heat-treated cells led to the identification of two thermostable PTMs, whose individual application reproduced disease protection and defense activation, demonstrating their role **independently of living bacterial cells**.

Building on these findings, the current study investigated the role of L-SDS and D-SDS derived from *L. capsici* AZ78 to further elucidate the molecular basis of grapevine plant protection. Earlier studies have demonstrated that species within the genus *Lysobacter* actively secrete extracellular enzymes and bioactive compounds into the surrounding environment (Christensen and Cook 1978). Moreover, secondary metabolite biosynthesis in bacteria is frequently enhanced during the transition from exponential to stationary growth phases, particularly under nutrient-limited conditions, while prolonged cultivation can promote cell lysis and subsequent accumulation of extracellular bioactive compounds in the culture medium (Tashiro *et al*., 2012; Almeida *et al*., 2017).

In our experiments using SDS derived from *L. capsici* AZ78 cultures, we observed that prolonged cultivation in liquid medium resulted in the accumulation of biologically active extracellular compounds associated with enhanced grapevine protection. Monitoring bacterial growth

over time showed that *L. capsici* AZ78 maintained exponential growth up to 96 h, after which a decline in cell density indicated the onset of autolytic processes. This phase likely promoted the release of membrane-associated PTMs and other bioactive metabolites into the culture supernatant. This observation is consistent with previous reports (Chen et al., 2020), which demonstrated that SDS of *L. enzymogenes* retains strong antimicrobial activity even after heat treatment and long-term storage due to extracellular enzymes and thermostable metabolites present in the culture filtrate.

In this regard, our experiments showed that the SDS collected at 96 h exhibited the highest plant protection efficacy against *P. viticola* in grapevine plants, outperforming SDS obtained at earlier or later time points at both full-strength and 1/10 dilution. Growth monitoring confirmed exponential growth up to 96 h, followed by declining cell density indicative of autolysis. Furthermore, D-SDS retained strong protective activity, confirming that the active components are heat-stable and supporting the involvement of thermostable metabolites in plant protection.. However, we observed that in the full strength SDS treatments, the medium control (PYKM) also showed protective efficacy. To rule out the involvement of media in plant protection, the treatments were diluted to 1/10 times and reapplied in another set of grapevine plants. Here we observed that the PYKM 1/10 treatment showed higher disease severity, whereas the 96 h SDS treatments retained protective ability (8.79 ± 2.09% in 96L-SDS 1/10 and 9.93 ± 2.04% in 96Hd-sds 1/10 disease severity) comparable to the commercial copper-based fungicide (14.81 ± 8.37% disease severity). Based on these results, subsequent analyses were focused on the 96 h time point.. This protection mediated by *L. capsici* AZ78 SDS is in line with the results demonstrated in the study by Chen *et al.* (2020), which exhibited protection potential against animal and plant-pathogenic fungal and oomycete pathogens. They detected the presence of several enzymes (phosphatase, protease and lysozyme) in the SDS of *L. enzymogenes* LE16. A study on *Bacillus subtilis* strain HA1 showed that the culture filtrates derived

from this BCA exhibited significant efficacy as a biocontrol agent against Tobacco mosaic virus in tomato under greenhouse conditions. Applying the culture filtrate to leaves before and after TMV inoculation improved plant growth and reduced viral accumulation by up to 91%. The treatment also improved the plant's defense responses by raising the levels of phenolics and flavonoids, boosting the activities of antioxidant enzymes (PPO, SOD, and POX), and lowering the levels of oxidative stress markers (H_2O_2 and MDA). Gene expression analysis demonstrated the upregulation of defense-related genes (*PR-1, PAL, CHS,* and *HQT*), signifying the activation of induced systemic resistance (El-gendi *et al.*, 2022). These results show that the BCAs can release antimicrobial compounds in their surrounding environment, which can help combat plant pathogens (Compant *et al.*, 2005).

Beyond direct antimicrobial effects, our results demonstrate that *L. capsici* AZ78-derived SDS also modulates grapevine defense responses. Hormonal regulation plays a central role in resistance to biotrophic pathogens and involves coordinated signalling among SA, JA, and ET pathways (S. Trouvelot *et al.*, 2008; Walters *et al.*, 2011; Gao *et al*., 2012). While SA signalling is classically associated with hypersensitive response (HR) and systemic acquired resistance (SAR), increasing evidence indicates that JA and ET signalling contribute significantly to resistance against *P. viticola*, particularly during early infection stages (Gauthier *et al*., 2014; Figueiredo *et al*., 2015). In this study, SDS treatment alone did not induce detectable defense gene expression prior to pathogen inoculation (T0), whereas strong transcriptional activation occurred following *P. viticola* challenge (T1). This pattern indicates that *L. capsici* AZ78-derived metabolites function primarily through **immune priming rather than constitutive activation of defense responses**.. Priming enables plants to maintain a sensitized physiological state that allows faster and stronger defense activation upon pathogen attack (Thomma *et al*., 2001; Mian *et al*., 2023; Verhagen *et al*., 2010). The absence of basal

induction in SDS treated grapevine plants before *P. viticola* inoculation strongly supports this mechanism.

The transcriptional responses observed encompassed structural defense genes (*CalS7, HSR*), hormone biosynthesis and signalling genes (*ACO, LOX9, AOC*), transcription factors (*ERF1, JAZ1*), pathogenesis-related proteins (*PR2, PR3*), and secondary metabolism markers (*PAL, STS*), collectively indicating activation of a multilayered immune response in grapevine following treatment and pathogen challenge.

Structural defense mechanisms represent the earliest barriers restricting pathogen establishment. The strong induction of *CalS7* in SDS treated plants after *P. viticola* inoculation correlates with callose deposition, a well-established defense response that reinforces cell walls and limits pathogen penetration at stomatal entry sites (Brown *et al.*, 1998; Gomez-Gomez *et al*., 1999; Yang *et al.*, 2015b). This transcriptional activation is consistent with our previous observations showing callose accumulation induced by *L. capsici* AZ78 viable and heat-treated cells and purified PTMs even at low concentrations (2.5 mg/L), suggesting that these metabolites prime physical defense barriers prior to infection. **In this study, we also observed that D-SDS was able to induce the expression of CalS7, similar to L-SDS**,, underlining the role of thermostable metabolites in gene regulation in infected plants. Similarly, increased *HSR* expression indicates activation of HR associated processes, including localized programmed cell death and ROS production, both commonly linked to resistance against *P. viticola* and restriction of biotrophic pathogen spread (Xing *et al*., 1997; Kawasaki *et al.*, 1999). In our experiments we **observed elevated HSR expression in D-SDS-treated plants, whereas it was lower in L-SDS-treated plants**. Notably, comparable activation of HR related mechanisms has been reported in resistant grapevine cultivars during incompatible interactions with *P. viticola*, where rapid ROS accumulation and localized cell death contribute to the effective limitation of pathogen

colonization (Gauthier *et al.*, 2014; Figueiredo *et al*., 2015). This result is also in accordance with our previous studies where we observed that *L. capsici* AZ78 cells (viable and heat-treated) ROS production in response to infection by *P. viticola* and *P. belbahrii* in grapevine and basil leaf discs, respectively.

Hormone-mediated defense pathways play a central role in grapevine responses to *P. viticola*, with ET and JA pathways being particularly critical. The SDS treatments derived from *L. capsici* AZ78 strongly induced key genes involved in these pathways. *ACO* encodes a rate-limiting enzyme in ethylene biosynthesis, catalysing the conversion of ACC to ethylene, and its upregulation following pathogen inoculation indicates that SDS primes plants for enhanced ET production, a hormonal signal essential for activating defense-related transcription factors and downstream defense genes (Glazebrook, 2005; Yang and Hoffman, 1984). Additionally, genes involved in JA biosynthesis, including *AOC* and *LOX9* were also strongly upregulated. *AOC* mediates the formation of 12-oxophytodienoic acid (OPDA), a critical intermediate in JA biosynthesis, while *LOX9* catalyses the oxidation of polyunsaturated fatty acids, providing substrates for JA production (Dave and Graham, 2012; Park et al., 2010). This coordinated activation of *LOX9* and *AOC* indicates that SDS primes JA synthesis, enabling rapid JA accumulation upon pathogen challenge. The induction of *JAZ1*, a transcriptional repressor of JA-responsive genes, reflects the dynamic regulation of the JA pathway, where pathogen-triggered degradation of pre-existing *JAZ* proteins releases JA-responsive transcription factors such as *MYC2*, followed by de novo *JAZ* synthesis to fine-tune defense responses (Tripathi *et al.*, 2018). Notably, similar patterns of *ACO, AOC*, and *LOX9* induction have been observed in resistant grapevine cultivars during *P. viticola* infection, supporting the role of coordinated JA and ET signalling in effective disease resistance (Gauthier *et al*., 2014; Figueiredo *et al*., 2015; Polesani *et al*., 2010). The upregulation of these genes in SDS-treated plants after pathogen

inoculation demonstrates that *L. capsici* AZ78 metabolites prime grapevine for enhanced JA- and ET-mediated defense, contributing to a robust, multi-layered immune response.

Simultaneously, the *ERF1* gene encodes an ethylene response factor that integrates multiple hormonal signals, particularly ET, JA, SA to orchestrate defense responses. In our study, SDS-treated grapevine plants exhibited strong *ERF1* induction in 1/10 diluted SDS treatments. *ERF1* acts as a central regulatory node that activates downstream defense genes, including *PR* proteins, and modulates JA/ET-responsive pathways, thereby coordinating transcriptional reprogramming during pathogen attack (Müller and Munné-bosch, 2015; Dong *et al*., 2015; C. Xing *et al*., 2023; Xing *et al*., 2017).

Downstream of hormone signalling and transcriptional regulation, *PR2* (β-1,3-glucanase) and *PR3* (chitinase) proteins constitute critical components of grapevine defense against *P. viticola*. In SDS-treated plants, PR2 expression was strongly induced in both L-SDS- and D-SDS-treated plants, whereas *PR3* was strongly induced only in D-SDS treated plants after pathogen inoculation, consistent with the concept of priming. These enzymes degrade pathogen cell walls, with *PR2* targeting β-1,3-glucans and PR3 hydrolysing chitin, thereby limiting pathogen colonization and spread (Adams, 2004; Singh and Singh, 2018). Their activation also contributes to SAR, which is largely SA-dependent, and reflects hormonal crosstalk. Importantly, the induction pattern observed in SDS-treated plants parallels that reported in resistant grapevine cultivars challenged with *P. viticola*, further supporting the role of *PR2* and *PR3* in effective biotrophic pathogen restriction (Giannakis *et al*., 1998; Polesani *et al*., 2010). The basal expression of these genes in untreated or copper-treated plants, including media controls, confirms that their upregulation in SDS-treated plants is specifically associated with pathogen-activated priming by *L. capsici* AZ78 SDS. Furthermore, the upregulation of all these genes

in D-SDS as well as D-SDS 1/10 treatments suggests the involvement of thermostable metabolites released by *L. capsici* AZ78 into the SDS.

Activation of secondary metabolism represents a crucial downstream component of grapevine defense against *P. viticola*, particularly through the phenylpropanoid and stilbene biosynthetic pathways. In the present study, SDS treatments derived from *L. capsici* AZ78 significantly induced the expression of *PAL* and *STS* following pathogen inoculation, indicating activation of phytoalexin-associated defense responses. *PAL* catalyses the first committed step of the phenylpropanoid pathway, linking primary metabolism to the biosynthesis of diverse defense-related compounds, including phenolics, lignin precursors, and salicylic acid, all of which contribute to reinforcement of plant immunity (Saigne-Soulard *et al*., 2015). Downstream of *PAL* activity, *STS* catalyses the formation of resveratrol (trans-3,5,4′-trihydroxystilbene), a key grapevine phytoalexin synthesized in response to biotic and abiotic stresses (Favaron *et al*., 2009). Increased expression of *PAL* and *STS* in SDS-treated plants corresponded with enhanced accumulation of stilbenes, including piceid and trans-ε-viniferin, compounds widely recognized for their antimicrobial activity against oomycete pathogens (Hain *et al*., 1993; Khattab *et al*., 2021; Marti *et al*., 2014; Latruffe and Vervandier-Fasseur, 2018). Stilbene accumulation is a hallmark of resistant grapevine cultivars, which typically produce higher concentrations of resveratrol derivatives and viniferins compared with susceptible genotypes (Alonso-villaverde *et al.*, 2011). Similar activation of *PAL* and *STS* pathways has been reported in resistant grapevine interactions with pathogens such as *Botrytis cinerea* and following application of resistance-inducing compounds, further supporting the association between stilbene accumulation and disease resistance (Tziros *et al*., 2022). In our experiments, we observed that SDS treatments enhanced gene upregulation and led to significant accumulation of phytoalexins following *P. viticola* inoculation. Analysis of phytoalexins by UPHLC revealed elevated levels of piceid, resveratrol and

its dimer, trans-ε-viniferin, in SDS-treated plants. The accumulation pattern was particularly notable over time, with resveratrol and trans-ε-viniferin levels increasing progressively after pathogen challenge, demonstrating that SDS primes the grapevine for an amplified secondary metabolite response upon infection, which progresses overtime. Importantly, this effect was observed with both full-strength and diluted SDS treatments, although full-strength SDS generally induced higher phytoalexin accumulation. These findings align with previous reports in resistant grapevine cultivars, which similarly produce elevated levels of resveratrol derivatives and viniferins in response to biotic stress, reinforcing their role as biochemical barriers to pathogen establishment (Mijailovic *et al*., 2022).

Taken together, these results demonstrate that SDS derived from *L. capsici* AZ78 provides grapevine protection through a combination of direct antimicrobial activity and indirect priming of host defense and phytoalexin accumulation. The SDS contains antimicrobial and thermostable bioactive metabolites capable of both restricting *P. viticola* growth and enhancing grapevine immune responses upon pathogen challenge, thereby exhibiting dual mode of action against the pathogen. Importantly, the enhanced phytoalexin accumulation observed over time reflects a sustained and pathogen-responsive chemical barrier, complementing the transcriptional activation of defense genes. These defense responses were observed only after pathogen inoculation, confirming the priming effect of SDS. Overall, the findings underscore the relevance of SDS as a biologically active formulation, even in its heat-treated and diluted state capable of integrating pathogen suppression, phytoalexin-mediated chemical defense, and host immune activation.

4.6 Conclusions

This study provides the first comprehensive evidence that SDS derived from *L. capsici* AZ78 (L-SDS and D-SDS) functions as an effective biocontrol strategy against *P. viticola* by combining

direct antimicrobial effects with induced systemic resistance in grapevine. The SDS was found to be active in its heat-inactivated sate as well as in its diluted form against *P. viticola.* Our findings demonstrate that thermostable metabolites released during bacterial autolysis not only suppress pathogen growth but also prime multiple layers of host immunity, including structural defense, hormone signalling, *PR* protein activation, and the accumulation of phytoalexins such as piceid, resveratrol and trans-ε-vaneferin. Notably, these results are consistent with our previous work showing that both viable and heat-inactivated *L. capsici* AZ78 cells, as well as purified PTMs, could trigger callose deposition, ROS accumulation, and disease protection, supporting the role of membrane-associated thermostable PTMs in plant defense. The ability of SDS to enhance phytoalexin production upon pathogen challenge highlights its role in reinforcing chemical barriers critical for disease resistance. By elucidating the molecular, biochemical, and metabolite-based mechanisms underlying SDS-mediated protection, this work emphasizes the potential of *L. capsici* AZ78 derived SDS as a sustainable and multifunctional alternative to chemical fungicides and provides new insights into the mode of action underlying its role as a biocontrol agent.

CHAPTER 5

SOIL SUPPRESSION OF *PYTHIUM ULTIMUM* BY *LYSOBACTER CAPSICI* AZ78: CONTRIBUTIONS OF ORGANIC AMENDMENTS, BACTERIAL CELLS, VOLATILE-MEDIATED ACTIVITY, AND SOIL MICROBIOME MODULATION

Abstract

Soil-borne oomycete plant pathogens represent a major constraint to agricultural productivity due to their persistence in soil and the severe crop losses they cause. Among them, *Pythium ultimum*, the causal agent of damping-off disease in a wide range of hosts, is particularly difficult to manage because of its high infectivity and ability to survive under diverse soil conditions. In this study, we evaluated the biocontrol potential of *Lysobacter capsici* AZ78 against *P. ultimum* under soil conditions using tomato as a host plant. Specifically, we investigated the relative contributions of bacterial cells and bacterial volatiles to pathogen suppression through the modulation of soil properties. Both *L. capsici* AZ78 cells and their volatiles significantly altered soil pH and ammonia concentration, generating conditions unfavourable for pathogen development. Volatilome analysis revealed the production of multiple antimicrobial volatile organic compounds, such as mono-alkyl and di-alkyl methylpyrazines which have been previously reported to inhibit *P. ultimum* and other soil-borne pathogens. Greenhouse experiments demonstrated that both *L. capsici* AZ78 cells and volatiles effectively suppressed disease and increased tomato seed germination, indicating plant growth-promoting effects in addition to biocontrol activity. The application of nutrient-rich organic amendments further enhanced these beneficial effects. Shotgun metagenomic analysis revealed that *L. capsici* AZ78 treatments differentially reshaped soil microbial communities, particularly when combined with hoof meal amendment, which resulted in the highest seed germination and disease

suppression. Microbiome shifts were associated with enrichment of taxa linked to disease suppression and nitrogen cycling. Functional metagenomics further showed that *L. capsici* AZ78 treatments restructured soil nitrogen metabolism by promoting microbial nitrogen assimilation via the glutamine synthase-glutamate synthase (GS-GOGAT) pathway and enhancing dissimilatory nitrate reduction, leading to increased ammonium availability and elevated soil pH, while nitrification remained a minor pathway. Collectively, these findings demonstrate that *L. capsici* AZ78 suppresses *P. ultimum* through an integrated mechanism involving bacterial cells, volatile-mediated soil modification, microbiome restructuring, and nitrogen-cycle-driven changes in soil properties. This study provides new mechanistic insight into how *L. capsici* AZ78 and organic amendments interact to create disease-suppressive soils, highlighting it as a promising strategy for sustainable management of soil-borne oomycete plant pathogens.

Keywords: *Lysobacter capsici* AZ78, *Pythium ultimum*, organic amendments, volatile organic compounds, soil microbiome, nitrogen cycling.

5.1 Introduction

Soil-borne fungal and oomycete plant pathogens represent some of the most destructive threats to global crop production and food security (Kamoun *et al.*, 2015). Their persistence in soil ecosystems and their ability to produce long-lived survival structures, such as spores and sclerotia, enable recurrent infections and make their management particularly challenging (Ruano-Rosa and Mercado-Blanco, 2015). Among these pathogens, species belonging to the genus *Pythium* affect a wide range of crop, pasture, and orchard plants due to their broad host range. *Pythium ultimum* is especially notorious for causing damping-off diseases, leading to severe yield losses by killing seedlings before or shortly after emergence (Hendrix and Campbell., 1973). Conventional management strategies rely largely on chemical fungicides, crop rotation, and resistant cultivars; however, these approaches often provide only partial or temporary control and raise serious concerns related to environmental sustainability, human health, and the emergence of pathogen resistance (Parry *et al*., 1995; Nguyen *et al.*, 2016).

Given the challenges, increasing attention has been given to understanding the functional roles of beneficial microbes in soil microbial interactions and the suppression of soil-borne pathogens. Among the known beneficial microbes, biological control agents (BCAs) and plant growth-promoting rhizobacteria (PGPR) represent a diverse group of microorganisms capable of inhibiting or suppressing soil-borne pathogens and protecting host plants (Morra *et al*., 2010; Hakim *et al*., 2021; Callaghan 2016). Many beneficial microbes exhibit overlapping functions, acting simultaneously as BCAs and PGPRs, often working synergistically by deploying a complex array of mechanisms to counter pathogen invasion (Sheoran *et al.*, 2025). They can compete with plant pathogens in the soil for resources and space as well as inhibit their growth through direct antagonism (Alqahtani, 2025).

In addition, they can produce a variety of antimicrobial substances, including lipopeptides, biosurfactants, enzymes, and volatile organic compounds (VOCs), as well as induce resistance mechanisms in host plants which contributes to pathogen suppression (Caulier *et al*., 2019; Gao *et al*., 2021; Compant *et al*., 2005).

Among the antimicrobial compounds, VOCs have garnered significant attention due to their low molecular weight (<300 Da), which allows them to diffuse over longer distances in soil microenvironments (Chuankun *et al.*, 2004). Numerous studies have demonstrated that bacterial VOCs can inhibit the growth of soil-borne pathogens, while simultaneously promoting plant defense and growth (Syed-ab-rahman *et al.*, 2019; Costa Almeida *et al.*, 2023; Ávila-Oviedo *et al.*, 2024). VOCs produced by microbes belong to diverse chemical classes, including alcohols (1-butanol, 3-methyl-1-butanol), ketones (2-nonanone, 2-heptanone), pyrazines (2,5-dimethylpyrazine, 2-methylpyrazine), and sulphur-containing compounds (dimethyl disulfide), which have been reported to inhibit soil-borne pathogens under *in vitro* and *in vivo* conditions (Giorgio *et al*., 2015; Hassan *et al*., 2019; Munjal *et al*., 2016; Song *et al*., 2022; Stocki *et al*., 2025; Wang *et al*., 2022a; Guevara-avendaño *et al*., 2019; Montejano-ram *et al*., 2024; Yin *et al*., 2021).

Within this context, members of the genus *Lysobacter* have emerged as particularly promising BCAs because of their multifaceted antagonistic strategies. These bacteria are frequently associated with disease-suppressive soils, and their abundance is negatively correlated with the incidence of several soil-borne pathogens, including fungi, oomycetes, nematodes, and bacteria (Expósito *et al*., 2015; Castillo *et al*., 2017; do Rêgo Barros *et al*., 2022; Postma *et al.*, 2010a; Rosenzweig *et al*., 2012). *Lysobacter* spp. exhibit a broad arsenal of antagonistic traits, including competition for nutrients and space, microbial predation, induction of plant defense responses, and the production of

bioactive secondary metabolites, lytic enzymes, and VOCs (Brescia *et al*., 2021; Nakayama *et al*., 1999; Palumbo *et al*., 2003; Puopolo *et al*., 2014a, b; Zhang and Yuen 2000; Puopolo *et al*., 2010).

Although the production of non-volatile antimicrobial metabolites by *Lysobacter* spp. has been extensively investigated, the ecological relevance and biocontrol function of VOCs emitted by this genus remain largely unexplored. A comprehensive study addressed this gap by characterizing the VOCs profile of four *Lysobacter* type strains (*L. antibioticus, L. capsici, L. enzymogenes* and *L. gummosus*) grown on media differing in nutrient composition. This work demonstrated that VOCs production is strongly influenced by substrate availability, with protein-rich media stimulating the emission of antimicrobial compounds, particularly pyrazines, pyridine derivatives, pyrrole, alcohols, and aldehydes. These VOC blends showed marked inhibitory activity against *Phytophthora infestans* (Lazazzara *et al.*, 2017). Building on these observations, *Lysobacter capsici* AZ78 (AZ78), a strain with established rhizosphere competence and production of antimicrobial metabolites (Puopolo *et al*., 2016), has been studied for VOC-mediated pathogen suppression. Subsequent studies demonstrated that in vitro split-Petri dish assays of AZ78 VOCs completely inhibited the growth of *Pythium ultimum* and *Sclerotinia minor* and strongly reduced the growth of *Rhizoctonia solani*. Chemical analysis identified pyrazines as the dominant class of VOCs, together with alcohols such as 3-methyl-butanol and 2-ethyl-1-hexanol, which are known for their antifungal and anti-oomycete properties. Among the VOCs produced by AZ78, 2,5-dimethylpyrazine, 2-ethyl-3-methoxypyrazine, and 2-isopropyl-3-methoxypyrazine accumulated on the growth medium and were confirmed to inhibit the growth of *P. ultimum* when tested as synthetic compounds. These results provided the first direct evidence that AZ78 can suppress *P. ultimum* via volatile-mediated mechanisms under controlled *in vitro* conditions (Vlassi *et al*., 2020a)

Recent studies have also demonstrated that AZ78 produces ammonia, an inorganic volatile that can exert antimicrobial effects either directly or indirectly by altering the environmental pH (Vlassi *et al*., 2020b). Ammonia-induced alkalisation has been shown to inhibit the growth of several soil-borne pathogens, as many fungi and oomycetes prefer mildly acidic conditions (Eno *et al*., 1955; Omar and Ismail 1999). Ammonia contributes to soil fungistasis, a phenomenon in which the germination and growth of fungal and oomycete propagules is strongly inhibited in soil (Howell *et al*., 1988). Importantly, ammonia production by AZ78 is influenced by nutrient availability, suggesting that environmental conditions and substrate composition may strongly affect its biocontrol efficacy. Similar ammonia-based suppression mechanisms have been reported for other soil-borne pathogens. For instacne, Zhao *et al*. (2017a) showed that *Fusarium* can be suppressed in the soil by the application of ammonia gas, reducing the disease and abundance of fungal communities in the soil. In another study they found that the application of ammonium carbonate, which releases ammonia was able to control *Fusarium* pathogen causing the wilt diseases (Sun *et al.*, 2015).

In parallel, organic amendments (OAs) have long been recognised as key drivers of soil health and disease suppressiveness. OAs have been used in agriculture for more than 2000 years and are known to play multiple roles, including improving overall soil health, suppressing soil-borne pathogens, enhancing plant disease resistance, and promoting plant growth (Janvier *et al*., 2007; Lazarovits 2010; Goss *et al*., 2013). The suppressive effects of OAs arise from a combination of chemical, physical, and biological changes induced in the soil environment (Naghman *et al.*, 2023). The suppression of soil-borne plant pathogens by OAs is largely attributed to the release of ammonia during microbial degradation of these materials (Lazarovits and Lazarovits, 2010). During decomposition, soil microorganisms mineralize organic nitrogen; nitrogen present in excess of microbial demand is released as ammonium (NH_4^+), which leads to an increase in soil pH, making the

soil environment less suitable for fungal and oomycete soil-borne plant pathogens (Angelova *et al*., 2013; Naghman *et al*., 2023; Diacono *et al*., 2020). Beyond ammonia-mediated effects, OAs suppress pathogens by stimulating antagonistic microbial populations and altering the ecological niches (Tamm *et al.*, 2010; Jaiswal *et al.*, 2017). A study by Siegel-hertz *et al*. (2018) demonstrated that the resident soil microbiota can be deliberately manipulated through OA application to convert the soil into disease-suppressive systems. Therefore, OAs act by altering soil physical, chemical, and biological properties, making them more effective for sustainable crop management (Zhao *et al.*, 2009). .

Importantly, several studies have shown that OAs selectively promote the proliferation of *Lysobacter* spp**.**, thereby enhancing soil suppressiveness against soil-borne pathogens. A study by Postma and Schilder (2015) showed that the application of OAs increased *Lysobacter* populations, resulting in enhanced suppression of *R. solani*. Similarly, Wang *et al*. (2020) reported that the application of spent mushroom substrate reduced *Fusarium* incidence, coinciding with an increased abundance of *Lysobacter* spp. alongside other beneficial microorganisms. Further evidence suggests that amendment-driven enrichment of *Lysobacter* spp. is closely linked to nitrogen cycling and biocontrol stimulation. Ma *et al*. (2025) demonstrated that OAs promoted the recruitment of nitrogen-mineralizing bacteria, including *Lysobacter* spp., leading to elevated ammonium levels and enhanced pathogen suppression. Likewise, Lin *et al*. (2023) showed that the incorporation of OAs significantly increased *Lysobacter* abundance in the rhizosphere, resulting in reduced populations of *Ralstonia solanacearum*, an effect attributed to the production of bioactive compounds by *Lysobacter* spp. These findings indicate that OAs not only modify soil physicochemical properties but also reshape the soil microbiome in ways that favour the recruitment of antagonistic bacteria

5.2 Aim of the work

Despite substantial evidence demonstrating the antagonistic potential of *Lysobacter* spp., studies performed with AZ78 to date have primarily been conducted under in vitro conditions. In particular, although AZ78 has been shown to produce a wide array of VOCs with activity against soilborne pathogens, its biocontrol efficacy and underlying mechanisms of action in soil environments remain poorly understood. There is a noticeable gap in the literature between the *in vitro* studies and soil conditions. Therefore, the objective of this study was to bridge this gap by linking in vitro observations with in vivo soil-based biocontrol activity. We investigated both the effects of AZ78 cells and volatiles against *Pythium ultimum* in soil under greenhouse conditions, focusing on pathogen suppression mediated by bacterial cells, volatile emissions, soil pH modulation, and the reshaping of the soil microbial community. In addition, protein-rich OAs were evaluated for their capacity to enhance AZ78-mediated disease suppression. By integrating physiological, chemical and omics technologies, this study provides a comprehensive assessment of the mechanisms through which AZ78 contributes to soilborne disease suppression and advances its potential application under realistic agricultural conditions.

5.3 Material and methods

5.3.1 Maintenance of microorganism

AZ78 was routinely preserved in 40% glycerol stocks at -80 °C. For experimental use, the strain was cultured on Nutrient Agar (NA) in 90 mm Petri dishes (Sarstedt, Nümbrecht, Germany, or VWR International, Leuven, Belgium) and incubated for 48 hours at 27 °C. To prepare bacterial suspensions, each Petri dish was flooded with 5 mL of sterile distilled water, and the bacterial cells were gently scraped off using sterile L-shaped spatulas. The resulting cell suspension was homogenized in sterile distilled water. The optical density (OD) at 600 nm was adjusted to 0.1 using a spectrophotometer (UV-2450, Shimadzu, Kyoto, Japan), corresponding to approximately 1×10^8 Colony Forming Unit

(CFU)/mL using a spectrophotometer (UV-2450, Shimadzu, Kyoto, Japan) (Puopolo *et al*., 2014b). A portion of the obtained solution was further diluted to achieve a final concentration of 1×10^6 CFU/mL. The concentration of AZ78 cells used in each experiment is specified in the corresponding subsection.

5.3.2 Preparation of Pythium ultimum *inoculum*

P. ultimum from the in-house culture collection of Fondazione Edmund Mach was routinely grown on potato dextrose agar (PDA, Oxoid) in 90 mm Petri dishes at 25 °C in the dark for 48 h. Pathogen inoculum was prepared according to the procedure of Pane *et al*. (2011) with some modifications. Briefly, common millet seeds were placed in a 50 mL conical flask, containing 20 mL of potato dextrose broth (PDB; 1/10 *w/w*) and 24 g of millet seeds. The contents were autoclaved twice at 121°C for 20 min. The autoclaved millets were infested with a plug of 48 h old *P. ultimum* mycelium grown on PDA and incubated under dark conditions at 20 °C for 21 days. The resulting pathogen-millet inoculum was air dried for 3 days and then ground into a fine powder using a clean mortar and pestle. The freshly prepared pathogen inoculum was always used at a concentration of 0.3% *w/w* in soil.

5.3.3 Evaluation of the antagonistic effect of Lysobacter capsici *AZ78 against* Pythium ultimum *in soil*

5.3.3.1 Experiment I: assessing the effect of *Lysobacter capsici* AZ78 cells application against *Pythium ultimum*

To investigate the long-term effects of AZ78 cell application in soil and its role in suppressing *P. ultimum*, a prolonged soil incubation experiment was conducted. Briefly, 40 g of soil were transferred into sterile 50 mL centrifuge tubes and inoculated with an AZ78 cell suspension adjusted

to 1×10^6 CFU/mL at a rate of 1 mL per 15 g of soil and mixed thoroughly. Uninoculated soil samples served as controls. The tubes were then sealed with parafilm, perforated to allow aeration, and incubated at 27 °C for 21 days. Each treatment consisted of five replicates.

After 21 days, freshly prepared *P. ultimum* inoculum was incorporated into the treated soil samples and mixed thoroughly. Soil samples that did not receive the pathogen inoculum were included as corresponding controls. The following treatments were established: (1) soil (S); (2) soil + AZ78 (SB); (3) soil + *P. ultimum* (S+P); and (4) soil + AZ78 + *P. ultimum* (SB+P).

Following this, the soil from each treatment was transferred into pots (7 × 7 × 8 cm) with perforated bases to allow excess water drainage. Each pot was sown with five surface-sterilized tomato seeds (*Solanum lycopersicum* cv. Moneymaker), sterilized using 2% (*v/v*) sodium hypochlorite for one minute and rinsed three times with sterile distilled water. Each treatment consisted of five biological replicates. For each biological replicate, three technical replicates were included. The experiment was repeated.

The experimental units were arranged in a randomized block design and incubated in a controlled greenhouse under the following conditions: 25 ± 1 °C, 70 ± 10% RH, and a 16/8 h light/dark photoperiod. Seed germination was assessed 21 days after sowing and expressed as a percentage using the following formula:

$$\text{Germination (\%)} = \left(\frac{\text{Number of germinated seedlings}}{\text{Total number of seeds sown}}\right) \times 100$$

5.3.3.2 Experiment II: assessing the effect of exposure to *Lysobacter capsici* AZ78 volatiles against *Pythium ultimum*

The indirect effects of volatile compounds emitted by AZ78 were evaluated using an *in vitro* soil exposure system prior to greenhouse experimentation. Soil samples were exposed to AZ78 volatiles emitted from NA cultures without direct physical contact between the bacteria and the soil.

AZ78 cultures were prepared by inoculating 100 µL of a bacterial suspension (1×10^8 CFU/mL) onto sterile NA Petri dishes. The inoculum was spread evenly using sterile loops and allowed to air-dry under a laminar flow hood. Once dried, the Petri dishes were sealed with parafilm and perforated to allow aeration. Uninoculated NA Petri dishes were used as controls.

For soil preparation, 40 g of soil were weighed and transferred into an arable cloth pouch, which was later sealed. An exposure unit was designed for each treatment which consisted of a sterile 1.5 L airtight container in which two NA Petri dishes were stacked horizontally above each other and separated by a sterilized metallic mesh to prevent direct contact. A second metallic mesh was placed above the upper Petri dish, and the soil pouch was positioned on top of this mesh, ensuring that no direct contact occurred between the soil and the Petri dishes. The container was then sealed tightly to prevent volatile loss.

The containers were incubated at 27 °C for 21 days. To maintain bacterial viability and ensure continuous volatile emission, the NA Petri dishes were replaced every seven days with freshly inoculated Petri dishes throughout the incubation period. Two treatments were applied during the volatile exposure phase, which included NA only and NA inoculated with AZ78. Each treatment consisted of five replicates.

After 21 days of exposure, the soil exposed to each type of treatment was collected and divided into two portions. One portion was amended with *P. ultimum* inoculum, while the other portion remained pathogen free. The soils were mixed thoroughly, and the soil from each treatment was

transferred into sterile pots (7 × 7 × 8 cm) with perforated bases. Five tomato seeds were sown in each pot, and the experimental units were arranged under controlled greenhouse conditions as described in Section 5.3.3.1. Seed germination was assessed and expressed as a percentage as described above.

The resulting treatments were: (1) soil exposed to NA (SV); (2) soil exposed to NA inoculated with AZ78 (SBV); (3) soil exposed to NA + *P. ultimum* (SV+P); and (4) soil exposed to NA inoculated with AZ78 + *P. ultimum* (SBV+P). Each treatment included five biological and three technical replicates, and the experiment was repeated.

5.3.4 Assessing the effects of organic amendments on enhancing the antagonistic effect of Lysobacter capsici *AZ78 against* Pythium ultimum *in soil*

5.3.4.1 Organic amendments

The OAs we used in our experiments were as follows: fish meal, feather meal and hoof meal (Plagron, Netherlands). The soil was amended with these OAs at a concentration of 0.3% (*w/w*) unless stated otherwise. The same concentration was used in NA Petri dishes for the preparation of AZ78 cultures used for volatile emission assays.

5.3.4.2 Experiment III: Experimental setup for assessing the effect of *Lysobacter capsici* AZ78 cells against *Pythium ultimum* in soil with organic amendments

This experiment (experiment III) was conducted following the same soil incubation, *P. ultimum* inoculation, and plant germination assays following the procedures described in Section 5.3.3.1, with the inclusion of OAs as additional experimental treatments.

Briefly, soil samples were initially amended with fish meal, feather meal, or hoof meal and inoculated with AZ78 cells (1×10^6 CFU/mL). Unamended and uninoculated soils served as

respective controls for each type of treatment. After a 21 days incubation period at 27 °C under aerobic conditions, *P. ultimum* was added to the soil samples, where applicable. Soil samples without pathogen addition were included as corresponding controls (Table 7).

Subsequent soil handling, tomato seed sowing and germination assay were identical to those described for Experiment I in the section 5.3.3.1. The treatments were as follows. Each treatment had five biological and three technical replicates, respectively and the experiment was repeated.

Table 7. Treatments used in Experiment III

Organic amendment in soil	**AZ78**	***P. ultimum***	**Treatment name**	**Treatment code**
None	–	–	Soil	S
	+	–	Soil + AZ78*	SB
	–	+	Soil + *P. ultimum*	SP
	+	+	Soil + AZ78 + *P. ultimum*	SBP
Fish meal	–	–	Soil + fish meal	SFi
	+	–	Soil + fish meal + AZ78	SFiB
	–	+	Soil + fish meal + *P. ultimum*	SFiP
	+	+	Soil + fish meal + AZ78 + *P. ultimum*	SFiBP
Feather meal	–	–	Soil + feather meal	SFe
	+	–	Soil + feather meal + AZ78	SFeB
	–	+	Soil + feather meal + *P. ultimum*	SFeP

	+	+	Soil + feather meal + AZ78 + *P. ultimum*	SFeBP
Hoof meal	–	–	Soil + hoof meal	SH
	+	–	Soil + hoof meal + AZ78	SHB
	–	+	Soil + hoof meal + *P. ultimum*	SHP
	+	+	Soil + hoof meal + AZ78 + *P. ultimum*	SHBP

AZ78: *Lysobacter capsici* AZ78

5.3.4.3 Experiment IV: Experimental setup for assessing the effect of *Lysobacter capsici* AZ78 volatiles against *Pythium ultimum* in soil with organic amendments

In this experiment IV, the effects of volatile compounds produced by AZ78 in the presence of OAs were assessed using the same *in vitro* soil exposure system described in Section 5.3.3.2, with the inclusion of organic nitrogen amendments in the growth medium on which AZ78 was grown as additional experimental treatments.

Briefly, NA Petri dishes were prepared either without amendment or amended with fish meal, feather meal, or hoof meal. All media components were autoclaved prior to plating. Petri dishes were either inoculated with AZ78 (100 µL, 1×10^8 CFU/mL) or left uninoculated as controls. The soil exposure setup and assembly were identical to those described in Section 5.3.3.2. Experimental units were incubated at 27 °C for 21 days, however, the NA Petri dishes corresponding to each treatment were replaced every seven days with freshly inoculated Petri dishes. Treatments during the volatile exposure phase included NA alone or NA amended with OAs, each with or without AZ78 inoculation (Table 8).

After 21 days of volatile exposure, soils were collected and divided into two portions. One portion was inoculated with *P. ultimum*, while the other remained pathogen-free. Subsequent soil handling, tomato seed sowing, greenhouse conditions, and germination assessment were conducted as described in Section 5.3.3.2. Each treatment had five biological and three technical replicates and the experiment was repeated.

Table 8. Treatments used in Experiment IV

Organic amendment in NA	**AZ78**	***P. ultimum***	**Treatment name**	**Treatment code**
None	–	–	Soil exposed to NA*	SV
	+	–	Soil exposed to NA + AZ78*	SBV
	–	+	Soil exposed to NA + *P. ultimum*	SV+P
	+	+	Soil exposed to NA + AZ78 + *P. ultimum*	SBV+P
Fish meal	–	–	Soil exposed to NA + fish meal	SFiV
	+	–	Soil exposed to NA + fish meal + AZ78	SFiBV
	–	+	Soil exposed to NA + fish meal + *P. ultimum*	SFiV+P
	+	+	Soil exposed to NA + fish meal + AZ78 + *P. ultimum*	SFiBV+P
	–	–	Soil exposed to NA + feather meal	SFeV

Feather meal	+	–	Soil exposed to NA + feather meal + AZ78	SFeBV
	–	+	Soil exposed to NA + feather meal + *P. ultimum*	SFeV+P
	+	+	Soil exposed to NA + feather meal + AZ78 + *P. ultimum*	SFeBV+P
Hoof meal	–	–	Soil exposed to NA + hoof meal	SHV
	+	–	Soil exposed to NA + hoof meal + AZ78	SHBV
	–	+	Soil exposed to NA + hoof meal + *P. ultimum*	SHV+P
	+	+	Soil exposed to NA + hoof meal + AZ78 + *P. ultimum*	SHBV+P

NA: nutrient agar; AZ78: *Lysobacter capsici* AZ78

5.3.5 Soil physiochemical analysis

5.3.5.1 Measurement of soil pH

Soil pH was measured using a calibrated pH meter by gently stirring the soil slurry for approximately 10 s, and values were recorded to the nearest 0.01 pH unit. The pH electrode was rinsed with deionized water between measurements to prevent cross-contamination (Robertson and VanderWulp., 2023).

Soil pH was measured in soil samples collected from Experiments I-IV described above. In Experiments I and II, soil samples were collected prior to pathogen inoculation at four time points: day 1, day 7, day 14, and day 21. At each sampling time point, 5 g of soil was transferred into sterile 15 mL centrifuge tubes, and sterile deionized water was added at a soil-to-water ratio of 1:2 (*w/v*). The suspensions were briefly vortexed to ensure homogenization and allowed to equilibrate at room temperature for 30 min with the tube caps closed. In Experiment I, soil pH was measured for the following treatments: (1) S and (2) SB. In Experiment II, the treatments included: (1) SV and (2) SBV.

Soil pH in samples obtained from Experiments III and IV was determined using the same procedures described above. In both experiments, soil samples were collected on day 1 and day 21 prior to pathogen inoculation, and analyses were performed following identical extraction protocols, equilibration conditions, and measurement procedures. Each treatment consisted of five biological replicates, and the experiments were independently repeated. The treatments analysed in Experiment III included: (1) S; (2) SFi; (3) SFe; (4) SH; (5) SB; (6) SFiB; (7) SFeB; and (8) SHB. In Experiment IV, the treatments included: (1) SV; (2) SFiV; (3) SFeV; (4) SHV; (5) SBV; (6) SFiBV; (7) SFeBV; and (8) SHBV.

5.3.5.2 Ammonia quantification

Soil ammonia was measured in the soil samples obtained from experiment III and experiment IV. In both experiments, soil samples were collected on day one and day 21 before pathogen inoculation. The following reagents were prepared for ammonia nitrogen analysis according to the procedure of Liu et al. (2022):

a) **Ammonia nitrogen standard solution**: An ammonia nitrogen stock solution (100 mg/L) was prepared using anhydrous ammonium sulfate dissolved in sterile distilled water. A working standard solution with a concentration of 2 mg/L was obtained by appropriate dilution of the stock solution.

b) **Phenol solution**: Prepared by dissolving phenol (10 g) and sodium nitroprusside (100 mg) in 1 L of sterile distilled water. The solution was stored in a brown bottle wrapped with aluminium foil at 4 °C.

c) **Alkaline sodium hypochlorite solution**: Prepared by dissolving sodium hydroxide (10 g), disodium hydrogen phosphate (7.06 g), and sodium phosphate (31.8 g) in sterile distilled water, followed by the addition of sodium hypochlorite solution (10 mL, 52.5 g/L), and dilution to a final volume of 1 L. This solution was freshly prepared and stored in a brown bottle at 4 °C.

d) **Masking agent**: Prepared by mixing potassium sodium tartrate (400 g/L) and disodium EDTA (100 g/L) solutions in equal volumes. Sodium hydroxide (10 mol/L) was added at a rate of 0.5 mL per 100 mL of the mixed solution.

Ammonia nitrogen in soil samples was determined following the method described by Liu et al. (2022), with minor modifications. Briefly, five g of soil from each treatment was extracted with 25 mL of 2 mol/L KCl solution in an Erlenmeyer flask. Each treatment was analysed in triplicate. The flasks were sealed with sterile corks and incubated at 25 °C with shaking at 230 rpm for 1 h. After incubation, the suspensions were filtered through Whatman filter paper into sterile 50 mL centrifuge tubes. The filtrate was designated as the soil extract. An aliquot (5 mL) of this solution was transferred to a 50 mL volumetric flask, followed by the addition of 10 mL of 2 mol/L KCl, 5 mL of phenol solution, and 5 mL of alkaline sodium hypochlorite solution. The mixture was homogenized and incubated at room temperature for 1 h in the dark to allow colour development. Subsequently, 1 mL

of masking agent was added to dissolve any precipitate formed, and the volume was adjusted to 50 mL with double-distilled water. Aliquots of the final solution were transferred to a 96-well microplate, and absorbance was measured at 650 nm using a microplate reader.

For calibrating the standard curve, aliquots of 0, 2, 4, 6, 8, and 10 mL of the ammonia nitrogen working standard solution were transferred into separate 50 mL volumetric flasks. Each flask received 10 mL of 2 mol/L KCl, 5 mL of phenol solution, and 5 mL of alkaline sodium hypochlorite solution. The mixtures were gently shaken and incubated at room temperature for 1 h in the dark. Aliquots were then transferred to a 96-well microplate, and absorbance was measured at 650 nm using the same microplate reader. The resulting absorbance values were used to construct a standard calibration curve for ammonia nitrogen quantification (Liu et al., 2022). Each treatment consisted of five biological replicates and the experiment was repeated.

5.3.6 Dynamic headspace Gas chromatography-mass spectrometry analysis (DHS–GC–MS) of Lysobacter capsici *AZ78 VOCs*

Sterile 20 mL headspace vials (Gerstel GmbH & Co. KG, Mülheim an der Ruhr, Germany) were filled with 5 mL of NA or NA supplemented with 0.3% (*w/v*) hoof meal (NAH). The vials were positioned at an angle under laminar airflow overnight to maximize the available surface area for inoculation and to prevent condensation. Subsequently, each vial received 50 µL of AZ78 cell suspension adjusted to 1×10^8 CFU/mL, while uninoculated vials served as controls. The bacterial suspension was evenly spread across the medium surface using sterile loops and allowed to air-dry for 2h under laminar airflow. After drying, vials were sealed with sterile metal caps fitted with 1.3 mm silicone/PTFE septa (Gerstel) and incubated at 27 °C for 7 days (168h). GC-MS analyses were performed at 7 days post-inoculation (dpi). The experimental treatments were: (i) NA alone; (ii) NA

inoculated with AZ78; (iii) NAH alone; and (iv) NAH inoculated with AZ78. Five replicates (HS vials) were analysed for each treatment in a randomized block design (Vlassi., *et al.*, 2020a).

All analyses were performed using a gas-chromatograph 8890 GC System (Agilent Technologies, CA, United States) coupled with a quadrupole mass selective detector (MSD) 5977C (Agilent). The GC-MS was additionally equipped with a multi-purpose autosampler (MPS 2XL, Gerstel) with a dynamic headspace system (DHS, Gerstel), a thermal desorption unit 2.0 (TDU, Gerstel) and a cooled injection system 4 (CIS, Gerstel) unit. Samples were pre-incubated at 30 °C for 15 min and simultaneously agitated at 1000 rpm every 10 sec. VOCs were then collected dynamically (N_2 purge flow 20 mL/min to a final volume of 100 mL) onto a 2 cm TENAX® TA trap (Gerstel) at 30°C. Subsequently, the loaded trap was dried at 30 °C in a N_2 gas stream (50 mL/min to a final volume of 200 mL) and transferred to the TDU. Primary desorption was conducted at 300 °C for 3 min with a desorption flow of 30 mL/min, during which analytes were transferred to a cryofocusing trap containing 15 mg of TENAX® TA maintained at 0 °C, applying a septum purge flow of 3 mL/min. Following primary desorption, the cold trap was rapidly heated to 300 °C and held for 4.10 min to inject analytes into the GC system. Chromatographic separation was performed using a DB-WAX Ultra Inert capillary column (60 m, 250 μm diameter, 0.5 μm film thickness, Agilent) Helium was used as the carrier gas at a constant flow rate of 1 mL/min. The oven temperature program consisted of an initial hold at 35 °C for 2 min, followed by a ramp of 5 °C/min to 200 °C and a second ramp of 20 °C/min to a final hold at 240 °C for 5 min. Analytes were ionized at 70 eV in the ion source at 230 °C and detected in full scan (14-330 amu). Raw data were acquired and processed using the Agilent software packages MassHunter Workstation Unknowns Analysis (v. 12) and MassHunter Workstation Quantitative Analysis (v. 12). The following parameter settings were used: deconvolution peak detection, ion peak signal to noise ratio (SNR) threshold 10, absolute area ≥ 1000 counts. Detected

compounds were annotated using Agilent Unknowns Analysis software by comparing their mass spectra with entries in the NIST 20 mass spectral library (National Institute of Standards and Technology, United States; http://www.nist.gov). Only matches with a similarity score above 70 were considered for compound annotation. The data were initially curated by manual inspection and subsequently imported into MetaboAnalyst 6.0 (https://www.metaboanalyst.ca). Prior to data analysis, integrity checks were performed, including verification of class labels and the detection of non-numeric values, missing values, and features with constant values. To reduce bias resulting from truncated data omissions, missing values were imputed using one-fifth of the minimum positive value of the corresponding variable. Variables exhibiting a relative standard deviation (RSD) greater than 25% across all samples were excluded. Data were then mean-centered to adjust for systematic differences among samples. Significant metabolites were obtained using one-way ANOVA with a p-value threshold of 0.05. Subsequently, sparse partial least squares-discriminant analysis and random forest analysis were performed. For the random forest analysis, the number of trees was set to 500, and the number of variables randomly sampled at each split was set to seven.

5.3.7Analysis of soil microbial community shifts induced by Lysobacter capsici *AZ78*

5.3.7.1 *In vitro* monitoring of soil microbial community changes

The effect of AZ78 cells and volatiles on the microbial population density was monitored periodically at day 1 and day 21 in all the treatments mentioned in experiment III and experiment IV prior to pathogen inoculation. Serial dilution plating was used for this purpose. The protocol was as follows: we started by taking one gram of soil from each sample for every treatment, and it was mixed with 9 mL of sterile NaCl solution (0.95% *w/v*) in 15 mL sterile centrifuge tubes. The contents were vortexed and allowed to stand and equilibrate at room temperature for 30 min. The samples were diluted at different concentrations depending on the targeted microbial population to be analysed. For

monitoring bacterial population density, we diluted the samples ranging from 10^{-4} to 10^{-6}, and 100 µL of each dilution was plated on Reasoner's 2A agar (R2A) Petri dishes amended with cycloheximide (100 mg/L). Three technical replicates (three Petri dishes) per treatment were used. The Petri dishes were incubated at 27 °C, and bacterial cells were counted after 72 h of incubation under dark conditions. For fungal samples, the dilutions were prepared ranging from 10^{-2} to 10^{-4}, and the procedure outlined above was used to plate the dilutions on PDA media acidified with lactic acid (10 mL/L). The incubation conditions for fungi were for one week at 25°C (Mokni-tlili, Markowicz and Hamdi, 2024).

5.3.7.2 Metagenomic analysis of soil microbial community structure of different soil treatments

Soil samples from the experiments described in Sections 5.3.4.2 and 5.3.4.3 were collected before *P. ultimum* inoculation. The collected samples corresponded to the treatments labeled “none” and “hoof meal” in Table 7 and 8. All soil samples were stored at -20 °C until further processing.

Total soil DNA was extracted using the PureLink™ Microbiome DNA Purification Kit (Thermo Fisher Scientific, USA) according to the manufacturer’s instructions. DNA concentration was determined using a Qubit 4 Fluorometer (Thermo Fisher Scientific) with the Qubit™ dsDNA High-Sensitivity Assay Kit (Invitrogen, USA). DNA quality was assessed by agarose gel electrophoresis on a 1% (*w/v*) agarose gel. The extracted DNA was subsequently stored at -20 °C for downstream metagenomic analysis.

For library preparation, the VAHTS Universal Plus DNA Library Prep Kit V4 (ND801, Vazyme, Nanjing, China) was used, following the manufacturer’s recommendations Library quality control was performed using the QSep-400 (BiOptic, Taipei, China) and Qubit 3.0 (Thermo Fisher Scientific, Wilmington, USA). The qualified library was sequenced on the Illumina Novaseq X

platform (Illumina, San Diego, USA) with paired-end 150 bp (PE150) mode. Library construction and sequencing were performed at Biomarker Technologies (BMKGENE) GmbH.

5.3.8 Statistical analysis

All statistical analyses were performed in R v4.3.0 using RStudio v2024.12.1-563. Data are presented as mean ± standard error. Normality and homogeneity of variance were assessed using the Shapiro-Wilk and Levene's tests, respectively. When assumptions were met, differences among treatments were analysed using one-way analysis of variance (ANOVA) followed by Tukey's HSD test for multiple comparisons ($\alpha = 0.05$). Pairwise comparisons were performed using Student's *t*-test. These analyses were conducted using the emmeans (v1.10.0) and agricolae (v1.3-7) packages. VOCs data were analysed using one-way ANOVA to identify significantly different compounds ($p < 0.05$), and relative abundances were visualized using $\log_{10}$-transformed normalized heatmaps generated in MetaboAnalyst 6.0. Multivariate analysis of VOC profiles was performed using principal component analysis (PCA) and treatment differences were assessed using PERMANOVA. Microbial community analyses were conducted using the BMK-Cloud platform (BMKGene). Alpha diversity (Chao1 and Shannon indices) was analysed using the Kruskal–Wallis test followed by Dunn's multiple comparison test ($p < 0.05$). Beta diversity was evaluated using Bray–Curtis dissimilarity and visualized by principal coordinates analysis (PCoA). Relationships between environmental variables and microbial taxa were explored using redundancy analysis (RDA). Differences in nitrogen cycling functional gene abundances were assessed using one-way ANOVA followed by Tukey's HSD test, and results were visualized using row Z-score normalized heatmaps. Treatments sharing the same letter were considered not significantly different ($p < 0.05$).

5.4 Results

5.4.1 Lysobacter capsici *AZ78 shows antagonistic effect against* Pythium ultimum *in soil and improves seed germination*

In Experiment I, tomato seed germination was evaluated in soils inoculated with AZ78 cells and subsequently challenged with *P. ultimum*. The symptoms of the damping-off disease were evaluated after 21 days. Application of AZ78 cells to soil in the absence of *P. ultimum* (SB) significantly increased tomato seed germination from 52 ± 4.9% in untreated soil (S) to 64 ± 4.0%. This enhancement suggests a plant growth-promoting effect of AZ78 cells in the soil in the absence of *P. ultimum*. In contrast, inoculation of soil with *P. ultimum* in the absence of AZ78 (S+P) markedly reduced seed germination to 32 ± 4.9%, a value lower than that observed in the control treatment S. However, soil treated with AZ78 cells and challenged with *P. ultimum* (SB+P) exhibited a higher germination percentage (40 ± 6.3%) than the pathogen-only treatment. Although germination in the SB+P treatment remained lower than in soil treated with AZ78 cells alone (SB), the observed increase indicates that AZ78 cells mitigated the negative effects of *P. ultimum* to a certain extent, providing measurable protection against this soil-borne pathogen (**Figure *21***).

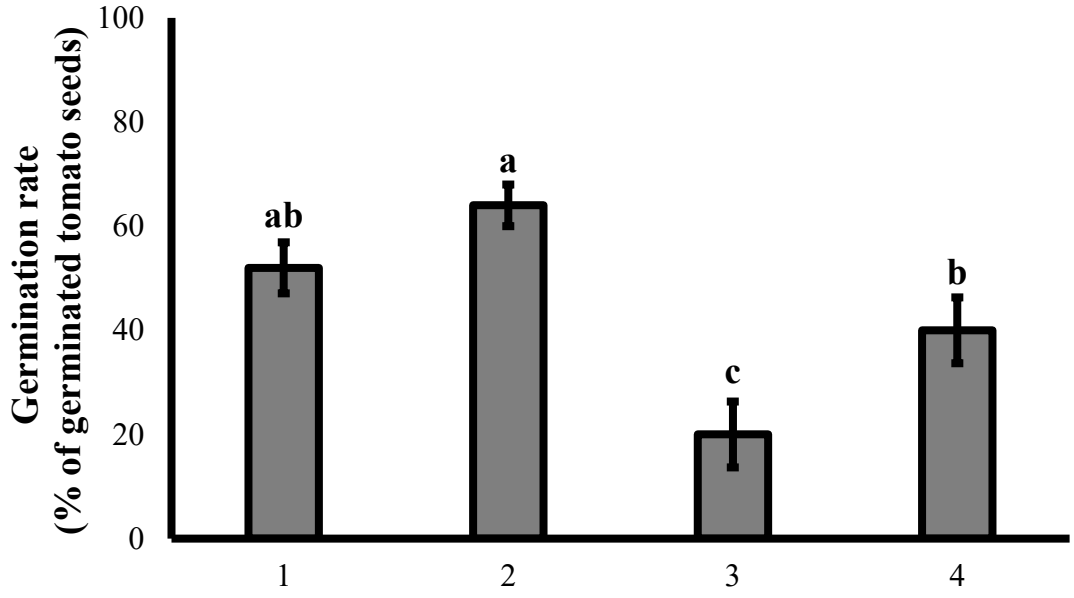

Figure 21. Effect of *Lysobacter capsici* AZ78 on the germination rate (%) of tomato seedlings infected with *Pythium ultimum* after 21 days. Different treatments included: 1) soil (S); 2) soil + *L. capsici* AZ78 (SB); 3) soil + *P. ultimum* (S+P); and 4) soil + + *L. capsici* AZ78 + *P. ultimum* (SB+P). Data represent mean ± standard error (n = 5). Differences among treatments were analysed by one-way ANOVA followed by Tukey's HSD test (α = 0.05). Columns sharing the same letter are not significantly different.

In Experiment II, the effects of the soil exposed for 21 days to volatile compounds produced by AZ78 were evaluated against *P. ultimum*. Soil exposed to the control treatment i.e., NA Petri dishes (SV) exhibited a germination rate of 36 ± 4.0%, whereas the treatment in which soil was exposed to NA Petri dishes inoculated with AZ78 cells able to produce volatiles (SBV) increased seed germination to 48 ± 4.9% (**Figure *22***). This confirms the role of AZ78 emitted volatiles in plant growth promotion. When these treatments were challenged with *P. ultimum*, a general reduction in germination percentage was observed. However, soil exposed to AZ78 derived volatiles and subsequently challenged with *P. ultimum* (SBV+P) showed a higher germination rate (24 ± 7.5%) compared with soil exposed to NA alone and challenged with the *P. ultimum* (SV+P), which exhibited

only 12 ± 4.9% germination (**Figure *22***). Notably, germination in the SV+P treatment was approximately threefold lower than that observed in the untreated control (SV).

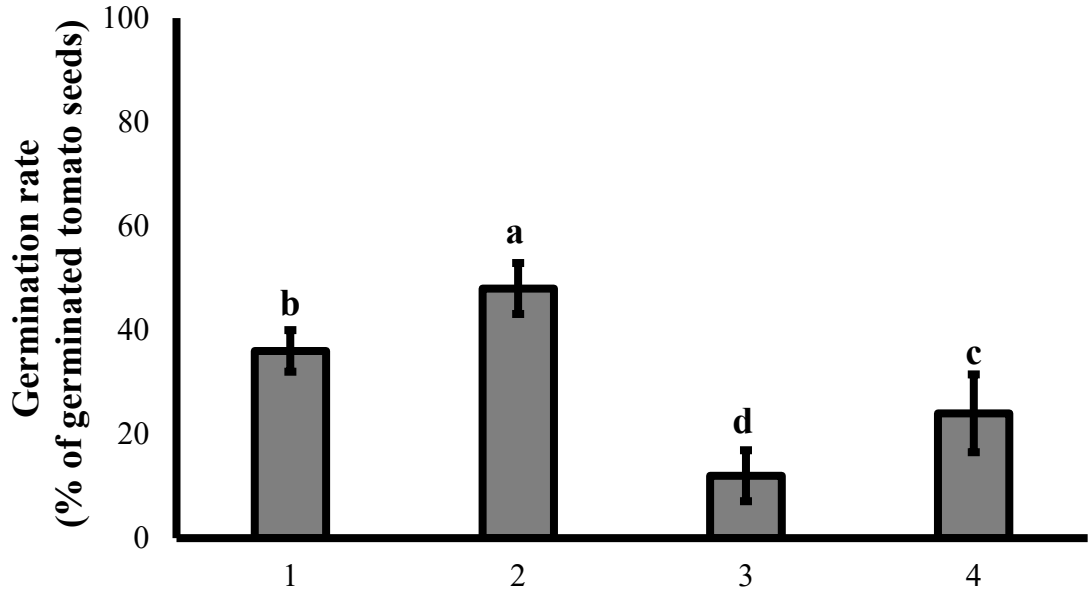

Figure 22. Effect of *Lysobacter capsici* AZ78 on the germination rate (%) of tomato seedlings infected with *Pythium ultimum* after 21 days. Different treatments included: **1)** soil exposed to nutrient agar (NA), (SV); **2)** soil exposed to NA with *L. capsici* AZ78 (SBV); **3)** soil exposed to NA + *P. ultimum* (SV+P); and **4)** soil exposed to NA with *L. capsici* AZ78 + *P. ultimum* (SBV+P). Data represent mean ± standard error (n = 5). Differences among treatments were analysed by one-way ANOVA followed by Tukey's HSD test (α = 0.05). Columns sharing the same letter are not significantly different.

5.4.2 Addition of organic amendments improves the antagonistic effect of Lysobacter capsici *AZ78 against* Pythium ultimum *in soil and improves seed germination*

In experiment III, distinct treatment-dependent effects were observed (**Figure *23***). Statistically significant differences were detected among treatments receiving OAs, when compared to the treatments without the OAs. Across all the treatments, the application of AZ78 cells increased tomato seed germination, confirming its plant growth-promoting potential. This effect was further enhanced when AZ78 was applied in combination with OAs, resulting in higher germination rates than those

observed with AZ78 treatment alone. Among the amendments tested, hoof meal produced the most pronounced synergistic effect, boosting seed germination to nearly twice that of the unamended control (increased from 33.33% in S-untreated to 66.66 ± 1.54% in SH-untreated). Notably, OAs also increased germination in the absence of AZ78 cells. In contrast, inoculation with *P. ultimum* in the absence of AZ78 cells had a strong negative impact on seed germination, with germination rates remaining below 30% across all amendment treatments. OAs alone were insufficient to counteract pathogen-induced suppression of germination, indicating that they did not directly inhibit *P. ultimum* (**Figure *23***). Notably, when *P. ultimum* was introduced into soils previously inoculated with AZ78 cells, germination rates increased markedly, demonstrating the biocontrol and protective role of AZ78. Compared with pathogen-only treatments, germination increased approximately twofold in AZ78-treated soils, reaching 40.00 ± 6.66% in unamended soil (S- *Lysobacter capsici* AZ78 + *Pythium ultimum*) and further increasing to 53.33 ± 8.16%, 66.66 ± 10.54%, and 80.00 ± 8.16% in soils amended with fish meal (SFi- *Lysobacter capsici* AZ78 + *Pythium ultimum*), feather meal (SFe- *Lysobacter capsici* AZ78+*Pythium ultimum*), and hoof meal (SH- *Lysobacter capsici* AZ78+*Pythium ultimum*), respectively. The highest germination rate (80.00 ± 8.16%) observed with hoof meal in the presence of both AZ78 and *P. ultimum* (SH- *Lysobacter capsici* AZ78+*Pythium ultimum*) was comparable to that observed in AZ78-treated soil without *P. ultimum*, indicating near-complete mitigation of pathogen effects.

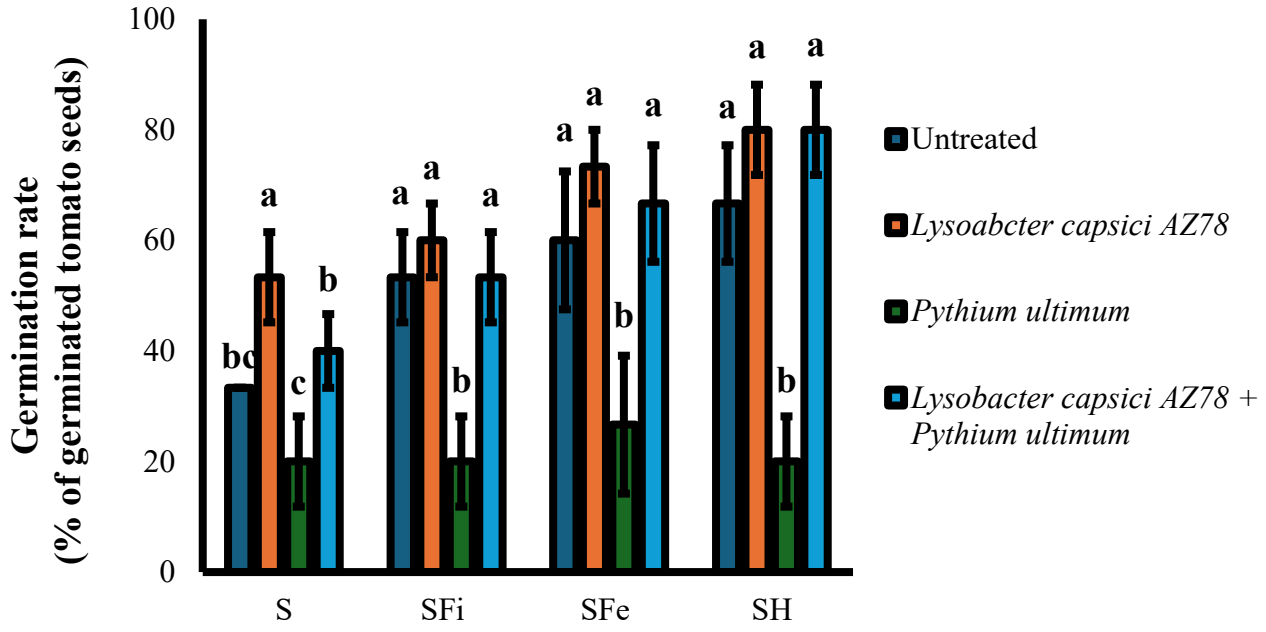

Figure 23. Effect of *Lysobacter capsici* AZ78 inoculation and organic amendments on tomato seedling germination (%) after 21 days in soil infected with *Pythium ultimum*. Treatment groups were: 1) soil (S), 2) soil + fish meal (SFi), 3) soil + feather meal (SFe), and 4) soil + hoof meal (SH). Each group was either: untreated, inoculated with *L. capsici* AZ78, infected with *P. ultimum*, or both inoculated with *L. capsici* AZ78 and infected with *P. ultimum*. Data represent mean ± standard error (n = 5). Differences among treatments were analysed by one-way ANOVA followed by Tukey's HSD test (α = 0.05). Columns sharing the same letter are not significantly different.

In the experiment IV, the soil treatment SV belonging to the group untreated exhibited a germination rate of 40.00 ± 6.66%. In contrast, soil exposed to NA amended with OAs (SFi- untreated, SFe- untreated, and SHV- untreated) markedly enhanced seed germination, with feather meal and hoof meal increasing germination to 86.66 ± 8.16% and 80.00 ± 8.16%, respectively (**Figure *24***). A similar trend was observed in soils exposed to AZ78-derived volatiles. In the absence of OAs, exposure to AZ78 volatiles slightly increased germination in the unamended soil treatment (46.66 ± 8.16%; SV- *Lysobacter capsici* AZ78). Among amended soils, feather meal and hoof meal resulted in higher germination rates than fish meal, reaching 86.66 ± 8.16% and 80.00 ± 13.33%, respectively (SFeV- *Lysobacter capsici* AZ78 and SHV- *Lysobacter capsici* AZ78). Notably, these values were

comparable to those observed in amended soils not exposed to AZ78 volatiles, suggesting that OAs were the primary drivers of enhanced germination under non-pathogen conditions. When treatments were challenged with *P. ultimum*, pathogen inoculation in the absence of AZ78 volatiles markedly reduced tomato seed germination across all amendment types (**Figure *24***). In contrast, exposure to AZ78 volatiles mitigated the negative effects of the pathogen, resulting in improved germination across all treatments. The highest germination rate was observed in soil amended with hoof meal and exposed to AZ78 volatiles (73.33 ± 12.47%; SHV- *Lysobacter capsici* AZ78+*Pythium ultimum*), followed by feather meal (60.00 ± 12.47%; SFeV- *Lysobacter capsici* AZ78+*Pythium ultimum*) and fish meal (53.33 ± 8.16%; SFiV- *Lysobacter capsici* AZ78+*Pythium ultimum*). The unamended soil exposed to AZ78 volatiles and challenged with the pathogen (SV- *Lysobacter capsici* AZ78+*Pythium ultimum*) showed a germination rate of 33.33 ± 0.00%, indicating partial but limited protection in the absence of OAs.

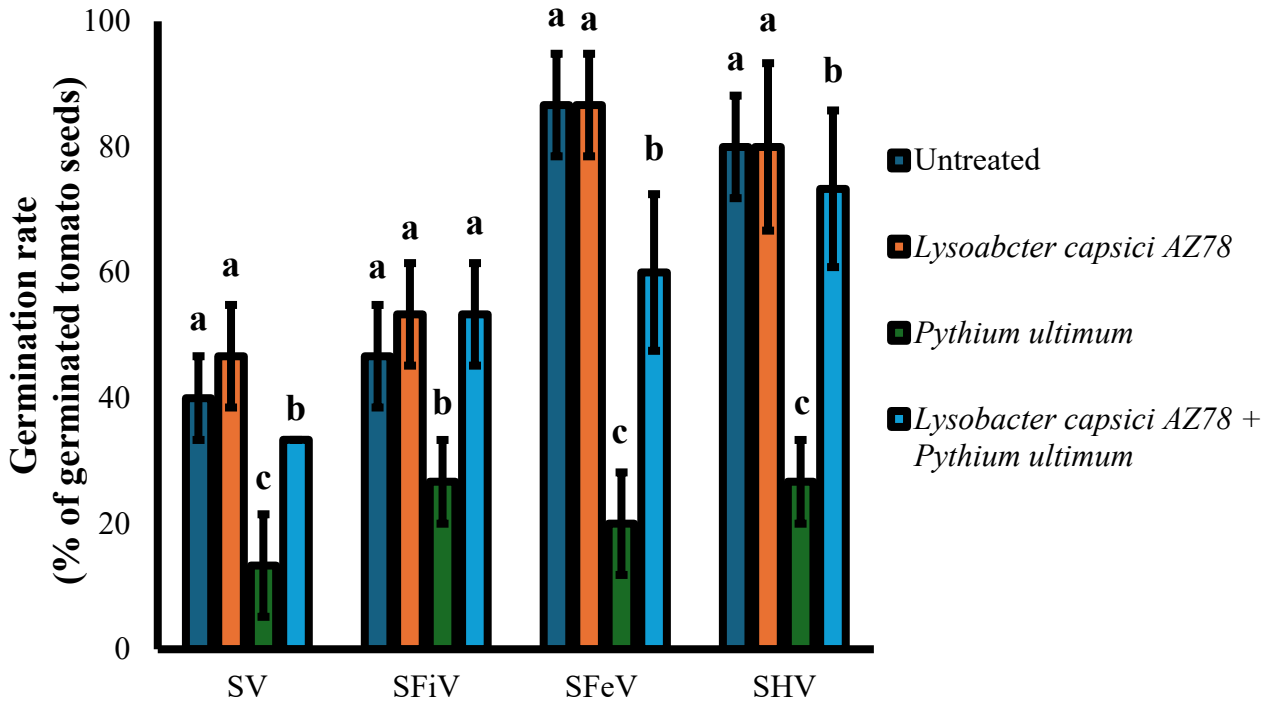

Figure 24. Effect of exposure to *Lysobacter capsici* AZ78 volatiles and organic amendments on tomato seedling germination (%) after 21 days in soil infected with *Pythium ultimum*. Treatment groups were: 1) soil exposed to nutrient agar (NA) volatiles (SV), 2) soil exposed to NA with fish meal (SFiV), 3) soil exposed to NA with feather meal (SFeV), and 4) soil exposed to NA with hoof meal (SHV). Each soil treatment was either left untreated, exposed to volatiles from *L. capsici* AZ78, infected with *P. ultimum*, or both exposed to *L. capsici* AZ78 volatiles and infected with *P. ultimum*. Data represent mean ± standard error (n = 5). Differences among treatments were analysed by one-way ANOVA followed by Tukey's HSD test ($\alpha = 0.05$). Columns sharing the same letter are not significantly different.

5.4.3 Change in soil pH

Soil pH was measured at two time points: day 1 (one day after inoculation with AZ78 cells and/or exposure of soil to AZ78 volatiles) up to day 21, with an interval of every 7 days to evaluate the change in soil physiochemical characteristics via AZ78 cells or AZ78 volatiles. The experiment was performed before *P. ultimum* inoculation in soil to understand the changes leading to plant protection ability of AZ78.

5.4.3.1 Change in soil pH in soil inoculated with *Lysobacter capsici* AZ78 cells

In Experiment I, untreated soil (S) exhibited a pH of 7.77 ± 0.01 on day 1, which decreased slightly to 7.65 ± 0.03 by day 21. However, there was no or negligible change in pH on day 7 and day 12. In contrast, the SB treatment showed a slight increase in pH, from 7.81 ± 0.01 at day 1 to 7.86 ± 0.01 at day 21. Similar to the untreated soil samples (S), there was no significant change in the pH on day 7 and day 14 (**Figure *25***).

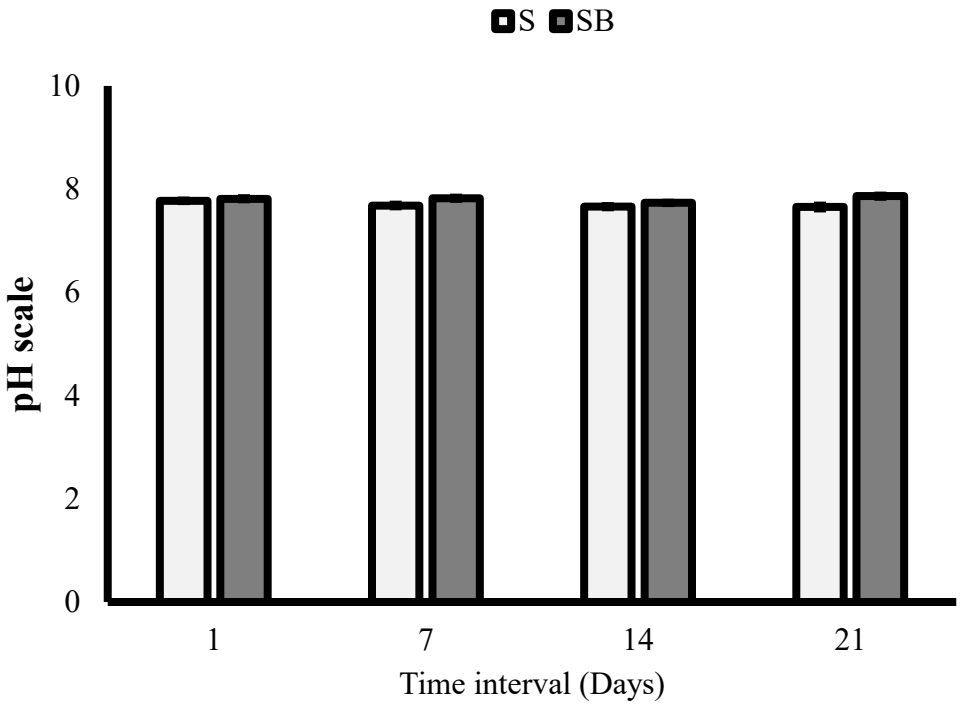

Figure 25. Changes in soil pH over time in soils inoculated with *Lysobacter capsici* AZ78 cells at 1, 7, 14, and 21 days. Treatments included soil (S) and soil + *L. capsici* AZ78 (SB). Data represent mean ± standard error (n = 5). Differences between treatments were assessed using Student's t-test ($p \leq 0.05$).

5.4.3.2 Change in soil pH in soil exposed to *Lysobacter capsici* AZ78 volatiles

In Experiment II, untreated samples (SV) showed a pH of 7.56 ± 0.01 at day 1, which increased marginally to 7.59 ± 0.03 by day 21. In contrast, soil exposed to AZ78-derived volatiles for 21 days

(SBV) exhibited a pronounced increase in pH, from 7.58 ± 0.01 at day 1 to 8.37 ± 0.11 at day 21There was a gradual increase in pH from day 1 to day 7 (7.84 ± 0.02) and day 14 (8.08 ± 0.05), reaching its highest value on day 21.Overall, these results suggest that volatiles emitted by AZ78 cells have a stronger alkalinizing effect on soil pH than the direct application of AZ78 cells (**Figure *26***).

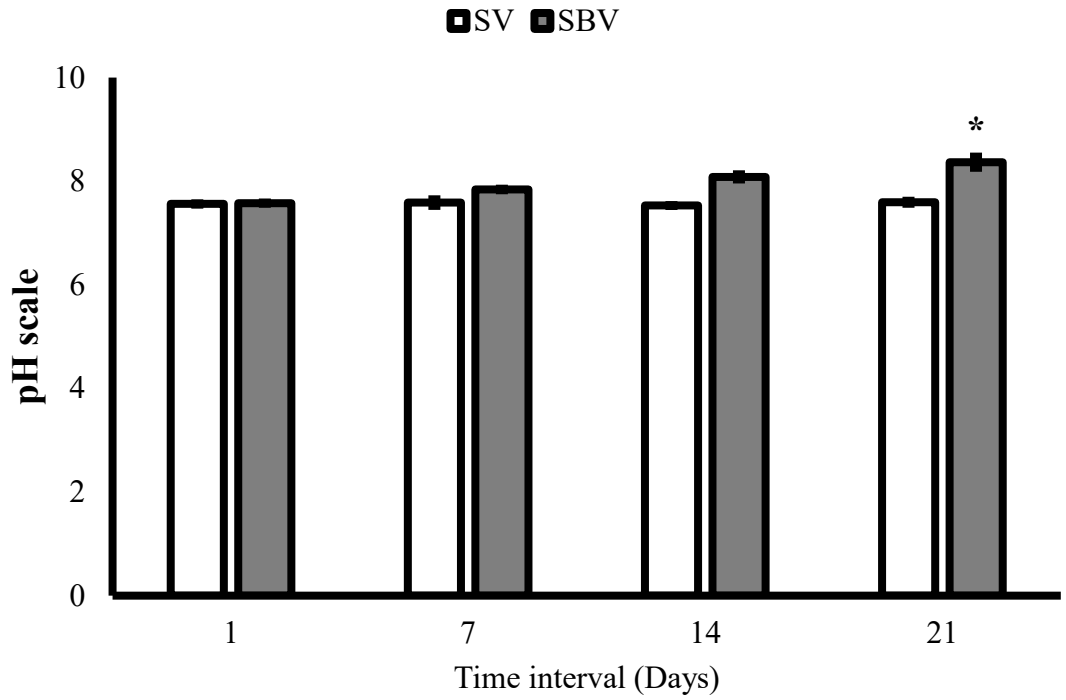

Figure 26. Changes in soil pH over time in soils exposed to volatiles produced by *Lysobacter capsici* AZ78 at 1, 7, 14, and 21 days. Treatments included soil exposed to nutrient agar (NA) volatiles (SV) and soil exposed to NA with *L. capsici* AZ78 (SBV). Data represent mean ± standard error (n = 5). Differences between treatments were assessed using Student's t-test ($p \leq 0.05$).

5.4.3.3 Addition of organic amendments can change the soil pH in soil inoculated with *Lysobacter capsici* AZ78 cells

In soil samples collected from Experiment III, soil pH was measured on day 1 and day 21 to evaluate the effects of AZ78 cells and OAs on the pH. In untreated soil (S), pH remained stable throughout the experimental period, showing only a negligible change from 7.36 ± 0.02 on day 1 to

7.35 ± 0.05 on day 21 (**Figure *27***). Similarly, soils amended with organic materials alone showed no marked pH variation. Treatments SFi, SFe, and SH recorded initial pH values of 7.36 ± 0.01, 7.40 ± 0.02, and 7.44 ± 0.02, respectively, with only very slight increases by day 21 (7.41 ± 0.01, 7.50 ± 0.01, and 7.45 ± 0.00). None of these changes were statistically significant. The application of AZ78 cells to soil also resulted in minimal pH variation, with values changing slightly from 7.48 ± 0.03 on day 1 to 7.45 ± 0.04 on day 21 (**Figure *27***). When AZ78 cells were applied in combination with OAs, a minor decrease in pH was observed over time. Specifically, pH values in SB, SFiB, SFeB, and SHB treatments decreased from 7.48 ± 0.03, 7.63 ± 0.03, 7.44 ± 0.02, and 7.45 ± 0.05 on day 1 to 7.45 ± 0.04, 7.37 ± 0.04, 7.33 ± 0.00, and 7.29 ± 0.04 on day 21, respectively. Although a decreasing trend was observed in treatments inoculated with AZ78 cells, these pH changes were small and not statistically significant (**Figure *27***).

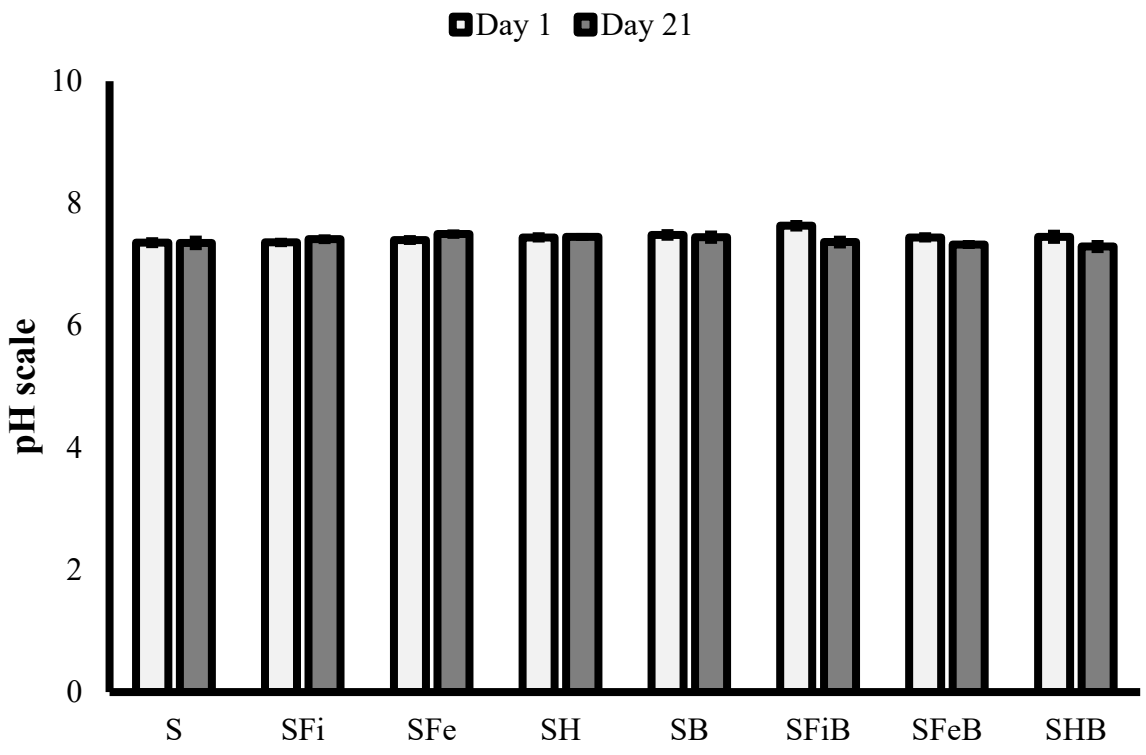

Figure 27. Changes in soil pH measured at day 1 and day 21 in soils inoculated with *Lysobacter capsici* AZ78 cells. Treatments included unamended soil (S), soils + fish meal (SFi), soil + feather meal (SFe), and soil + hoof meal (SH), each either inoculated with *L. capsici* AZ78 (SB, SFiB, SFeB, and SHB) or left uninoculated. Data represent mean ± standard error (n = 5). Differences between treatments were assessed using Student's t-test ($p \leq 0.05$).

5.4.3.4 Addition of organic amendments can change the soil pH in soil exposed to *Lysobacter capsici* AZ78 volatiles

Exposure of soil to AZ78-derived volatile compounds resulted in pronounced changes in soil pH. Soils exposed to NA plates without AZ78 inoculation, both with and without OAs, showed only minor increases in pH over time. Untreated soil (SV) exhibited a slight increase in pH from 7.03 ± 0.02 on day 1 to 7.12 ± 0.04 on day 21. A similar trend was observed in soils amended with fish meal (SFiV), feather meal (SFeV), and hoof meal (SHV), **with initial pH values of 7.05 ± 0.07, 7.06 ± 0.03, and 6.99 ± 0.03, respectively, increasing slightly to 7.15 ± 0.02, 7.14 ± 0.06, and 7.04 ± 0.00 by day 21** (**Figure *28***). These changes were not statistically significant. By contrast, soils exposed to

volatiles emitted by AZ78-inoculated (SBV) showed a significant increase in pH over the experimental period, rising from 7.04 ± 0.06 on day 1 to 7.97 ± 0.09 on day 21, even in the absence of OAs. The presence of OAs further enhanced this effect. The amended soil SFiBV, SFeBV, and SHBV exhibited initial pH values of 7.03 ± 0.06, 6.98 ± 0.10, and 7.05 ± 0.01, respectively, which increased markedly to 8.10 ± 0.12, 8.20 ± 0.10, and 8.20 ± 0.05 by day 21. All the soil treatments exposed to AZ78-derived volatiles showed statistically significant pH increases, with the largest effects observed in soils amended with feather meal and hoof meal (**Figure *28***).

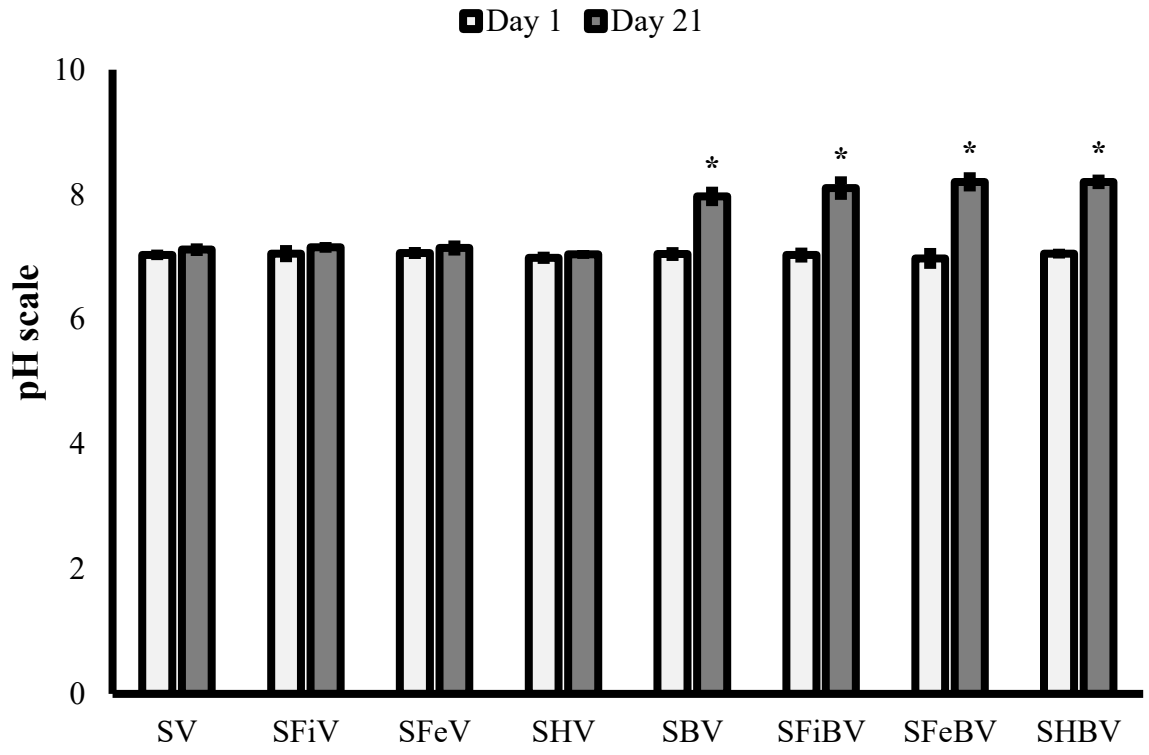

Figure 28. Changes in soil pH measured at day 1 and day 21 in soils exposed to volatiles produced by *Lysobacter capsici* AZ78. Treatments included soils exposed to nutrient agar (NA) volatiles (SV), soil exposed to NA with fish meal (SFiV), soil exposed to NA with feather meal (SFeV), and soil exposed to NA with hoof meal (SHV), and the treatments exposed to *L. capsici* AZ78 volatiles (SBV, SFiBV, SFeBV, and SHBV). Data represent mean ± standard error (n = 5). Differences between treatments were assessed using Student's t-test ($p \leq 0.05$).

5.4.4 Ammonia quantification in soil

5.4.4.1 Ammonia quantification in soil inoculated with *Lysobacter capsici* AZ78 cells

Soil ammonia nitrogen was quantified according to the procedure described in Section 5.3.5.2. After addition of the required reagents and thorough mixing, absorbance was measured at 650 nm using a microplate reader on day 1 and day 21 in Experiments III and IV. Absorbance values for all treatments were recorded, and ammonia nitrogen concentrations were calculated and expressed as parts per million (ppm).

In Experiment III, untreated soil (S) exhibited the lowest ammonia nitrogen concentration, measuring 1.01 ± 0.00 ppm on day one and showing only a slight, statistically insignificant increase to 1.02 ± 0.01 ppm by day 21. Soils amended with organic materials but without AZ78 cells (SFi, SFe, and SH) displayed higher ammonia nitrogen concentrations at day 1 (1.07 ± 0.01, 1.06 ± 0.00, and 1.06 ± 0.00 ppm, respectively) compared to the treatment S, but no significant changes were observed by day 21 (1.09 ± 0.00, 1.05 ± 1.01, and 1.07 ± 0.01 ppm, respectively) (**Figure *29***). These results indicate that OAs alone increased initial ammonia nitrogen levels but did not result in significant variation. In contrast, soils inoculated with AZ78 cells showed a different trend. In soil amended with AZ78 cells (SB), ammonia nitrogen concentration increased from 1.02 ± 0.01 ppm on day one to 1.06 ± 0.04 ppm on day 21. When AZ78 cells were combined with OAs, this effect was more pronounced. In treatments SFiB, SFeB, and SHB, ammonia nitrogen concentrations increased significantly from 1.02 ± 0.06, 1.02 ± 0.07, and 1.03 ± 0.00 ppm on day 1 to 3.12 ± 0.03, 3.11 ± 0.05, and 4.11 ± 0.02 ppm on day 21, respectively (**Figure *29***). These increases were statistically significant, demonstrating that AZ78 activity in combination with organic substrates enhanced ammonia nitrogen accumulation in soil.

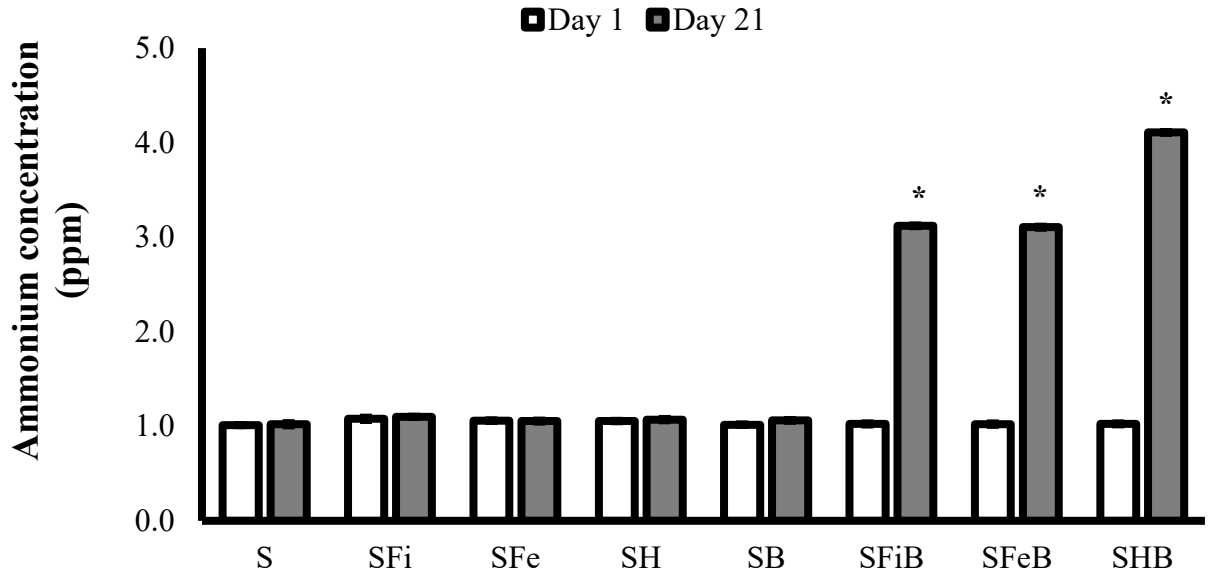

Figure 29. Changes in soil ammonia concentration (ppm) measured at day 1 and day 21 in soils inoculated with *Lysobacter capsici* AZ78 cells. Treatments included soil (S), soil + fish meal (SFi), soil + feather meal (SFe), and soil + hoof meal (SH), each either inoculated with *L. capsici* AZ78 (SB, SFiB, SFeB, and SHB) or left uninoculated. Data represent mean ± standard error (n = 5). Differences between treatments were assessed using Student's t-test ($p \leq 0.05$).

5.4.4.2 Ammonia quantification in soil exposed to *Lysobacter capsici* AZ78 volatiles

In experiment IV, untreated soil (SV) showed only a slight insignificant increase in ammonia nitrogen concentration from 1.09 ± 0.02 ppm on day one to 1.11 ± 0.02 ppm on day 21. A similar trend was observed in soils exposed to NA plates with OAs, where concentrations increased modestly from 1.08 ± 0.02, 1.08 ± 0.02, and 1.08 ± 0.01 ppm to 1.11 ± 0.02, 1.13 ± 0.03, and 1.11 ± 0.02 ppm in SFiV, SFeV, and SHV treatments, respectively (**Figure *30***). By contrast, soils exposed to volatiles emitted by AZ78-inoculated NA plates without OAs (SBV) exhibited a significant increase in ammonia nitrogen concentration, rising from 1.06 ± 0.01 ppm on day one to 5.12 ± 0.03 ppm on day 21. Notably, the treatments SFiBV, SFeBV, and SHBV displayed significant increases in ammonia nitrogen concentration. They exhibited increases from 1.03 ± 0.01, 1.07 ± 0.02, and 1.04 ± 0.01 ppm on day one to 6.18 ± 0.04, 6.18 ± 0.04, and 6.21 ± 0.05 ppm on day 21, respectively (**Figure *30***).

These results demonstrate that volatile compounds produced by AZ78, particularly when organic substrates are present, have a strong and significant effect on soil ammonia nitrogen dynamics.

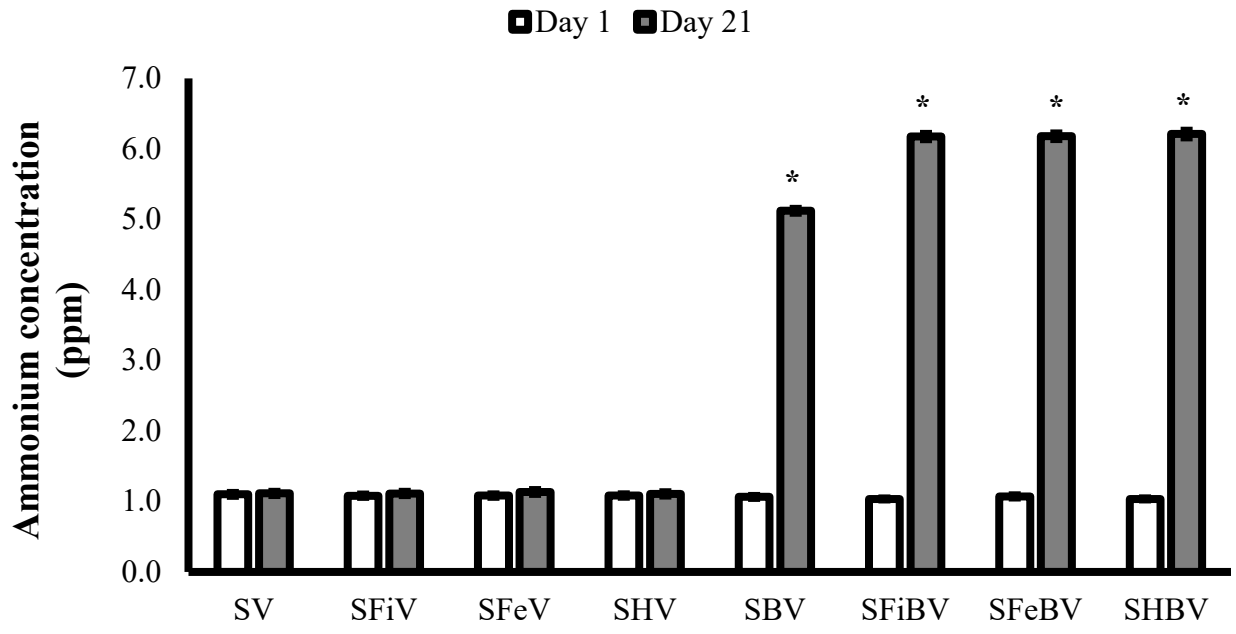

Figure 30. Changes in soil ammonia concentration (ppm) measured at day 1 and day 21 in soils exposed to volatiles produced by *Lysobacter capsici* AZ78. Treatments included soils exposed to nutrient agar (NA) volatiles (SV), soil exposed to NA with fish meal (SFiV), soil exposed to NA with feather meal (SFeV), and soil exposed to NA with hoof meal (SHV), soil exposed to *L. capsici* AZ78 volatiles (SBV), soil exposed to NA with fish meal + *L. capsici* AZ78 (SFiBV), soil exposed to NA with feather meal + *L. capsici* AZ78 (SFeBV), and soil exposed to NA with hoof meal + *L. capsici* AZ78 (SHBV). Data represent mean ± standard error (n = 5). Differences between treatments were assessed using Student's t-test ($p \leq 0.05$).

5.4.5 Volatile organic compounds emitted by Lysobacter capsici *AZ78 in different growth conditions*

In this study, VOCs produced by AZ78 were analysed under two growth conditions, NA_78 and NAH_78, with the corresponding uninoculated media (NA and NAH) serving as controls. VOCs collected in HS vials were analysed on day seven using GC-MS, leading to the identification of 77 compounds across all treatments. These VOCs belonged to diverse chemical classes, including alcohols, ketones, aldehydes, furans and their derivatives, pyrazines, phenols, and sulphur- and nitrogen-containing compounds. One-way ANOVA identified 25 compounds as statistically

significant ($p < 0.05$), and their relative abundances were visualized in a normalized heatmap (log_{10}-transformed average peak area).

Overall, VOC abundance was highest in NAH_78, followed by NA_78, whereas the uninoculated controls (NA and NAH) showed markedly fewer and lower-abundance VOCs. Among all treatments, NAH_78 exhibited the most pronounced metabolic divergence, indicating a strong effect of hoof meal on AZ78 volatile production (**Figure *31***).

Consistent with the heatmap analysis, principal component analysis (PCA) revealed a clear separation of treatments based on their VOC profiles. Samples clustered primarily along principal component 1 (PC1), with AZ78-inoculated treatments (NA_78 and NAH_78) clearly separated from the uninoculated controls (NA and NAH), indicating that AZ78 inoculation was the dominant factor shaping VOC emissions. Within the AZ78-treated samples, NAH_78 formed a distinct cluster separated from NA_78, reflecting the strong influence of hoof meal on AZ78-mediated VOC production. This separation was consistent with the enhanced emission of pyrazines observed in NAH_78 (**Figure *32***). In contrast, control treatments clustered together on the negative side of PC1, indicating comparatively low and less diverse VOC emissions. A moderate separation between NA and NAH along PC2 suggested that hoof meal alone also contributed to shifts in VOC composition, although to a lesser extent than AZ78 inoculation. These treatment-specific differences were statistically supported by PERMANOVA.

The most prominent feature of the AZ78 volatilome was the dominance of pyrazines, particularly methoxypyrazine derivatives. While pyrazines were detected only at baseline levels in the control treatments, inoculation with AZ78 resulted in a clear accumulation of this compound class in both NA_78 and NAH_78, with a substantially stronger enrichment in NAH_78 (**Figure *31***). Several monoalkyl-methoxypyrazines, including 2-methoxy-3-(1-methylpropyl)-pyrazine, 2-methoxy-3-sec-

butyl-5-methylpyrazine, 2-methoxy-3-(1-methylethyl)-pyrazine, 2-methoxy-3-methylpyrazine, and 2-methoxy-5-methyl-3-propan-2-yl-pyrazine, were detected at high abundance. In addition, dialkyl-methoxypyrazines such as 3-methoxy-2,5-dimethylpyrazine and 2-methoxy-3,5-dimethylpyrazine were particularly abundant in NAH_78 treatments. Notably, 2,5-dimethylpyrazine, previously reported to exhibit toxicity against *P. ultimum* (Vlassi., *et al.*, 2020a), was present at higher levels in NAH_78 than in NA_78. All monoalkyl- and dialkyl-methoxypyrazines were detected at substantially lower abundance in the uninoculated controls (**Figure *31***).

Beyond pyrazines, several additional VOCs were enriched in AZ78-inoculated treatments. These included the alcohol 3-methyl-1-butanol, the furan derivative 3,4-dimethoxyfuran, and the nitrogen-containing compound pyrrole. 3-methyl-1-butanol and 3,4-dimethoxyfuran were more abundant in NAH_78 than in NA_78, whereas pyrrole showed comparable abundance across both AZ78-inoculated treatments. All three compounds were detected at lower levels in the uninoculated controls. A distinct group of VOCs was specifically associated with hoof meal amended media (NAH and NAH_78). These included thiazole, 2-methoxymethyl-furan, and the ketones 2-octanone and 2-nonanone. These compounds were present at baseline or low abundance in treatments lacking hoof meal, regardless of AZ78 inoculation. In contrast, aldehydes such as benzaldehyde and nonanal were detected at higher abundance exclusively in the uninoculated control treatments (NA and NAH). Another aldehyde, 3-furaldehyde, was most abundant in AZ78-inoculated NA vials (NA_78) but occurred at low levels in hoof meal amended treatments. Two compounds, 2-(1-phenylethyl)-phenol and 2,3-heptadien-1-ol, were detected at elevated levels only in NA_78 vials and were present at low abundance in all other treatments (**Figure *31***).

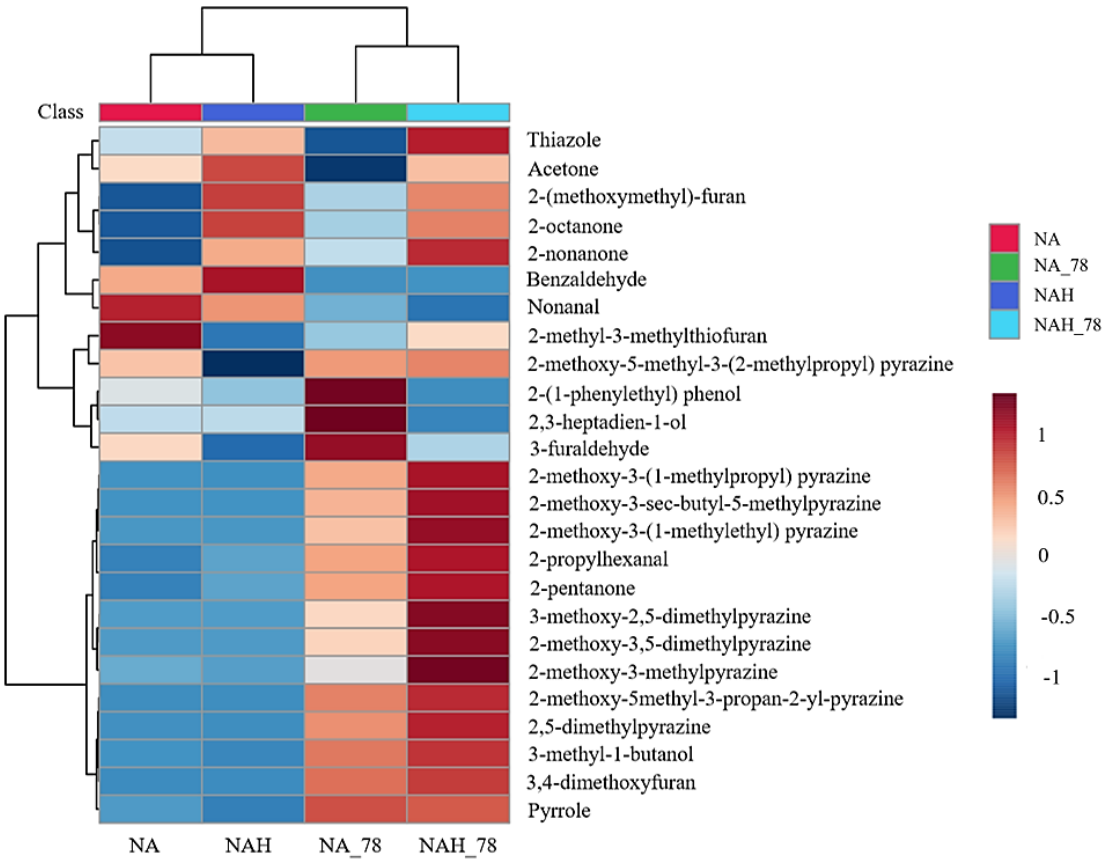

Figure 31. Heatmap of $\log_{10}$ transformed average peak areas of volatile organic compounds detected at 144 h in nutrient agar (NA) without amendment (NA) or with hoof meal (NAH), in the absence or presence of *Lysobacter capsici* AZ78 inoculation (NA_78 and NAH_78, respectively). Data were $\log_{10}$ transformed, mean-centred, and hierarchically clustered using Euclidean distance and Ward's minimum variance method. VOC abundance is indicated by a colour scale from blue (low) to red (high). The heatmap includes only VOCs showing significant differences among treatments (one-way ANOVA, $p \leq 0.05$).

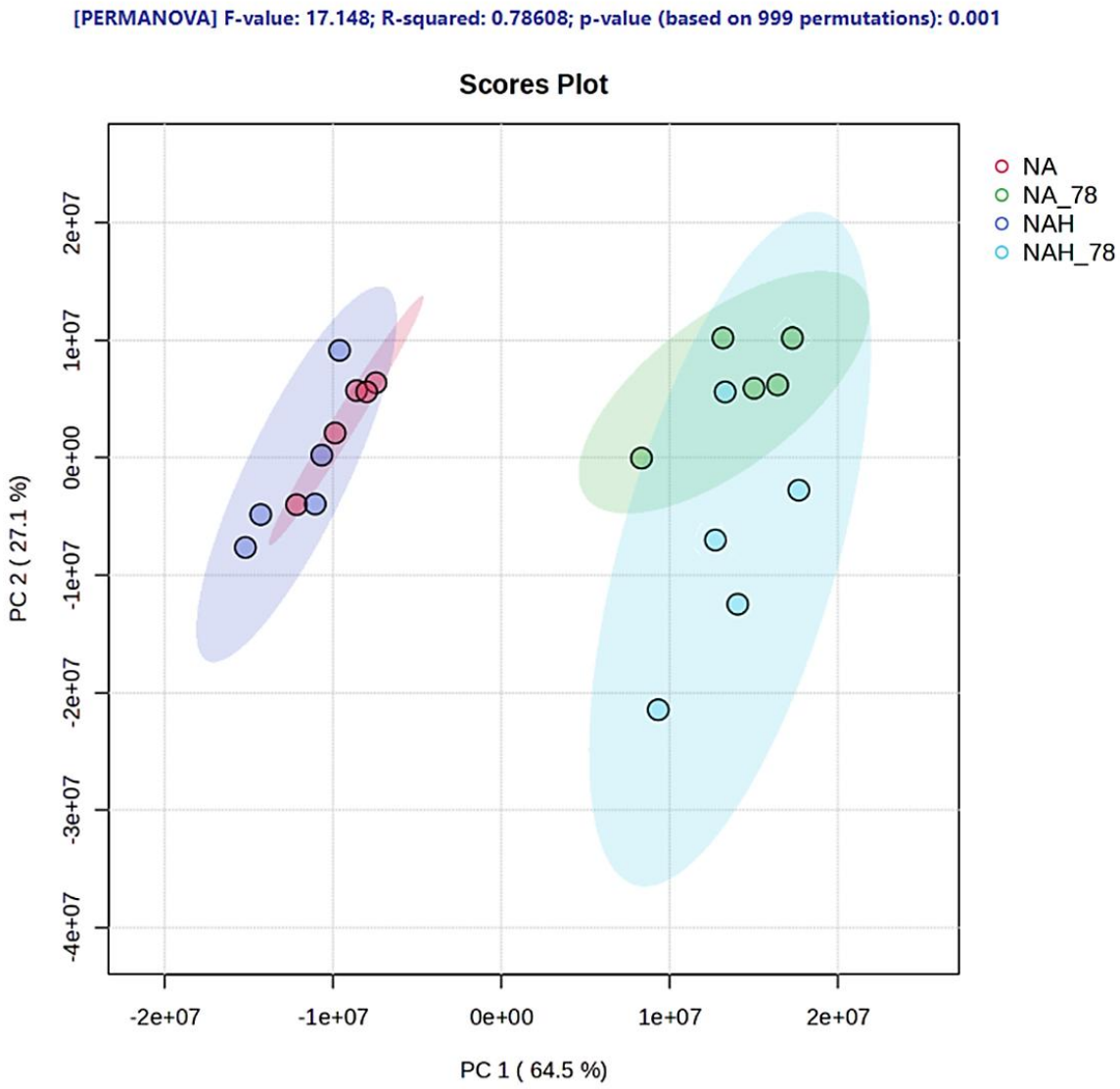

Figure 32. Principal component analysis (PCA) score plot and PERMANOVA test of volatile organic compound profiles in nutrient agar without amendment (NA) or with hoof meal (NAH), in the absence or presence of *Lysobacter capsici* AZ78 inoculation (NA_78 and NAH_78, respectively). Points represent replicates and ellipses indicate 95% confidence intervals. The first two principal components explained 91.6% of the total variance (PC1: 64.5%; PC2: 27.1%).

5.4.6 Impact of pH change on the bacterial and fungal populations in the soil

5.4.6.1 Impact of pH change on the bacterial and fungal populations in the soil treatments without organic amendments

In Experiment I, where the soil was directly inoculated with AZ78 cells, a slight reduction in bacterial cell density was observed at day 21 in SB treatment compared to the untreated control (S). No significant differences were detected at the earlier sampling points (**Figure *33***). A comparable trend was observed in Experiment II, in which soils were exposed to volatiles emitted by AZ78 grown on NA. At day 21, bacterial cell density was slightly lower in the treatment SBV than in its respective control (SV), whereas no differences were detected at days 1 and 7 (**Figure *33***). Overall, AZ78 cells and their volatiles had only minor and late effects on bacterial abundance. In contrast, fungal populations were markedly affected. In Experiment I, fungal counts in SB declined by day 14 and were completely inhibited by day 21, while remaining relatively stable in the untreated control (S) (**Figure *33***). In Experiment II, exposure to AZ78 volatiles led to an even earlier suppression of fungal growth, with inhibition evident by day 7 and complete suppression by days 14 and 21. These findings suggest that AZ78 volatiles exert a stronger and more rapid antifungal effect than the inoculation of AZ78 cells themselves.

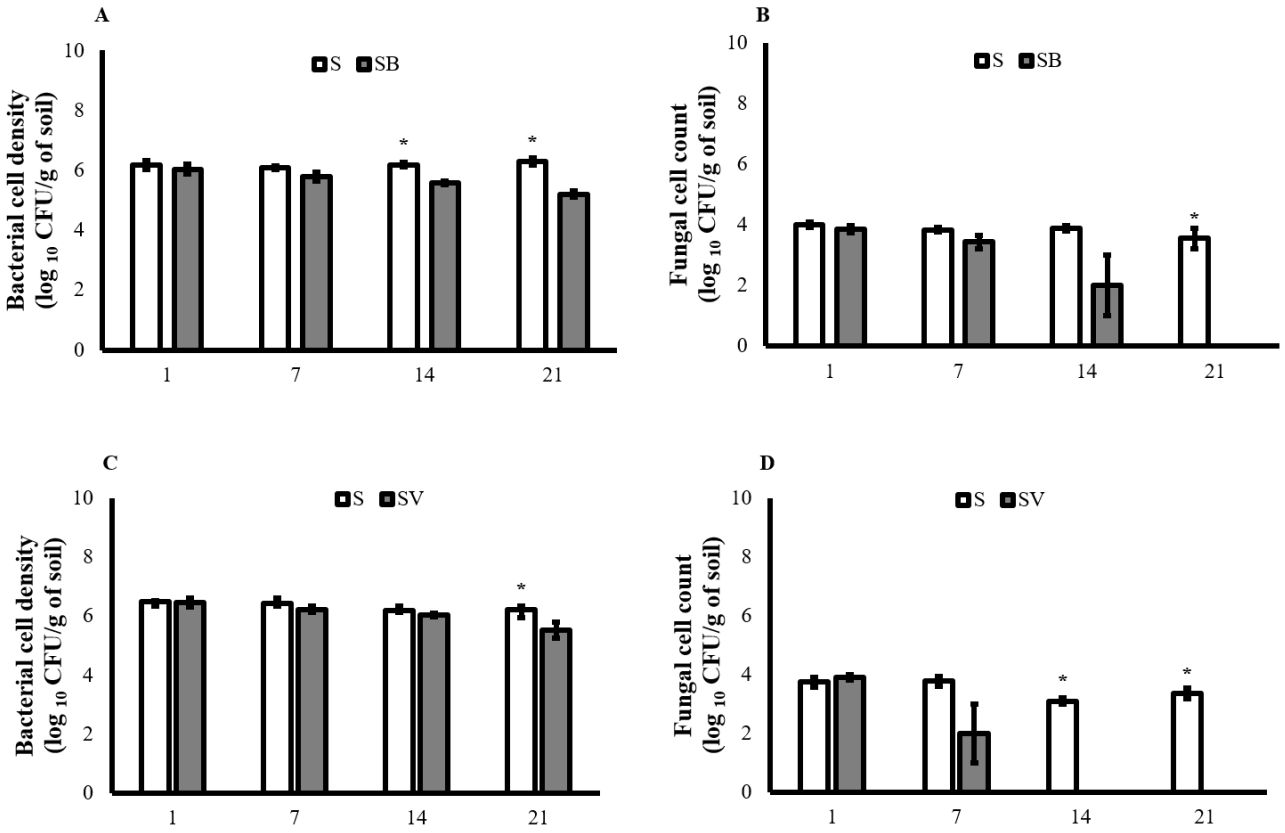

Figure 33. Change in the bacterial and fungal cell density in (**A** and **B**) soil inoculated with *Lysobacter capsici* AZ78 cells and (**C** and **D**) soil exposed to volatiles produced by *L. capsici* AZ78 at 1, 7, 14, and 21 days. The treatments in **A** and **B** included soil (S) and soil + *L. capsici* AZ78 (SB). The treatments in **C** and **D** included soil exposed to nutrient agar (NA) volatiles (SV) and soil exposed to NA with *L. capsici* AZ78 (SBV). Data represent mean ± standard error (n = 5). Differences between treatments were assessed using Student's t-test ($p \leq 0.05$).

5.4.6.2 Impact of pH change on the bacterial and fungal populations in the soil treatments with organic amendments

Experiments III and IV evaluated the impact of hoof meal amendment on bacterial and fungal populations in both AZ78-inoculated soils and soils exposed to AZ78 volatiles, alongside their respective controls. In Experiment III, neither hoof meal amendment nor AZ78 cell inoculation significantly influenced bacterial density at day 1 or day 21. Bacterial populations remained relatively stable in both uninoculated controls (S, SH) and AZ78-inoculated treatments (SB, SHB). However, soils exposed to AZ78 volatiles (SBV and SHBV) showed slight changes in bacterial density by day

21 compared to day 1, whereas their corresponding controls (SV and SHV) did not exhibit such variation. Regarding fungal populations in Experiments III and IV, a pronounced decline was observed by day 21 in all AZ78-related treatments (SB, SHB, SBV, and SHBV) (**Figure *34***). Complete inhibition of fungal growth was recorded at this time point, irrespective of hoof meal amendment.

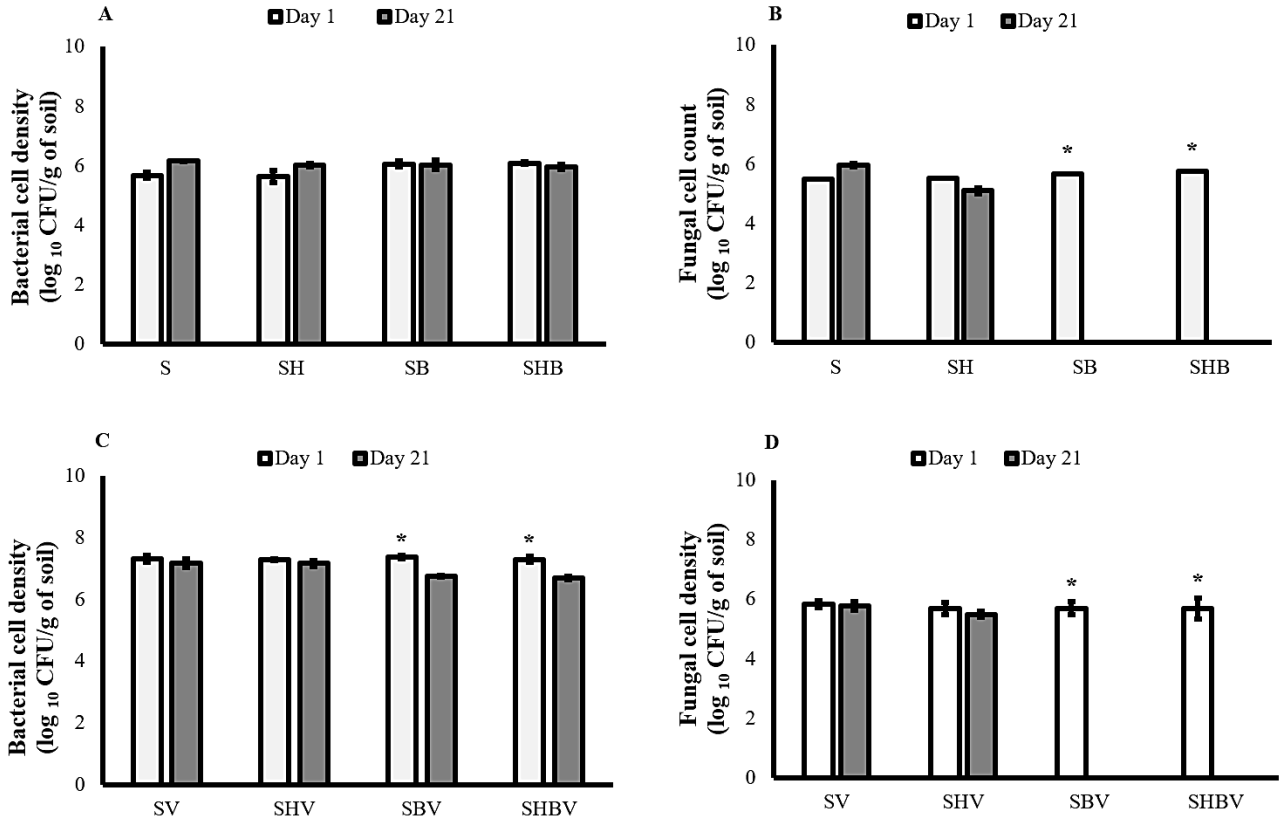

Figure 34. Change in the bacterial and fungal cell density in (**A** and **B**) soil inoculated with *Lysobacter capsici* AZ78 cells and (**C** and **D**) soil exposed to volatiles produced by *L. capsici* AZ78 at day 1 and day 21. Treatments in **A** and **B** included soil (S), soil + *L. capsici* AZ78 (SB), soil + hoof meal (SH), and soil + hoof meal + *L. capsici* AZ78 (SHB). Treatments in **C** and **D** included soil exposed to nutrient agar (NA) volatiles (SV), soil exposed to *L. capsici* AZ78 volatiles (SBV), soil + NA with hoof meal (SHV), Soil exposed to NA with hoof meal + *L. capsici* AZ78 volatiles (SHBV). Data represent mean ± standard error (n = 5). Differences between treatments were assessed using Student's t-test ($p \leq 0.05$).

5.4.7 Taxonomic diversity

5.4.7.1 Taxonomic composition and treatment-driven shifts in soil microbial communities

The soil microbial community exhibited a hierarchical response to the experimental treatments. Bacteria dominated all the samples, comprising an average of 98.85% relative abundance, while Archaea were consistently present at low levels, representing a minor component across most of the treatments (**Figure *35***).

Phylum-level taxonomic profiling revealed treatment-dependent shifts in community composition. *Actinobacteria* and *Proteobacteria* were the most abundant phyla across all treatments, though their relative proportions varied considerably. *Actinobacteria* were significantly enriched in volatile-exposed soils, particularly in the absence of hoof meal (SV, 55.12%; SBV, 55.42%), followed by treatments containing hoof meal (SHV, 43.37%; SHBV, 51.40%). *Proteobacteria* reached the highest relative abundance in SHB (40.24%), whereas in all other treatments they ranged between 20-30%. Additional phyla contributing to the core soil microbiome included *Chloroflexi*, *Acidobacteria*, and *Gemmatimonadetes*. *Chloroflexi* and *Acidobacteria* maintained relatively stable abundances in S, SB, and SH soils but showed slight reductions in volatile-exposed treatments, with the lowest levels observed in SHB (**Figure *35***).

At the genus level, treatment-specific effects were more pronounced and provided insight into the drivers of phylum-level shifts. The enrichment of *Actinobacteria* was largely attributable to the genera *Nocardioides* and *Streptomyces*, which dominated volatile-exposed soils. A stable core of genera, including *Gaiella*, *Solirubrobacter*, and *Sphingomonas*, persisted across most treatments, although *Gaiella* and *Solirubrobacter* declined sharply in SHB, coinciding with an increase in *Sphingomonas*. *Mesorhizobium*, a Gram-negative nitrogen-fixing bacterium, was enriched in SHB but depleted in volatile-exposed soils (**Figure *35***). *Nitrospira* exhibited its lowest abundance in SHB, whereas it was moderately represented across other treatments. *Nitrosococcus* was restricted to

volatile-exposed soils, the highest abundance observed in SBV. Additional genera selectively enriched in SHB included *Lysobacter*, *Microvirga*, and *Arthrobacter*. A proportion of unassigned genera (others) was consistently observed across all treatments.

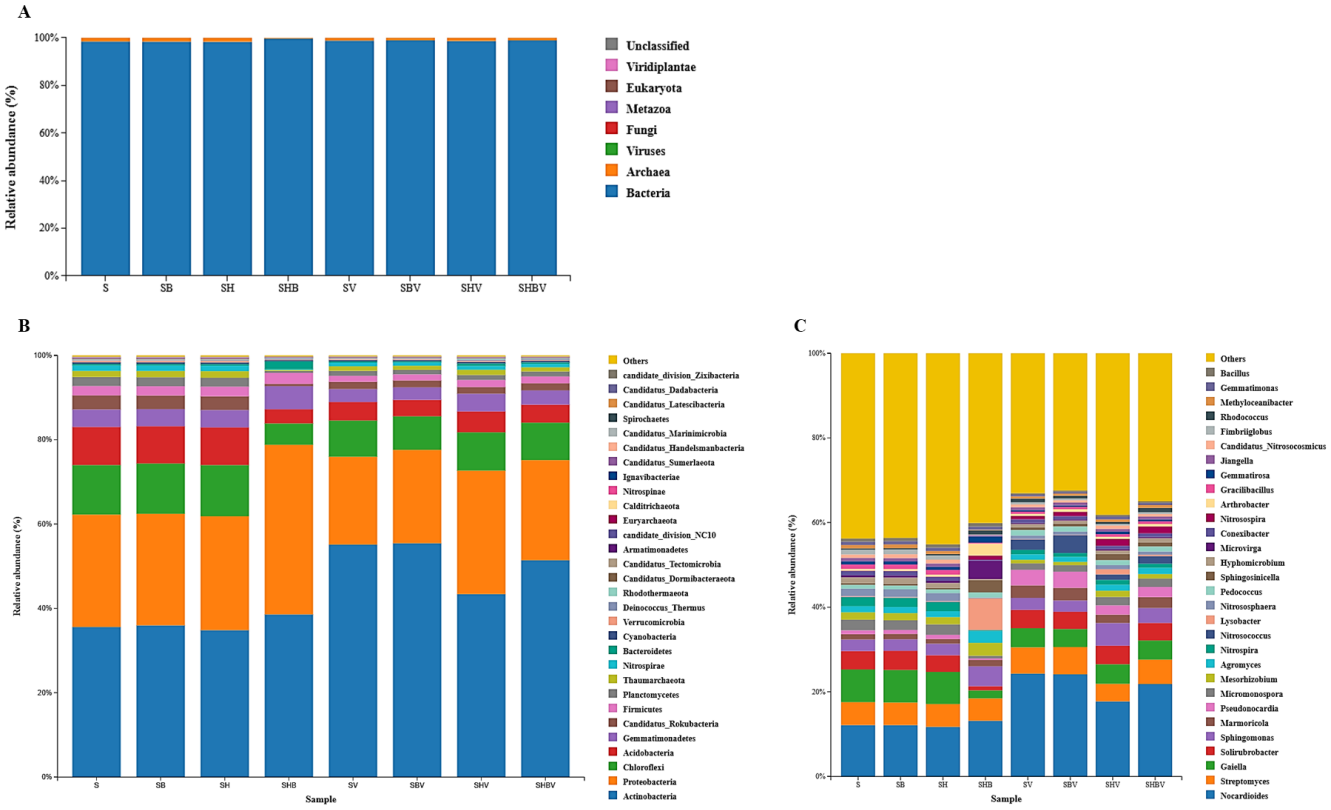

Figure 35. Taxonomic composition and relative abundance of microbial communities determined by shotgun metagenomic sequencing at the (A) domain, (B) phylum, and (C) genus levels. Treatments included soil (S), soil + *Lysobacter capsici* AZ78 (SB), soil + hoof meal (SH), and soil + hoof meal + *L. capsici* AZ78 (SHB), soils exposed to nutrient agar (NA) volatiles (SV), soil exposed to NA with *L. capsici* AZ78 (SBV), soil exposed to NA with hoof meal (SHV), Soil exposed to NA with hoof meal + *L. capsici* AZ78 (SHBV). The top 30 most abundant taxa are shown at the phylum and genus levels. "Unassigned" represents sequences that could not be taxonomically annotated. Relative abundances are expressed as percentages of total classified reads

5.4.7.2 Alpha diversity analysis reveals treatment-dependent changes

Alpha diversity was assessed using the Chao1 richness estimator and the Shannon diversity index to evaluate treatment-induced changes in microbial richness and diversity. Chao1 analysis

revealed clear treatment-specific differences in estimated richness. The SHB treatment exhibited the highest richness (Chao1 = 12,481.59), markedly exceeding all other treatments (**Figure *36***). In contrast, other treatments like S, SB, and SH maintained comparable baseline richness levels. Among soils exposed to volatile treatments, SHV displayed elevated richness, followed by SHB. The presence of hoof meal in the media generally increased richness relative to soil exposed to NA alone (SV and SBV). However, richness in SHBV was lower than in SHV, indicating that exposure to AZ78 volatiles may slightly reduce species richness compared to hoof meal alone. Overall, richness followed the trend: SHB > SHV > SHBV, whereas all remaining treatments, including controls (S and SV), remained at baseline levels.

Shannon diversity analysis showed a similar pattern. SHB exhibited the highest diversity (Shannon index = 6.50), indicating both high richness and evenness (**Figure *36***). In general, volatile-exposed soils demonstrated higher Shannon diversity compared to treatments inoculated with AZ78 cells. Within the volatile group, hoof meal amendment further increased diversity, with SHV showing the highest Shannon value (6.43), followed by SHBV (6.36). Among AZ78 cell treatments, only SHB displayed a marked increase in diversity, whereas other treatments remained comparable to their respective controls. Collectively, these results indicate that the combined application of AZ78 cells and hoof meal (SHB) had the strongest positive effect on both richness and diversity (**Figure *36***).

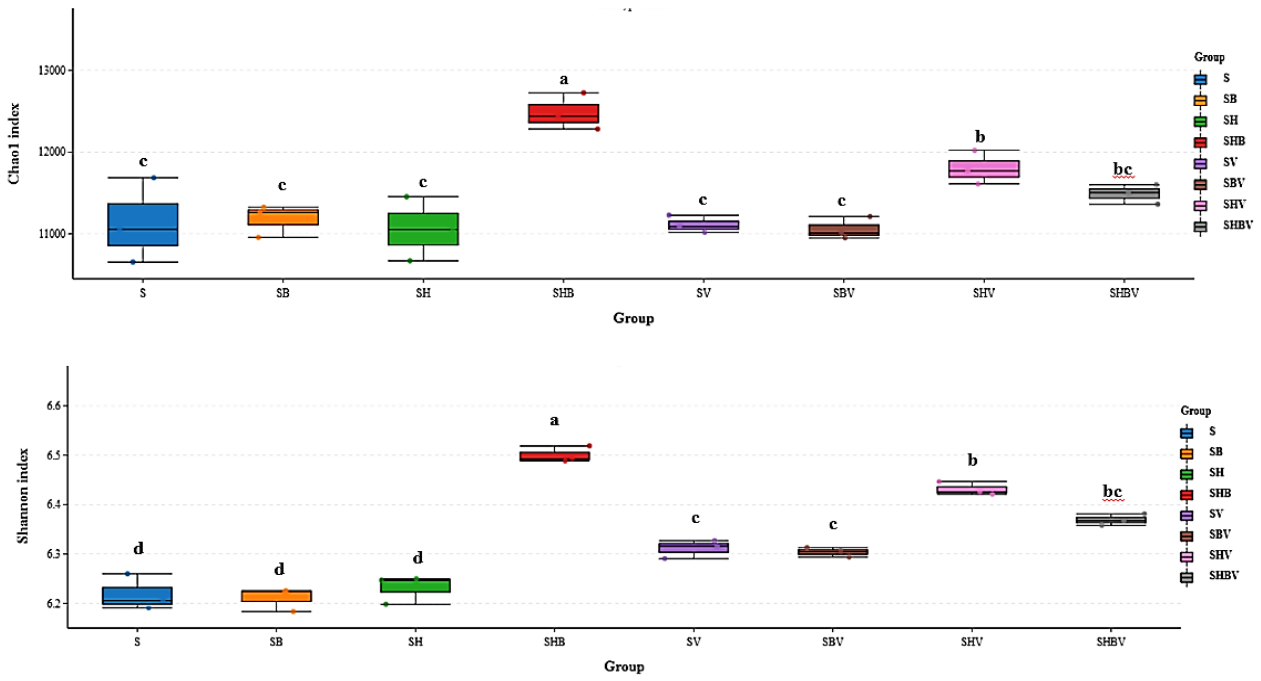

Figure 36. Alpha diversity of microbial communities across soil treatments measured by richness (Chao1 index; p = 0.0001) and diversity (Shannon index; p = 7.6e-11). Treatments included soil (S), soil + *Lysobacter capsici* AZ78 (SB), soil + hoof meal (SH), and soil + hoof meal + *L. capsici* AZ78 (SHB), soils exposed to nutrient agar (NA) volatiles (SV), soil exposed to NA with *L. capsici* AZ78 (SBV), soil exposed to NA with hoof meal (SHV), Soil exposed to NA with hoof meal + *L. capsici* AZ78 (SHBV). Boxplots show median values (line within the box), with boxes representing the interquartile range and whiskers indicating the data range (n = 3). Differences among treatments were assessed using the Kruskal–Wallis test followed by Dunn's multiple comparisons. Treatments sharing the same letter do not differ significantly ($p < 0.05$).

5.4.7.3 Beta diversity and community structure

Consistent with the alpha diversity patterns, beta diversity analysis was performed to determine whether treatment-induced differences in microbial richness and diversity were accompanied by shifts in overall community composition. Beta diversity was calculated using Bray–Curtis dissimilarity and visualized using Principal Coordinates Analysis (PCoA). The PCoA revealed a clear separation among treatments (**Figure *37***), with the first axis having 64.33% of the total variation and the second axis 29.18%. This indicates strong treatment driven structuring of microbial communities. These patterns were consistent with alpha diversity trends, as the SHB treatment

previously shown to have high richness and diversity formed a distinct cluster along PCoA1, leading to a pronounced shift in community composition compared to all other treatments. The other AZ78 cell treatments (S, SB, and SH) clustered together on the left side of PCoA1, separated from SHB, and exhibited minimal internal variation, as confirmed by Bray–Curtis distance matrix boxplots (**Figure *37***). A distinct clustering pattern separated the AZ78 volatile-exposed soil treatments from AZ78 inoculated soil treatments, highlighting the unique effects of volatile-mediated exposure. Within this group, SV and SBV formed tight clusters, whereas the samples SHBV and SHV clustered slightly further apart, suggesting subtle differences in community responses. Control treatments (S and SV) exhibited tight clustering, reflecting a stable baseline community structure. PERMANOVA confirmed that the treatments significantly influenced microbial community composition ($R^2 = 0.940$, $p = 0.001$), underscoring that the observed variation in relative abundance and alpha diversity **was treatment-dependent**.

.

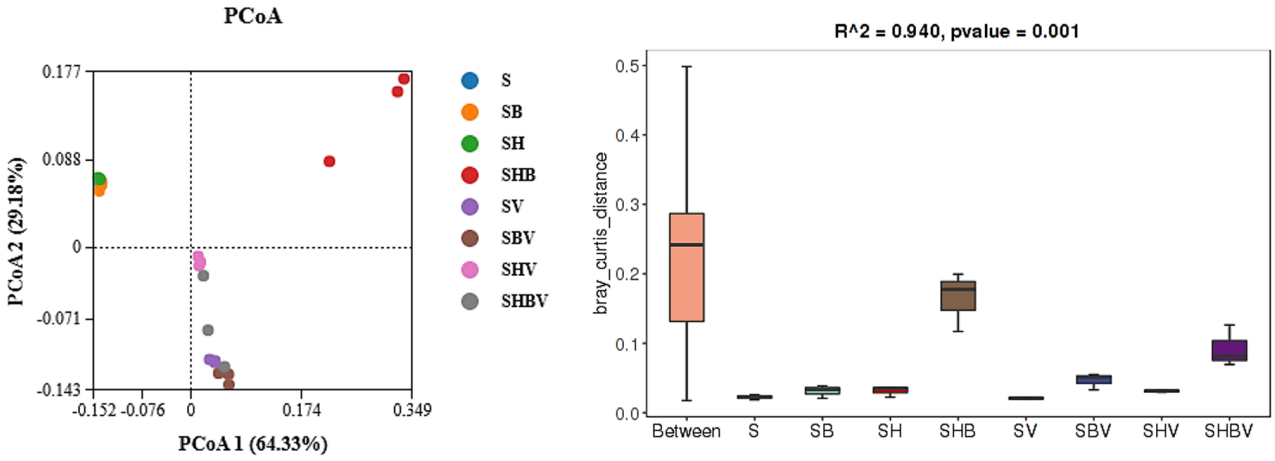

Figure 37. Beta diversity analysis of microbial communities across soil treatments based on Bray–Curtis dissimilarity. **(A)** Principal coordinates analysis (PCoA) showing differences in microbial community composition among treatments. The percentage of variance explained by each axis is indicated. **(B)** Boxplot of Bray–Curtis dissimilarity values illustrating beta diversity between treatment groups. "Between" represents distances among samples from different treatments.

Treatments included soil (S), soil + *Lysobacter capsici* AZ78 (SB), soil + hoof meal (SH), and soil + hoof meal + *L. capsici* AZ78 (SHB), soils exposed to nutrient agar (NA) volatiles (SV), soil exposed to NA with *L. capsici* AZ78 (SBV), soil exposed to NA with hoof meal (SHV), Soil exposed to NA with hoof meal + *L. capsici* AZ78 (SHBV).

5.4.7.4 Linking microbial community composition and soil environmental factors using redundancy analysis (RDA) and heatmap analyses

To evaluate how soil environmental variables shape microbial community composition, RDA was performed using soil pH and ammonia concentration (ppm) as explanatory factors (**Figure *38***). The first two RDA axes explained 11.95% of the total variation in the microbial communities, with RDA1 contributing 7.96% and RDA2 contributing 3.99%. Both soil pH and ammonia vectors were oriented toward the positive side of RDA1, indicating that microbial variation along this axis is positively associated with these soil parameters. Several genera clustered along the ammonia vector, including *Micromonospora*, *Streptomyces*, *Nocardioides*, *Pseudonocardia*, and *Solirubrobacter*, suggesting a strong positive correlation with increased ammonia availability, whereas *Gaiella*, *Agromyces*, and *Mesorhizobium* displayed negative associations with pH and ammonia shifts. These multivariate patterns were further supported by a correlation heatmap, which revealed genus-level relationships with soil variables and highlighted enrichment trends across treatments (**Figure *38***). Genera such as *Micromonospora*, *Gracilibacillus*, *Methyloceanibacter*, *Streptomyces*, *Mycobacterium*, *Nitrococcus*, and *Pseudonocardia* exhibited strong positive correlations and enrichment with higher soil pH and ammonia, while *Bacillus*, *Lysobacter*, *Agromyces*, *Nitrospira*, *Azospirillum*, *Rhodococcus*, *Nocardia*, *Arthrobacter*, *Nitrosococcus*, and *Actinomyces* showed moderate positive associations. In contrast, taxa such as *Candidatus*, *Paracoccus*, *Sphingomonas*, and *Rhizobium* displayed comparatively weak correlations and basal abundance patterns. Together, the RDA and heatmap analyses indicate that soil pH and ammonia availability are central drivers of

microbial community structure, shaping both overall community composition and genus-level enrichment patterns, consistent with the differentiation observed in beta diversity analyses.

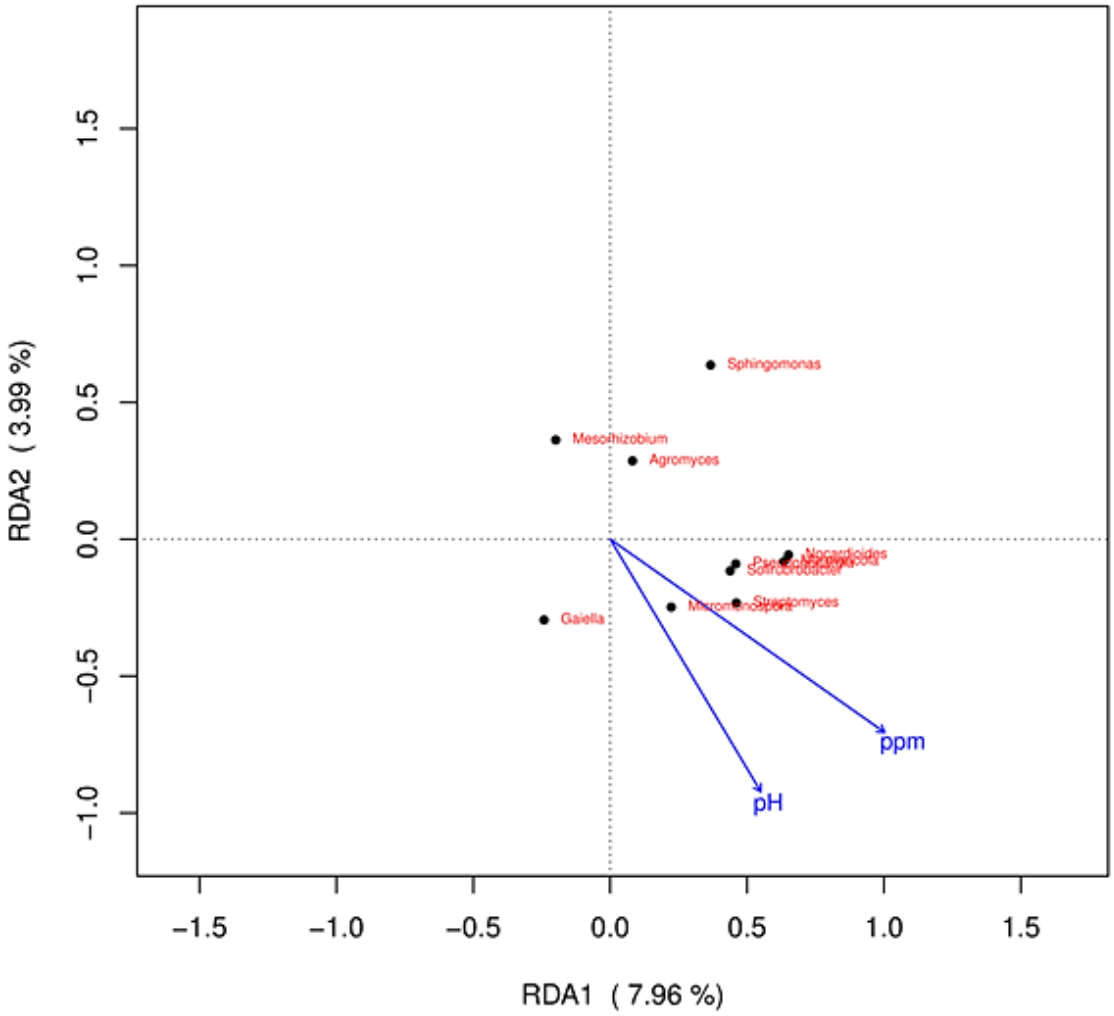

Figure 38. Redundancy analysis (RDA) showing the relationships between soil physicochemical parameters and the relative abundance of significantly enriched microbial genera in soil samples ($p < 0.05$). Blue arrows represent environmental variables, including soil pH and ammonia concentration (ppm). The direction and length of the arrows indicate the strength and magnitude of their influence on microbial community composition.

5.4.8 Functional and taxonomic drivers of soil nitrogen cycling across treatments

5.4.8.1 Functional gene profiling of soil nitrogen cycle

Metagenomic analysis revealed that the relative abundance of functional genes associated with key steps of the soil nitrogen (N) cycle varied among treatments, reflecting differences in nitrogen transformation potential. Among all nitrogen-cycle processes, nitrogen assimilation (NAS) genes were the most abundant across treatments. The S, SB, and SH treatments exhibited higher NAS gene abundance, whereas SHB showed slightly lower NAS levels (**Figure *39***). Genes involved in denitrification (DNIT) displayed notable treatment-dependent variation, with the SHB treatment exhibiting the highest relative abundance. Ammonium nitrogen reduction (ANR) genes were moderately abundant, with S, SB, and SH slightly higher than other treatments and SHB showing the lowest levels. Dissimilatory nitrate reduction (DNR) genes were also moderately represented, with SHB and AZ78 volatile-treated soils showing the highest relative abundance. Nitrification (NIT) genes were least abundant overall, though SBV soils exposed to AZ78 volatiles showed relatively higher gene abundance compared to cell-treated soils (**Figure *39***).

At the individual gene level, NAS genes such as *gltD* showed moderate abundance across treatments, whereas *glnA* was negligible, and *gltB* was enriched in S, SB, and SH. NIT-related genes (*amoA, amoB, amoC, hao*) were higher in volatile-treated soils, particularly in SBV, while among cell-treated soils, SHB displayed higher abundance of *amoA, amoC,* and *hao*, but lower *amoB* (**Figure 40**). For ANR, *nasB* was enriched in SHB and volatile groups, while *nasC* showed opposite trends, and *nirA* was lower in SHB. DNR genes (*nirB, nirD*) were most abundant in SHB and volatile-treated soils, while *nrfH* was higher in cell-treated soils. DNIT genes showed highest abundance in SHB, particularly *narI, napB, nirK, norB,* and *nosZ*, whereas *napA* was lower in volatile-treated soils, and *narI* and *nirK* were enriched in volatile-treated groups (**Figure 40**).

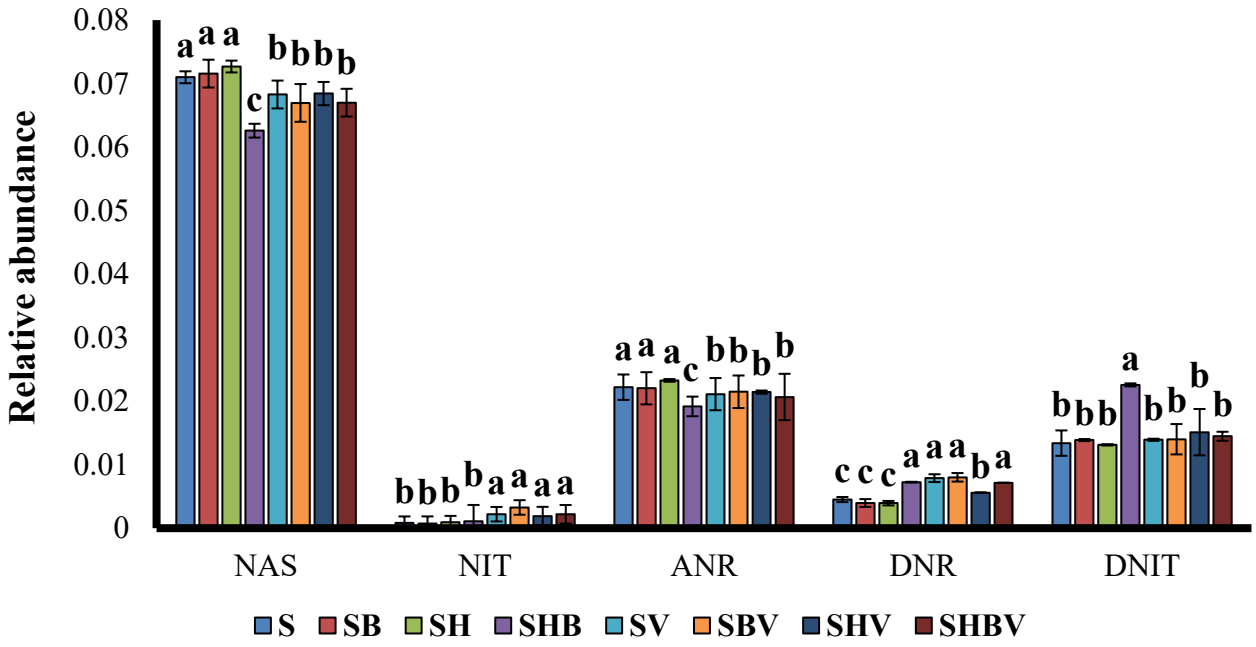

Figure 39. Differences in the abundance of functional genes associated with nitrogen (N) cycling processes under different treatments. Treatments included soil (S), soil + *Lysobacter capsici* AZ78 (SB), soil + hoof meal (SH), and soil + hoof meal + *L. capsici* AZ78 (SHB), soils exposed to nutrient agar (NA) volatiles (SV), soil exposed to NA with *L. capsici* AZ78 (SBV), soil exposed to NA with hoof meal (SHV), Soil exposed to NA with hoof meal + *L. capsici* AZ78 (SHBV). Nitrogen cycling processes included nitrogen assimilation (NAS), nitrification (NIT), assimilatory nitrogen reduction (ANR), dissimilatory nitrogen reduction (DNR), and denitrification (DNIT). Data are presented as mean ± standard error (n = 5). Differences among treatments were analyzed using one-way ANOVA followed by Tukey's HSD test ($\alpha = 0.05$). Columns sharing the same letter are not significantly different.

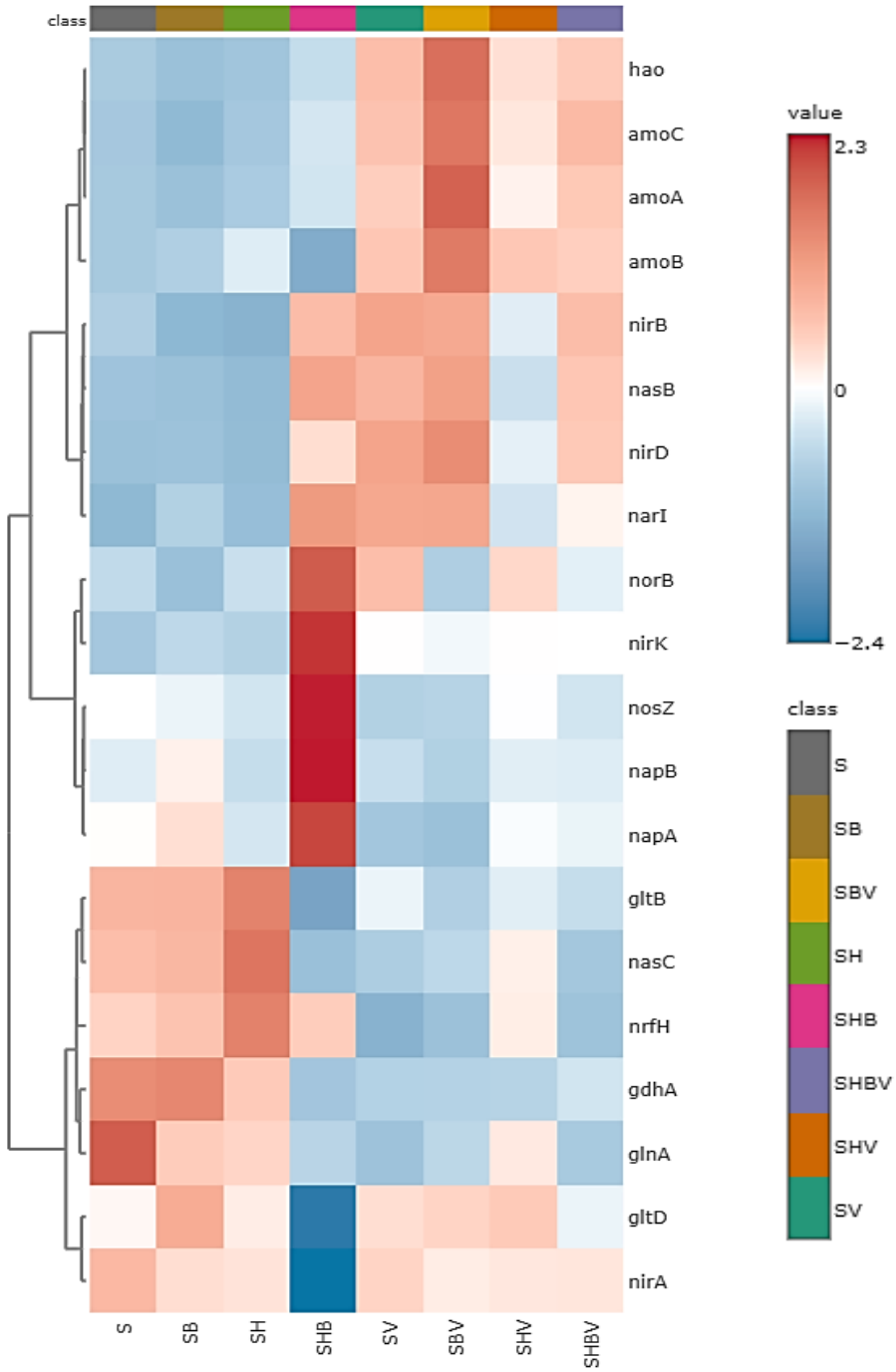

Figure 40. Heatmap of normalized abundance values (row Z-scores) illustrating differences in the abundance of nitrogen cycling functional genes annotated in the KEGG database across different treatments. Treatments included soil (S), soil + *Lysobacter capsici* AZ78 (SB), soil + hoof meal (SH), and soil + hoof meal + *L. capsici* AZ78 (SHB), soils exposed to nutrient agar (NA) volatiles (SV), soil exposed to NA with *L. capsici* AZ78 (SBV), soil exposed to NA with hoof meal (SHV), Soil exposed to NA with hoof meal + *L. capsici* AZ78 (SHBV).

5.5 Discussion

The present study demonstrates that AZ78 enhances tomato seed germination and suppresses damping-off caused by *Pythium ultimum* through multiple complementary mechanisms, including direct antagonism, emission of bioactive volatile organic compounds (VOCs), modification of soil physicochemical properties, and restructuring of the soil microbiome. Across experiments, tomato germination consistently improved in soils inoculated with AZ78 cells or exposed to AZ78-derived volatiles compared with untreated controls. The strongest plant growth-promoting and biocontrol effects occurred when AZ78 treatments were combined with OAs, particularly hoof meal, indicating that nutrient availability and substrate composition strongly influence AZ78 performance in soil.

In Experiment I, prolonged soil inoculation with AZ78 for 21 days significantly increased germination under both pathogen-free (SB) and pathogen-inoculated (SBP) conditions, demonstrating that AZ78 functions not only as a BCA but also as a PGPR even in the presence of the pathogen. Comparable improvements observed in VOC-exposed soils indicate that volatile-mediated interactions alone can influence plant protection and growth promotion. These findings support earlier *in vitro* observations showing anti-oomycete activity of AZ78 VOCs against *P. ultimum* (Vlassi *et al*., 2020a), while extending their relevance to greenhouse soil conditions and confirming AZ78 functionality under semi-realistic soil environment.

The disease suppressiveness observed in AZ78-treated soils aligns with the broader concept that beneficial microbial communities regulate soil-borne diseases through antagonism, competition, and ecological changes (Marín-guirao *et al.*, 2025). Similar mechanisms have been described for several BCAs, including *Bacillus* and *Trichoderma* species (Correa-delgado *et al.*, 2024; Huang *et al.*, 2024). Within the genus *Lysobacter*, suppressive soils have previously been associated with high abundances of antagonistic species such as *L. antibioticus* and *L. gummosus* (Postma *et al*., 2008), and increased

L. capsici populations have been linked to suppression of *Rhizoctonia solani* (Postma *et al*., 2010a). Our results support the hypothesis that AZ78 contributes to disease-suppressive soil conditions through active microbial interactions. Improved germination in soils exposed only to AZ78 volatiles further indicates that diffusible gaseous metabolites accumulated during incubation and inhibited pathogen activity, consistent with reports showing microbial VOC-mediated suppression of *Fusarium oxysporum*, *R. solani*, and *Pythium* species (Agtmaal *et al.*, 2018).

Organic amendments amplified AZ78 activity, acting primarily as enhancers rather than direct antimicrobial agents. OAs are known to stimulate beneficial microbial communities and increase soil biological activity, thereby disrupting pathogen life cycles (Yadav *et al.*, 2015). Feather meal has been shown to enhance suppressiveness against *R. solani* (Postma *et al*., 2014), while fish meal amendments historically improved crop performance and reduced several soil-borne diseases through stimulation of microbial activity (Wilhelm, 1951; Akhthar and Mahmiid, 1995; Blatt and Mcrae, 1998; Abbasi, 2011). In agreement, OAs alone improved germination under pathogen-free conditions but failed to suppress *P. ultimum* independently, indicating a supportive rather than direct protective role. Among amendments, hoof meal produced the strongest synergistic interaction with AZ78, doubling protection relative to control treatments (S and SV) under pathogen pressure. These findings highlight that biological control efficacy depends not only on the presence of a BCA but also on the surrounding nutrient environment.

Disease suppression was closely associated with shifts in soil physicochemical properties. Soil pH is a major ecological determinant of microbial activity and survival (Fernández-calviño *et al.*, 2011). AZ78 cell inoculation caused minor pH changes, whereas volatile-exposed soils showed pronounced alkalinization, particularly in amendment treatments (SFiBV, SFeBV, SHBV), where pH exceeded 8.0. Because these soils subsequently displayed strong disease suppression, alkaline

conditions likely contributed to reduced pathogen activity, consistent with reports that *Pythium* pathogenicity declines at higher pH (Mondal and Hyakumachi, 2000).

Ammonia accumulation represented an additional suppressive factor. Soil ammonia contributes to fungistasis (Chuankun *et al.*, 2004), especially when elevated pH promotes formation of toxic non-ionized NH_3. OAs increasing soil pH have previously been shown to generate inhibitory nitrogen compounds that suppress oomycete development (Tsao and Oster 1980). In our study, treatments with low pH and low ammonia showed limited protection, whereas AZ78-inoculated and VOC-exposed amended soils accumulated higher ammonia concentrations (~3 ppm in cell treatments, ~4 ppm in SHB, and ~6 ppm in volatile treatments), coinciding with improved germination. These results suggest that AZ78 activity and amendment-driven nitrogen transformations jointly created conditions unfavourable for pathogen establishment.

Beyond ammonia, AZ78 volatile metabolites appear central to pathogen suppression. AZ78 produces diverse VOCs including alcohols, ketones, pyrazines, and pyrroles, with methoxypyrazines dominating the volatilome (Vlassi *et al*., 2020a). Compounds such as 2,5-dimethylpyrazine directly inhibit *P. ultimum*, indicating that volatile-mediated antagonism represents a key anti-oomycete mechanism. Enhanced enrichment of pyrazines in NAH_78 provides a plausible explanation for superior disease suppression in hoof meal treatments. Pyrazines and related volatiles are characteristic of fungistatic soils and inhibit fungal germination at low concentrations (Chuankun *et al*., 2004). Similarly, suppressive soils contain volatile ketones such as 2-octanone and 2-nonanone that inhibit *Pythium* species (Agtmaal *et al.*, 2015). Additional compounds detected in AZ78 treatments, including pyrroles and thiazole derivatives, have documented anti-oomycete activity (Vlassi *et al*., 2020a). These findings indicate that pathogen suppression results from combined VOC blends rather than single compounds, which is consistent with our findings where these compounds were uniquely and

strongly enriched in NAH_78 compared to all other treatments. The differentiation of volatilomes among treatments therefore suggests that amendment type and microbial activity jointly shape soil volatile composition, ultimately driving differential disease suppressiveness outcomes.

In addition to chemical changes, hoof meal and AZ78 significantly reorganized soil bacterial communities. OAs are known to reshape microbiomes and promote long-term disease suppressiveness (Kurm *et al.*, 2023). Organic matter inputs increase microbial biomass and activity while reducing root disease incidence (Bailey and Lazarovits, 2003; Yadav *et al*., 2015). Consistent with these findings, alpha and beta diversity analyses revealed significant treatment effects ($p < 0.05$), with the SHB treatment showing the highest Shannon diversity and Chao1 richness and forming a distinct microbial cluster (Bray–Curtis, $p = 0.001$). Bacterial enrichment correlated positively with soil pH and ammonia concentrations (Lazarovits *et al.*, 2009; Wen *et al.*, 2020). Proteobacteria and Actinobacteria dominated across treatments, consistent with their preference for neutral to alkaline soils (Gai *et al.*, 2021; Yunchen Zhao *et al.*, 2021b). Actinobacteria enrichment in volatile-treated soils agreed with previous reports linking this group to elevated pH and ammonia (Nie *et al.*, 2018), while amendment-enhanced VOC effects have been observed previously (Yuan *et al.*, 2017).

At the genus level, treatment-specific shifts in soil microbial communities were observed, indicating that both AZ78 activity and OAs selectively enriched distinct functional groups. Soils amended with hoof meal (SHB) and soils exposed to AZ78 volatiles (SV, SBV, SHV, SHBV) exhibited the strongest enrichment of beneficial and metabolically active genera compared with other treatments (S, SB, SV). Among antagonistic taxa, *Nocardioides* markedly increased in SV and SBV treatments, followed by SHBV and SHV, and remained abundant in SHB soils, suggesting that AZ78-derived volatiles and elevated nitrogen availability favoured Actinobacteria adapted to nutrient-rich and alkaline environments. Similarly, *Streptomyces* abundance slightly increased in SV and SBV,

consistent with its known role in antibiosis and disease suppression through production of antifungal metabolites (Expósito *et al*., 2015; Lazcano *et al*., 2021; Lee *et al*., 2023). Genera such as *Gaiella*, which were relatively more abundant in S, SB, and SH treatments, declined in the other treatments, indicating sensitivity to increased pH and ammonia concentrations. The enrichment of *Lysobacter* in SHB soils further supports the role of hoof meal in promoting persistence of antagonistic populations, whereas its low abundance in SB treatments suggesting reduced ecological establishment potential without nutrient supplementation and carbon availability. *Marmoricola* also increased in soils exposed to AZ78 volatiles, consistent with its adaptation to high alkaline soils (pH 6-9) and its ability to produce bioactive metabolites against pathogens (Jiang *et al.*, 2018; Schumann *et al.*, 2018). Another genus enriched in volatile-exposed soils was *Pseudonocardia*, which is known to produce antifungal and antibacterial compounds in high pH environments (Kiranmayi *et al.*, 2011; Omran and Kadhem, 2016). The SHB treatment showed increased abundance of *Mesorhizobium*, which is involved in plant growth promotion and nitrogen cycling (Soe *et al.*, 2020), and *Agromyces*, which serves as an indicator of good soil health, is plant growth-promoting, and correlates with soil pH and total nitrogen content (Wang *et al.*, 2017; Chiodi *et al.*, 2025).Additionally, the ammonia-oxidizing genus *Nitrosococcus* was detected in AZ78-volatile exposed soils, reflecting its key role in ammonia oxidation within the nitrogen cycle (Campbell *et al.*, 2011). Enrichment of *Microvirga* in SHB soils contributes to rhizosphere nitrogen cycling, supporting nitrogen availability and plant growth promotion (Zhou *et al.*, 2025). *Arthrobacter*, which participates in nitrification and denitrification and can produce ammonia from nitrate or nitrite, was also enriched (Liu *et al.*, 2023).

The taxonomic shifts observed are consistent with functional gene evidence showing enhanced nitrogen metabolism. Nitrogen addition through OAs further reshaped nitrogen cycling functions. Nitrogen assimilation genes dominated across treatments, reflecting microbial immobilization of

inorganic nitrogen via the glutamine synthase/ glutamate synthase **(**GS-GOGAT) pathway availability (Kumar and Shimizu, 2010; Liu *et al*., 2025; Mehmood *et al*., 2022; Singh et al., 2020). Lower *glnA* abundance in amendment-free soils likely reflected ammonium limitation at low pH, where microbes prioritize glutamate production over glutamine synthesis (Huang *et al.*, 2020). As ammonium accumulated, we saw that nitrogen flux shifted toward dissimilatory pathways. Nitrification genes remained comparatively low, although *amoA*, *amoC*, and *hao* increased in treatments with higher pH and ammonium concentrations, nitrification remained a minor nitrogen transformation pathway overall, limited by incomplete coupling between ammonium production and oxidation capacity. This observation aligns with studies demonstrating that nitrification is strongly controlled by soil pH, with ammonia-oxidizing archaea dominating acidic soils and bacterial nitrifiers becoming more competitive under neutral to alkaline conditions and elevated ammonium supply (Aoyagi *et al.*, 2025; Coca-salazar *et al*., 2021; Zhou *et al*., 2025). The limited abundance of NIT genes in our system suggests that ammonia oxidation did not keep up with ammonium production, allowing NH_4^+ to accumulate due to insufficient nitrification under high-pH conditions. In contrast, dissimilatory nitrate reduction genes (*nirB*, *nirD*) were strongly enriched in hoof meal + AZ78 treatments. DNR is favoured in carbon-rich environments where nitrate is reduced to ammonium rather than lost as gas (Pandey *et al.*, 2020; Cheng *et al.*, 2022), explaining the observed ammonium accumulation. Denitrification genes (*narI*, *nirK*) also increased under alkaline, nitrogen-rich conditions, consistent with previous studies (Kandeler *et al*., 2006; Nogales *et a*l., 2002; Simek and Cooper, 2002). However, it is interesting to note that all the genes related to DNIT step were in highest abundance in the treatment SHB, followed by AZ78-volite based treatments. Recent meta-analyses further demonstrate that responses of *nirS* and *nosZ* to nitrogen fertilization are particularly pronounced at pH values above 8, which is in consistent with our results (Zhou *et al*., 2025), matching the conditions observed in the SHB treatment.

These nitrogen-cycle shifts provide a mechanistic explanation for disease suppression, linking microbial nitrogen transformations directly to pathogen suppression via chemical soil changes. Treatments enriched in DNR and DNIT genes also exhibited higher pH, increased ammonia, and improved plant protection. Ammonia released by rhizosphere bacteria is known to inhibit *P. ultimum* even at low concentrations (Howell *et al*., 1988). Many pathogenic fungi actively acidify their surrounding environment to promote virulence and host colonization (Vylkova, 2017). The shift toward alkaline conditions observed in AZ78-amended soils may therefore counteract pathogen-driven acidification and reduce infection success. In this framework, nitrogen transformations act not only as nutrient cycling processes but also as regulators of soil chemical conditions that influence disease outcomes.

Collectively, our findings demonstrate that AZ78-mediated disease suppression emerges from interconnected biological and chemical processes, including VOC production, nitrogen transformation, alkalinization, and microbiome restructuring. Rather than a single mechanism, suppression of *P. ultimum* appears to result from coordinated ecological shifts that collectively create a soil environment unfavourable for pathogen development.

5.6 Conclusion

In conclusion, this study demonstrates that AZ78 effectively suppresses *P. ultimum* damping-off and enhances tomato seed germination through multiple mechanisms operating within the soil environment. To our knowledge, this is the first study evaluating the capacity of AZ78 to control *P. ultimum* under semi-realistic soil and greenhouse conditions, moving beyond previous *in vitro* observations and providing experimental validation of its functionality in a more complex soil environment. By integrating microbiological, chemical, and metagenomic analyses, this work aimed to elucidate the mechanisms underlying AZ78-mediated disease suppression and revealed that AZ78

acts against the pathogen through multiple modes of action, including direct antagonism, emission of bioactive VOCs, modification of soil physicochemical properties, and modulation of soil microbial communities as well as nitrogen-cycling processes. The combination of AZ78 with nitrogen-rich OAs, particularly hoof meal, enhanced these effects by promoting alkalinization, ammonia accumulation, and enrichment of beneficial microbial taxa, collectively creating soil conditions unfavourable for pathogen establishment while supporting plant growth. These findings highlight that effective biological control depends not only on the presence of a BCA but also on the surrounding soil environment that regulates microbial activity and nutrient transformations. Overall, this study advances our understanding of how microbial inoculants and OAs can be strategically combined to promote soil suppressiveness and provides a foundation for developing more robust and sustainable disease management strategies, while improving soil health and crop performance.

CHAPTER 6

ENHANCING THE BIOCONTROL POTENTIAL OF *LYSOBACTER CAPSICI* AZ78 AGAINST *PYTHIUM ULTIMUM* IN SOIL UTILISING ORGANIC AMENDMENTS

Amulya Jain Dinesh Kothari[1,2], Gerardo Puopolo[1,2]

[1]*Center of Agriculture, Food, Environment, University of Trento, San Michele all'Adige, Italy*

[2]*Research and Innovation Centre, Fondazione Edmund Mach, San Michele all'Adige, Italy*

Published on Biological and integrated control of plant pathogens, IOBC-WPRS Bulletin Vol. 177, 2023 pp. 37-38

Soil disease suppressiveness has been linked to *Lysobacter* species, known for their antagonistic activity against soilborne plant pathogens (Postma et al., 2010a). Organic and protein-rich materials can also stimulate *Lysobacter* populations, enhancing soil suppressiveness (Postma and Schilder, 2015). Recently, *Lysobacter capsici* AZ78 (AZ78) showed detrimental effects on soil-borne plant pathogens, including *Pythium ultimum* under *in vitro* conditions (Vlassi., *et al.*, 2020a). Building on this knowledge, this study investigated the role of organic amendments, namely chitin, feather meal, fish meal, hoof meal, and yeast, in enhancing the biocontrol efficacy of AZ78 against *P. ultimum* in tomato seedlings. Sandy loam soil was incorporated with organic amendments at 0.3% (w/w), followed by inoculation with AZ78 (1×10^6 CFU/mL). *Pythium ultimum* inoculum was prepared by culturing the plant pathogen on saturated millet seeds for 21 days and introduced into the soil at 0.3% (w/w) dry weight. Control treatments received non-inoculated millet. The experiment consisted of four treatment groups: (1) soil only, (2) soil + AZ78, (3) soil + *P. ultimum*, and (4) soil + *P. ultimum* + AZ78, each group tested under both amended and unamended conditions. Tomato seeds (Five seeds

per treatment) were sown equidistantly in the soil and incubated in a greenhouse at 25 ± 1°C. The seedling germination rate was recorded after 14 days. Results showed that soil inoculated with *P. ultimum* alone exhibited the lowest germination rate. In contrast, treatment with AZ78 significantly increased germination rates, surpassing even the untreated control, highlighting its potential as a plant growth-promoting rhizobacterium. Organic amendments influenced the AZ78 effectiveness, with hoof, feather, and fish meal yielding the highest germination rates. In contrast, yeast amendment hindered germination. These findings suggest that specific organic amendments can enhance the AZ78 protective effects. This is the first study to demonstrate the protective capability of AZ78 against *P. ultimum* under semi-natural soil conditions. Furthermore, using organic amendments aligns with sustainable agricultural practices and has promising implications for field applications.

CHAPTER 7

APPLICATION OF HEAT-TREATED *LYSOBACTER CAPSICI* AZ78 CELLS AND ITS POLYCYCLIC TETRAMATE LACTAMS EFFECTIVELY CONTROLS *PLASMOPARA VITICOLA* BY STIMULATING GRAPEVINE DEFENCE MECHANISMS

Amulya Jain Dinesh Kothari[1,2], Stefano Nadalini[1,2], Marco Masi[3], Alessio Cimmino[3], Gerardo Puopolo[1,2]

[1]Center of Agriculture, Food, Environment, University of Trento, San Michele all'Adige, Italy; [2]Research and Innovation Centre, Fondazione Edmund Mach, San Michele all'Adige, Italy; [3]Department of Chemical Sciences, University of Naples Federico II, Naples, Italy. E-mail:

Published on Biological and integrated control of plant pathogens, IOBC-WPRS Bulletin Vol. 177, 2023 pp. 85-86

7.1 Abstract

The genus *Lysobacter* controls a broad range of plant pathogens through diverse modes of action, including the production of Polycyclic Tetramate Lactams (PTMs), secondary metabolites resistant to high temperatures and exhibiting strong antifungal activity. As PTMs are stored in the cell membranes, this study investigated the efficacy of applying heat-treated cells of *L. capsici* AZ78 in controlling *Plasmopara viticola*, the causal agent of grapevine downy mildew. Moreover, it sheds light on the ability of *L. capsici* AZ78 cells and PTMs to stimulate defence mechanisms in grapevine plants.

Keywords: *Lysobacter capsici*, *Plasmopara viticola*, polycyclic tetramate lactams, callose, reactive oxygen species

7.3 Introduction

The *Lysobacter* genus includes bacterial species that efficiently control plant pathogenic fungi and oomycetes by releasing antifungal secondary metabolites (Puopolo et al., 2018). Polycyclic Tetramate Lactams (PTMs) are the most studied, given their broad host range and resistance to high temperatures (Yu et al., 2007; Li et al., 2009). Beyond inhibiting hyphal growth, PTMs also trigger apoptotic processes in yeasts (Ding *et al.*, 2016). Notably, Yue et al. (2021) showed that *L. enzymogenes* PTMs are primarily localised within bacterial cell membranes. Recently, Brescia et al. (2021) detected PTMs in cell-free supernatants of *L. capsici* AZ78 (AZ78), a biocontrol agent of *Plasmopara viticola*. However, little is known about their presence in AZ78 cell membranes and if they play a role in controlling *P. viticola*.

Based on this, we evaluated the biocontrol efficacy of heat-treated AZ78 cells against *P. viticola*. In parallel, we assessed the capacity of these treatments to trigger plant defence responses. To further substantiate the involvement of PTMs, we isolated them directly from the AZ78 cell membranes and tested them against *P. viticola*.

7.3 Materials and methods

7.3.1 Plant protection efficacy assays

Grapevine leaf discs and two-year-old Pinot Noir plants were used in *in vitro* and *in planta* assays, respectively. Two-year-old *V. vinifera* cv. Pinot Noir grapevine plants, grafted onto Kober 5BB were used for *in planta* assays. Heat-treated AZ78 cells were prepared by incubating AZ78 cell

suspension (1×10^8 CFU/mL) at 90°C for 20 min, followed by incubation at −20 °C for 5 min. Viable and heat-treated AZ78 cells (1×10^8 CFU/mL) were sprayed 24 h before *P. viticola* inoculation (2.5×10^5 sporangia/mL). For PTM assays, mixtures of PTMs (50 mg/L–2.5 mg/L) were mixed in equal volumes with the *P. viticola* inoculum and drop-inoculated onto grapevine leaf discs. In all the cases, samples were incubated under greenhouse conditions for six days (Brescia *et al.*, 2021). Then, disease severity was assessed according to the EPPO standard scale (EPPO, 2004). Untreated and copper-treated leaf discs (Coprantol Hi Bio; 2g/L) were negative and positive controls, respectively. Five leaf discs per Petri dish were used, and each treatment consisted of five replicates (Petri dishes) for *in vitro assays*. For *in planta assays,* each treatment was carried out on five grapevine plants (replicates).

In planta and *in vitro* assays were repeated, and results were statistically analysed using R on R studio version 4.3.0. Data related to disease severity were analysed using One-Way ANOVA, and means were compared with Tukey's test ($\alpha = 0.01$).

7.3.2 Grapevine plant response to treatments

The ability of PTMs and AZ78 cells to stimulate grapevine defence mechanisms was investigated by assessing callose accumulation and reactive oxygen species (ROS) production. Callose was visualised via aniline blue staining using fluorescence microscopy, with callose appearing as turquoise fluorescence (Palmieri *et al.*, 2012). ROS production was detected using 3' 3' diaminobenzidine (DAB) staining (1 mg/mL) (Trouvelot et al., 2008). ROS was visible as a dark brown precipitate under the bright field microscoP. The experiments were repeated.

7.4 Results and discussion

In the plant protection efficacy assays, the untreated control had the highest severity, ranging between 80% and 100% in all cases, whereas the copper-based fungicide showed a plant protection

efficacy higher than 90%. Notably, our results demonstrated that heat-treated AZ78 cells retained strong protective efficacy against *P. viticola*, comparable to AZ78 viable cells and the commercial copper-based fungicide. This indicates that the associated thermostable PTMs could play a role in the control of *P. viticola*.

To confirm the involvement of PTMs in *P. viticola* control, we isolated the PTM mixture from AZ78 cell membranes and applied it to grapevine leaves. The PTM mixture provided significant protection against *P. viticola* even at the lowest concentration (2.5 mg/L), mirroring the effects of AZ78 cells. Furthermore, the PTMs independently induced plant defence responses, validating their role in controlling *P. viticola.*

Together, these results prove that PTMs are associated with AZ78 cell membranes and are involved in biocontrol activity. This study, the first to highlight the ability of PTMs to trigger defence mechanisms in plants, could potentially lead to the development of non-viable AZ78 cells and/or PTMs as novel plant protection products for the control of *P. viticola* on grapevines, offering hope for more effective and sustainable wine production.

CHAPTER 8

DISCUSSIONS

The present study provides comprehensive evidence of the anti-oomycete activity of *Lysobacter capsici* AZ78 (AZ78) against both foliar and soil-borne oomycete plant pathogens through a multifaceted and integrated approach combining microbiological, molecular, chemical, and omics-based analyses. By adopting this multidisciplinary framework, we demonstrated the biocontrol efficacy of AZ78 against *Plasmopara viticola* in grapevine, *Peronospora belbahrii* in basil, and *Pythium ultimum* in tomato under controlled experimental conditions.

Our results demonstrate that AZ78 exhibits direct antagonistic activity against *P. viticola* and *P. belbahrii* in grapevine and basil plants, providing more than 90% plant protection under greenhouse conditions, a level comparable to that achieved with commercially available copper-based fungicides. We further showed that not only viable cells but also heat-treated AZ78 cells were effective against these pathogens. This activity was demonstrated to result from thermostable secondary metabolites belonging to the polycyclic tetramate macrolactam (PTM) family. These metabolites are membrane-associated and are released upon disturbance or damage to the bacterial membrane in *Lysobacter* spp. In this study, two PTMs, dihydromaltophilin/heat-stable antifungal factor (DMP/HSAF) and maltophilin (MP), were extracted from AZ78 cell extracts. These metabolites exhibited antagonistic activity against *P. viticola* even at concentrations as low as 2.5 mg/ L. This finding confirms that the retained anti-oomycete activity of heat-treated AZ78 cells is attributable to these thermostable PTMs.

In addition, we investigated the effects of AZ78 cells and PTMs on host plants. Microscopic visualization using aniline blue staining and 3,3′-diaminobenzidine revealed that both viable and heat-

treated AZ78 cells induced callose accumulation and reactive oxygen species (ROS) production in grapevine and basil plants following challenge with *P. viticola* and *P. belbahrii*, respectively. Furthermore, the PTM mixture also induced callose deposition in grapevine plants, and the number of stomata displaying callose increased in a dose-dependent manner. Along with callose deposition and ROS production, AZ78 cells and PTMs showed toxicity toward *P. viticola* sporangia, demonstrating that AZ78 acts through multiple modes of action, including both direct and indirect mechanisms, when applied to plants.

We also demonstrated that the self-digestive solution (SDS) of AZ78, enriched in antimicrobial secondary metabolites including PTMs, exhibited antagonistic activity against *P. viticola*. The SDS was obtained through prolonged growth of AZ78 in nutrient limited liquid medium, which resulted in bacterial autolysis and release of cellular contents, including secondary metabolites. The retention of plant protection activity after exposure to thermal shock at 90 °C indicates that membrane-associated PTMs were released into the medium upon thermal treatment, explaining the observed protective activity. In addition to its direct antagonistic action, SDS application triggered defense responses in plants against the pathogen. However, these responses were observed only in infected plants following *P. viticola* inoculation and not in uninfected plants, indicating that AZ78-derived SDS acts as a priming agent, enabling activation of defense responses only upon pathogen challenge.

Several defense-related genes were analysed, including those involved in structural defense (*CalS7, HSR*), hormonal biosynthesis and signalling (*ACO, AOC, LOX9*), pathogenesis-related proteins (*PR2, PR3*), transcription factors (*ERF1, JAZ1*), and genes associated with stilbene synthesis and phytoalexin accumulation (*STS, PAL*). The upregulation of these genes in plants treated with SDS obtained at the 96-h time point, corresponding to the autolysis phase, indicates that AZ78 application primes grapevine plants and enhances gene expression upon pathogen infection. Furthermore,

phytoalexin accumulation analyses showed increased production of compounds such as piceid, resveratrol, and trans-ε-viniferin. The increased accumulation of resveratrol and trans-ε-viniferin over time suggests sustained induction and accumulation of these phytoalexins during infection, contributing to pathogen inhibition.

In addition to foliar oomycete pathogens, the biocontrol ability of AZ78 was also evaluated against *P. ultimum*. The effects of AZ78 cells and AZ78 volatiles were tested in soil samples inoculated with bacterial cells and in soils exposed to bacterial volatiles, respectively. AZ78 volatiles altered soil pH, whereas both AZ78 cells and volatiles increased ammonia concentration in soil, with the strongest increase observed in volatile-treated soils. Through modulation of soil physicochemical properties, AZ78 reduced the growth of *P. ultimum* in soil. Both AZ78 cells and volatiles acted as plant growth promoters and plant protectants. Furthermore, the addition of nutrient-rich organic amendments enhanced the efficacy of AZ78. In particular, hoof meal resulted in germination rates exceeding 80% in infected tomato seedlings, whereas infection with *P. ultimum* reduced germination to 20-30% in treatments lacking AZ78 or organic amendments. Although AZ78 treatments alone provided protection, the strongest effects were observed when AZ78 was combined with hoof meal.

The increase in ammonia concentration was identified as one of the factors contributing to inhibition of *P. ultimum* growth in soil. Volatile analysis revealed additional antimicrobial volatile organic compounds, including mono- and di-alkyl methylpyrazines, pyrrole, ketones such as octanone and nonane, and thiazole, all previously reported to be toxic to *P. ultimum*. Volatilome analysis further showed that the addition of hoof meal to nutrient agar enhanced volatile production compared with AZ78 grown on nutrient agar alone. Control treatments showed negligible volatile accumulation, confirming that emission of toxic volatiles by AZ78 contributed to inhibition of *P. ultimum* growth in volatile-exposed soils.

Shotgun metagenomic analysis further demonstrated that environmental factors, including soil pH and ammonia concentration, influenced the antagonistic activity of soil treatments against *P. ultimum*. Soils characterized by low pH and low ammonia concentrations exhibited poor pathogen suppression, whereas soils with higher pH and ammonia levels showed enhanced protection. These findings link soil physicochemical properties with **the survival and infectivity of soil-borne oomycete** plant **pathogens**. Moreover, the addition of hoof meal to AZ78-inoculated soils increased microbial richness and diversity, promoting taxa associated with plant protection and disease suppression. Beneficial genera such as *Nocardioides*, *Streptomyces*, *Mesorhizobium*, *Lysobacter*, *Pseudonocardia*, *Arthrobacter*, and *Microvirga* were enriched in treatments exhibiting strong disease suppression, whereas sensitive genera such as *Gaiella* declined. Increased microbial abundance was also observed in soils exposed to AZ78 volatiles, with or without organic amendments, indicating that bacterial volatiles can also modulate soil microbiome composition.

We additionally analysed genes involved in nitrogen cycling to identify links between soil properties and disease suppression. Nitrogen assimilation genes associated with the GS-GOGAT pathway dominated across treatments. As ammonium accumulated, microbial metabolism shifted toward dissimilatory nitrate reduction and denitrification pathways, reflected by increased abundance of genes such as *nirB*, *nirD*, *narI*, and *nirK*. Nitrification remained comparatively low even under higher pH conditions, suggesting preferential ammonium accumulation. These microbial functional shifts explain the observed soil alkalinization and elevated ammonium concentrations, providing a mechanistic link between microbiome composition, nitrogen transformations, and pathogen suppression.

Organic amendments primarily functioned as enhancers rather than direct antimicrobial agents. They supplied additional nitrogen and carbon sources that supported AZ78 growth and promoted

metabolically active genera associated with disease suppression and nitrogen cycling. Among the tested amendments, hoof meal showed the strongest synergistic effect, improving both plant growth and pathogen suppression when combined with AZ78 cells or volatiles. Organic amendments alone improved germination under pathogen-free conditions but were insufficient to suppress *P. ultimum*, emphasizing the importance of combining AZ78 with supportive nutrient substrates to achieve maximal biocontrol efficacy.

Collectively, our findings demonstrate that AZ78-mediated suppression results from the interaction of multiple complementary mechanisms: (i) direct antimicrobial activity mediated by PTMs and volatile compounds, (ii) priming of host structural and biochemical defense, (iii) soil chemical modification leading to alkaline and ammonia-rich conditions unfavourable for pathogen establishment, and (iv) microbiome restructuring that favours nitrogen-cycling and antagonistic microbial taxa. This multilayered suppression strategy provides a robust approach that enables AZ78 to maintain efficacy under semi-realistic soil conditions where single-mode interventions often fail.

CHAPTER 9

EXTENDED CONCLUSIONS

This study demonstrates that *Lysobacter capsici* AZ78 represents a highly versatile biocontrol agent capable of suppressing both foliar and soil-borne oomycete pathogens through an integrated and multi-level mode of action. By combining microbiological assays, metabolite characterization, plant defense analyses, soil physicochemical measurements, volatilome profiling, and shotgun metagenomics, we established a comprehensive mechanistic framework that explains how AZ78 enhances plant protection across different host–pathogen systems.

AZ78 exhibited strong antagonistic activity against *Plasmopara viticola*, *Peronospora belbahrii*, and *Pythium ultimum*, achieving disease suppression levels comparable to conventional chemical fungicides under greenhouse conditions. A key finding of this work is that bacterial viability is not strictly required for efficacy. Heat-treated cells and autolysate preparations retained strong anti-oomycete activity due to the presence of thermostable polycyclic tetramate macrolactams (PTMs), including dihydromaltophilin and maltophilin. These metabolites **both directly inhibited pathogen structures and simultaneously induced plant immune responses**.

AZ78 and its derived metabolites functioned not only as antimicrobial agents but also as plant defense primers. Treated plants exhibited enhanced callose deposition, reactive oxygen species production, activation of defense-related genes, and accumulation of phytoalexins such as resveratrol and trans-ε-viniferin following pathogen challenge. The priming effect ensured that defense responses were activated specifically upon infection, **thereby minimizing unnecessary metabolic costs to the host plant**.

In the soil, AZ78 cells and volatile emissions modified key soil physicochemical parameters, particularly soil pH and ammonia concentration, creating conditions unfavourable for *P. ultimum*. Volatile organic compounds produced by AZ78 contributed directly to pathogen inhibition and indirectly shaped soil microbial communities. The integration of organic amendments, especially hoof meal, further enhanced AZ78 performance by stimulating metabolite production and supporting beneficial microbial populations.

Metagenomic analyses revealed that AZ78 reshaped soil microbiome composition and nitrogen cycling functions. Enrichment of beneficial taxa and increased abundance of nitrogen assimilation, dissimilatory nitrate reduction, and denitrification genes promoted ammonium accumulation and soil alkalinization, both associated with disease suppression. These findings demonstrate that nitrogen transformations act not only as nutrient cycling processes but also as ecological regulators influencing pathogen survival.

Overall, AZ78-mediated biocontrol emerges from a wide range of complementary mechanisms: direct pathogen antagonism, host defense priming, soil modulation, and microbiome restructuring. This multi-layered strategy provides stability and effectiveness under complex environmental conditions, highlighting the potential of AZ78 as a sustainable alternative to chemical pesticides.

The results presented in this study support the development of AZ78-based formulations and emphasize the importance of combining microbial inoculants with specific organic amendments to design next-generation suppressive soils. Future field validation and formulation optimization will be essential steps toward translating these findings into practical agricultural applications for environmentally friendly management of oomycete diseases.

APPENDIX A. LIST OF PUBLICATIONS

Chapter 1 is a book chapter, Kothari, A. D. J., Martini, A., and Puopolo, G., 2026.

Chapter 2 is an article accepted in European Journal of Plant pathology on 5th March 2026.

Chapter 6 and chapter 7 are published as a conference proceeding for the XVII IOBC-WPRS meetings in Uppsala (Sweden) as Dinesh Kothari and Puopolo (2025) and Kothari *et al.,* (2025), respectively.

Papers in peer-review journals

- **Kothari**, A. D. J., Martini, A., Puopolo, G., 2026. *Lysobacter*: an emerging frontier in sustainable control of soilborne phytopathogenic microorganisms. Book chapter in Soil microorganisms for plant growth promotion and soil health, 327-365. https://doi.org/10.1016/B978-0-443-34055-0.00013-8.
- **Kothari**, A. D. J., Nadalini, S., Lucii, L., *et al*., 2026. Heat-inactivated *Lysobacter capsici* AZ78 cells effectively control *Peronospora belbahrii* and *Plasmopara viticola* through direct and indirect mechanisms. Accepted in European Journal of Plant Pathology
- **Kothari**, A. D. J., Martini, A., Puopolo, G., *et al*., 2026. Tentative title: Anti-oomycete activity of *Lysobacter capsici* AZ78 autolysates and their role in inducing grapevine defense responses. In preparation.
- **Kothari**, A. D. J., Puopolo, G., *et al*., 2026. Tentative title: Soil suppression of *Pythium ultimum* by *Lysobacter capsici* AZ78: contributions of organic amendments, bacterial cells, volatile-mediated activity, and soil microbiome modulation. In preparation.

Conference proceedings

- **Kothari**, A. D. J., and Puopolo, G., 2025. Enhancing the biocontrol potential of *Lysobacter capsici* AZ78 against *Pythium ultimum* in soil utilising organic amendments. *IOBC-WPRS Bulletin Vol. 177. Proceedings of the XVII meeting,* Uppsala, Sweden, 11-14 June 2025.
- **Kothari**, A. D. J., Nadalini, S., Puopolo, G., *et al*., 2025. Application of heat-treated *Lysobacter capsici* AZ78 cells and its polycyclic tetramate lactams effectively controls *Plasmopara viticola* by stimulating grapevine defence mechanisms. *IOBC-WPRS Bulletin Vol. 177. Proceedings of the XVII meeting,* Uppsala, Sweden, 11-14 June 2025.
- Sinna, M., Manganiello, A., **Dinesh Kothari**, **A.,** *et al*., 2025. Effects of microbial biocontrol agents on tomato physiology productivity and response to biotic and abiotic stresses. *IOBC-WPRS Bulletin Vol. 177. Proceedings of the XVII meeting,* Uppsala, Sweden, 11-14 June 2025.

Oral presentations at conferences

- **Kothari**, A. D. J., Nadalini, S., Lucii, L., *et al*., 2025. *Lysobacter capsici* AZ78 and its derived metabolites aid the grapevine in activating plant defense mechanisms against *Plasmopara viticola. Soil and Plant Health in a Changing Environment* (*SoiPHE*), Reims, France, 26-28 May 2025.
- **Kothari**, A. D. J., and Puopolo, G., 2025. Enhancing the biocontrol potential of *Lysobacter capsici* AZ78 against *Pythium ultimum* in soil utilising organic amendments. *IOBC-WPRS XVII conference*, Torino, Italy 11-14 June 2025.
- **Kothari**, A. D. J., Nadalini, S., Puopolo, G., *et al*., 2025. Application of heat-treated *Lysobacter capsici* AZ78 cells and its polycyclic tetramate lactams effectively controls

Plasmopara viticola by stimulating grapevine defence mechanisms. *IOBC-WPRS XVII conference*, Torino, Italy 11-14 June 2025.

- **Kothari**, A. D. J., Nadalini, S., Puopolo, G., *et al*., 2025. Antifungal factors or resistance elicitors? Role of polycyclic tetramate macrolactams in the biological control of *Peronospora belbahrii* and *Plasmopara viticola* by *Lysobacter capsici* AZ78. *XXX SIPaV congress*, Catania, Italy. 1-17 September 2025.

Poster presentations at conferences

- **Kothari**, A. D. J., and Puopolo, G., 2024. Evaluation of a *Lysobacter* biocontrol strain for the eco-friendly management of basil downy. *XXIX SIPaV congress*, Trento, Italy. 9-11 September 2024.

-

REFERENCES

Abbasi, P.A., 2011. Exploiting and Understanding Disease Suppressing Effects of Fish Emulsion for Soil-borne and Foliar Diseases. Am. J. Plant Sci. Biotechnol. 5 (2): 61-68. https://doi.org/10.1080/07060661.2012.740076

Adams, D.J., 2004. Mini-Review Fungal cell wall chitinases and glucanases. Microbiology, 150 (7): 2029-2035. https://doi.org/10.1099/mic.0.26980-0.

Agisha, V.N. *et al.*, 2019. Broad-spectrum antimicrobial activity of volatile organic compounds from endophytic *Pseudomonas putida* BP25 against diverse plant pathogens. Biocontrol Sci. Technol. 29 (11): 1069-1089. https://doi.org/10.1080/09583157.2019.1657067.

Agtmaal, M. Van *et al.*, 2015. Legacy effects of anaerobic soil disinfestation on soil bacterial community composition and production of pathogen-suppressing volatiles. Front. Microbiol. 6: 1-12. https://doi.org/10.3389/fmicb.2015.00701.

Agtmaal, M. Van *et al.*, 2018. Volatile-mediated suppression of plant pathogens is related to soil properties and microbial community composition. Soil Biol. Biochem.117: 164-174. https://doi.org/10.1016/j.soilbio.2017.11.015.

Ahn, I. *et al.*, 2007. Rhizobacteria-induced priming in *Arabidopsis* is dependent on ethylene , jasmonic acid , and NPR1. MPMI. 20 (7): 759–768. https://doi.org/10.1094/mpmi-20-7-0759.

Akhthar, M. and Mahmiid, I., 1995. Supression of nematode populations with animal by-products. Bioresour. Technol. 51 (2-3): 269-271. https://doi.org/10.1016/0960-8524(94)00111-D.

Al-khayri, J.M. *et al.*, 2023. Plant Secondary Metabolites : The Weapons for Biotic Stress Management. Metabolites, 13 (6): 716. https://doi.org/10.3390/metabo13060716.

Ali, Q. *et al*., 2025. Antimicrobial metabolites of *Bacillus velezensis* FZB42 reshape rice rhizosphere microbial community composition and induce host resistance against *Rhizoctonia solani.* Curr. Plant Biol. 41: 100440. https://doi.org/10.1016/j.cpb.2025.100440

Almeida, C. *et al*., 2017. Time-dependent production of the bioactive peptides endolides A and B and the polyketide mariline A from the Sponge-derived Fungus *Stachylidium bicolor* 293K04. Fermentation, 3 (3): 45. https://doi.org/10.3390/fermentation3030045.

Alonso-villaverde, V. *et al.*, 2011. Plant Physiology and Biochemistry The effectiveness of stilbenes in resistant Vitaceae : Ultrastructural and biochemical events during *Plasmopara viticola* infection process. Plant Physiol. Biochem. 49 (3): 265–274. https://doi.org/10.1016/j.plaphy.2010.12.010.

Alqahtani, F.S., 2025. The utilization of microorganisms for biological control of soil-borne plant pathogens : a sustainable strategy for managing plant diseases - a comprehensive review. J. Plant Pathol. 1815–1839. https://doi.org/10.1007/s42161-025-01984-1

Angelova, V.R. *et al.*, 2013. The effect of organic amendments on soil chemical characteristics. Bulg.

J. Agric. Sci. 19 (5): 958–971.

Aoyagi, L.N. *et* al., 2025. Diversity and characterization of the ammonia-oxidizing bacteria responsible for nitrification in tea field soils. Sci. Rep. 15 (1): 33221. https://doi.org/10.1038/s41598-025-18596-5.

Aslam, Z. *et al.*, 2009. *Lysobacter oryzae* sp. nov., isolated from the rhizosphere of rice (*Oryza sativa* L.). Int. J. Syst. Evol. Microbiol. 59 (4): 675–680. https://doi.org/10.1099/ijs.0.000588-0.

Ávila-Oviedo, J.L. *et al.*, 2024. Antagonistic effects and volatile organic compound profiles of rhizobacteria in the biocontrol of *Phytophthora capsici*. Plants, 13 (22): 3224. https://doi.org/10.3390/plants13223224.

Averyanov, A., 2009. Oxidative burst and plant disease resistance. Front. Biosci. (Elite Ed.). 1: 142–152. https://doi.org/10.2741/E14.

Aziz, A. *et al.*, 2016. Effectiveness of beneficial bacteria to promote systemic resistance of grapevine to gray mold as related to phytoalexin production in vineyards. Plant Soil. 405 (1): 141-153. https://doi.org/10.1007/s11104-015-2783-z.

Babadoost, M., 2017. Oomycete diseases of cucurbits : history , significance , and management. Hortic. Rev. 44: 279-314. https://doi.org/10.1002/9781119281269.ch6

Bae, H.S. *et al*., 2005. *Lysobacter concretionis* sp. nov., isolated from anaerobic granules in an upflow anaerobic sludge blanket reactor. Int. J. Syst. Evol. Microbiol. 55 (3): 1155–1161. https://doi.org/10.1099/ijs.0.63399-0.

Bai, H. *et al.*, 2020. *Lysobacter oculi* sp. nov., isolated from human Meibomian gland secretions. Antonie van Leeuwenhoek. Int. J. Gen. Mol. Microbiol. 113 (1): 13–20. https://doi.org/10.1007/s10482-019-01289-1.

Bailey, K.L. and Lazarovits, G., 2003. Suppressing soil-borne diseases with residue management and organic amendments. Soil Tillage Res. 72 (2): 169-180. https://doi.org/10.1016/S0167-1987(03)00086-2.

Barceló, A.M. *et al.*, 2016. Climatología del Balneario de Villavieja. Real Acad Farm. 82 (5): 108–126.

Bartram, A.K. *et al.*, 2014. Exploring links between pH and bacterial community composition in soils from the Craibstone Experimental Farm. FEMS Microbiol. Ecol. 87 (2): 403–415. https://doi.org/10.1111/1574-6941.12231.

Baudoin, A. *et al.*, 2008. QoI Resistance of *Plasmopara viticola* and *Erysiphe necator* in the Mid-Atlantic United States. Plant Health Prog. 9 (1): 25. https://doi.org/10.1094/PHP-2008-0211-02-RS.Abstract.

Bejarano, A. and Puopolo, G., 2022. A step out of the lab: the importance of formulations in the development of biopesticides. In Microbial biocontrol agents: developing effective biopesticides. GB: CABI. 20–44. https://doi.org/10.1079/9781789249200.0002.

Bem, B.P. De *et al.*, 2016. Effect of four training systems on the temporal dynamics of downy mildew in two grapevine cultivars in southern Brazil. Trop. Plant Pathol. 41 (6): 370-379. https://doi.org/10.1007/s40858-016-0110-8.

Ben-Naim, Y., *et al*., 2018 Transfer of downy mildew resistance from wild basil (*Ocimum americanum*) to sweet basil (*O. basilicum*). Phytopathol. 108 (1): 114–123. https://doi.org/10.1094/PHYTO-06-17-0207-R

Bickel, J.T. and Koehler, A.M., 2021. Review of *Pythium* species causing damping-off in corn. PHP. 22 (3): 219–225. https://doi.org/10.1094/PHP-02-21-0046-FI

Blatt, C.R. and Mcrae, K.B., 1998. Comparison of four organic amendments with a chemical fertilizer applied to three vegetables in rotation. Can. J. Plant Sci. 78 (4): 641-646. https://doi.org/10.4141/P97-089

Blum, M., *et al*., 2010. A single point mutation in the novel *PvCesA3* gene confers resistance to the carboxylic acid amide fungicide mandipropamid in *Plasmopara viticola*. Fungal Genet. Biol. 47 (6): 499–510. https://doi.org/10.1016/j.fgb.2010.02.009.

De Boer, W. *et al*., 2019. Pathogen suppression by microbial volatile organic compounds in soils. FEMS Microbiol. Ecol. 95 (8): 1–10. https://doi.org/10.1093/femsec/fiz105.

Bonanomi, G. *et al.*, 2010. Identifying the characteristics of organic soil amendments that suppress soilborne plant diseases. Soil Biol. Biochem. 42 (2): 136–144. https://doi.org/10.1016/j.soilbio.2009.10.012.

Austin Bourke, P.M., 1964. Emergence of potato blight. Nature, 45 (203): 805–808. https://doi.org/10.1038/203805A0

Brescia, F. *et al.*, 2020. The rhizosphere signature on the cell motility, biofilm formation and secondary metabolite production of a plant-associated *Lysobacter* strain. Microbiol. Res. 234: 12642. https://doi.org/10.1016/j.micres.2020.126424.

Brescia, F. *et al.*, 2021. Characterisation of the antibiotic profile of *Lysobacter capsici* AZ78, an effective biological control agent of plant pathogenic microorganisms. Microorganisms, 9 (6): 1320. https://doi.org/10.3390/microorganisms9061320.

Brown, I. *et al.*, 1998. Localization of components of the oxidative cross-linking of glycoproteins and of callose synthesis in papillae formed during the interaction between non-pathogenic strains of *Xanthomonas campestris* and French bean mesophyll cells. Plant J. 15 (3): 333-343. https://doi.org/10.1046/j.1365-313X.1998.00215.x.

de Bruijn, I. *et al.*, 2015. Comparative genomics and metabolic profiling of the genus *Lysobacter.* BMC Genomics, 16 (1): 1–16. https://doi.org/10.1186/s12864-015-2191-z.

Burki, F. *et al.*, 2020. The new tree of Eukaryotes. Trends Ecol. Evol. 35 (1): 43–55. https://doi.org/10.1016/j.tree.2019.08.008.

Callaghan, M.O., 2016. Microbial inoculation of seed for improved crop performance : issues and

opportunities. 100 (13): 5729-5746. https://doi.org/10.1007/s00253-016-7590-9.

Campbell, M.A. *et al.*, 2011. *Nitrosococcus watsoniisp*.nov.,a new species of marine obligate ammonia-oxidizing bacteria that is not omnipresent in the world's oceans:calls to validate the names '*Nitrosococcushalophilus*' and '*Nitrosomonasmobilis*'. FEMS Microbiol. Ecol. 76 (1): 39-48. https://doi.org/10.1111/j.1574-6941.2010.01027.x.

Capinera, J.L. and Dickens, K., 2016. Some effects of copper-based fungicides on plant-feeding terrestrial molluscs : A role for repellents in mollusc management. Crop Prot. 83: 76-82. https://doi.org/10.1016/j.cropro.2016.01.018.

Caulier, S. *et al.*, 2019. Overview of the antimicrobial compounds produced by members of the Bacillus subtilis group. Front. Microbiol. 10: 1–19. https://doi.org/10.3389/fmicb.2019.00302.

de Chaves, M.A. *et al.*, 2022. Fungicide resistance in *Fusarium graminearum* species complex. Curr. Microbiol. 79 (2): 1–9. https://doi.org/10.1007/s00284-021-02759-4.

Cheema, N. and Qureshi, A.W., 2024. Isolated bacterial strains with antibiotics production. Pak. Biomed. J. 7 (3): 62–69. https://doi.org/https://doi.org/10.54393/pbmj.v7i03.1059.

Chen, D. *et al.*, 2020. Total synthesis and a systematic structure-activity relationship study of WAP-8294A2. Bioorg. Med. Chem. 28 (18): 115677. https://doi.org/10.1016/j.bmc.2020.115677.

Chen, D.M. *et al.*, 2020. *Lysobacter enzymogenes* LE16 autolysates have potential as biocontrol agents *Lysobacter* sp. autolysates as biofungicide. J. Appl. Microbiol. 129 (6): 1684–1692. https://doi.org/10.1111/jam.14752.

Chen, J. *et al.*, 2018. Two direct gene targets contribute to *Clp*-dependent regulation of type IV pilus-mediated twitching motility in *Lysobacter enzymogenes* OH11. Appl. Microbiol. Biotechnol. 102 (17): 7509–7519. https://doi.org/10.1007/s00253-018-9196-x.

Chen, W. *et al.*, 2007. At least two origins of fungicide resistance in grapevine downy mildew populations. Appl. Environ. Microbiol. 73 (16): 5162–5172. https://doi.org/10.1128/AEM.00507-07.

Chen, W. *et al.*, 2024. The natural polycyclic tetramate macrolactam HSAF inhibit *Fusarium graminearum* through altering cell membrane integrity by targeting *FgORP1*. Int. J. Biol. Macromol. 261: 129744. https://doi.org/10.1016/j.ijbiomac.2024.129744.

Cheng, Y. *et al.*, 2022. Global patterns and drivers of soil dissimilatory nitrate reduction to ammonium. Environ. Sci. Technol. 56 (6): 3791-3800. https://doi.org/10.1021/acs.est.1c07997.

Chiodi, C. *et al.*, 2025. Organic amendments influence soil properties , soil microbial diversity , and winter barley traits in a five - year field trial with contaminated soils at a former wood preservation site. Chem. Biol. Technol. Agric. 12 (1): 1–20. https://doi.org/10.1186/s40538-025-00810-1?urlappend=%3Futm_source%3Dresearchgate.net%26utm_medium%3Darticle

Choi, J.H. *et al.*, 2014. *Lysobacter panacisoli* sp. nov., isolated from ginseng soil. Int. J. Syst. Evol. Microbiol. 64 (PART 7): 2193–2197. https://doi.org/10.1099/ijs.0.062034-0.

Christensen, P. and Cook, F.D., 1978. *Lysobacter*, a new genus of nonfruiting, gliding bacteria with a high base ratio. Int. J. Syst. Bacteriol. 28 (3): 367–393. https://doi.org/10.1099/00207713-28-3-367.

Chuankun, X. *et al.*, 2004. Soil volatile fungistasis and volatile fungistatic compounds. Soil Biol. Biochem. 36 (12): 1997–2004. https://doi.org/10.1016/j.soilbio.2004.07.020.

Cimmino, A. *et al.*, 2021. Isolation of 2,5-diketopiperazines from *Lysobacter capsici* AZ78 with activity against *Rhodococcus fascians*. Nat. Prod. Res. 35 (23): 4969–4977. https://doi.org/10.1080/14786419.2020.1756803.

Clippinger, J.I. *et* al., 2024. Traditional and emerging approaches for disease management of *Plasmopara viticola*, causal agent of downy mildew of grape. Agriculture, 14 (3): 1–24. https://doi.org/10.3390/agriculture14030406

Coca-salazar, A. *et al.*, 2021. Response of ammonia-oxidizing bacteria and archaea abundance and activity to land use changes in agricultural systems of the Central Andes. Eur. J. Soil Biol. 102: 103263. https://doi.org/10.1016/j.ejsobi.2020.103263.

Cohen, Y., an Rubin, A, E., 2015. Daytime solar heating controls downy mildew *Peronospora belbahrii* in sweet basil. PLOS One, 10: 1–25. https://doi.org/10.1371/journal.pone.0126103.

Compant, S. *et al.*, 2005. Use of plant growth-promoting bacteria for biocontrol of plant diseases : principles , mechanisms of action , and future prospects. Appl. Environ. Microbiol. 71 (9): 4951–4959. https://doi.org/10.1128/AEM.71.9.4951.

Compant, S., Brader, G., Muzammil, S. *et al.*, 2013. Use of beneficial bacteria and their secondary metabolites to control grapevine pathogen diseases. BioControl. 58 (4): 435-455. https://doi.org/10.1007/s10526-012-9479-6.

Correa-Delgado, R., Brito-López, P., Jaizme Vega, M. C. *et al.*, 2024. Biodiversity of Trichoderma species of healthy and Fusarium wilt-infected banana rhizosphere soils in Tenerife (Canary Islands, Spain). Front. Microbiol. 15: 1376602. https://doi.org/10.3389/fmicb.2024.1376602.

Costa Almeida, O. A. C., De Araujo, N. O., Dias, B. H. S. *et al.*, 2023. The power of the smallest : The inhibitory activity of microbial volatile organic compounds against phytopathogens. Front. Microbiol. 13: 951130. https://doi.org/10.3389/fmicb.2022.951130.

Cram, M.M. (2003). Damping-Off. Tree planter's notes. 50 (1): 9–13.

Cucu, M.A., Gilardi, G., Pugliese, M. *et al.*, 2020a. An assessment of the modulation of the population dynamics of pathogenic *Fusarium oxysporum* f. sp. *lycopersici* in the tomato rhizosphere by means of the application of *Bacillus subtilis* QST 713, *Trichoderma* sp. TW2 and two composts. Biol. Control 142: 104158. https://doi.org/10.1016/j.biocontrol.2019.104158.

Cucu, M.A., Gilardi, G., Pugliese, M. *et al.*, 2020b. Effects of biocontrol agents and compost against the *Phytophthora capsici* of zucchini and their impact on the rhizosphere microbiota. Appl. Soil Ecol. 142: 104158. https://doi.org/10.1016/j.apsoil.2020.103659.

Dai, Z., Ahmed, W., Yang, J. *et al.*, 2023. Seed coat treatment by plant-growth-promoting

rhizobacteria *Lysobacter antibioticus* 13–6 enhances maize yield and changes rhizosphere bacterial communities. Biol. Fertil. Soils. 59 (3): 317–331. https://doi.org/10.1007/s00374-023-01703-x.

Darine, T., Alaeddine, C., Fethi, B. *et al.*, 2015. Fluazifop-P-butyl (herbicide) affects richness and structure of soil bacterial communities. Soil Biol. Biochem. 81: 89-97. https://doi.org/10.1016/j.soilbio.2014.10.030.

Daudi, A., and O'Brien, J. A., 2012. Detection of hydrogen peroxide by DAB Staining in *Arabidopsis* leaves. Bio Protoc. 2 (18): 262.

Dave, A., and Graham, I. A., 2012. Oxylipin signaling: a distinct role for the jasmonic acid precursor cis-(+)-12-oxo-phytodienoic acid (cis-OPDA). Front. Plant Sci. 3: 42

Delame, M., Prado, E., Blanc, S. *et al.*, 2019. Introgression reshapes recombination distribution in grapevine interspecific hybrids. Theor. Appl. Genet. 132 (4): 1073–1087. https://doi.org/10.1007/s00122-018-3260-x.

Delledonne, M., Zeier, J., Marocco, A. *et al*., 2001. Signal interactions between nitric oxide and reactive oxygen intermediates in the plant hypersensitive disease resistance response. Proc. Natl. Acad. Sci. U.S.A. 98 (23): 13454–13459. https://doi.org/10.1073/pnas.231178298

Delmas, C. E., Fabre, F., Jolivet, J. *et al*., 2016. Adaptation of a plant pathogen to partial host resistance : selection for greater aggressiveness in grapevine downy mildew. Evol. Appl. 9 (5): 709–725. https://doi.org/10.1111/eva.12368

Di Marco, M., Baker, M. L., Daszak, P. *et al*., 2020. Sustainable development must account for pandemic risk. Proc. Natl. Acad. Sci. U.S.A. 117 (8): 3888–3892. https://doi.org/10.1073/pnas.2001655117.

Diacono, M., and Montemurro, F., 2011. Long-term effects of organic amendments on soil fertility. In: Sustainable Agriculture 2: 761–786. https://doi.org/10.1007/978-94-007-0394-0_34

Ding, Y., Li, Z., Li, Y. *et al*., 2016. HSAF-induced antifungal effects in *Candida albicans* through ROS-mediated apoptosis. RSC Adv. 6 (37): 30895–30904. https://doi.org/10.1039/C5RA26092B

do Rêgo Barros, F. M., Pedrinho, A., da Cunha Sant'Ana, G. *et al*., 2023. Plant-parasitic nematode community and enzyme activities in soils under no-till soybean crops in Brazil. Rhizosphere. 27: 100736https://doi.org/10.1016/j.rhisph.2023.100736.

Dong, L., Cheng, Y., Wu, J. *et al*., 2015. Overexpression of *GmERF5*, a new member of the soybean EAR motif-containing ERF transcription factor, enhances resistance to *Phytophthora sojae* in soybean. J. Exp. Bot. 66 (9): 2635–2647. https://doi.org/10.1093/jxb/erv078.

Dufour, M. C., Lambert, C., Bouscaut, J. *et al*., 2013. Benzothiadiazole-primed defence responses and enhanced differential expression of defence genes in *Vitis vinifera* infected with biotrophic pathogens *Erysiphe necator* and *Plasmopara viticola*. Plant Pathol. 62 (2): 370–382. https://doi.org/10.1111/j.1365-3059.2012.02628.x.

Duke, S. O., 2018. Interaction of chemical pesticides and their formulation ingredients with microbes

associated with plants and plant pests. J. Agric. Food Chem. 66 (29): 7553–7561. https://doi.org/10.1021/acs.jafc.8b02316.

Durrant, W.E. and Dong, X., 2004. Systemic acquired resistance. **Annu. Rev. Phytopathol.** 35 (1): 235–270. https://doi.org/10.1146/annurev.phyto.42.040803.140421.

El-Gendi, H., Al-Askar, A. A., Király, L. *et al*., 2022. Foliar applications of *Bacillus subtilis* HA1 culture filtrate enhance tomato growth and induce systemic resistance against tobacco mosaic virus infection. Horticulturae, 8 (4): 301. https://doi.org/10.3390/horticulturae8040301

Eno, C. F., Blue, W. G., and Good, J. M., 1955. The effect of anhydrous ammonia on nematodes, fungi, bacteria, and nitrification in some Florida soils. Soil Sci. Soc. Am. J. 19 (1): 55–58. https://doi.org/10.2136/sssaj1955.03615995001900010013x.

EPPO., 2004. EPPO Standards PP1/31(3). Efficacy evaluation of fungicides & bactericides. 2: 37–39.

Gómez Expósito, R., Postma, J., Raaijmakers, J. M. *et al*., 2015. Diversity and activity of *Lysobacter* species from disease suppressive soils. Front. Microbiol. 6: 1243. https://doi.org/10.3389/fmicb.2015.01243.

FAO, 2017. The State of Food and Agriculture 2017: Leveraging food systems for inclusive rural transformation.http://www.fao.org/3/a-i7658e.pdf (accessed 23 March 2026).

Favaron, F., Lucchetta, M., Odorizzi, S. *et al*., 2009. The role of grape polyphenols on trans-resveratrol activity against *Botrytis cinerea* and of fungal laccase on the solubility of putative grape PR proteins. J. Plant Pathol. 91: 579–588. https://doi.org/10.4454/JPP.V91I3.549

Felsenstein, J., 1985. Confidence limits on phylogenies: an approach using the bootstrap. Evolution 39 (4): 783–791. https://doi.org/10.1111/j.1558-5646.1985.tb00420.x

Fernández-Calviño, D., Rousk, J., Brookes, P. C. *et al*., 2011. Bacterial pH-optima for growth track soil pH, but are higher than expected at low pH. Soil Biol. Biochem. 43 (7): 1569–1575. https://doi.org/10.1016/j.soilbio.2011.04.007.

Fernandez, M. R., Zentner, R. P., Basnyat, P., et al., 2009. Glyphosate associations with cereal diseases caused by *Fusarium* spp. in the Canadian Prairies. Eur. J. Agron. 31 (3): 133–143. https://doi.org/10.1016/j.eja.2009.07.003.

Figueiredo, A., Monteiro, F., and Sebastiana, M., 2015. First clues on a jasmonic acid role in grapevine resistance against the biotrophic fungus *Plasmopara viticola*. Eur. J. Plant Pathol. 142 (3): 645–652. https://doi.org/10.1007/s10658-015-0634-7.

Folman, L. B., De Klein, M. J. E. M., Postma, J. *et al*., 2004. Production of antifungal compounds by *Lysobacter enzymogenes* isolate 3.1 T8 under different conditions in relation to its efficacy as a biocontrol agent of *Pythium aphanidermatum* in cucumber. Biol. Control. 31 (2): 145–154. https://doi.org/10.1016/j.biocontrol.2004.03.008.

Folman, L. B., Postma, J., and van Veen, J. A., 2003. Characterisation of *Lysobacter enzymogenes* (Christensen and Cook 1978) strain 3.1 T8, a powerful antagonist of fungal diseases of cucumber.

Microbiol. Res. 158 (2): 107–115. https://doi.org/10.1078/0944-5013-00185.

Fontaine, M. C., Austerlitz, F., Giraud, T., et al., 2013. Genetic signature of a range expansion and leap-frog event after the recent invasion of Europe by the grapevine downy mildew pathogen *Plasmopara viticola*. Mol. Ecol. 22 (10): 2771–2786. https://doi.org/10.1111/mec.12293

Fröbel, S., and Zyprian, E., 2019. Colonization of different grapevine tissues by *Plasmopara viticola*—a histological study. Front. Plant Sci. 10: 951. https://doi.org/10.3389/fpls.2019.00951

Fu, L., Penton, C. R., Ruan, Y. *et al*., 2017. Inducing the rhizosphere microbiome by biofertilizer application to suppress banana *Fusarium* wilt disease. Soil Biol. Biochem. 104: 39–48. https://doi.org/10.1016/j.soilbio.2016.10.008.

Fu, L., Li, H., Wei, L. *et al*., 2018. Antifungal and biocontrol evaluation of four *Lysobacter* strains against clubroot disease. Indian J. Microbiol. 58 (3): 353–359. https://doi.org/10.1007/s12088-018-0716-2.

Fu, Y., Luo, Y., Tang, C. *et al*., 2022. Succession of the soil bacterial community as resource utilization shifts from plant residues to rhizodeposits. Soil Biol. Biochem. 173: 108785. https://doi.org/10.1016/j.soilbio.2022.108785.

Gabaston, J., Richard, T., Biais, B. *et al*., 2017. Stilbenes from common spruce (*Picea abies*) bark as natural antifungal agent against downy mildew (*Plasmopara viticola*). Ind. Crops Prod. 103: 267–273. https://doi.org/10.1016/j.indcrop.2017.04.009.

Gai, X., Zhong, Z., Zhang, X. *et al*., 2021. Effects of chicken farming on soil organic carbon fractions and fungal communities in a Lei bamboo (*Phyllostachys praecox*) forest in subtropical China. For. Ecol. Manage. 479: 118603. https://doi.org/10.1016/j.foreco.2020.118603.

Gamliel, A., Austerweil, M., and Kritzman, G., 2000. Non-chemical approach to soilborne pest management–organic amendments. Crop Prot. 19 (8–10): 847–853. https://doi.org/10.1016/S0261-2194(00)00112-5.

Gao, H., Zhu, F., Jiang, Y., et al., 2012. Genetic analysis and molecular mapping of a new powdery mildew resistant gene *Pm46* in common wheat. Theor. Appl. Genet. 125 (5): 967–973. https://doi.org/10.1007/s00122-012-1886-7.

Gao, M., Xiong, C., Gao, C. *et al*., 2021. Disease-induced changes in plant microbiome assembly and functional adaptation. Microbiome, 9 (1): 187. https://doi.org/10.1186/s40168-021-01138-2.

Gao, Y., Wang, J., Ge, Y. *et al*., 2024. Partial substitution of nitrogen fertilizers by organic products of rural waste co-composting impacts on farmland soil quality. Environ. Technol. Innov. 33: 103470. https://doi.org/10.1016/j.eti.2023.103470.

García-Salamanca, A., Molina-Henares, M. A., van Dillewijn, P. *et al*., 2013. Bacterial diversity in the rhizosphere of maize and the surrounding carbonate-rich bulk soil. Microb. Biotechnol. 6 (1): 36–44. https://doi.org/10.1111/j.1751-7915.2012.00358.x.

De Cara García, M., Michel, V., and Molendijk, L., 2020. Soil borne diseases: Practical information.

Best4Soil Factsheet, 3–5. https://www.best4soil.eu/factsheets/17

Gauthier, A., Trouvelot, S., Kelloniemi, J. *et al*., 2014. The sulfated laminarin activates a stress transcriptome before priming the SA- and ROS-dependent defenses during grapevine's induced resistance against *Plasmopara viticola*. PLoS One, 9 (2): e88145. https://doi.org/10.1371/journal.pone.0088145.

Geberetsadik, G., Inaizumi, A., Nishiyama, A. *et al*., 2022. Lysocin E targeting menaquinone in the membrane of *Mycobacterium tuberculosis* is a promising lead compound for antituberculosis drugs. Antimicrob. Agents Chemother. 66 (9): e00171-22. https://doi.org/10.1128/aac.00171-22.

Gessler, C., Pertot, I., and Perazzolli, M., 2011. *Plasmopara viticola*: a review of knowledge on downy mildew of grapevine and effective disease management. Phytopathol. Mediterr. 50 (1): 3–44. https://doi.org/10.14601/Phytopathol_Mediterr-9360

Gianessi, L., and Reigner, N., 2006. The importance of fungicides in US crop production. Outlook Pest Manag. 17 (5): 209. https://doi.org/10.1564/17oct06.

Giannakis, C., Bucheli, C. S., Skene, K. G. M. *et al*., 1998. Chitinase and β-1,3-glucanase in grapevine leaves: a possible defence against powdery mildew infection. Aust. J. Grape Wine Res. 4 (1): 14–22. https://doi.org/10.1111/j.1755-0238.1998.tb00130.x

Giesler, L. J., and Yuen, G. Y., 1998. Evaluation of *Stenotrophomonas maltophilia* strain C3 for biocontrol of brown patch disease. Crop Prot. 17 (6): 509–513. https://doi.org/10.1016/S0261-2194(98)00049-0.

Gilardi, G., Demarchi, S., Garibaldi, A. *et al*., 2013. Management of downy mildew of sweet basil (*Ocimum basilicum*) caused by *Peronospora belbahrii* by means of resistance inducers, fungicides, biocontrol agents and natural products. Phytoparasitica, 41 (1): 59–72. https://doi.org/10.1007/s12600-012-0264-y.

Gilardi, G., Garibaldi, A., and Gullino, M. L., 2020. Integrated management of downy mildew of basil. Crop Prot. 137: 105202. https://doi.org/10.1016/j.cropro.2020.105202.

Gindro, K., Pezet, R., and Viret, O., 2003. Histological study of the responses of two *Vitis vinifera* cultivars (resistant and susceptible) to *Plasmopara viticola* infections. Plant Physiol. Biochem. 41 (9): 846–853. https://doi.org/10.1016/S0981-9428(03)00124-4

Giorgio, A., De Stradis, A., Lo Cantore, P. *et al*., 2015. Biocide effects of volatile organic compounds produced by potential biocontrol rhizobacteria on *Sclerotinia sclerotiorum*. Front. Microbiol. 6: 1056. https://doi.org/10.3389/fmicb.2015.01056.

Glazebrook, J., 2005. Contrasting mechanisms of defense against biotrophic and necrotrophic pathogens. Annu. Rev. Phytopathol. 43 (1): 205–227. https://doi.org/10.1146/annurev.phyto.43.040204.135923.

Gómez-Gómez, L., Felix, G., and Boller, T., 1999. A single locus determines sensitivity to bacterial flagellin in *Arabidopsis thaliana*. Plant J. 18 (3): 277–284. https://doi.org/10.1046/j.1365-313X.1999.00451.x.

Goodwin, S. B., 1997. The population genetics of *Phytophthora*. Phytopathology, 87 (4): 462–473. https://doi.org/10.1094/phyto.1997.87.4.462

Goss, M. J., Tubeileh, A., and Goorahoo, D., 2013. A review of the use of organic amendments and the risk to human health. Adv. Agron. 120: 275–379. https://doi.org/10.1016/B978-0-12-407686-0.00005-1

Graupner, P. R., Thornburgh, S., Mathieson, J. T. *et al*., 1997. Dihydromantophilin; a novel fungicidal tetramic acid-containing metabolite from *Streptomyces* sp. J. Antibiot. 50 (12): 1014–1019. https://doi.org/10.7164/antibiotics.50.1014.

Gruau, C., Trotel-Aziz, P., Villaume, S. *et al*., 2015. *Pseudomonas fluorescens* PTA-CT2 triggers local and systemic immune response against *Botrytis cinerea* in grapevine. Mol. Plant-Microbe Interact. 28 (10): 1117–1129. https://doi.org/10.1094/MPMI-04-15-0092-R

Guevara-Avendaño, E., Bejarano-Bolívar, A. A., Kiel-Martínez, A. L. *et al*., 2019. Avocado rhizobacteria emit volatile organic compounds with antifungal activity against *Fusarium solani*, *Fusarium* sp. associated with Kuroshio shot hole borer, and *Colletotrichum gloeosporioides*. Microbiol. Res. 219: 74–83.: https://doi.org/10.1016/j.micres.2018.11.009.

Hadar, Y., and Mandelbaum, R., 1986. Suppression of *Pythium aphanidermatum* damping-off in container media containing composted liquorice roots. Crop Prot. 5 (2): 88–92. https://doi.org/10.1016/0261-2194(86)90086-4

Hain, R., Reif, H. J., Krause, E. *et al.*, 1993. Disease resistance results from foreign phytoalexin expression in a novel plant. Nature, 361 (6408): 153–156. https://doi.org/10.1038/361153a0

Hakim, S., Naqqash, T., Nawaz, M. S. *et al*., 2021. Rhizosphere engineering with plant growth-promoting microorganisms for agriculture and ecological sustainability. **Front. Sustain. Food Syst.** 5: 617157. https://doi.org/10.3389/fsufs.2021.617157.

Hamamoto, H., Urai, M., Ishii, K. *et al*., 2015. Lysocin E is a new antibiotic that targets menaquinone in the bacterial membrane. Nat. Chem. Biol. 11 (2): 127–133. https://doi.org/10.1038/nchembio.1710.

Hamiduzzaman, M. M., Jakab, G., Barnavon, L. *et al*., 2005. β-Aminobutyric acid-induced resistance against downy mildew in grapevine acts through the potentiation of callose formation and jasmonic acid signaling. Mol. Plant-Microbe Interact. 18 (8): 819–829. https://doi.org/10.1094/mpmi-18-0819

Hassan, Z. U., Al Thani, R., Alnaimi, H. *et al*., 2019. Investigation and application of *Bacillus licheniformis* volatile compounds for the biological control of toxigenic *Aspergillus* and *Penicillium* spp. ACS Omega, 4 (17): 17186–17193. https://doi.org/10.1021/acsomega.9b01638.

He, F., Li, B., Ai, G. *et al*., 2018. Transcriptomics analysis of the Chinese pear pathotype of *Alternaria alternata* gives insights into novel mechanisms of HSAF antifungal activities. Int. J. Mol. Sci. 19 (7): 1841. https://doi.org/10.3390/ijms19071841

Helepciuc, F. E., and Todor, A., 2022. EU microbial pest control: A revolution in waiting. **Pest** Manag. Sci. 78 (4): 1314–1325. https://doi.org/10.1002/ps.6721

Hendrix, F. F., and Campbell, W. A., 1973. *Pythiums* as plant pathogens. Annu. Rev. Phytopathol. 11 (1): 77–98. https://doi.org/10.1146/annurev.py.11.090173.000453

Hönig, M., Roeber, V. M., Schmülling, T., et al., 2023. Chemical priming of plant defense responses to pathogen attacks. Front. Plant Sci. 14: 1146577. https://doi.org/10.3389/fpls.2023.1146577

Homa, K., Barney, W. P., Ward, D. L. *et al*., 2014. Evaluation of fungicides for the control of *Peronospora belbahrii* on sweet basil in New Jersey. Plant Dis. 98 (11): 1561–1566. https://doi.org/10.1094/pdis-02-14-0200-re

Howell, C. R., Beier, R. C., and Stipanovic, R. D., 1988. Production of ammonia by *Enterobacter cloacae* and its possible role in the biological control of *Pythium* preemergence damping-off by the bacterium. Phytopathology, 78 (8): 1075–1078. https://doi.org/10.1094/Phyto-78-1075

Hu, H. Y., Li, H., Hao, M. M. *et al*., 2021. Nitrogen fixation and crop productivity enhancements co-driven by intercrop root exudates and key rhizosphere bacteria. J. Appl. Ecol. 58 (10): 2243–2255. https://doi.org/10.1111/1365-2664.13964.

Hu, L., Robert, C. A., Cadot, S. *et al*., 2018. Root exudate metabolites drive plant-soil feedbacks on growth and defense by shaping the rhizosphere microbiota. Nat. Commun. 9: 2738. https://doi.org/10.1038/s41467-018-05122-7.

Huang, B., Chen, Y., Cao, Y. *et al*., 2024. The structure and function of rhizosphere bacterial communities: impact of chemical vs. bio-organic fertilizers on root disease, quality, and yield of *Codonopsis pilosula*. Front. Microbiol. 15: 1484727. https://doi.org/10.3389/fmicb.2024.1484727.

Huang, X., Weisener, C. G., Ni, J. *et al*., 2020. Nitrate assimilation, dissimilatory nitrate reduction to ammonium, and denitrification coexist in *Pseudomonas putida* Y-9 under aerobic conditions. Bioresour. Technol. 312: 123597. https://doi.org/10.1016/j.biortech.2020.123597.

Im, W. T., Siddiqi, M. Z., Kim, S. Y. *et al*., 2020. *Lysobacter lacus* sp. nov., isolated from lake sediment. Int. J. Syst. Evol. Microbiol. 70 (4): 2211–2216. https://doi.org/10.1099/ijsem.0.003950.

Islam, M. T., Hashidoko, Y., Deora, A. *et al*., 2005. Suppression of damping-off disease in host plants by the rhizoplane bacterium *Lysobacter* sp. strain SB-K88 is linked to plant colonization and antibiosis against soilborne *Peronosporomycetes*. Appl. Environ. Microbiol. 71 (7): 3786–3796. https://doi.org/10.1128/AEM.71.7.3786-3796.2005.

Islam, S., Akanda, A. M., Prova, A. *et al*., 2016. Isolation and identification of plant growth promoting rhizobacteria from cucumber rhizosphere and their effect on plant growth promotion and disease suppression. Front. Microbiol. 6: 1360. https://doi.org/10.3389/fmicb.2015.01360.

Itoh, H., Tokumoto, K., Kaji, T. *et al*., 2017. Total synthesis and biological mode of action of WAP-8294A2: a menaquinone-targeting antibiotic. J. Org. Chem. 83 (13): 6924–6935. https://doi.org/10.1021/acs.joc.7b02318.

Jain, A., Singh, S., Kumar Sarma, B. *et al*., 2012. Microbial consortium–mediated reprogramming of defense network in pea to enhance tolerance against *Sclerotinia sclerotiorum*. **J. Appl. Microbiol.** 112 (3): 537–550. https://doi.org/10.1111/j.1365-2672.2011.05220.x.

Jaiswal, A. K., Elad, Y., Paudel, I. *et al*., 2017. Linking the belowground microbial composition, diversity and activity to soilborne disease suppression and growth promotion of tomato amended with biochar. Sci. Rep. 7: 44382. https://doi.org/10.1038/srep44382.

Jakobi, M., Winkelmann, G., Kaiser, D. *et al*., 1996. Maltophilin: A new antifungal compound produced by *Stenotrophomonas maltophilia* R3089. J. Antibiot. 49 (11): 1101–1104. https://doi.org/10.7164/antibiotics.49.1101.

Janvier, C., Villeneuve, F., Alabouvette, C. *et al*., 2007. Soil health through soil disease suppression: which strategy from descriptors to indicators? Soil Biol. Biochem. 39 (1): 1–23. https://doi.org/10.1016/j.soilbio.2006.07.001.

Jeandet, P., Delaunois, B., Conreux, A. *et al*., 2010. Biosynthesis, metabolism, molecular engineering, and biological functions of stilbene phytoalexins in plants. Biofactors, 36 (5): 331–341. https://doi.org/10.1002/biof.108.

Jeandet, P., Hébrard, C., Deville, M. A. *et al*., 2014. Deciphering the role of phytoalexins in plant-microorganism interactions and human health. Molecules, 19 (11): 18033–18056. https://doi.org/10.3390/molecules191118033.

Jeandet, P., Vannozzi, A., Sobarzo-Sánchez, E. *et al*., 2021. Phytostilbenes as agrochemicals: biosynthesis, bioactivity, metabolic engineering and biotechnology. Nat. Prod. Rep. 38 (7): 1282–1329. https://doi.org/10.1039/d0np00030b.

Jermini, M., Blaise, P., and Gessler, C., 2010. Quantification of the influence of the downy mildew (*Plasmopara viticola*) epidemics on the compensatory capacities of *Vitis vinifera* 'Merlot' to limit the qualitative yield damage. Vitis – J. Grapevine Res. 49 (4): 153–160. https://doi.org/10.5073/vitis.2010.49.153-160

Jiang, Z. K., Tuo, L., Huang, D. L. *et al*., 2018. Diversity, novelty, and antimicrobial activity of endophytic actinobacteria from mangrove plants in Beilun Estuary National Nature Reserve of Guangxi, China. Front. Microbiol. 9: 868. https://doi.org/10.3389/fmicb.2018.00868.

Jin, C. Z., Song, X., Sung, Y. J. *et al*., 2020. *Lysobacter profundi* sp. nov., isolated from freshwater sediment and reclassification of *Lysobacter panaciterrae* as *Luteimonas panaciterrae* comb. nov. Int. J. Syst. Evol. Microbiol. 70 (6): 3878–3887. https://doi.org/10.1099/ijsem.0.004253.

Jochum, C. C., Osborne, L. E., and Yuen, G. Y., 2006. *Fusarium* head blight biological control with *Lysobacter enzymogenes* strain C3. Biol. Control 39 (3): 336–344. https://doi.org/10.1016/j.biocontrol.2006.05.004.

Jung, Y., Chhetri, G., Kim, I. *et al*., 2024. *Lysobacter ponds* sp. nov. and *Limnohabitans lacus* sp. nov., isolated from a pond. Int. J. Syst. Evol. Microbiol. 74 (5): 006400. https://doi.org/10.1099/ijsem.0.006400.

Kamoun, S., Furzer, O., Jones, J. D. G. *et al*., 2015. The top 10 oomycete pathogens in molecular plant pathology. Mol. Plant Pathol. 16 (4): 413–434. https://doi.org/10.1111/mpp.12190.

Kandeler, E., Deiglmayr, K., Tscherko, D. *et al*., 2006. Abundance of *narG*, *nirS*, *nirK*, and *nosZ*

genes of denitrifying bacteria during primary successions of a glacier foreland. Appl. Environ. Microbiol. 72 (9): 5957–5962. https://doi.org/10.1128/AEM.00439-06.

Katan, J., 1999. The methyl bromide issue: problems and potential solutions. J. Plant Pathol. 81: 153–159. https://www.jstor.org/stable/41998968.

Katan, J., 2000. Physical and cultural methods for the management of soil-borne pathogens. Crop Prot. 19 (8–10): 725–731. https://doi.org/10.1016/S0261-2194(00)00096-X

Kaur, S., Samota, M. K., Choudhary, M. *et al*., 2022. How do plants defend themselves against pathogens—biochemical mechanisms and genetic interventions. Physiol. Mol. Biol. Plants. 28 (2): 485–504. https://doi.org/10.1007/s12298-022-01146-y.

Kawasaki, T., Henmi, K., Ono, E. *et al*., 1999. The small GTP-binding protein Rac is a regulator of cell death in plants. Proc. Natl. Acad. Sci. U.S.A. 96 (19): 10922–10926. https://doi.org/10.1073/pnas.96.19.10922.

Khattab, I. M., Sahi, V. P., Baltenweck, R. *et al*., 2021. Ancestral chemotypes of cultivated grapevine with resistance to Botryosphaeriaceae-related dieback allocate metabolism towards bioactive stilbenes. New Phytol. 229 (2): 1133–1146. https://doi.org/10.1111/nph.16919.

Kiesewalter, H. T., Lozano-Andrade, C. N., Wibowo, M. *et al*., 2021. Genomic and chemical diversity of *Bacillus subtilis* secondary metabolites against plant pathogenic fungi. mSystems. 6 (1): e01128-20. https://doi.org/10.1128/mSystems.00770-20

Kilic-Ekici, O., and Yuen, G. Y., 2003. Induced resistance as a mechanism of biological control by *Lysobacter enzymogenes* strain C3. Phytopathology, 93 (9): 1103–1110. https://doi.org/10.1094/PHYTO.2003.93.9.1103.

Kim, I., Chhetri, G., So, Y. *et al*., 2022. Characteristics and biological activity of exopolysaccharide produced by *Lysobacter* sp. MMG2 isolated from the roots of *Tagetes patula*. Microorganisms, 10 (7): 1257. https://doi.org/10.1007/s10482-019-01256-w.

Kim, I., Chhetri, G., So, Y. *et al*., 2023. Characterization and antioxidant activity of exopolysaccharides produced by *Lysobacter soyae* sp. nov isolated from the root of *Glycine max* L. Microorganisms, 11 (8): 1900. https://doi.org/10.3390/microorganisms11081900.

Kim, J. S., and Crowley, D. E., 2007. Microbial diversity in natural asphalts of the Rancho La Brea Tar Pits. Appl. Environ. Microbiol. 73 (14): 4579–4591. https://doi.org/10.1128/AEM.01372-06.

Kim, S. J., Ahn, J. H., Weon, H. Y. *et al*., 2017. *Lysobacter solanacearum* sp. nov., isolated from rhizosphere of tomato. Int. J. Syst. Evol. Microbiol. 67 (5): 1102–1106. https://doi.org/10.1099/ijsem.0.001729.

Kimura, M., 1980. A simple method for estimating evolutionary rates of base substitutions through comparative studies of nucleotide sequences. J. Mol. Evol. 16 (2): 111–120. https://doi.org/10.1007/BF01731581.

Kiranmayi, M. U., Sudhakar, P., Sreenivasulu, K. *et al*., 2011. Optimization of culturing conditions

for improved production of bioactive metabolites by *Pseudonocardia* sp. VUK-10. Mycobiology, 39 (3): 174–181. https://doi.org/10.5941/MYCO.2011.39.3.174

Klopping, H. L., and Delp, C. J., 1980. 2-Cyano-N-[(ethylamino) carbonyl]-2-(methoxyimino) acetamide, a new fungicide. J. Agric. Food Chem. 28 (2): 467–468. https://doi.org/10.1021/jf60228a010

Ko, H. S., Jin, R. D., Krishnan, H. B. *et al*., 2009. Biocontrol ability of *Lysobacter antibioticus* HS124 against *Phytophthora* blight is mediated by the production of 4-hydroxyphenylacetic acid and several lytic enzymes. Curr. Microbiol. 59 (6): 608–615. https://doi.org/10.1007/s00284-009-9481-0.

Kobayashi, D. Y., Reedy, R. M., Palumbo, J. D. *et al*., 2005. A *clp* gene homologue belonging to the *Crp* gene family globally regulates lytic enzyme production, antimicrobial activity, and biological control activity expressed by *Lysobacter enzymogenes* strain C3. Appl. Environ. Microbiol. 71 (1): 261–269. https://doi.org/10.1128/AEM.71.1.261-269.2005.

Koledenkova, K., Esmaeel, Q., Jacquard, C. *et al*., 2022. *Plasmopara viticola* the causal agent of downy mildew of grapevine: from its taxonomy to disease management. Front. Microbiol. 13: 889472. https://doi.org/10.3389/fmicb.2022.889472.

Kong, H. G., Song, G. C., Sim, H. J. *et al*., 2021. Achieving similar root microbiota composition in neighboring plants through airborne signaling. ISME J. 15 (2): 397–408. https://doi.org/10.1038/s41396-020-00759-z.

Koornneef, Annemart and Pieterse, C.M.J., 2008. Cross talk in defense signaling. Plant Physiol. 146 (3): 839–844. https://doi.org/10.1104/pp.107.112029.

Koroch, A. R., Villani, T. S., Pyne, R. M. *et al*., 2013. Rapid staining method to detect and identify downy mildew (*Peronospora belbahrii*) in basil. Appl. Plant Sci. 1 (7): 1300032. https://doi.org/10.3732/apps.1300032

Kortekamp, A., and Zyprian, E., 2003. Characterization of *Plasmopara* resistance in grapevine using in vitro plants. J. Plant Physiol., 160 (11): 1393–1400. https://doi.org/10.1078/0176-1617-01021

Kothari, A. J. D., Martini, A., *et al*., 2026. *Lysobacter*: an emerging frontier in sustainable control of soilborne phytopathogenic microorganisms. In Soil Microorganisms for Plant Growth Promotion and Soil Health, 327–365. Elsevier. https://doi.org/10.1016/B978-0-443-34055-0.00013-8

Kudryakova, I. V., Shishkova, N. A., and Vasilyeva, N. V., 2016. Outer membrane vesicles of *Lysobacter* sp. XL1: biogenesis, functions, and applied perspectives. Appl. Microbiol. Biotechnol., 100 (11): 4791–4801. https://doi.org/10.1007/s00253-016-7524-6.

Kuhn, P. J., Pitt, D., Lee, S. A. *et al*., 1991. Effects of dimethomorph on the morphology and ultrastructure of *Phytophthora*. Mycol. Res. 95 (3): 333–340. https://doi.org/10.1016/S0953-7562(09)81244-6.

Kumar, R., Gupta, S. K., and Gupta, M., 2018. Investigation on etiology and epidemiology of damping-off of tomato seedlings in mid hills of Himachal Pradesh. Indian Phytopathol. 71 (4): 513–518. https://doi.org/10.1007/s42360-018-0092-1.

Kumar, R., and Shimizu, K., 2010. Metabolic regulation of *Escherichia coli* and its *gdhA, glnL, gltB,* D mutants under different carbon and nitrogen limitations in the continuous culture. Microb. Cell Fact. 9 (1): 8. https://doi.org/10.1186/1475-2859-9-8

Kurm, V., Visser, J., Schilder, M. *et al*., 2023. Soil suppressiveness against *Pythium ultimum* and *Rhizoctonia solani* in two land management systems and eleven soil health treatments. Microb. Ecol. 86 (3): 1709–1724. https://doi.org/10.1007/s00248-023-02215-9.

La Placa, L., Cornali, S., Bertinaria, F. *et al*., 2025. Cropping system support in downy mildew control in basil in organic farming: a two-year open field experiment. J. Plant Pathol. 107 (1): 167–179. https://doi.org/10.1007/s42161-024-01651-x

Lamichhane, J. R., Osdaghi, E., Behlau, F. *et al*., 2018. Thirteen decades of antimicrobial copper compounds applied in agriculture: A review. Agron. Sustain. Dev. 38 (3): 28. https://doi.org/10.1007/s13593-018-0503-9.

Langcake, P., 1981. Disease resistance of *Vitis* spp. and the production of the stress metabolites resveratrol, ε-viniferin, α-viniferin and pterostilbene. Physiol. Plant Pathol. 18 (2): 213–226. https://doi.org/10.1016/S0048-4059(81)80043-4.

Langcake, P., and Pryce, R. J., 1976. The production of resveratrol by *Vitis vinifera* and other members of the Vitaceae as a response to infection or injury. Physiol. Plant Pathol. 9 (1): 77–86. https://doi.org/10.1016/0048-4059(76)90077-1

Latijnhouwers, M., de Wit, P. J., and Govers, F., 2003. Oomycetes and fungi: similar weaponry to attack plants. Trends Microbiol. 11 (10): 462–469. https://doi.org/10.1016/j.tim.2003.08.002.

Latruffe, N. and Vervandier-Fasseur, D., 2018. Strategic syntheses of vine and wine resveratrol derivatives to explore their effects on cell functions and dysfunctions. Diseases. 6 (4): 110. https://doi.org/10.3390/diseases6040110.

Lazarovits, G., Hawke, M. A., Tomlin, A. D. *et al*., 1991. Soil solarization to control *Verticillium dahliae* and *Pratylenchus penetrons* on potatoes in central Ontario. Can. J. Plant Pathol. 13 (2): 116–123. https://doi.org/10.1016/0048-4059(76)90077-1.

Lazarovits, G., Conn, K. L., Potter, J. *et al*., 1999. Reduction of potato scab, verticillium wilt, and nematodes by soymeal and meat and bone meal in two Ontario potato fields. Can. J. Plant Pathol. 21 (4): 345–353. https://doi.org/10.1080/07060669909501170.

Lazarovits, G., 2010. Managing soilborne disease of potatoes using ecologically based approaches. Am. J. Potato Res. 87 (5): 401–411. https://doi.org/10.1007/s12230-010-9157-0.

Lazarovits, G., 2001. Management of soil-borne plant pathogens with organic soil amendments: a disease control strategy rescued from the past. Can. J. Plant Pathol. 23 (1): 1–7. https://doi.org/10.1080/07060660109506901.

Lazazzara, V., Perazzolli, M., Pertot, I. *et al*., 2017. Growth media affects the volatilome and antimicrobial activity against *Phytophthora infestans* in four *Lysobacter* type strains. Microbiol. Res. 201: 52–62. https://doi.org/10.1016/j.micres.2017.04.015.

Lazcano, C., Boyd, E., Holmes, G. *et al*., 2021. The rhizosphere microbiome plays a role in the resistance to soil-borne pathogens and nutrient uptake of strawberry cultivars under field conditions. Sci. Rep. 11 (1): 3188. https://doi.org/10.1038/s41598-021-82768-2.

Lee, J., Kim, S., Jung, H. *et al*., 2023. Exploiting bacterial genera as biocontrol agents: mechanisms, interactions and applications in sustainable agriculture. J. Plant Biol. 66 (6): 485–498. https://doi.org/10.1007/s12374-023-09404-6.

Lee, J. C., and Whang, K. S., 2021. *Lysobacter telluris* sp. nov., isolated from Korean rhizosphere soil. Arch. Microbiol. 203 (1): 287–293. https://doi.org/10.1007/s00203-020-02032-5.

Lee, J. W., Im, W. T., Kim, M. K. *et al*., 2006. *Lysobacter koreensis* sp. nov., isolated from a ginseng field. Int. J. Syst. Evol. Microbiol. 56 (1): 231–235. https://doi.org/10.1099/ijs.0.63955-0.

Lee, Y. S., Anees, M., Hyun, H. N. *et al*., 2013. Biocontrol potential of *Lysobacter antibioticus* HS124 against the root-knot nematode, *Meloidogyne incognita*, causing disease in tomato. Nematology, 15 (5): 545–555. https://doi.org/10.1163/15685411-00002700.

Lee, Y. S., Nguyen, X. H., Naing, K. W. *et al*., 2015. Role of lytic enzymes secreted by *Lysobacter capsici* YS1215 in the control of root-knot nematode of tomato plants. Indian J. Microbiol. 55 (1): 74–80. https://doi.org/10.1007/s12088-014-0499-z.

Lenzi, L., Caruso, C., Bianchedi, P. L. *et al*., 2016. Laser microdissection of grapevine leaves reveals site-specific regulation of transcriptional response to *Plasmopara viticola*. Plant Cell Physiol. 57 (1): 69–81. https://doi.org/10.1093/pcp/pcv166.

Li, C., Tang, B., Cao, S. *et al*., 2021. Biocontrol ability and action mechanism of dihydromaltophilin against *Colletotrichum fructicola* causing anthracnose of pear fruit. Pest Manag. Sci. 77 (2): 1061–1069. Available at: https://doi.org/10.1002/ps.6122.

Li, S., Du, L., Yuen, G. *et al*., 2006. Distinct ceramide synthases regulate polarized growth in the filamentous fungus *Aspergillus nidulans*. Mol. Biol. Cell 17 (3): 1218–1227. https://doi.org/10.1091/mbc.e05-06-0533.

Li, S., Calvo, A. M., Yuen, G. Y. *et al*., 2009. Induction of cell wall thickening by the antifungal compound dihydromaltophilin disrupts fungal growth and is mediated by sphingolipid biosynthesis. J. Eukaryot. Microbiol. 56 (2): 182–187. https://doi.org/10.1111/j.1550-7408.2008.00384.x.

Li, Y., Wang, H., Liu, Y. *et al*., 2018. Biosynthesis of the polycyclic system in the antifungal HSAF and analogues from *Lysobacter enzymogenes*. Angew. Chem. 130 (21): 6329–6333. https://doi.org/10.1002/anie.201802488.

Liang, J., Sun, S., Ji, J. *et al*., 2014. Comparison of the rhizosphere bacterial communities of Zigongdongdou soybean and a high-methionine transgenic line of this cultivar. PLoS One 9 (7): e103343. https://doi.org/10.1371/journal.pone.0103343.

Lin, L., Xu, K., Shen, D. *et al*., 2021. Antifungal weapons of *Lysobacter*, a mighty biocontrol agent. Environ. Microbiol. 23 (10): 5704–5715. https://doi.org/10.1111/1462-2920.15674.

Lin, L., Yang, Z., Tao, M. *et al*., 2023. *Lysobacter enzymogenes* prevents *Phytophthora* infection by inhibiting pathogen growth and eliciting plant immune responses. Front. Plant Sci. 14: 1116147. https://doi.org/10.3389/fpls.2023.1116147.

Lin, S. Y., Hameed, A., Wen, C. Z. *et al*., 2015. *Lysobacter lycopersici* sp. nov., isolated from tomato plant *Solanum lycopersicum*. Antonie van Leeuwenhoek 107 (5): 1261–1270. https://doi.org/10.1007/s10482-015-0419-1.

Liu, X., Wu, D., Abid, A. A. *et al*., 2022. Determination of paddy soil ammonia nitrogen using rapid detection kit coupled with microplate reader. Toxics, 10 (12): 725. https://doi.org/10.3390/toxics10120725

Liu, Y., Zhang, Y., Huang, Y. *et al*., 2023. Spatial and temporal conversion of nitrogen using *Arthrobacter* sp. 24S4–2, a strain obtained from Antarctica. Front. Microbiol. 14: 1040201. https://doi.org/10.3389/fmicb.2023.1040201.

Liu, Y., Qiao, J., Liu, Y. *et al*., 2019. Characterization of *Lysobacter capsici* strain NF87–2 and its biocontrol activities against phytopathogens. Eur. J. Plant Pathol. 155 (3): 859–869. https://doi.org/10.1007/s10658-019-01817-9.

Liu, Z., Jiang, P., Niu, G. *et al*., 2022. *Lysobacter antarcticus* sp. nov., an SUF-system-containing bacterium from Antarctic coastal sediment. Int. J. Syst. Evol. Microbiol. 72 (2): 005250. https://doi.org/10.1099/ijsem.0.005250.

López-López, A., Koller, M., Herb, C. *et al*., 2013. Influence of light management on the sporulation of downy mildew on sweet basil. In II Int. Symp. Org. Greenh. Hortic. 1041: 213–219. https://doi.org/10.17660/ActaHortic.2014.1041.24

Lou, L., Qian, G., Xie, Y. *et al*., 2011. Biosynthesis of HSAF, a tetramic acid-containing macrolactam from *Lysobacter enzymogenes*. J. Am. Chem. Soc. 133 (4): 643–645. https://doi.org/10.1021/ja105732c.

Lucena, T., Sánchez, O., Sanz-Saez, I. *et al*., 2022. *Parvicella tangerina* gen. nov., sp. nov. (*Parvicellaceae* fam. nov., *Flavobacteriales*), first cultured representative of the marine clade UBA10066, and *Lysobacter luteus* sp. nov., from activated sludge of a seawater-processing wastewater treatment plant. Int. J. Syst. Evol. Microbiol. 72 (8): 005498. https://doi.org/10.1099/ijsem.0.005498.

Lumsden, R. D., and Locke, J. C., 1989. Biological control of damping-off caused by *Pythium ultimum* and *Rhizoctonia solani* with *Gliocladium virens* in soilless mix. Phytopathology, 79 (3): 361–366. https://doi.org/10.1094/PHYTO-79-361

Luo, G., Shi, Z., and Wang, G., 2012. *Lysobacter arseniciresistens* sp. nov., an arsenite-resistant bacterium isolated from iron-mined soil. Int. J. Syst. Evol. Microbiol. 62 (7): 1659–1665. https://doi.org/10.1099/ijs.0.034405-0.

Ma, Y., Wu, Q., Wang, X. *et al*., 2025. Carbon components in organic amendments drive nitrogen metabolism in one-year-long anaerobic soil microcosms. Front. Microbiol. 16: 1588169. https://doi.org/10.3389/fmicb.2025.1588169.

Manorantitham, S. K., Prakasam, V., and Rajappan, K., 2001. Biocontrol of damping off of tomato caused by *Pythium aphanidermatum*. Indian Phytopathol. 54: 59–61.

Mao, S., Li, S., Guo, B. *et al*., 2022. *Lysobacter selenitireducens* sp. nov., isolated from river sediment. Int. J. Syst. Evol. Microbiol. 72 (10): 005550. https://doi.org/10.1099/ijsem.0.005550.

Marant, B., Flourat, A. L., Lanoue, A. *et al*., 2025. Peroxidase 4-based enzymatic synthesis of stilbene oligomers in methyl jasmonate-elicited grapevine cell suspensions. J. Agric. Food Chem. 73 (3): 1929–1939. https://doi.org/10.1021/acs.jafc.4c09502.

Marchive, C., Léon, C., Kappel, C. *et al*., 2013. Over-expression of *VvWRKY1* in grapevines induces expression of jasmonic acid pathway-related genes and confers higher tolerance to the downy mildew. PLoS One 8 (1): e54185. https://doi.org/10.1371/journal.pone.0054185.

Marín-Guirao, J. I., Yan, D., Di Gioia, F. *et al*., 2025. Soil microbial communities to promote suppressiveness against soil-borne pathogens and diseases. Front. Microbiol. 16: 1677158. https://doi.org/10.3389/fmicb.2025.1677158

Markellou, E., Kapaxidi, E., Karamaouna, F. *et al*., 2022. Evaluation of plant protection efficacy in field conditions and side effects of *Lysobacter capsici* AZ78, a biocontrol agent of *Plasmopara viticola*. Biocontrol Sci. Technol. 32 (8): 930–951. https://doi.org/10.1080/09583157.2022.2064431

Marti, G., Schnee, S., Andrey, Y. *et al*., 2014. Study of leaf metabolome modifications induced by UV-C radiations in representative *Vitis*, *Cissus* and *Cannabis* species by LC-MS based metabolomics and antioxidant assays. Molecules, 19 (9): 14004–14021. https://doi.org/10.3390/molecules190914004.

Martínez-Servat, S., Pinyol-Escala, L., Daura-Pich, O. *et al*., 2023. Characterization of *Lysobacter enzymogenes* B25, a potential biological control agent of plant-parasitic nematodes, and its mode of action. AIMS Microbiol. 9 (1): 151. https://doi.org/10.3934/microbiol.2023010.

Meena, R. S., Kumar, S., Datta, R. *et al*., 2020. Impact of agrochemicals on soil microbiota and management: A review. Land. 9 (2): 34. https://doi.org/10.3390/land9020034.

Meers, P. R., Liu, C., Chen, R. *et al*., 2018. Vesicular delivery of the antifungal antibiotics of *Lysobacter enzymogenes* C3. Appl. Environ. Microbiol. 84 (20): e01353-18. https://doi.org/10.1128/AEM.01353-18.

Mehmood, M. A., Fu, Y., Zhao, H. *et al*., 2022. Enrichment of bacteria involved in the nitrogen cycle and plant growth promotion in soil by sclerotia of rice sheath blight fungus. Stress Biol. 2 (1): 32. https://doi.org/10.1007/s44154-022-00049-y.

Mersha, Z., Zhang, S., Raid, R. N., *et al*., 2012. Evaluation of systemic acquired resistance inducers for control of downy mildew on basil. Crop Prot. 40: 83–90. https://doi.org/10.1016/j.cropro.2012.04.031

Meziane, H., Van Der Sluis, I., Van Loon, L. C. *et al*., 2005. Determinants of *Pseudomonas putida* WCS358 involved in inducing systemic resistance in plants. Mol. Plant Pathol. 6 (2): 177–185. https://doi.org/10.1111/j.1364-3703.2005.00276.x

Mian, G., Musetti, R., Belfiore, N. *et al*., 2023. Chitosan application reduces downy mildew severity on grapevine leaves by positively affecting gene expression pattern. Physiol. Mol. Plant Pathol. 125: 102025. https://doi.org/10.1016/j.pmpp.2023.102025

Miclot, A. S., Guimier, S., Delmotte, F. *et al*., 2019. Sustainable management of grapevine resistance. Detect the emergence of breakdown, of new diseases and adapt crop systems. Innov. Agron. 77: 19–30. https://dx.doi.org/10.15454/8bbz-t493

Mihajlovic, M., 2017. Methods for management of soilborne plant pathogens. Pestic. Fitomed. 32 (3–4): 1–10. https://doi.org/10.2298/pif1701009m.

Mijailovic, N., Nesler, A., Perazzolli, M. *et al*., 2022. Foliar application of a tagatose-based product reduces downy mildew symptoms through induction of grapevine resistance and anti-oomycete action. Agronomy, 12 (2): 498. https://doi.org/10.2298/PIF1701009M

Mokni-Tlili, S., Markowicz, A., and Sułowicz, S., 2024. Culture-based and molecular investigation of antibiotic and metal resistance in a semi-arid agricultural soil repeatedly amended with urban sewage sludge. Environ. Res. 263: 120182. https://doi.org/10.1016/j.envres.2024.120182.

Mondal, S. N., and Hyakumachi, M., 2000. Soil factors affecting carbon loss and pathogenicity of oospores of *Pythium aphanidermatum*. Soil Biol. Biochem. 32 (1): 111–118. https://doi.org/10.1016/S0038-0717(99)00139-X

Montejano-Ramírez, V., Ávila-Oviedo, J. L., Campos-Mendoza, F. J. *et al*., 2024. Microbial volatile organic compounds: Insights into plant defense. Plants 13 (15): 2013. https://doi.org/10.3390/plants13152013

Moon, J. H., Won, S. J., Maung, C. E. H. *et al*., 2021. The role of *Lysobacter antibioticus* HS124 on the control of fall webworm (*Hyphantria cunea* Drury) and growth promotion of Canadian poplar (*Populus canadensis* Moench) at Saemangeum reclaimed land in Korea. Microorganisms, 9 (8): 1580. https://doi.org/10.3390/microorganisms9081580.

Morra, L., Pagano, L., Iovieno, P. *et al*., 2010. Soil and vegetable crop response to addition of different levels of municipal waste compost under Mediterranean greenhouse conditions. Agron. Sustain. Dev. 30 (3): 701–709. https://doi.org/10.1051/agro/2009046.

Müller, M., and Munné-Bosch, S., 2015. Ethylene response factors: a key regulatory hub in hormone and stress signaling. Plant Physiol. 169 (1): 32–41. https://doi.org/10.1104/pp.15.00677.

Munjal, V., Nadakkakath, A. V., Sheoran, N. *et al*., 2016. Genotyping and identification of broad spectrum antimicrobial volatiles in black pepper root endophytic biocontrol agent, *Bacillus megaterium* BP17. Biol. Control, 92: 66–76. https://doi.org/10.1016/j.biocontrol.2015.09.005.

Mur, L. A. J., Kenton, P., Atzorn, R. *et al*., 2006. The outcomes of concentration-specific interactions between salicylate and jasmonate signaling include synergy, antagonism, and oxidative stress leading to cell death. Plant Physiol. 140 (1): 249–262. https://doi.org/10.1104/pp.105.072348.was.

Musetti, R., Stringher, L., Borselli, S. *et al*., 2005. Ultrastructural analysis of *Vitis vinifera* leaf tissues showing atypical symptoms of *Plasmopara viticola*. Micron, 36 (1): 73–80.

https://doi.org/10.1016/j.micron.2004.05.002.

Naghman, R., Bhatti, M. T., Najabat, Z. *et al*., 2023. Organic amendments: a natural way to suppress phytopathogens: a sustainable approach to go green. Turk. J. Agric. For. 47 (5): 602–622. https://doi.org/10.1080/07060669909501173.

Nakayama, T., Homma, Y., Hashidoko, Y. *et al*., 1999. Possible role of xanthobaccins produced by *Stenotrophomonas* sp. strain SB-K88 in suppression of sugar beet damping-off disease. Appl. Environ. Microbiol. 65 (10): 4334–4339. https://doi.org/10.1128/aem.65.10.4334-4339.1999.

Nannipieri, P., Ascher, J., Ceccherini, M. *et al*., 2017. Microbial diversity and soil functions. Eur. J. Soil Sci. 68 (1): 12–26. https://doi.org/10.1111/ejss.4.

Naushad, S., Adeolu, M., Wong, S. *et al*., 2015. A phylogenomic and molecular marker based taxonomic framework for the order Xanthomonadales: proposal to transfer the families Algiphilaceae and Solimonadaceae to the order Nevskiales ord. nov. and to create a new family within the order Xanthomonadales, the family Rhodanobacteraceae fam. nov., containing the genus *Rhodanobacter* and its closest relatives. Antonie van Leeuwenhoek, 107 (2): 467–485. https://doi.org/10.1007/s10482-014-0344-8.

Nawrocka, J. and Małolepsza, U., 2013. Diversity in plant systemic resistance induced by *Trichoderma*. Biol. Control 67 (2): 149–156. https://doi.org/10.1016/j.biocontrol.2013.07.005.

Ngo, H. T., Won, K., Du, J. *et al*., 2015. *Lysobacter terrae* sp. nov. isolated from *Aglaia odorata* rhizosphere soil. Int. J. Syst. Evol. Microbiol. 65 (Pt 2): 587–592. https://doi.org/10.1099/ijs.0.067397-0.

Nguyen, N. H., Song, Z., Bates, S. T. *et al*., 2016. FUNGuild: an open annotation tool for parsing fungal community datasets by ecological guild. Fungal Ecol. 20: 241–248. https://doi.org/10.1016/j.funeco.2015.06.006.

Nian, J., Yu, M., Bradley, C. A. *et al*., 2021. *Lysobacter enzymogenes* strain C3 suppresses mycelium growth and spore germination of eight soybean fungal and oomycete pathogens and decreases disease incidences. Biol. Control 152: 104424. https://doi.org/10.1016/j.biocontrol.2020.104424.

Nie, Y., Wang, M., Zhang, W. *et al*., 2018. Ammonium nitrogen content is a dominant predictor of bacterial community composition in an acidic forest soil with exogenous nitrogen enrichment. Sci. Total Environ. 624: 407–415. https://doi.org/10.1016/j.scitotenv.2017.12.142.

Nimbeshaho, F., Nihorimbere, G., Arias, A. A. *et al*., 2024. Unravelling the secondary metabolome and biocontrol potential of the recently described species *Bacillus nakamurai*. Microbiol. Res. 288: 127841. https://doi.org/10.1016/j.micres.2024.127841

Niu, B. Y., Ren, D. J., Zhang, F. B. *et al*., 2023. *Lysobacter changpingensis* sp. nov., a novel species of the genus *Lysobacter* isolated from a rhizosphere soil of strawberry in China. Folia Microbiol. 68 (6): 991–998. https://doi.org/10.1007/s12223-023-01058-8.

Nogales, B., Timmis, K. N., Nedwell, D. B. *et al*., 2002. Detection and diversity of expressed denitrification genes in estuarine sediments after reverse transcription-PCR amplification from

mRNA. Appl. Environ. Microbiol. 68 (10): 5017–5025. https://doi.org/10.1128/AEM.68.10.5017.

Núñez-Palenius, H. G., Orosco-Alcalá, B. E., Espitia-Vázquez, I. *et al*., 2022. Biological control of downy mildew and yield enhancement of cucumber plants by *Trichoderma harzianum* and *Bacillus subtilis* (Ehrenberg) under greenhouse conditions. Horticulturae, 8 (12): 1133. https://www.mdpi.com/2311-7524/8/12/1133

OIV, 2022. State of the World Vitivinicultural Sector in 2021.https://www.oiv.int/public/medias/8702/oiv-state-of-the-world-vitivinicultural-sector-in-2021.pdf(accessed 23 March 2026).

Olson, J. D., Damicone, J. P., Kahn, B. A. *et al*., 2016. Identification and characterization of isolates of *Pythium* and *Phytophthora* spp. from snap beans with cottony leak. Plant Dis. 100 (7): 1446–1453. https://doi.org/10.1094/pdis-06-15-0662-re

Omar, S. A., and Ismail, M. A., 1999. Microbial populations, ammonification and nitrification in soil treated with urea and inorganic salts. Folia Microbiol. 44 (2): 205–212. https://doi.org/10.1007/BF02816244.

Omoboye, O. O., Oni, F. E., Batool, H. *et al*., 2019. *Pseudomonas* cyclic lipopeptides suppress the rice blast fungus *Magnaporthe oryzae* by induced resistance and direct antagonism. Front. Plant Sci. 10: 901. https://doi.org/10.3389/fpls.2019.00901

Omran, R. A. B. A. B., and Kadhem, M. F., 2016. Production, purification, and characterization of bioactive metabolites produced from rare actinobacteria *Pseudonocardia alni*. Asian J. Pharm. Clin. Res. 9 (3): 1. https://doi.org/10.22159/ajpcr.2016.v9s3.14961

Palmieri, M. C., Perazzolli, M., Matafora, V. *et al*., 2012. Proteomic analysis of grapevine resistance induced by *Trichoderma harzianum* T39 reveals specific defense pathways activated against downy mildew. J. Exp. Bot. 63 (17): 6237–6251. https://doi.org/10.1093/jxb/ers279.

Palumbo, J. D., Sullivan, R. F., and Kobayashi, D. Y., 2003. Molecular characterization and expression in *Escherichia coli* of three β-1,3-glucanase genes from *Lysobacter enzymogenes* strain N4-7. J. Bacteriol. 185 (15): 4362–4370. https://doi.org/10.1128/JB.185.15.4362-4370.2003.

Pandey, C. B., Kumar, U., Kaviraj, M. *et al*., 2020. DNRA: a short-circuit in biological N-cycling to conserve nitrogen in terrestrial ecosystems. Sci. Total Environ. 738: 139710. https://doi.org/10.1016/j.scitotenv.2020.139710.

Pane, C., Spaccini, R., Piccolo, A. *et al*., 2011. Compost amendments enhance peat suppressiveness to *Pythium ultimum*, *Rhizoctonia solani* and *Sclerotinia minor*. Biol. Control, 56 (2): 115–124. https://doi.org/10.1016/j.biocontrol.2010.10.002.

Panthee, S., Hamamoto, H., Paudel, A. *et al*., 2016. *Lysobacter* species: a potential source of novel antibiotics. Arch. Microbiol. 198 (9): 839–845. https://doi.org/10.1007/s00203-016-1278-5.

Park, J. H., Kim, R., Aslam, Z. *et al*., 2008. *Lysobacter capsici* sp. nov., with antimicrobial activity, isolated from the rhizosphere of pepper, and amended description of the genus *Lysobacter*. Int. J. Syst. Evol. Microbiol. 58 (2): 387–392. https://doi.org/10.1099/ijs.0.65290-0.

Park, Y. S., Kunze, S., Ni, X. *et al*., 2010. Comparative molecular and biochemical characterization of segmentally duplicated 9-lipoxygenase genes ZmLOX4 and ZmLOX5 of maize. Planta 231 (6): 1425–1437. https://doi.org/10.1007/s00425-010-1143-8.

Parry, D. W., Jenkinson, P., and McLeod, L., 1995. Fusarium ear blight (scab) in small grain cereals—a review. Plant Pathol. 44 (2): 207–238. https://doi.org/10.1111/j.1365-3059.1995.tb02773.x.

Patel, J. S., Wyenandt, C. A., and McGrath, M. T., 2021. Effective downy mildew management in basil using resistant varieties, environment modifications, and fungicides. Plant Health Prog. 22 (3): 226–234. https://doi.org/10.1094/PHP-02-21-0041-FI

Perazzolli, M., Roatti, B., Bozza, E. *et al*., 2011. *Trichoderma harzianum* T39 induces resistance against downy mildew by priming for defense without costs for grapevine. Biol. Control 58 (1): 74–82. https://doi.org/10.1016/j.biocontrol.2011.04.006.

Peressotti, E., Wiedemann-Merdinoglu, S., Delmotte, F. *et al*., 2010. Breakdown of resistance to grapevine downy mildew upon limited deployment of a resistant variety. BMC Plant Biol. 10 (1): 147. https://doi.org/10.1186/1471-2229-10-147

Pérez-Jaramillo, J. E., De Hollander, M., Ramírez, C. A. *et al*., 2019. Deciphering rhizosphere microbiome assembly of wild and modern common bean (*Phaseolus vulgaris*) in native and agricultural soils from Colombia. Microbiome 7 (1): 114. https://doi.org/10.1186/s40168-019-0727-1.

Pezet, R., Perret, C., Jean-Denis, J. B. *et al*., 2003. δ-Viniferin, a resveratrol dehydrodimer: one of the major stilbenes synthesized by stressed grapevine leaves. J. Agric. Food Chem. 51 (18): 5488–5492. https://doi.org/10.1021/jf030227o

Pieterse, C. M., Van der Does, D., Zamioudis, C. *et al*., 2012. Hormonal modulation of plant immunity. Annu. Rev. Cell Dev. Biol. 28: 489–521. https://doi.org/10.1146/annurev-cellbio-092910-154055.

Polesani, M., Bortesi, L., Ferrarini, A. *et al*., 2010. General and species-specific transcriptional responses to downy mildew infection in a susceptible (*Vitis vinifera*) and a resistant (*V. riparia*) grapevine species. BMC Genomics 11 (1): 117. https://doi.org/10.1186/1471-2164-11-117

Postma, J., Schilder, M. T., Bloem, J. *et al*., 2008. Soil suppressiveness and functional diversity of the soil microflora in organic farming systems. Soil Biol. Biochem. 40 (9): 2394–2406. https://doi.org/10.1016/j.soilbio.2008.05.023.

Postma, J., Nijhuis, E. H., Yassin, A. F., *et al*., 2010a. Genotypic and phenotypic variation among *Lysobacter capsici* strains isolated from *Rhizoctonia* suppressive soils. Syst. Appl. Microbiol. 33 (4): 232–235. https://doi.org/10.1016/j.syapm.2010.03.002.

Postma, J., Scheper, R. W. A., Schilder, M. T., *et al*., 2010b. Effect of successive cauliflower plantings and *Rhizoctonia solani* AG 2-1 inoculations on disease suppressiveness of a suppressive and a conducive soil. Soil Biol. Biochem. 42 (5): 804–812. https://doi.org/10.1016/j.soilbio.2010.01.017.

Postma, J., and Schilder, M. T., 2015. Enhancement of soil suppressiveness against *Rhizoctonia solani*

in sugar beet by organic amendments. Appl. Soil Ecol. 94: 72–79. https://doi.org/10.1016/j.apsoil.2015.05.002.

Postma, J., Schilder, M. T., van Hoof, R. A., *et al*., 2011. Indigenous populations of three closely related *Lysobacter* spp. in agricultural soils using real-time PCR. Microb. Ecol. 62 (4): 948–958. https://doi.org/10.1007/s00248-011-9847-2.

Postma, J., Schilder, M. T., and Stevens, L. H., 2014. The potential of organic amendments to enhance soil suppressiveness against *Rhizoctonia solani* disease in different soils and crops. In VIII Int. Symp. Chem. Non-Chem. Soil Substrate Disinfestation, 1044: 127–132. https://doi.org/10.17660/ActaHortic.2014.1044.14

Pozo, M. J., Van Der Ent, S., Van Loon, L. C. *et al*., 2008. Transcription factor MYC2 is involved in priming for enhanced defense during rhizobacteria-induced systemic resistance in *Arabidopsis thaliana*. New Phytol. 180 (2): 511–523. https://doi.org/10.1111/j.1469-8137.2008.02578.x

Parveen, T., and Sharma, K., 2015. *Pythium* diseases, control and management strategies: a review. Int. J. Plant Anim. Environ. Sci. 5 (1): 244–257.

Puopolo, G., Cimmino, A., Palmieri, M. C. *et al*., 2014a. *Lysobacter capsici* AZ78 produces cyclo(l-Pro-l-Tyr), a 2,5-diketopiperazine with toxic activity against sporangia of *Phytophthora infestans* and *Plasmopara viticola*. J. Appl. Microbiol. 117 (4): 1168–1180. https://doi.org/10.1111/jam.12611.

Puopolo, G., Tomada, S., Sonego, P. *et al*., 2016. The *Lysobacter capsici* AZ78 genome has a gene pool enabling it to interact successfully with phytopathogenic microorganisms and environmental factors. Front. Microbiol. 7: 96. https://doi.org/10.3389/fmicb.2016.00096.

Puopolo, G., Giovannini, O., amd Pertot, I., 2014b. *Lysobacter capsici* AZ78 can be combined with copper to effectively control *Plasmopara viticola* on grapevine. Microbiol. Res. 169 (7–8): 633–642. https://doi.org/10.1016/j.micres.2013.09.013.

Puopolo, G., Raio, A., and Zoina, A., 2010. Identification and characterization of *Lysobacter capsici* strain PG4: a new plant health-promoting rhizobacterium. J. Plant Pathol. 157–164. https://doi.org/10.4454/jpp.v92i1.25.

Puopolo, G., Tomada, S., and Pertot, I., 2018. The impact of the omics era on the knowledge and use of *Lysobacter* species to control phytopathogenic micro-organisms. J. Appl. Microbiol. 124 (1): 15–27. https://doi.org/10.1111/jam.13607.

Qi, G., Chen, S., Ke, L. *et al*., 2020. Cover crops restore declining soil properties and suppress bacterial wilt by regulating rhizosphere bacterial communities and improving soil nutrient contents. Microbiol. Res. 238: 126505. https://doi.org/10.1016/j.micres.2020.126505.

Qian, G. L., Hu, B. S., Jiang, Y. H. *et al*., 2009. Identification and characterization of *Lysobacter enzymogenes* as a biological control agent against some fungal pathogens. Agric. Sci. China 8 (1): 68–75. https://doi.org/10.1016/S1671-2927(09)60010-9.

Qian, Y., Lynch, J. H., Guo, L. *et al*., 2019. Completion of the cytosolic post-chorismate phenylalanine biosynthetic pathway in plants. Nat. Commun. 10 (1): 15. https://doi.org/10.1038/s41467-018-07969-

2.

Qu, J., Dry, I., Liu, L. *et al*., 2021. Transcriptional profiling reveals multiple defense responses in downy mildew-resistant transgenic grapevine expressing a *TIR-NBS-LRR* gene located at the *MrRUN1*/*MrRPV1* locus. Hortic. Res. 8. https://doi.org/10.1038/s41438-021-00597-w.

Quesada-Moraga, E., González-Mas, N., Yousef-Yousef, M. *et al*., 2024. Key role of environmental competence in successful use of entomopathogenic fungi in microbial pest control. J. Pest Sci. 97 (1): 1–15. https://doi.org/10.1007/s10340-023-01622-8.

Raio, A., and Puopolo, G., 2021. *Pseudomonas chlororaphis* metabolites as biocontrol promoters of plant health and improved crop yield. World J. Microbiol. Biotechnol. 37 (6): 99. https://doi.org/10.1007/s11274-021-03063-w

Ray, P., Lakshmanan, V., Labbé, J. L. *et al*., 2020. Microbe to microbiome: a paradigm shift in the application of microorganisms for sustainable agriculture. Front. Microbiol. 11: 622926. https://doi.org/10.3389/fmicb.2020.622926

Rahman, A., Siddiqui, S. A., Rahman, M. O. *et al*., 2020. Cyclo(L-Pro-L-Tyr) from *Streptomyces* sp. 150: exploiting in vitro potential in controlling foodborne pathogens and phytopathogens. Anti-Infect. Agents, 18 (2): 169–177. https://doi.org/10.2174/2211352517666190716155147.

Reichenbach, H., 1992. The genus *Lysobacter*. In: Balows, A., Trüper, H. G., Dworkin, M., Harder, W., Schleifer, K. H. (eds.) *The Prokaryotes: A Handbook on the Biology of Bacteria: Ecophysiology, Isolation, Identification, Applications*. Springer, New York, pp. 3256–3275. https://doi.org/10.1007/978-1-4757-2191-1_14.

Reimer-Michalski, E. M., and Conrath, U., 2016. Innate immune memory in plants. In *Seminars in Immunology* 28 (4): 319–327. Academic Press. https://doi.org/10.1016/j.smim.2016.05.006.

Ren, X., Ren, S., Xu, G. *et al*., 2020. Knockout of diguanylate cyclase genes in *Lysobacter enzymogenes* to improve production of antifungal factor and increase its application in seed coating. Curr. Microbiol. 77 (6): 1006–1015. https://doi.org/10.1007/s00284-020-01902-x

Rodrigues, R. R., Rodgers, N. C., Wu, X. *et al*., 2018. COREMIC: a web-tool to search for a niche associated CORE MICrobiome. PeerJ 6: e4395. https://doi.org/10.7717/peerj.4395.

Romanenko, L. A., Uchino, M., Tanaka, N. *et al*., 2008. *Lysobacter spongiicola* sp. nov., isolated from a deep-sea sponge. Int. J. Syst. Evol. Microbiol. 58 (2): 370–374. https://doi.org/10.1099/ijs.0.65391-0.

Ruano-Rosa, D., and Mercado-Blanco, J., 2015. Combining biocontrol agents and organic amendments to manage soil-borne phytopathogens. In: *Organic Amendments and Soil Suppressiveness in Plant Disease Management*, pp. 457–478. Springer, Cham. https://doi.org/10.1007/978-3-319-23075-7_22.

Saigne-Soulard, C., Abdelli-Belhadj, A., Télef-Micouleau, M. *et al*., 2015. Oligosaccharides from *Botrytis cinerea* and elicitation of grapevine defense. In: *Polysaccharides: Bioactivity and Biotechnology*, pp. 939–958. https://doi.org/10.1007/978-3-319-16298-0.

Saikai, K. K., Oduori, C., Situma, E. *et al*., 2023. Biocontrol-based strategies for improving soil health and managing plant-parasitic nematodes in coffee production. Front. Plant Sci. 14: 1196171. https://doi.org/10.3389/fpls.2023.1196171.

Saito, A., Dohra, H., Hamada, M. *et al*., 2023. Physiological and genomic analyses of cobalamin (vitamin B12)-auxotrophy of *Lysobacter auxotrophicus* sp. nov., a methionine-auxotrophic chitinolytic bacterium isolated from chitin-treated soil. Int. J. Syst. Evol. Microbiol. 73 (5): 005899. https://doi.org/10.1099/ijsem.0.005899.

Saitou, N., and Nei, M., 1987. The neighbor-joining method: a new method for reconstructing phylogenetic trees. Mol. Biol. Evol. 4 (4): 406–425. https://doi.org/10.1093/oxfordjournals.molbev.a040454.

Salas-Marina, M. A., Silva-Flores, M. A., Uresti-Rivera, E. E. *et al*., 2011. Colonization of *Arabidopsis* roots by *Trichoderma atroviride* promotes growth and enhances systemic disease resistance through jasmonic acid/ethylene and salicylic acid pathways. Eur. J. Plant Pathol. 131 (1): 15–26. https://doi.org/10.1007/s10658-011-9782-6.

Sang, M., Wang, H., Shen, Y. *et al*., 2019. Identification of an anti-MRSA cyclic lipodepsipeptide, WBP-29479A1, by genome mining of *Lysobacter antibioticus*. Org. Lett. 21 (16): 6432–6436. https://doi.org/10.1021/acs.orglett.9b02333.

Sang, M. K., Kim, J. D., Kim, B. S. *et al*., 2011. Root treatment with rhizobacteria antagonistic to *Phytophthora* blight affects anthracnose occurrence, ripening, and yield of pepper fruit in the plastic house and field. Phytopathology 101 (6): 666–678. https://doi.org/10.1094/PHYTO-08-10-0224.

Santiago, M., Lee, W., Fayad, A. A. *et al*., 2018. Genome-wide mutant profiling predicts the mechanism of a Lipid II binding antibiotic. Nat. Chem. Biol. 14 (6): 601–608. https://doi.org/10.1038/s41589-018-0041-4.

Sarrocco, S., 2023. Biological disease control by beneficial (micro) organisms: Selected breakthroughs in the past 50 years. Phytopathology 113 (4): 732–740. https://doi.org/10.1094/PHYTO-11-22-0405-KD

Savary, S., Willocquet, L., Pethybridge, S. J. *et al*., 2019. The global burden of pathogens and pests on major food crops. Nat. Ecol. Evol. 3 (3): 430–439. https://doi.org/10.1038/s41559-018-0793-y.

Schobert, R., and Schlenk, A., 2008. Tetramic and tetronic acids: an update on new derivatives and biological aspects. Bioorg. Med. Chem. 16 (8): 4203–4221. https://doi.org/10.1016/j.bmc.2008.02.069

Schroeder, K. L., Martin, F. N., de Cock, A. W. *et al*., 2013. Molecular detection and quantification of *Pythium* species: evolving taxonomy, new tools, and challenges. Plant Dis. 97 (1): 4–20. https://doi.org/10.1094/pdis-03-12-0243-fe

Schüder, I., Port, G., and Bennison, J., 2004. The behavioral response of slugs and snails to novel molluscicides, irritants and repellents. Pest Manag. Sci. 60 (12): 1171–1177. https://doi.org/10.1002/ps.942.

Schumann, P., Zhang, D. C., França, L. *et al*., 2018. *Marmoricola silvestris* sp. nov., a novel actinobacterium isolated from alpine forest soil. Int. J. Syst. Evol. Microbiol. 68 (4): 1313–1318. https://doi.org/10.1099/ijsem.0.002674.

Seccareccia, I., Kost, C., and Nett, M., 2015. Quantitative analysis of *Lysobacter* predation. Appl. Environ. Microbiol. 81 (20): 7098–7105. https://doi.org/10.1128/AEM.01781-15.

Segarra, G., Puopolo, G., Giovannini, O. *et al*., 2015. Stepwise flow diagram for the development of formulations of non-spore-forming bacteria against foliar pathogens: the case of *Lysobacter capsici* AZ78. J. Biotechnol. 216: 56–64. https://doi.org/10.1016/j.jbiotec.2015.10.004.

Sekulska-Nalewajko, J., Gocławski, J., Chojak-Koźniewska, J. *et al*., 2016. Automated image analysis for quantification of reactive oxygen species in plant leaves. Methods 109: 114–122. https://doi.org/10.1016/j.ymeth.2016.05.018.

Seo, S., and Matthews, K. R., 2012. Influence of the plant defense response to *Escherichia coli* O157:H7 cell surface structures on survival of that enteric pathogen on plant surfaces. Appl. Environ. Microbiol. 78 (16): 5882–5889. https://doi.org/10.1128/AEM.01095-12

Shen, X., Wang, B., Yang, N. *et al*., 2021. *Lysobacter enzymogenes* antagonizes soilborne bacteria using the type IV secretion system. Environ. Microbiol. 23 (8): 4673–4688. https://doi.org/10.1111/1462-2920.15662.

Sheoran, A. R., Lakra, N., Saharan, B. S. *et al*., 2025. Enhancing plant disease resistance: insights from biocontrol agent strategies. J. Plant Growth Regul. 44 (2): 436–459. https://doi.org/10.1007/s00344-024-11480-y.

Shukla, N., Singh, E. A. N. A., Kabadwa, B. C. *et al*., 2019. Present status and future prospects of bio-agents in agriculture. Int. J. Curr. Microbiol. Appl. Sci. 8 (4): 2138–2153. https://doi.org/10.20546/ijcmas.2019.804.251.

Siddiqi, M. Z., and Im, W. T., 2016. *Lysobacter hankyongensis* sp. nov., isolated from activated sludge and *Lysobacter sediminicola* sp. nov., isolated from freshwater sediment. Int. J. Syst. Evol. Microbiol. 66 (1): 212–218. https://doi.org/10.1099/ijsem.0.000699.

Siegel-Hertz, K., Edel-Hermann, V., Chapelle, E. *et al*., 2018. Comparative microbiome analysis of a *Fusarium* wilt suppressive soil and a *Fusarium* wilt conductive soil from the Châteaurenard region. Front. Microbiol. 9: 568. https://doi.org/10.3389/fmicb.2018.00568.

Šimek, M., and Cooper, J. E., 2002. The influence of soil pH on denitrification: progress towards the understanding of this interaction over the last 50 years. Eur. J. Soil Sci. 53 (3): 345–354.

Singh, A., and Singh, I. K. (eds.), 2018. *Molecular aspects of plant-pathogen interaction*. Vol. 10, pp. 978–981. Springer, Singapore.

Singh, H., Du, J., Ngo, H. T. *et al*., 2015. *Lysobacter fragariae* sp. nov. and *Lysobacter rhizosphaerae* sp. nov. isolated from rhizosphere of strawberry plant. Antonie van Leeuwenhoek 107 (6): 1437–1444. https://doi.org/10.1007/s10482-015-0439-x.

Singh, R. K., Singh, P., Li, H. B. *et al*., 2020. Diversity of nitrogen-fixing rhizobacteria associated with sugarcane: a comprehensive study of plant–microbe interactions for growth enhancement in *Saccharum* spp. BMC Plant Biol. 20 (1): 220. https://doi.org/10.1186/s12870-020-02400-9

Singh, V., Hallan, V., and Pati, P. K., 2024. *Withania somnifera* osmotin (WsOsm) confers stress tolerance in tobacco and establishes novel interactions with the defensin protein (WsDF). Physiol. Plant. 176 (5): e14513. https://doi.org/10.1111/ppl.14513.

Soe, K. M., Htwe, A. Z., Moe, K., Tomomi, A., & Yamakawa, T. (2020). Diversity and effectivity of indigenous Mesorhizobium strains for chickpea (Cicer arietinum L.) in Myanmar. *Agronomy* , *10* (2), 287. https://doi.org/10.3390/agronomy10020287

Song, S., Jeon, E. K., and Hwang, C. W., 2022. Characteristic analysis of soil-isolated *Bacillus velezensis* HY-3479 and its antifungal activity against phytopathogens. Curr. Microbiol. 79 (12): 357. https://doi.org/10.1007/s00284-022-03060-8.

Song, Y., and Liu, M., 2025. Empowering sustainable farming: harnessing digital technology for green and low-carbon agricultural practices. Sustainability 17 (4): 1617. https://doi.org/10.3390/su17041617

Stocki, M., Stocka, N., Borowik, P. *et al*., 2025. Use of volatile organic compounds produced by *Bacillus* bacteria for the biological control of *Fusarium oxysporum*. Forests 16 (8): 1220. https://doi.org/10.3390/f16081220

Stummer, B. E., Francis, I. L., Zanker, T. *et al*., 2005. Effects of powdery mildew on the sensory properties and composition of Chardonnay juice and wine when grape sugar ripeness is standardised. Aust. J. Grape Wine Res. 11 (1): 66–76. https://doi.org/10.1111/j.1755-0238.2005.tb00280.x.

Sullivan, R. F., Holtman, M. A., Zylstra, G. J. *et al*., 2003. Taxonomic positioning of two biological control agents for plant diseases as *Lysobacter enzymogenes* based on phylogenetic analysis of 16S rDNA, fatty acid composition and phenotypic characteristics. J. Appl. Microbiol. 94 (6): 1079–1086. https://doi.org/10.1046/j.1365-2672.2003.01932.x.

Sun, L., Song, S., Fu, L. *et al*., 2015. Exploring a soil fumigation strategy based on ammonium bicarbonate to control *Fusarium* wilts of cucurbits. Crop Prot. 70: 53–60. https://doi.org/10.1016/j.cropro.2015.01.004.

Syed-Ab-Rahman, S. F., Carvalhais, L. C., Chua, E. T. *et al*., 2019. Soil bacterial diffusible and volatile organic compounds inhibit *Phytophthora capsici* and promote plant growth. Sci. Total Environ. 692: 267–280. https://doi.org/10.1016/j.scitotenv.2019.07.061.

Tamm, L., Thürig, B., Bruns, C. *et al*., 2010. Soil type, management history, and soil amendments influence the development of soil-borne (*Rhizoctonia solani*, *Pythium ultimum*) and air-borne (*Phytophthora infestans*, *Hyaloperonospora parasitica*) diseases. Eur. J. Plant Pathol. 127 (4): 465–481. https://doi.org/10.1007/s10658-010-9612-2.

Tamura, K., Stecher, G., Kumar, S., *et al*., 2021. MEGA11: molecular evolutionary genetics analysis version 11. Mol. Biol. Evol. 38 (7): 3022–3027. https://doi.org/10.1093/molbev/msab120.

Tashiro, Y., Uchiyama, H., Nomura, N., *et al*., 2012. Multifunctional membrane vesicles in *Pseudomonas aeruginosa*. Environ. Microbiol. 14 (6): 1349–1362. https://doi.org/10.1111/j.1462-2920.2011.02632.x

Thomma, B. P., Penninckx, I. A., Cammue, B. P. *et al*., 2001. The complexity of disease signaling in *Arabidopsis*. Curr. Opin. Immunol. 13 (1): 63–68. https://doi.org/10.1016/s0952-7915(00)00183-7

Tian, G. L., Bi, Y. M., Jiao, X. L. *et al*., 2021. Application of vermicompost and biochar suppresses *Fusarium* root rot of replanted American ginseng. Appl. Microbiol. Biotechnol. 105 (18): 6977–6991. https://doi.org/10.1007/s00253-021-11464-y.

Toffolatti, S. L., Russo, G., Campia, P. *et al*., 2018a. A time-course investigation of resistance to the carboxylic acid amide mandipropamid in field populations of *Plasmopara viticola* treated with anti-resistance strategies. Pest Manag. Sci. 74 (12): 2822–2834. https://doi.org/10.1002/ps.5072.

Toffolatti, S. L., De Lorenzis, G., Costa, A. *et al*., 2018b. Unique resistance traits against downy mildew from the center of origin of grapevine (*Vitis vinifera*). Sci. Rep. 8 (1): 12523. https://doi.org/10.1038/s41598-018-30413-w.

Tomada, S., Puopolo, G., Perazzolli, M. *et al*., 2016. Pea broth enhances the biocontrol efficacy of *Lysobacter capsici* AZ78 by triggering cell motility associated with biogenesis of type IV pilus. Front. Microbiol. 7: 1136. https://doi.org/10.3389/fmicb.2016.01136.

Tomada, S., Sonego, P., Moretto, M. *et al*., 2017. Dual RNA-seq of *Lysobacter capsici* AZ78–*Phytophthora infestans* interaction shows the implementation of attack strategies by the bacterium and unsuccessful oomycete defense responses. Environ. Microbiol. 19 (10): 4113–4125. https://doi.org/10.1111/1462-2920.13861

Tripathi, A. N., Meena, B. R., Pandey, K. K. *et al*., 2020. Microbial bioagents in agriculture: current status and prospects. In: *New Frontiers in Stress Management for Durable Agriculture*, pp. 331–368. https://doi.org/10.1007/978-981-15-1322-0.

Tripathi, D., Zhang, T., Koo, A. J. *et al*., 2018. Extracellular ATP acts on jasmonate signaling to reinforce plant defense. Plant Physiol. 176 (1): 511–523. https://doi.org/10.1104/pp.17.01477.

Trouvelot, S., Varnier, A. L., Allegre, M. *et al*., 2008. A β-1,3 glucan sulfate induces resistance in grapevine against *Plasmopara viticola* through priming of defense responses, including HR-like cell death. Mol. Plant-Microbe Interact. 21 (2): 232–243. https://doi.org/10.1094/MPMI-21-2-0232.

Tsao, P. H., and Oster, J. J., 1981. Relation of ammonia and nitrous acid to suppression of *Phytophthora* in soils amended with nitrogenous organic substances. Phytopathology 71 (1): 53–59. https://doi.org/10.1094/PHYTO-71-53

Tu, C. K., Wang, P. H., Lee, M. H., *et al*., 2023. Endophytic bacterium *Lysobacter firmicutimachus* strain 5-7 is a promising biocontrol agent against rice seedling disease caused by *Pythium arrhenomanes* in nursery trays. Plant Dis. 107 (4): 1075–1086. https://doi.org/10.1094/PDIS-05-22-1195-RE.

Turnbull, A. L., Liu, Y., Lazarovits, G., *et al*., 2012. Isolation of bacteria from the rhizosphere and

rhizoplane of potato (*Solanum tuberosum*) grown in two distinct soils using semi-selective media and characterization of their biological properties. Am. J. Potato Res. 89 (4): 294–305. https://doi.org/10.1007/s12230-012-9253-4.

Tyler, B. M., 2002. Molecular basis of recognition between *Phytophthora* pathogens and their hosts. Annu. Rev. Plant Pathol. 40 (1): 137–167. https://doi.org/10.1146/annurev.phyto.40.120601.125310.

Tziros, G. T., Ainalidou, A., Samaras, A. *et al*., 2022. Differences in defense-related gene expression and metabolite accumulation reveal insights into the resistance of Greek grape wine cultivars to *Botrytis* bunch rot. OENO One 56 (2): 111–123. https://doi.org/10.20870/oeno-one.2022.56.2.5451.

Uddin, N., 2022. Studies on the effect of pesticides on the mycoflora diversity in the agricultural environments. J. Mycopathol. Res. 60 (4): 603–608. https://doi.org/10.57023/jmycr.60.4.2022.603.

Ul Haq, I., Rahim, K., Yahya, G. *et al*., 2024. Eco-smart biocontrol strategies utilizing potent microbes for sustainable management of phytopathogenic diseases. Biotechnol. Rep. 44: e00859. https://doi.org/10.1016/j.btre.2024.e00859.

Van der Ent, S., Verhagen, B. W., Van Doorn, R. *et al*., 2008. MYB72 is required in early signaling steps of rhizobacteria-induced systemic resistance in *Arabidopsis*. Plant Physiol. 146 (3): 1293–1304. https://doi.org/10.1104/pp.107.113829

Van der Plaats-Niterink, A. J., 1981. *Monograph of the genus Pythium*. Vol. 21, p. 242. Baarn: Centraalbureau voor Schimmelcultures.

Van Overbeek, L., and Van Elsas, J. D., 2008. Effects of plant genotype and growth stage on the structure of bacterial communities associated with potato (*Solanum tuberosum* L.). FEMS Microbiol. Ecol. 64 (2): 283–296. https://doi.org/10.1111/j.1574-6941.2008.00469.x.

Velmourougane, K., Prasanna, R., Saxena, A. K., *et al*., 2017. Agriculturally important microbial biofilms: present status and future prospects. J. Basic Microbiol. 57 (7): 548–573. https://doi.org/10.1002/jobm.201700046.

Verhagen, B. W., Trotel-Aziz, P., Couderchet, M. *et al*., 2010. *Pseudomonas* spp.-induced systemic resistance to *Botrytis cinerea* is associated with induction and priming of defence responses in grapevine. J. Exp. Bot. 61 (1): 249–260. https://doi.org/10.1093/jxb/erp295.

Villaverde, J. J., Sevilla-Morán, B., Sandín-España, P. *et al*., 2014. Biopesticides in the framework of the European Pesticide Regulation (EC) No. 1107/2009. Pest Manag. Sci. 70 (1): 2–5. https://doi.org/10.1002/ps.3663.

Vinale, F., Ghisalberti, E. L., Sivasithamparam, K. *et al*., 2009. Factors affecting the production of *Trichoderma harzianum* secondary metabolites during the interaction with different plant pathogens. Lett. Appl. Microbiol. 48 (6): 705–711. https://doi.org/10.1111/j.1472-765X.2009.02599.x

Vlassi, A., Nesler, A., Perazzolli, M. *et al*., 2020a. Volatile organic compounds from *Lysobacter capsici* AZ78 as potential candidates for biological control of soilborne plant pathogens. Front. Microbiol. 11: 1748. https://doi.org/10.3389/fmicb.2020.01748.

Vlassi, A., Nesler, A., Parich, A. *et al*., 2020b. Volatile-mediated inhibitory activity of rhizobacteria as a result of multiple factors interaction: The case of *Lysobacter capsici* AZ78. Microorganisms 8 (11): 1761. https://doi.org/10.3390/microorganisms8111761.

Vraka, C., Nics, L., Wagner, K. H. *et al*., 2017. LogP, a yesterday's value? Nucl. Med. Biol. 50: 1–10. https://doi.org/10.1016/j.nucmedbio.2017.03.003

Vylkova, S., 2017. Environmental pH modulation by pathogenic fungi as a strategy to conquer the host. PLoS Pathog. 13 (2): e1006149. https://doi.org/10.1371/journal.ppat.1006149.

Walnut, J., 2019. Hormonal signaling induced in soybean by *Lysobacter enzymogenes* strain C3. Masters Thesis. University of Nebraska-Lincoln, Lincoln, NE.

Walters, D. R., Havis, N. D., Sablou, C. *et al*., 2011. Possible trade-off associated with the use of a combination of resistance elicitors. Physiol. Mol. Plant Pathol. 75 (4): 188–192. https://doi.org/10.1016/j.pmpp.2011.02.001.

Wang, C. Y., Zhou, X., Guo, D. *et al*., 2019. Soil pH is the primary factor driving the distribution and function of microorganisms in farmland soils in northeastern China. Ann. Microbiol. 69 (13): 1461–1473. https://doi.org/10.1007/s13213-019-01529-9.

Wang, H. W., Xu, M., Cai, X. Y. *et al*., 2020. Application of spent mushroom substrate suppresses *Fusarium* wilt in cucumber and alters the composition of the microbial community of the cucumber rhizosphere. Eur. J. Soil Biol. 101: 103245. https://doi.org/10.1016/j.ejsobi.2020.103245.

Wang, R., Zhang, H., Sun, L. *et al*., 2017. Microbial community composition is related to soil biological and chemical properties and bacterial wilt outbreak. Sci. Rep. 7 (1): 343. https://doi.org/10.1038/s41598-017-00472-6.

Wang, W. Y., Kong, W. L., Liao, Y. C. Z. *et al*., 2022a. Identification of *Bacillus velezensis* SBB and its antifungal effects against *Verticillium dahliae*. J. Fungi 8 (10): 1021. https://doi.org/10.3390/jof8101021

Wang, X., Zhou, C., Xiao, X. *et al*., 2022b. Phytoextraction potential of arsenic and cadmium and response of rhizosphere microbial community by intercropping with two types of hyperaccumulators. Environ. Sci. Pollut. Res. 29 (60): 91356–91367. https://doi.org/10.1007/s11356-022-21994-1.

Wang, Y., Li, X., Fan, B. *et al*., 2021. Regulation and function of defense-related callose deposition in plants. Int. J. Mol. Sci. 22 (5): 2393. https://doi.org/10.3390/ijms22052393

Wang, Y., Liu, C., Jiang, J. *et al*., 2024. Mechanism of KOH-modified biochar application under water-saving and nitrogen-reducing conditions to inhibit soybean root rot and improve quality and efficiency. J. Soil Sci. Plant Nutr. 24 (3): 5370–5383. https://doi.org/10.1007/s42729-024-01913-8.

Wang, Y., Govers, F., and Wang, Y., 2025. Oomycete plant pathogens: biology, pathogenesis and emerging control strategies. Nat. Rev. Microbiol.: 1–18. https://doi.org/10.1038/s41579-025-01248-w.

Weindling, R., and Fawcett, H. S., 1936. Experiments in the control of *Rhizoctonia* damping-off of

citrus seedlings. Hilgardia 10 (1): 1–16. https://doi.org/10.3733/HILG.V10N01P001

Wen, Y. C., Li, H. Y., Lin, Z. A. *et al*., 2020. Long-term fertilization alters soil properties and fungal community composition in fluvo-aquic soil of the North China Plain. Sci. Rep. 10 (1): 7198. https://doi.org/10.1038/s41598-020-64227-6.

Wilhelm, S., 1951. Effect of various soil amendments on the inoculum potential of the *Verticillium* wilt fungus. Phytopathology 41: 31–33. https://doi.org/10.1007/BF02853547

Willmann, R., Lajunen, H. M., Erbs, G. *et al*., 2011. *Arabidopsis* lysin-motif proteins LYM1, LYM3, CERK1 mediate bacterial peptidoglycan sensing and immunity to bacterial infection. Proc. Natl. Acad. Sci. U.S.A. 108 (49): 19824–19829. https://doi.org/10.1073/pnas.1112862108

Wood, S. L., Alam, M., Dupras, J., *et al*., 2019. Multiple pathways to more sustainable diets: shifts in dietary composition, caloric intake and food waste. Front. Sustain. Food Syst. 3: 89. https://doi.org/10.3389/fsufs.2019.00089.

Wyenandt, C. A., Simon, J. E., McGrath, M. T. *et al*., 2010. Susceptibility of basil cultivars and breeding lines to downy mildew (*Peronospora belbahrii*). HortScience. 45 (9): 1416–1419. https://doi.org/10.21273/hortsci.45.9.1416.

Wyenandt, C. A., Simon, J. E., Pyne, R. M. *et al*., 2015. Basil downy mildew (*Peronospora belbahrii*): discoveries and challenges related to its control. Phytopathology 105 (7): 885–894. https://doi.org/10.1094/PHYTO-02-15-0032-FI.

Xia, J., Chen, J., Chen, Y. *et al*., 2018. Type IV pilus biogenesis genes and their roles in biofilm formation in the biological control agent *Lysobacter enzymogenes* OH11. Appl. Microbiol. Biotechnol. 102 (2): 833–846. https://doi.org/10.1007/s00253-017-8619-4.

Xiao, M., Zhou, X. K., Chen, X. *et al*., 2019. *Lysobacter tabacisoli* sp. nov., isolated from rhizosphere soil of *Nicotiana tabacum* L. Int. J. Syst. Evol. Microbiol. 69 (7): 1875–1880. https://doi.org/10.1099/ijsem.0.003164.

Xing, C., Chen, Q., Qiao, Q. *et al*., 2023. *PbrWRKY70* increases pear (*Pyrus bretschneideri* Rehd.) black spot disease tolerance by negatively regulating ethylene synthesis via *PbrERF1B-2*. Plant Sci. 334: 111773. https://doi.org/10.1016/j.plantsci.2023.111773

Xing, L., Di, Z., Yang, W. *et al*., 2017. Overexpression of ERF1-V from *Haynaldia villosa* can enhance the resistance of wheat to powdery mildew and increase the tolerance to salt and drought stresses. Front. Plant Sci. 8: 1948. https://doi.org/10.3389/fpls.2017.01948

Xing, T., Higgins, V. J., Blumwald, E., *et al*., 1997. Race-specific elicitors of *Cladosporium fulvum* promote translocation of cytosolic components of NADPH oxidase to the plasma membrane of tomato cells. Plant Cell 9 (2): 249–259. https://doi.org/10.1105/tpc.9.2.249

Xiong, W., Guo, S., Jousset, A. *et al*., 2017. Bio-fertilizer application induces soil suppressiveness against *Fusarium* wilt disease by reshaping the soil microbiome. Soil Biol. Biochem. 114: 238–247. https://doi.org/10.1016/j.soilbio.2017.07.016.

Xu, L., Wu, P., Wright, S. J. *et al*., 2015. Bioactive polycyclic tetramate macrolactams from *Lysobacter enzymogenes* and their absolute configurations by theoretical ECD calculations. J. Nat. Prod. 78 (8): 1841–1847. https://doi.org/10.1021/acs.jnatprod.5b00099.

Xu, L., Han, Y., Yi, M. *et al*., 2019. Shift of millet rhizosphere bacterial community during the maturation of parent soil revealed by 16S rDNA high-throughput sequencing. Appl. Soil Ecol. 135: 157–165. https://doi.org/10.1016/j.apsoil.2018.12.004.

Yadav, R. S., Panwar, J., Meena, H. N. *et al*., 2015. Developing disease-suppressive soil through agronomic management, in: Organic amendments and soil suppressiveness in plant disease management. Springer International Publishing, Cham, pp. 61–94. https://doi.org/10.1007/978-3-319-23075-7.

Yan, Z. F., Trinh, H., Moya, G. *et al*., 2016. *Lysobacter rhizophilus* sp. nov., isolated from rhizosphere soil of mugunghwa, the national flower of South Korea. Int. J. Syst. Evol. Microbiol. 66 (11): 4754–4759. https://doi.org/10.1099/ijsem.0.001422.

Yang, S. F., and Hoffman, N. E., 1984. Ethylene biosynthesis and its regulation in higher plants. Annu. Rev. Plant Physiol. 35 (1): 155–189. https://doi.org/10.1146/annurev.pp.35.060184.001103

Yang, S. Z., Feng, G. D., Zhu, H. H. *et al*., 2015a. *Lysobacter mobilis* sp. nov., isolated from abandoned lead–zinc ore. Int. J. Syst. Evol. Microbiol. 65 (Pt 3): 833–837. https://doi.org/10.1099/ijs.0.000026.

Yang, W., Zhu, Y., Jiang, Y. *et al*., 2024. Dissolved organic matter of mature chicken compost contributes to the protection of microorganisms from the stress of heavy metals. J. Environ. Chem. Eng. 12 (5): 113590. https://doi.org/10.1016/j.jece.2024.113590.

Yang, Y., Ling, X., Chen, T. *et al*., 2015b. A cotton *Gbvdr5* gene encoding a leucine-rich-repeat receptor-like protein confers resistance to *Verticillium dahliae* in transgenic *Arabidopsis* and upland cotton. Plant Mol. Biol. Rep. 33 (4): 987–1001. https://doi.org/10.1007/s11105-014-0810-5.

Yano, S., Kanno, H., Tsuhako, H. *et al*., 2021. Cloning, expression, and characterization of a GH19-type chitinase with antifungal activity from *Lysobacter* sp. MK9-1. J. Biosci. Bioeng. 131 (4): 348–355. https://doi.org/10.1016/j.jbiosc.2020.11.005.

Yaxiong, W., Shasha, X., Wenbin, L. *et al*., 2017. Identification and location of grapevine sucker based on information fusion of 2D laser scanner and machine vision. Int. J. Agric. Biol. Eng. 10 (2): 84–93. https://doi.org/10.3965/j.ijabe.20171002.2489.

Yin, N., Liu, R., Zhao, J. L. *et al*., 2021. Volatile organic compounds of *Bacillus cereus* strain Bc-cm103 exhibit fumigation activity against *Meloidogyne incognita*. Plant Dis. 105 (4): 904–911. https://doi.org/10.1094/PDIS-04-20-0783-RE.

Yu, F., Zaleta-Rivera, K., Zhu, X. *et al*., 2007. Structure and biosynthesis of heat-stable antifungal factor (HSAF), a broad-spectrum antimycotic with a novel mode of action. Antimicrob. Agents Chemother. 51 (1): 64–72. https://doi.org/10.1128/AAC.00931-06.

Yu, L., Li, H., Zhou, Z. *et al*., 2021. An antifungal polycyclic tetramate macrolactam, heat-stable

antifungal factor (HSAF), is a novel oxidative stress modulator in *Lysobacter enzymogenes*. Appl. Environ. Microbiol. 87 (10): e03105-20. https://doi.org/10.1128/AEM.03105-20.

Yu, X., Feng, B., He, P. *et al*., 2017. From chaos to harmony: responses and signaling upon microbial pattern recognition. Annu. Rev. Plant Pathol. 55 (1): 109–137. https://doi.org/10.1146/annurev-phyto-080516-035649

Yuan, J., Zhao, M., Li, R. *et al*., 2017. Microbial volatile compounds alter the soil microbial community. Environ. Sci. Pollut. Res. 24 (28): 22485–22493. https://doi.org/10.1007/s11356-017-9839-y.

Yue, H., Jiang, J., Taylor, A. J. *et al*., 2021. Outer membrane vesicle-mediated codelivery of the antifungal HSAF metabolites and lytic polysaccharide monooxygenase in the predatory *Lysobacter enzymogenes*. ACS Chem. Biol. 16 (6): 1079–1089. https://doi.org/10.1021/acschembio.1c00260.

Yue, L., Jiao, L., Tao, M. *et al*., 2023. Dynamics of organic acid exudation and rhizobacteria in maize rhizosphere respond to N-CDs. Sci. Total Environ. 901: 166500. https://doi.org/10.1016/j.scitotenv.2023.166500.

Yuen, G. Y., Broderick, K. C., Jochum, C. C. *et al*., 2018. Control of cyst nematodes by *Lysobacter enzymogenes* strain C3 and the role of the antibiotic HSAF in the biological control activity. Biol. Control 117: 158–163. https://doi.org/10.1016/j.biocontrol.2017.11.007

Yuen, G. Y., Steadman, J. R., Lindgren, D. T. *et al*., 2001. Bean rust biological control using bacterial agents. Crop Prot. 20 (5): 395–402. https://doi.org/10.1016/S0261-2194(00)00154-X

Zhang, J., Wei, L., Yang, J. *et al*., 2020. Probiotic consortia: reshaping the rhizospheric microbiome and its role in suppressing root-rot disease of *Panax notoginseng*. Front. Microbiol. 11: 701. https://doi.org/10.3389/fmicb.2020.00701.

Zhang, Z., and Yuen, G. Y., 1999. Biological control of *Bipolaris sorokiniana* on tall fescue by *Stenotrophomonas maltophilia* strain C3. Phytopathology, 89 (9): 817–822. https://doi.org/10.1094/PHYTO.1999.89.9.817

Zhang, Z., and Yuen, G. Y., 2000. The role of chitinase production by *Stenotrophomonas maltophilia* strain C3 in biological control of *Bipolaris sorokiniana*. Phytopathology, 90 (4): 384–389. https://doi.org/10.1094/PHYTO.2000.90.4.384.

Zhao, J., Mei, Z., Zhang, X. *et al*., 2017a. Suppression of *Fusarium* wilt of cucumber by ammonia gas fumigation via reduction of *Fusarium* population in the field. Sci. Rep. 7 (1): 43103. https://doi.org/10.1038/srep43103.

Zhao, Y., Wang, P., Li, J. *et al*., 2009. The effects of two organic manures on soil properties and crop yields on a temperate calcareous soil under a wheat–maize cropping system. Eur. J. Agron. 31 (1): 36–42. https://doi.org/10.1016/j.eja.2009.03.001.

Zhao, Y., Qian, G., Ye, Y. *et al*., 2016. Heterocyclic aromatic N-oxidation in the biosynthesis of phenazine antibiotics from *Lysobacter antibioticus*. Org. Lett. 18 (10): 2495–2498. https://doi.org/10.1021/acs.orglett.6b01089.

Zhao, Y., Qian, G., Chen, Y. *et al*., 2017b. Transcriptional and antagonistic responses of biocontrol strain *Lysobacter enzymogenes* OH11 to the plant pathogenic oomycete *Pythium aphanidermatum*. Front. Microbiol. 8: 1025. https://doi.org/10.3389/fmicb.2017.01025.

Zhao, Y., Cheng, C., Jiang, T. *et al*., 2019. Control of wheat *Fusarium* head blight by heat-stable antifungal factor (HSAF) from *Lysobacter enzymogenes*. Plant Dis. 103 (6): 1286–1292. https://doi.org/10.1094/PDIS-09-18-1517-RE.

Zhao, Y., Jiang, T., Xu, H. *et al*., 2021a. Characterization of *Lysobacter* spp. strains and their potential use as biocontrol agents against pear anthracnose. Microbiol. Res. 242: 126624. https://doi.org/10.1016/j.micres.2020.126624.

Zhao, Y., Fu, W., Hu, C. *et al*., 2021b. Variation of rhizosphere microbial community in continuous mono-maize seed production. Sci. Rep. 11 (1): 1544. https://doi.org/10.1038/s41598-021-81228-1.

Zhou, S., Bi, J., Zhou, S. *et al*., 2025. Community assembly mechanisms underlying divergent responses of indica and japonica rice rhizosphere microbiota to drought stress. Microb. Ecol. 88 (1): 126. https://doi.org/10.1007/s00248-025-02647-5

Zhou, X., Qian, G., Chen, Y. *et al*., 2015. *PilG* is involved in the regulation of twitching motility and antifungal antibiotic biosynthesis in the biological control agent *Lysobacter enzymogenes*. Phytopathology, 105 (10): 1318–1324. https://doi.org/10.1094/PHYTO-12-14-0361-R.

Zorrilla, J. G., Giovannini, O., Nadalini, S. *et al*., 2023. Suppressive activity of *Glechoma hederacea* extracts against the phytopathogenic oomycete *Plasmopara viticola*, and first screening of the active metabolites. Agriculture, 14 (1): 58. https://doi.org/10.3390/agriculture14010058